

Spatial and Temporal Variability of In-Stream Functioning within a Forested,  
Headwater Piedmont Watershed

Luke Ethan Wildfire

Thesis submitted to the faculty of the Virginia Polytechnic Institute and State  
University in partial fulfillment of the requirements for the degree of

Master of Science  
In  
Biological Systems Engineering

Durelle T. Scott, Chair  
William C. Hession  
Kevin J. McGuire

November 25, 2013  
Blacksburg, VA

Keywords: Dissolved organic matter, in-stream metabolism, ammonium uptake,  
Piedmont

Copyright (2017)

# **SPATIAL AND TEMPORAL VARIABILITY OF IN-STREAM FUNCTIONING WITHIN A FORESTED, HEADWATER PIEDMONT WATERSHED**

**LUKE ETHAN WILDFIRE**

## **ABSTRACT**

As anthropogenic nutrient loads threaten the health of the Chesapeake Bay, lotic processes throughout its headwaters may buffer increased nitrogen inputs by converting them to stable forms, ultimately through denitrification to N<sub>2</sub> gas. However, the temporal environmental factors controlling baseflow nitrogen retention are poorly understood, particularly temperature, shading, and dissolved organic matter dynamics. This study therefore attempts to elucidate the effects of these environmental variables on nitrogen cycling within the Fair Hill Natural Resources Management Area (Fair Hill), a forested watershed within the Piedmont physiographic province of the Chesapeake Bay. As expected, groundwater and allochthonous organic matter inputs set the foundation for lotic biogeochemistry at Fair Hill, creating a nutrient-limited, heterotrophic reach. Within this setting, three temporal “hot-moments” of in-stream nutrient processing were observed: the release of ammonium and phosphate during the warm - but shaded - growing season; nitrate uptake during autumnal leaf-fall; and a unique spike of nitrate uptake and respiration-induced degradation of labile organic matter during a drought. Consequently, the baseflow capacity of this headwater stream to buffer nutrient exports to the Chesapeake Bay constantly varies throughout the year in response to light availability, temperature, and in-stream organic matter dynamics.

# **SPATIAL AND TEMPORAL VARIABILITY OF IN-STREAM FUNCTIONING WITHIN A FORESTED, HEADWATER PIEDMONT WATERSHED**

**LUKE ETHAN WILDFIRE**

## **GENERAL AUDIENCE ABSTRACT**

Throughout the Chesapeake Bay watershed, ecological processes known as nitrogen retention can naturally remove nitrogen pollution from small streams (a.k.a. headwater streams), and hence the Chesapeake Bay watershed. However, in-stream nitrogen retention varies throughout the year due to seasonal changes in temperature, shading (as leaves grow in the spring or fall off in the fall), and the amount and type of organic matter in the stream. This study examines how these three variables (temperature, shading, and dissolved organic matter dynamics) affect nitrogen retention in a headwater, forested stream within the Fair Hill Natural Resources Management Area (Fair Hill) located in the Piedmont region of the Chesapeake Bay watershed. As expected, groundwater and organic matter inputs set the foundation for in-stream conditions at Fair Hill, creating an environment with low concentrations of nitrate and phosphate (thus causing the stream to be nutrient-limited), while also creating a heterotrophic environment, which is an environment where more oxygen is consumed by microbes than produced by algae and plants. Additionally, three seasonal patterns regarding in-stream nutrient dynamics were observed at Fair Hill. Firstly, in-stream ammonium and phosphate concentrations increased during the warm - but shaded - growing season. Secondly, in-stream nitrate concentrations decreased when leaves fell in the fall. Thirdly, during a drought, in-stream nitrate removal increased while in-stream organic matter became more degraded. Consequently, in-stream nutrient retention at Fair Hill varies constantly throughout the year in response to light availability, temperature, and in-stream organic matter dynamics.

## ACKNOWLEDGEMENTS

To my amazing wife, Anna Wildfire, thank you for your endless love and support.

Thank you to my family for their encouragement throughout the thesis process: Mom, Dad, Nate, Gillian, Joe, Caitlin, Nolan, Jess, and Jake.

Thank you to my colleagues that helped with field work and lab work: Nate Jones, Tyler Kreider, Dan Chuquín, Ryan Fahs, Mike Nassry, Sally Walker, Kelly Fergusson, Janae Pinney. I couldn't have completed this thesis without your tireless work, late night contributions, and encouragement. Additional thanks to the many great friends that helped me stay sane throughout the process: Javier, James, Matt, Dan, Devin, Eric, Nancy, Kelsey, and many many others.

Lastly, thank you to the professors and researchers who helped guide me through the process, including my advisor, Dr. Scott, and the rest of the staff of the Virginia Tech Biological Systems Engineering Department. Also, thank you to Dr. Inamdar of the University of Delaware for his help and data contributed by his research group. Thank you to the National Science Foundation for supporting this research.

## TABLE OF CONTENTS

<b>1</b>	<b>LITERATURE REVIEW .....</b>	<b>1</b>
1.1	INTRODUCTION .....	1
1.2	WATERSHED NITROGEN RETENTION & EXPORT .....	4
1.2.1	Sources of reactive nitrogen to watersheds.....	5
1.2.2	Input-output models of watershed nitrogen retention.....	8
1.2.3	Watershed nitrogen flushing .....	12
1.3	IN-STREAM NITROGEN RETENTION AND EXPORT .....	16
1.3.1	In-stream dissolved organic nitrogen.....	16
1.3.2	In-stream dissolved inorganic nitrogen.....	18
1.3.2.1	Stoichiometric controls of in-stream inorganic nitrogen concentrations .....	18
1.3.2.2	Hydraulic controls on nutrient retention .....	21
1.3.2.3	Biotic controls on nutrient retention .....	25
<b>2</b>	<b>OBJECTIVES .....</b>	<b>30</b>
<b>3</b>	<b>STUDY AREA.....</b>	<b>32</b>
<b>4</b>	<b>FIELD METHODS.....</b>	<b>38</b>
4.1	24-HOUR IN-STREAM ENVIRONMENTAL DATA .....	38
4.2	CONTINUOUS NUTRIENT ADDITION EXPERIMENTS .....	39
4.3	SURFACE WATER LONGITUDINAL SURVEY .....	43
<b>5</b>	<b>LAB METHODS.....</b>	<b>44</b>
<b>6</b>	<b>STATISTICAL ANALYSIS .....</b>	<b>46</b>
<b>7</b>	<b>RESULTS .....</b>	<b>49</b>
7.1	HYDROLOGY .....	49
7.2	CONSERVATIVE SOLUTES & TRACERS .....	51
7.3	ECOSYSTEM METABOLISM.....	53
7.4	DISSOLVED ORGANIC MATTER .....	56
7.5	DISSOLVED INORGANIC NUTRIENTS.....	58
<b>8</b>	<b>DISCUSSION .....</b>	<b>62</b>

8.1	CATCHMENT INPUTS TO THE STREAM .....	62
8.1.1	Groundwater hydrologic inputs .....	63
8.1.2	Groundwater nutrient inputs .....	64
8.1.3	Catchment-wide organic inputs .....	65
8.2	HOT MOMENTS OF IN-STREAM PROCESSES .....	69
8.2.1	Nutrient export in the growing season .....	69
8.2.2	Fall nutrient retention.....	70
8.2.3	Biogeochemical cycling during drought.....	71
<b>9</b>	<b>CONCLUSION .....</b>	<b>73</b>

**APPENDIX A: LONGITUDINAL GRAPHS**

**APPENDIX B: DOWNSTREAM CONCENTRATION CHANGES WITH DISTANCE**

**APPENDIX C: MULTI-WAY PAIR-WISE ANALYSES**

**APPENDIX D: SINGLE-VARIABLE REGRESSION ANALYSES**

**APPENDIX E: DAILY VARIATIONS IN TEMPERATURE, DO, AND NEM**

**APPENDIX F: IN-STREAM AND SOURCE CONCENTRATIONS**

**APPENDIX G: SINGLE STATION METHOD FOR DETERMINING NEM**

**APPENDIX H: CONSTRAINT-RATE NUTRIENT INJECTION CALCULATIONS**

**APPENDIX I: EXAMPLE CALCULATIONS FOR AMMONIUM UPTAKE**

**APPENDIX J: CARBON AND AMMONIUM UPTAKE VALUES**

**APPENDIX K: MATLAB CODE**

K.1	NEM: FEBRUARY 2012, UPSTREAM
K.2	NEM: FEBRUARY 2012, DOWNSTREAM
K.3	NEM: APRIL 2011, UPSTREAM
K.4	NEM: APRIL 2011, DOWNSTREAM
K.5	NEM: JUNE 2011, UPSTREAM
K.6	NEM: JUNE 2011, DOWNSTREAM
K.7	NEM: AUGUST 2011, UPSTREAM
K.8	NEM: AUGUST 2011, DOWNSTREAM
K.9	NEM: SEPTEMBER 2010, UPSTREAM

- K.10 NEM: SEPTEMBER 2010, DOWNSTREAM
- K.11 NEM: NOVEMBER 2010, UPSTREAM
- K.12 NEM: NOVEMBER 2010, DOWNSTREAM
- K.13 MULTI-VARIABLE STATISTICAL ANALYSIS
- K.14 LINEAR REGRESSION, 1 VARIABLE
- K.15 MULTIPLE LINEAR REGRESSION, 2 VARIABLES
- K.16 MULTIPLE LINEAR REGRESSION, 3 VARIABLES
- K.17 MULTIPLE LINEAR REGRESSION, 4 VARIABLES
- K.18 LONGITUDINAL ANALYTE PLOTS

## **CITATIONS**

## FIGURES

Figure 1. Typical yearly cycle of in-stream nitrate concentrations in lotic systems dominated by watershed nitrogen retention in the growing season. ....	14
Figure 2. Typical yearly pattern of in-stream nitrate concentrations in lotic systems dominated by in-stream nitrogen retention in the spring and fall. ....	29
Figure 3. Fair Hill Natural Resource Management Area topographic map. ....	33
Figure 4. Fair Hill Natural Resource Management Area aerial imagery. ....	34
Figure 5. 15 minute discharge at Fair Hill, measured via a Parshall flume at the upstream sampling site. ....	36
Figure 6. Typical results from a well-mixed nutrient injection experiment. ....	42
Figure 7. Seasonal variations in discharge. ....	49
Figure 8. Palmer Hydrological Drought Index (PHDI) in the Northern Central Climate Division 6 of Maryland. ....	50
Figure 9. Seasonal variations in $\delta^{18}\text{O}$ . ....	51
Figure 10. Longitudinal variations in $\delta^{18}\text{O}$ . ....	53
Figure 11. Longitudinal variations in chloride. ....	53
Figure 12. Seasonal variations in average daily temperature (A), pH (B), net ecosystem metabolism (NEM) (C), and gross primary production (GPP) (D). ....	54
Figure 13. Longitudinal variations in DOC concentrations. ....	57
Figure 14. Seasonal variations in nitrate concentrations. ....	60
Figure 15: Seasonal variations in ammonium concentrations. ....	61
Figure 16: Seasonal variations in phosphate concentrations. ....	61



## TABLES

Table 1. Baseflow contributions to discharge, total nitrogen, and nitrate export in and near the Chesapeake Bay watershed (CBW). .....	3
Table 2. Disturbances that increase watershed nitrate export in and near the Chesapeake Bay watershed. ....	4
Table 3. Percentage of atmospheric nitrogen deposition by nitrogen species in and near the Chesapeake Bay watershed. ....	7
Table 4. Watershed retention of atmospheric nitrogen in and near the Chesapeake Bay watershed (CBW). ....	9
Table 5. Percentage of atmospheric contributions to in-stream nitrogen export in and near the Chesapeake Bay watershed. ....	12
Table 6: Riparian uptake of nitrate due to shallow groundwater within the Chesapeake Bay watershed. ....	13
Table 7: Watersheds in and near the Chesapeake Bay region that experience peak nitrate export during the winter similar to Figure 1. ....	15
Table 8. Lotic redox equations. ....	19
Table 9. Percentage of in-stream nitrate uptake that occurs in the hyporheic zone. ....	22
Table 10. In-stream geomorphic features that increase nitrogen uptake and/or decrease nitrogen concentrations/fluxes. ....	23
Table 11. Percent contribution of ammonium uptake via assimilation to total in-stream ammonium uptake. ....	26
Table 12. Percent contribution of biologically available DOC to total in-stream DOC. ....	27
Table 13: Watersheds in and near the Chesapeake Bay region that experience bi-modal peak nitrate export during the summer and winter. ....	29
Table 14. Stream discharge, width, and depth at the sampling locations. ....	37
Table 15. Sampling dates at Fair Hill. ....	38
Table 16. Continuous flow injection set-up including solute concentrations and pump rates. ....	40
Table 17. Station distance from injection site: Upstream experimental site. ....	42
Table 18. Station distance from injection site: Downstream experimental site. ....	42
Table 19. Annual amplitudes of $\delta^{18}\text{O}$ in precipitation and baseflow in Chesapeake Bay region	

watersheds.....	52
Table 20. Ecosystem metabolism at the upstream and downstream experimental sites measured over a 24 hr. period. ....	55
Table 21. Percent contribution of DON to TDN.....	57
Table 22. Percent contribution of BDOC to DOC.....	58
Table 23. In-stream nutrient concentrations of select basins near Fair Hill.....	65

## COMMONLY USED ACRONYMNS

**BDOC:** Biologically available dissolved organic carbon.

**CBW:** Chesapeake Bay watershed.

**DIC:** Dissolved inorganic carbon.

**DO:** Dissolved oxygen.

**DOC:** Dissolved organic carbon.

**DOM:** Dissolved organic matter.

**DON:** Dissolved organic nitrogen.

**GPP:** Gross primary production.

**ILTER:** Long term ecological research site.

**MDL:** Method detection limit.

**NEM:** Net ecosystem metabolism.

**P/R:** Gross primary production/Respiration.

**POC:** Particulate organic carbon.

**R:** Respiration.

**RDOC:** Refractory dissolved organic carbon.

**STP:** Standard temperature and pressure.

**TDN:** Total dissolved nitrogen.

**WS:** Watershed.

# 1 LITERATURE REVIEW

## 1.1 INTRODUCTION

Worldwide increases in anthropogenic nitrogen have dramatically altered the global nitrogen cycle (Galloway et al., 2003), contributing to eutrophication in coastal bodies across the globe (Vitousek et al., 1997). In the Chesapeake Bay watershed, nitrogen cycling was stable prior to European settlement (Brush, 2009), but modern-day increases in nitrogen inputs have led to Bay-wide degradation through the expansion of eutrophication and oxygen-starving “dead zones” (Brush, 2009; Hagy et al., 2004). These disruptions to the nitrogen cycle can be attenuated far away from the Chesapeake Bay in headwater catchments where reactive nitrogen is retained and converted to more stable forms, ultimately through denitrification to N<sub>2</sub> gas (Alexander et al., 2007; Mulholland et al., 2008; Peterson et al., 2001).

This study thus focuses on nutrient export during baseflow from a headwater forested stream, examining the roles of both catchment-wide and in-stream processes directly related to the study’s location within the Chesapeake Bay watershed. Throughout the region, baseflow is particularly influential, accounting for the majority of total discharge and total nitrogen export from headwater streams (Table 1). Accordingly, nitrate exports from Piedmont streams typically increase with groundwater discharge (Jordan et al., 1997b). Headwater streams likewise play a critical role in regulating downstream water quality. Typically, headwater streams are the predominant source of nutrients to downstream water bodies, such as in the northeast where they provide 45% of total nitrogen and 60% of discharge to downstream basins (Alexander et al., 2007). Accounting for more than 70% of all channel length in the US, headwater streams also provide perhaps the greatest biogeochemical link between terrestrial and aquatic ecosystems (Lowe and Likens, 2005; Meyer et al., 2003). For instance, headwater streams have been shown to facilitate groundwater-surface

water interactions (Bernot and Dodds, 2005; Thomas et al., 2001) promoting “hot-spots” of biogeochemical transformations (Groffman et al., 2009; McClain et al., 2003; Vidon et al., 2010) while retaining total nitrogen (Alexander et al., 2007; Alexander et al., 2000; Bernot and Dodds, 2005), ammonium (Peterson et al., 2001), and nitrate (Mulholland et al., 2008). Lastly, forested watersheds are particularly important to nutrient processing in the Chesapeake Bay region. While forested watersheds provide up to 15% of the nitrogen load to the Chesapeake Bay (Sprague et al., 2006), because forests are so widespread and store so much nitrogen (Galloway et al., 2003), nitrogen exports from forested catchments react non-linearly to catchment-wide disturbances (Pan et al., 2004; Sprague et al., 2006). For example, nitrogen inputs to the Chesapeake Bay only started increasing in the mid-seventeenth century after 40% of the watershed was deforested (Brush, 2009). Similar responses to disturbance at the catchment-scale are also ubiquitous throughout the Chesapeake region (Table 2). Therefore, nutrient export from watersheds within the Chesapeake Bay region reflect the net influence of both catchment-wide and in-stream processes.

**Table 1. Baseflow contributions to discharge, total nitrogen, and nitrate export in and near the Chesapeake Bay watershed (CBW).**

<b>State</b>	<b>Location/Basin</b>	<b>Baseflow contribution to total discharge (baseflow index)</b>	<b>% of total nitrogen exported via baseflow</b>	<b>% of nitrate exported via baseflow</b>	<b>Reference</b>
	Atlantic Coastal Plain	-	16%	23%	(Ator and Denver, 2012)
	CBW – non-tidal streams	54%	-	48%	(Bachman et al., 1998)
	CBW – Ridge & Valley, Blue Ridge, Piedmont	67%	-	-	(Rutledge and Mesko, 1996)
	CBW – Piedmont	57%	-	80%	(Bachman et al., 1998)
	CBW – Piedmont	54-86%	-	-	(Jordan et al., 1997b)
	CBW – Coastal Plain	55%	-	-	(Sinnott and Cushing, 1978)
<b>MD</b>	Beaverdam Creek	74%	-	-	(Olmsted and Hely, 1962)
	Big Elk Creek	63%	-	-	(Sloto, 2002)
	Fair Hill	24-47%	-	-	(Dhillon and Inamdar, 2013)
	USDA-Beltsville	~50%	-	~50%	(Angier et al., 2001; Angier and McCarty, 2008; Angier et al., 2005)
<b>NJ</b>	North Branch Rancocas Creek	64%	-	-	(Olmsted and Hely, 1962)
<b>PA</b>	Brandywine Creek	67%	-	-	(Olmsted and Hely, 1962)
	WE-38 – Mahantango Creek	56%	-	56%	(Pionke et al., 1999)
	FD-36 – Mahantango Creek	64%	65%	75%	(Zhu et al., 2011)
<b>VA</b>	Paine Run	65%	45%	46%	(Buffam et al., 2001)
	Polecat Creek	52%	-	-	(Speiran, 2003)

**Table 2. Disturbances that increase watershed nitrate export in and near the Chesapeake Bay watershed.**

<b>Disturbance</b>	<b>State</b>	<b>Location/Basin</b>	<b>Reference</b>
<b>Fire</b>	PA	Jews Run and others	(Lynch and Corbett, 1994)
	MD	Big Run Black Lick	(Eshleman et al., 2008)
<b>Insect defoliation</b>	MD	Big Run	(Eshleman et al., 1998)
	VA	Many	
	PA	West Fork Run East Fork Run	(Lewis and Likens, 2007)
	PA	Buchanan State Forest	(Lynch and Corbett, 1994)
	VA	Many	(Eshleman et al., 2000)
	VA	Many	(Riscassi and Scanlon, 2009)
	VA	Paine Run	(Scanlon et al., 2010)
	VA	White Oak Run	(Webb et al., 1995)
<b>Clear-cut logging</b>	NY	Neversink River	(Burns and Murdoch, 2005; McHale et al., 2007)
	PA	Leading Ridge	(Lynch and Corbett, 1990, 1991, 1994; Lynch et al., 1985)
	WV	WS 3 – Fernow	(Aubertin and Patric, 1974)
	VA	Nomini Creek	(Wynn et al., 2000)
<b>Partial harvesting</b>	NY	Neversink River	(Wang et al., 2006)
	PA	Baldwin Creek	(Herrmann et al., 2001)

## 1.2 WATERSHED NITROGEN RETENTION & EXPORT

Regarding watershed biogeochemistry, nitrogen-containing molecules and chemicals within a catchment are typically classified as inert (i.e. N<sub>2</sub> gas) or reactive. Reactive nitrogen consists of particulate and dissolved species that can be used for biotic growth and metabolism. The sum of all dissolved reactive nitrogen species is called “total dissolved nitrogen,” consisting of dissolved organic nitrogen – as a constituent of dissolved organic matter - and dissolved inorganic nitrogen – nitrate (NO<sub>3</sub><sup>-</sup>), nitrite (NO<sub>2</sub><sup>-</sup>), and ammonium (NH<sub>4</sub><sup>+</sup>). Total dissolved nitrogen and its constituents are thus examined at the catchment-level in order to illustrate their paths and processes from source to catchment to stream, ultimately setting the foundation for in-stream biogeochemistry.

### ***1.2.1 Sources of reactive nitrogen to watersheds***

Reactive nitrogen can be imported into watersheds through atmospheric deposition, import of food and feed, application of fertilizer, and biological fixation (Fisher and Oppenheimer, 1991; Galloway et al., 2003; Howarth et al., 1996). Atmospheric deposition and nitrogen fixation are typically the predominant sources of nitrogen to forested watersheds (Galloway et al., 2003; Howarth et al., 1996), but fixation is usually negligible in older forests (Boring et al., 1988; Galloway et al., 2003). Deposition therefore has been shown to be the largest contributor of reactive nitrogen to undisturbed, stable forests (Alexander et al., 2007; Fisher and Oppenheimer, 1991; Howarth et al., 1996). This is particularly true in northeast river basins, where nitrogen deposition is among the highest in the country (Holland et al., 2005; Peterjohn et al., 1996).

Nitrogen deposition encompasses all species of reactive nitrogen including nitrate, ammonium, and organic nitrogen - each originating from a variety of natural and anthropogenic sources. Atmospheric ammonium originates from fossil fuel combustion, fertilizer, animal excreta, and the breakdown of organic matter in soil (Howarth et al., 1996; Prospero et al., 1996; Scudlark et al., 2005). In the Chesapeake Bay region, agricultural activities and soil emissions to the west and southwest are the predominant sources for ammonium deposition (Russell et al., 1998). Atmospheric nitrate is derived naturally and anthropogenically from many sources including fossil fuel combustion, soil emissions and lightning (Galloway et al., 2003; Prospero et al., 1996; Vitousek et al., 1997). Nitrate deposition in the Chesapeake Bay region primarily originates from fossil fuel combustion to the west and northwest, such as from the Ohio River Valley (Russell et al., 1998). Of the two, nitrate deposition typically exceeds ammonium in the Chesapeake Bay region (Table 3). Lastly, atmospheric organic nitrogen originates from marine and terrestrial organic molecules, particulates from dust, and pollen (Cornell et al., 2003; Neff et al.,



2002). However, only about half of organic nitrogen deposition can be traced molecularly because it is a component of a complex suite of organic matter (Altieri et al., 2009; Cornell et al., 2003; Neff et al., 2002). In the Chesapeake Bay watershed, organic nitrogen accounts for about one third of nitrogen deposition (Table 3).

**Table 3. Percentage of atmospheric nitrogen deposition by nitrogen species in and near the Chesapeake Bay watershed.**

	Basin	% ON	% NO <sub>3</sub> <sup>-</sup>	% NH <sub>4</sub> <sup>+</sup>	% Inorganic nitrogen	Reference
<b>Meta-Analysis</b>	Global	34	-	-	66	(Neff et al., 2002)
	Global	29	-	-	71	(Cornell, 2011)
	N. America	38	-	-	62	(Cornell et al., 2003)
	N. America	35	-	-	75	(Cornell, 2011)
	Northeast USA	50	35	15	50	(Prospero et al., 1996)
<b>NY</b>	Catskills	1	72	26	99	(Lawrence et al., 2000)
	Ithaca	11	59	30	89	(Butler and Likens, 1995)
<b>NJ</b>	Camden	25	35	39	75	(Altieri et al., 2009)
<b>DE</b>	Lewes	15	-	-	85	(Russell et al., 1998)
	Lewes	2	47	51	98	(Russell et al., 1998)
	Lewes	21	48	31	79	(Scudlark et al., 1998)
	Newark	8	-	-	92	(Keene et al., 2002)
<b>PA</b>	Philadelphia	19-52	-	-	48-81	(Seitzinger and Sanders, 1999)
<b>MD</b>	Rhodes	15-35	41-54	24-32	65-85	(Jordan et al., 1995)
	Rhodes	29	45	26	71	(Correll and Weller, 1997)
<b>VA</b>	Charlottesville	6	-	-	94	(Keene et al., 2002)

### ***1.2.2 Input-output models of watershed nitrogen retention***

Deposited nitrogen can be stored on the landscape, assimilated by biota, lost to denitrification, exported via in-stream transport, or lost to anthropogenic export such as harvesting (Galloway et al., 2003; Jaworski et al., 1992; Prospero et al., 1996). “Nitrogen retention” is the percent of nitrogen deposition within a catchment that is not exported via surface water  $[(\text{input}-\text{output})/\text{input}]$ , typically calculated on an annual basis (Nadelhoffer et al., 1999). Nitrogen retention values in watersheds within the Chesapeake Bay region range from 24% to over 100%, with values typically around 75% (Table 4). Watershed nitrogen retention varies among physiographic provinces, watersheds and even inter-annually within the same watershed. In general, nitrogen retention is positively correlated with percent forest cover and negatively correlated with percent agricultural (Correll and Weller, 1997; Zheng et al., 2008) or urban land-use (Groffman et al., 2004; Shields et al., 2008).

**Table 4. Watershed retention of atmospheric nitrogen in and near the Chesapeake Bay watershed (CBW).**

	<b>Basin</b>	<b>N Deposition Kg/ha/yr</b>	<b>N Export Kg/ha/yr</b>	<b>N Retention Kg/ha/yr</b>	<b>% N Retained</b>	<b>Reference</b>
<b>Meta-analysis</b>	Global	-	-	-	70	(Curtis et al., 2011)
	Northeast USA	6.4	2	4.4	69	(Campbell et al., 2004)
	CBW - forested Land	14.3	2.9	11.4	80	(Fisher and Oppenheimer, 1991)
	CBW - forested Land	10	0.6	9.4	94	(Sheeder et al., 2002)
	CBW - forested Land	10	1.2	8.8	88	(Pan et al., 2004)
<b>NY</b>	Ithaca	8.3	0.9	7.4	90	(Goodale et al., 2009)
	Catskills	15	2.1	12.9	85	(Lawrence et al., 2000)
	Catskills	12.2	3.9	8.3	68	(Lovett et al., 2000)
	Catskills	7.4	4.1	3.3	45	(Campbell et al., 2004)
<b>PA</b>	York County	14	8.6	5.4	39	(Jordan et al., 1997a)
	Leading Ridge	7.2	0.12	7.1	99	(Williard et al., 1997)
	Southwest PA	12.1	3	9.1	75	(DeWalle and Pionke, 1994; Dow and DeWalle, 1997)
	Southwest PA	9.7	2.8	6.9	71	(DeWalle et al., 2005)
	North-central PA	11.9	1.4	10.5	88	(DeWalle and Pionke, 1994; Dow and DeWalle, 1997)
	North-central PA	7.9	1	6.9	87	(DeWalle et al., 2005)
<b>MD</b>	Rhode River - WS 110	12.7	2	10.7	84	(Correll and Weller, 1997)
	Rhode River - WS 110	12.7	1	11.7	92	(Correll et al., 1999; Correll and Weller, 1997)
	Rhode River	12.7	2.8	9.9	78	(Correll et al., 1999; Correll and Weller, 1997)
	Baltimore County	14	4.8	9.2	66	(Jordan et al., 1997a)
	Pond Branch	11.2	0.52	10.7	95	(Groffman et al., 2004)
	Upper Potomac	13.3	8.3	5	38	(Jaworski et al., 1992)
	Western MD	6.9	4.1	2.8	41	(DeWalle and Pionke, 1994; Williard et al., 1997)

	Basin	N Deposition Kg/ha/yr	N Export Kg/ha/yr	N Retention Kg/ha/yr	% N Retained	Reference
<b>MD (Cont.)</b>	Western MD	6.7	1.7	5	75	(Castro and Morgan II, 2000)
	Western MD	6.8	2.3	4.5	66	(Campbell et al., 2004)
	Western MD	6.6	9.5	0	143	(Castro et al., 2007)
<b>WV</b>	Fernow - WS 4	7.5	5.7	1.8	24	(Campbell et al., 2004)
	Fernow - WS 10	7.5	1.1	6.4	85	(Campbell et al., 2004)
	Fernow - WS 13	7.5	4.2	3.3	44	(Campbell et al., 2004)
	Fernow - WS 3 pretreatment*	9	3.1	5.9	65	(Adams et al., 2006)
	Fernow - WS 3 during treatment*	44.5	4.5	40	90	(Adams et al., 2006)
	Fernow - WS 4	9	5	4	45	(Adams et al., 2006)
	Little Laurel Run	13.8	7.4	6.4	46	(Rentch and Hicks, 1999)
<b>VA</b>	Shenandoah Nat'l Park	9.3	0.13	9.2	99	(Cosby et al., 1991)

\*After 1989 WS 3 experienced yearly catchment fertilization with ammonium sulfate (Adams et al., 2006)

Using historical observations of watershed retention, many watershed nitrogen input-output models attempt to predict nitrogen export based on deposition, but these models tend to oversimplify the systems they represent. Some speculate that export increases linearly with deposition (Howarth et al., 1996), but meta-analyses find that deposition explains less than a third of the variance in watershed nitrate export (Grigal, 2012; Pellerin et al., 2006). Others hypothesize a “nitrogen saturation” model whereby forested watersheds retain deposited nitrogen up to a certain threshold above which excess deposition is simply exported (Aber et al., 1998; Aber et al., 2003; Peterjohn et al., 1996). In other words, when deposition is below the saturation threshold, nitrogen export is a function of watershed retention; when nitrogen deposition exceeds the saturation threshold though, export simply increases co-linearly with deposition. Empirical studies, however, find that few forested watersheds adhere to this saturation model (Castro et al., 2007; Peterjohn et al., 1996). Likewise, meta-analyses fail to identify a saturation threshold, or a rate of deposition above which the capacity of a watershed to retain deposition is exhausted (Campbell et al., 2004), though some have found that nitrogen exports markedly increase when deposition exceeds 10 kg N/ha/yr (Aber et al., 2003; Grigal, 2012). These input-output models break down, therefore, due to the assumption that nitrogen export is simply the difference between deposition and retention, failing to account for other inputs and outputs, differing timescales of storage within the landscape, and biogeochemical transformations (Bernhardt et al., 2005; Hill, 1996). For example, even though watershed retention is typically measured annually, groundwater nitrogen exports in the Chesapeake Bay region can lag behind deposition from six months (Burns et al., 1998) to several decades (Böhlke and Denver, 1995; Lindsey et al., 2003). Therefore, a more robust, mechanistic hydrological/biogeochemical understanding is required to fully explain and predict nitrogen export from headwater catchments (Hill, 1996; Mitchell, 2001).

### ***1.2.3 Watershed nitrogen flushing***

Further questioning the utility of watershed-scale nitrogen input-output models, isotopic analyses from within the Chesapeake Bay region (Table 5) to around the world (Curtis et al., 2011; Nestler et al., 2011) show that over 80% of in-stream nitrate can be derived from nitrification within the landscape, while less than a fifth can be attributed directly to atmospheric deposition. Thus, it is not surprising that in response to catchment-wide ammonium fertilization experiments simulating increased deposition, some have observed that in-stream nitrate concentrations spike while ammonium concentrations remain relatively constant [e.g. (Adams et al., 2006; Peterjohn et al., 1996)]. In other words, as opposed to input-out analyses that assume that nitrate export is simply deposition that is not retained, landscape-wide processes play a critical role in managing watershed nitrogen export.

**Table 5. Percentage of atmospheric contributions to in-stream nitrogen export in and near the Chesapeake Bay watershed.**

<b>Basin</b>	<b>% of N atmospherically derived</b>	<b>% of N derived from soil</b>	<b>Reference</b>
PA & WV	5	95	(Williard et al., 2001)
Catskills, NY	8	92	(Burns and Kendall, 2002)
Ithaca, NY	8	95	(Goodale et al., 2009)
PA & WV (stormflow)	3-17	83-97	(Williard et al., 2001)
PA (stormflow)	33	67	(Buda and DeWalle, 2009)
Ithaca, NY (snowmelt)	45	55	(Goodale et al., 2009)

Wishing to gain deeper insight to the link between landscape processes and nitrogen export, hill-slope trenching experiments were used to observe that after logging, ammonium first accumulates in the soil, followed by increases in nitrate, followed by nitrate export (Vitousek et al., 1979). These observations led to a three-step mechanistic model: (1) organic matter mineralization, (2) in-ground nitrification, and (3) hydrologic nitrate export. Each step is limited by several factors: (1) mineralization by nitrogen-richness of organic inputs; (2) nitrification by

temperature, ammonium and oxygen; and (3) nitrate export by hydrologic transport (Vitousek et al., 1979). In fact, this three-step biogeochemical sequence scales-up, observed in disturbed watersheds where in-stream ammonium concentrations peak before nitrate (Aubertin and Patric, 1974; Lewis and Likens, 2007; Wang et al., 2006). In this model of nitrogen export, hydrology is not just an export mechanism, it is also a controlling biogeochemical factor (Cirimo and McDonnell, 1997; Manzoni and Porporato, 2011; McClain et al., 2003). Where water is transported below-ground close to the surface, nitrate retention increases due to increased residence times, suboxic environments, organic matter, and proximity to rooting depth (Hill, 1996; Lowrance et al., 1997; Vidon and Hill, 2004). This process is commonly associated with, but not limited to, nitrate retention in shallow groundwater by terrestrial uptake in riparian zones (Table 6). Given these complex hydro-biogeochemical controls on nitrogen export, it is not surprising that others propose similar mechanistic models to predict nitrogen export from small watersheds in lieu of input-output models (Jordan et al., 1997b; Nestler et al., 2011).

**Table 6: Riparian uptake of nitrate due to shallow groundwater within the Chesapeake Bay watershed.**

Physiographic province	State	Basin/Location	Reference
-	-	Chesapeake Bay watershed	(Lowrance et al., 1997)
<b>Coastal Plain</b>	MD	Rhode River	(Peterjohn and Correll, 1984)
	MD	Chester River	(Jordan et al., 1993)
	MD	Morgan Creek	(Böhlke and Denver, 1995)
	MD	Choptank River	(Correll et al., 1997)
	VA	Nomini Creek	(Snyder et al., 1998)
	VA	Magothy Bay	(Speiran, 2010)
<b>Piedmont</b>	PA	White Clay Creek	(Sweeney, 1992)
	PA	Brandywine Creek	(Newbold et al., 2010)



Given that landscape processes therefore directly affect in-stream nitrogen concentrations, the impact of temporal variations in catchment processes can be seen in temporal shifts in water quality. Indeed, landscape-wide terrestrial nitrogen uptake during the growing season has been observed to decrease nitrate export from catchments, decreasing in-stream nitrate concentrations; conversely, the lack of landscape-wide retention due to plant inactivity in the dormant season has been observed to increase export, increasing in-stream concentrations (Peterjohn et al., 1996). This cyclical seasonality of in-stream nitrate concentrations reflecting terrestrial processes (Figure 1) is ubiquitous across biomes (Goodale et al., 2009), and it clearly occurs in and near the Chesapeake Bay region (Table 7). Thus, in streams that experience peak nitrate concentrations in the winter and lowest concentrations in the summer, it is likely that landscape-wide nutrient retention and export play a predominant role in controlling in-stream nitrogen concentrations.

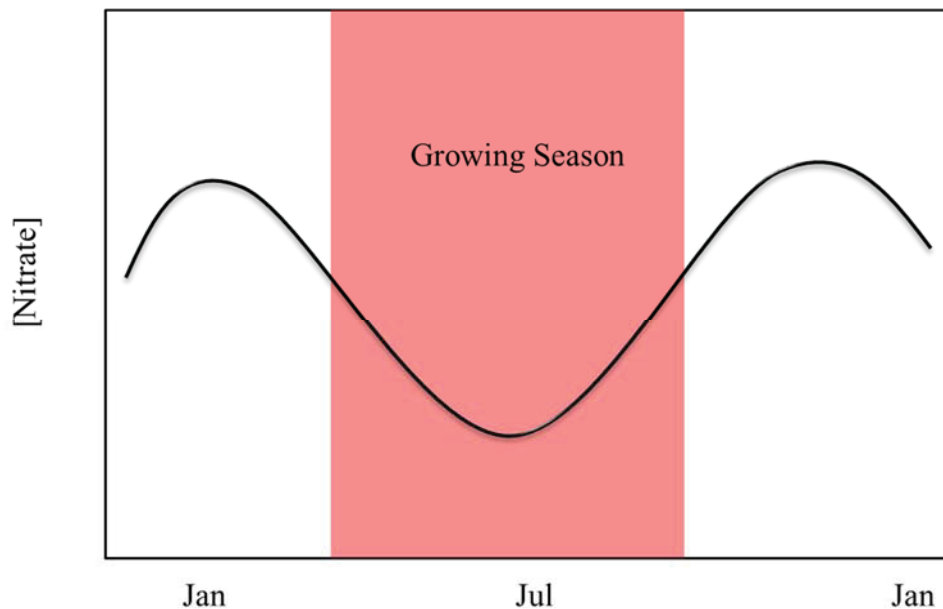


**Figure 1. Typical yearly cycle of in-stream nitrate concentrations in lotic systems dominated by watershed nitrogen retention in the growing season.**

**Table 7: Watersheds in and near the Chesapeake Bay region that experience peak nitrate export during the winter similar to Figure 1.**

<b>Physiographic province</b>	<b>State</b>	<b>Basin/Location</b>	<b>Reference</b>
<b>Allegheny Plateau</b>	MD	East Branch of Neff Run	(Castro et al., 2007)
	MD	Herrington Creek	(Castro and Morgan II, 2000)
	MD	Big Run Black Lick	(Eshleman et al., 2008)
	PA	Many	(Dow and DeWalle, 1997)
<b>Catskills</b>	NY	Many	(Lovett et al., 2000)
	NY	Neversink River	(Burns, 1998)
<b>Coastal Plain</b>	MD	USDA-Beltsville	(Angier et al., 2001; Angier and McCarty, 2008)
	MD	Rhode River	(Correll et al., 1999; Correll and Weller, 1997)
	VA	Nomini Creek	(Snyder et al., 1998)
<b>Piedmont</b>	PA	Upper Potomac River	(Jaworski et al., 1992)
	MD		
<b>Ridge and Valley</b>	PA	WE-38 – Mahantango Creek	(Pionke et al., 1999)
	PA	FD-36 – Mahantango Creek	(Zhu et al., 2011)
	WV	WS-4 – Fernow	(Peterjohn et al., 1996)
	WV	Little Laurel Run	(Rentch and Hicks, 1999)

## 1.3 IN-STREAM NITROGEN RETENTION AND EXPORT

While significant portions of nitrogen imported in to watersheds can be retained throughout the landscape, in-stream nitrogen retention often plays an overlooked role in controlling nitrogen export. In-stream dissolved nitrogen can be either organic or inorganic, which are both created, transformed, retained and exported throughout lotic systems. In-stream processing of organic nitrogen, as a component of organic matter, is dependent on inter-related organic matter and inorganic nitrogen dynamics. In-stream processing of inorganic nitrogen is fundamentally controlled by stoichiometry and thermodynamics, though in-stream hydraulics and biotic metabolism play a critical role in facilitating inorganic nitrogen uptake.

### *1.3.1 In-stream dissolved organic nitrogen*

In-stream dissolved organic nitrogen (DON) results from organic matter inputs to lotic systems and in-stream processes that retain or transform organic matter (e.g. respiration and mineralization) – which are driven by both organic matter and inorganic nutrient dynamics.

Dissolved organic nitrogen (DON) is nitrogen-containing, carbon-based dissolved organic matter (DOM) consisting of a complex suite of free and combined amino acids, proteins, nucleic acids, amino sugars, and humic substances (Berman and Bronk, 2003). DON is calculated by subtraction (1), compounding the uncertainties in measurements of total dissolved nitrogen (TDN), nitrate-nitrite ( $\text{NO}_3^-$ ), and ammonium ( $\text{NH}_4^+$ ) (Berman and Bronk, 2003; Martin and Harrison, 2011; Pellerin et al., 2006).

$$DON = TDN - NO_3^- - NH_4^+ \quad (1)$$

Due to the difficulties in measuring DON, organic matter nitrogen content is often analyzed with carbon to nitrogen ratios (DOC:DON), where higher ratios indicate more carbon-rich, recalcitrant DOM (Bernal et al., 2005; Kaushal and Lewis, 2005; Petrone et al., 2009; Wiegner et al., 2006).

This nitrogen-containing organic matter originates from either autochthonous (in-stream) or allochthonous (landscape) sources such as leaf fall, soil matter, micro-organisms and excrement (Berman and Bronk, 2003). Assimilation of inorganic nitrogen also contributes to in-stream DOM and hence DON (Scott et al., 2007). Groundwater, however, is not a significant source of organic matter, as DOC and DON concentrations typically dilute with baseflow (Bernal et al., 2005; Jordan et al., 1997b). At the basin scale, DON concentrations typically increase with stream order due to an increased influence of photosynthesis (Scott et al., 2007). Similarly, compared to forested streams, DON concentrations are also generally higher in agricultural streams also due to a lack of shading (Jordan et al., 1997a; Pellerin et al., 2006; Willett et al., 2004).

Though historically considered recalcitrant (Thurman, 1985), recent studies show that 5-70% of DON can be bio-available (Kaushal and Lewis, 2005; Petrone et al., 2009; Wiegner et al., 2006). However, in-stream DON uptake is affected by numerous factors, such as phosphorus availability (Johnson and Tank, 2009) and complex carbon-nitrogen dynamics (Lutz et al., 2011). For instance, concentrations of DOC and DON can co-vary, causing static DOC:DON ratios (Brookshire et al., 2007; Campbell et al., 2000; Inamdar and Mitchell, 2007), DIN and DON concentrations can be inversely related (Lovett et al., 2000; Lutz et al., 2011; Willett et al., 2004), or DON and nitrate concentrations can co-vary, causing an inverse relationship between DOC:DON ratios and nitrate concentrations (Brookshire et al., 2007). Overall, DON uptake tends to be energetically advantageous because an energy source (carbon) is provided concurrently with nitrogen (Lutz et al., 2011; Petrone et al., 2009; Wiegner et al., 2006). As such, DON uptake typically is proportionally greater than DOC uptake (Kaushal and Lewis, 2005; Petrone et al., 2009; Wiegner et al., 2006). Given the variability among dissolved organic matter sources, the uncertainty in measuring DON, and the complex in-stream biotic nitrogen demands, a complete mechanistic

model for predicting in-stream DON dynamics is still considered incomplete (Berman and Bronk, 2003; Lutz et al., 2011).

### ***1.3.2 In-stream dissolved inorganic nitrogen***

In-stream dissolved inorganic nitrogen encompasses both oxidized ( $\text{NO}_x$ ) and reduced ( $\text{NH}_x$ ) forms of nitrogen (Galloway et al., 2003). However, in-stream concentrations of nitrate ( $\text{NO}_3^-$ ) often exceed concentrations of nitrite ( $\text{NO}_2^-$ ) by an order of magnitude or more (Morgan II and Kline, 2011) leading many to simply report dissolved inorganic nitrogen as the sum of nitrate and ammonium [e.g. (Liu et al., 2000)]. In-stream concentrations of these dissolved inorganic nitrogen species result from the complex interactions of inputs, transformations and uptake in lotic environments. These biogeochemical processes are underlain and controlled by stoichiometry and thermodynamics. In-turn, in-stream hydraulics drive nitrogen processing by transporting reactants through micro-environments of differing redox states. Lastly, the biologic processes responsible for retaining nitrogen can ultimately be attributed to either in-stream autotrophic or heterotrophic uptake.

#### *1.3.2.1 Stoichiometric controls of in-stream inorganic nitrogen concentrations*

In-stream biogeochemical processing of inorganic nitrogen is often controlled by thermodynamics and stoichiometry through terminal electron accepting processes (TEAPs) which typically occur in the order of greatest energy yield.<sup>1</sup> Of the various electron donors, oxidation of

---

<sup>1</sup> For field studies see: (Baker et al., 1999; Battin et al., 2003; Butturini et al., 2000; Hedin et al., 1998; Hill et al., 1998a; Jones Jr. et al., 1995; Morrice et al., 2000; Sobczak and Findlay, 2002; Sobczak et al., 2003; Strauss and Lamberti, 2000; Strauss et al., 2002; Tiedje et al., 1983; Triska et al., 1993; Valett et al., 1994; Zarnetske et al., 2011).

For reviews see: (Boulton et al., 1998; Brunke and Gonser, 1997; Burgin and Hamilton, 2007; Dahm et al., 1998; Findlay, 1995; Jones Jr. et al., 1985; Krause et al., 2011; Manzoni and Porporato, 2011; Sophocleous, 2002; Storey et al., 1999; Thomas et al., 2001; Trimmer et al., 2012; Williams, 1993)

carbon-based organic matter produces the highest energy yield through aerobic respiration and anaerobic denitrification (Table 8). In particular, dissolved organic matter (DOM), operationally defined as organic matter smaller than 0.45 micrometers, typically makes up the majority of carbon supply in headwater streams (Fisher and Likens, 1973; Thurman, 1985). As such, the carbon measured in DOM is simply known as “dissolved organic carbon” (DOC) (Fisher and Likens, 1973; Thurman, 1985). Hence, DOC is typically the predominant electron donor and oxygen is typically the primary electron acceptor in lotic systems through aerobic respiration (Table 8). The entire suite of lotic TEAPs, including denitrification and respiration, is particularly influential at the soil-stream interface (typically but not always described as the hyporheic zone) because: (1) electron acceptors other than oxygen are used in suboxic conditions; (2) vertical redox gradients vary greatly across a few centimeters or less; (3) reactants are continuously supplied; and (4) wastes are continuously removed (Footnote 1). Combined, these various TEAPs form the backbone of most in-stream biogeochemical processes.

**Table 8. Lotic redox equations.**

*Adapted from Dahm et al. (1998) and Hedin et al. (1998).*

Process	Reaction	Free Energy (kJ)
<b>Terminal Electron Accepting Processes (Decreasing pE)</b>		
Aerobic Respiration	$\text{CH}_2\text{O} + \text{O}_2 \rightarrow \text{CO}_2 + \text{H}_2\text{O}$	-501
Denitrification	$\text{CH}_2\text{O} + (4/5)\text{NO}_3 + (4/5)\text{H}^+ \rightarrow (2/5)\text{N}_2 + \text{CO}_2 + (7/5)\text{H}_2\text{O}$	-476
Sulfate Reduction	$\text{CH}_2\text{O} + (1/2)\text{SO}_4^{2-} + (1/2)\text{H}^+ \rightarrow (1/2)\text{HS}^- + \text{CO}_2 + \text{H}_2\text{O}$	-102
Methanogenesis	a. $\text{CH}_2\text{O} \rightarrow (1/2)\text{CH}_4 + (1/2)\text{CO}_2$	-93
	b. $(1/2)\text{CO}_2 + 2\text{H}_2 \rightarrow (1/2)\text{CH}_4 + \text{H}_2\text{O}$	-66
<b>Chemoautotrophic Processes (Increasing pE)</b>		
Methane Oxidation	$\text{O}_2 + (1/2)\text{CH}_4 \rightarrow (1/2)\text{CO}_2 + \text{H}_2\text{O}$	-408
Sulfide Oxidation	$\text{O}_2 + (1/2)\text{HS}^- \rightarrow (1/2)\text{SO}_4^{2-} + (1/2)\text{H}^+$	-399
Nitrification	$\text{O}_2 + (1/2)\text{NH}_4^+ \rightarrow (1/2)\text{NO}_3 + \text{H}^+ + (1/2)\text{H}_2\text{O}$	-181

Of the lotic TEAPs, nitrification and denitrification are the most important to in-stream nitrogen cycling. Nitrification is the only natural process to convert ammonium to nitrate (Strauss et al., 2002), and denitrification is the primary process for removing reactive nitrogen from streams (Burgin and Hamilton, 2007; Knowles, 1982). Denitrification is heterotrophic dissimilatory reduction of nitrate to  $N_2$  gas in suboxic environments (less than 0.2 mg/L of  $O_2$ ); however micro-environments of anoxic denitrification can also exist in oxic conditions (Knowles, 1982; Paerl, 1984; Seitzinger et al., 2006). Conversely, nitrification is oxic chemoautotrophic conversion of ammonium to nitrate, and it competes for oxygen with the more energetically favorable, carbon-driven respiration (Baker et al., 1999; Hedin et al., 1998). Differences in in-stream redox potentials are mirrored by the relative predominance of these two processes, with nitrification sometimes causing wholly separate zones of ammonium and nitrate concentrations (Hedin et al., 1998). More commonly though, heterogeneous hyporheic zones cause interspersed patches of nitrification and denitrification [e.g. (Triska et al., 1993; Zarnetske et al., 2011)]. Other metabolic pathways for nitrogen uptake include assimilation of nitrate and ammonium to organic matter, the mineralization of organic nitrogen to ammonium, sulfate oxidation or fermentative dissimilatory reduction (DNRA) of nitrate to ammonium, chemoautotrophic denitrification via iron reduction, or anaerobic ammonium oxidation (anammox) to  $N_2$  gas (Burgin and Hamilton, 2007). In lotic systems though, assimilation, denitrification and nitrification dominate nitrogen processes except in highly sulfuric, ferric, or stagnant water (Burgin and Hamilton, 2007).

Due to this predominance of aerobic respiration and denitrification in lotic systems, in-stream carbon-nitrate dynamics are inextricably linked. For instance, when the C:N ratio of an organic source falls below Redfield C:N ratio of 106:16 or about 7:1, it is said to be carbon-limited where an excess of nitrogen limits its demand; conversely, when the C:N ratio exceeds the Redfield ratio,

it is nitrogen-limited, where nitrogen is relatively in higher demand (Redfield, 1958). Thus, the C:N ratios of benthic sediment, detritus, and particulate matter have been observed controlling in-stream nitrification and ammonium uptake (Arango and Tank, 2008; Dodds et al., 2004; Kemp and Dodds, 2002), while ambient dissolved C:N ratios have been observed similarly controlling nitrification in lab experiments (van Niel et al., 1993; Verhagen and Laanbroek, 1991) and natural streams (Strauss et al., 2002). Moreover, both particulate and ambient dissolved C:N ratios have been shown to control denitrification in many aquatic environments including rivers, streams, wetlands and oceans (Taylor and Townsend, 2010). Increased carbon quality (lability) likewise can have similar effects as quantity, driving nitrogen demand by increasing denitrification (Barnes et al., 2012; Newcomer et al., 2012). At the reach-scale, denitrification has also been found to increase with stream modifications that increase carbon availability, such as amending streambeds with particulate organic matter (Crenshaw et al., 2002), replacing streambed sediments with wood-based media bioreactors (Elgood et al., 2010; Robertson and Merkley, 2009), and installing in-stream structures that trap organic matter (Munn and Meyer, 1990; Roberts et al., 2007b). This simple carbon-nitrogen relationship stems directly from stoichiometric and thermodynamic controls (Table 8), leading some to recommend carbon amendments to treat in-stream nitrogen pollution (Craig et al., 2008; Hester and Gooseff, 2010; Passeport et al., 2013).

#### *1.3.2.2 Hydraulic controls on nutrient retention*

These biochemical processes are facilitated by lotic hydraulic flow paths that transport reactants through zones of varying redox states, such as at the surface-subsurface interface (the hyporheic zone). Consequentially, as nutrients are transported through the hyporheic zone, they are biochemically transformed in a suite of processes known as spiraling (Newbold et al., 1983; Workshop, 1990). Increased hyporheic flow therefore typically increases nutrient retention



(Alexander et al., 2007; Mulholland et al., 2008; Peterson et al., 2001) making the hyporheic zone a biogeochemical “hot-spot” of nutrient uptake (Groffman et al., 2009; McClain et al., 2003; Vidon et al., 2010). In fact, hyporheic nitrate uptake is so substantial that it has been observed accounting for up to 50% of total nitrate uptake in streams across many biomes (Table 9). Because headwater streams - compared to larger order streams - experience proportionally more hyporheic flow, headwater streams themselves are also considered nutrient retention “hot spots” (Hall Jr. et al., 2002). Moreover, because hyporheic flow is typically influenced by a stream’s geomorphology, most in-stream geomorphic features - such as debris dams and riffles – increase hyporheic flow and nitrogen uptake, decreasing nitrogen concentrations (Table 10). As a result, many in-stream nutrient retention models also include the effects of geomorphology on nutrient uptake [e.g. (Dahm et al., 1998; Thomas et al., 2001; Valett et al., 1996)], and in-stream geomorphic restoration is often recommended to increase nutrient retention (Craig et al., 2008; Hester and Gooseff, 2010; Passeport et al., 2013).

**Table 9. Percentage of in-stream nitrate uptake that occurs in the hyporheic zone.**

State	Basin	% Hyporheic nitrate uptake	Reference
<b>Antarctica</b>	Green Creek	0-26%	(Runkel, 2007)
<b>CA</b>	Elder Creek	29-46%	(O’Connor et al., 2009)
<b>MA</b>	Ipswich River	21%	(Stewart et al., 2011)
<b>NC</b>	Snake Den Branch	44-49%	(Thomas et al., 2003)
<b>WI</b>	Many	3-44%	(Powers et al., 2012)

**Table 10. In-stream geomorphic features that increase nitrogen uptake and/or decrease nitrogen concentrations/fluxes.**

<b>Geomorphic feature</b>	<b>State</b>	<b>Location/Basin</b>	<b>Analyte</b>	<b>Reference</b>
<b>Stream valley complexity</b>	CO	Many	Nitrate uptake	(Baker et al., 2012)
	NM	Many	Nitrate uptake	(Valett et al., 1997)
	OR	H.J. Andrews	Ammonium uptake	(Lamberti et al., 1989)
<b>Meander bends</b>	IL	Embarras River	Denitrification	(Opdyke et al., 2006)
	IL	Little Kickapoo Creek	Nitrate flux	(Peterson and Benning, 2013)
<b>Benthic habitat complexity</b>	-	Experimental flume	Nitrate uptake	(Cardinale, 2011)
	IL	Many	Ammonium concentrations Nitrate concentrations	(Heatherly et al., 2007)
	NY	Koxing Kill	Ammonium uptake	(Gibson and O'Reilly, 2012)
	OH	Many	Ammonium concentrations Inorganic nitrogen concentrations	(Miltner and Rankin, 1998)
	Spain	Irrigation canal	Ammonium uptake	(Argerich et al., 2011)
	WV	Many	Nitrate concentrations Total nitrogen concentrations	(Zheng et al., 2008)
	<b>Two-stage ditches</b>	IN	Shatto Ditch	Denitrification
OH		Portage River	Denitrification	(Powell and Bouchard, 2010)
<b>Geomorphic stream restoration</b>	KY	Wilson Creek	Nitrate uptake	(Bukaveckas, 2007)
	MD	Anne Arundel County	Total nitrogen flux	(Filoso and Palmer, 2011)
	MD	Baltimore LTER	Denitrification	(Klocker et al., 2009)
	MD	Baltimore LTER	Total nitrogen uptake	(Sivirichi et al., 2011)
	MI	Shane Creek	Ammonium uptake Nitrate uptake	(Hoellein et al., 2012)
	NC	Many	Nitrate uptake	(Sudduth et al., 2011)
	OH	Many	Denitrification	(Zika, 2008)
	<b>Restored riffles, baffles, cross-vanes, etc.</b>	NC	Many	Ammonium uptake
NY		Many	Nitrate uptake	(Daniluk et al., 2012)
Ontario		Many	Nitrate uptake	(Kasahara and Hill, 2006)

<b>Geomorphic feature</b>	<b>State</b>	<b>Basin</b>	<b>Analyte</b>	<b>Reference</b>
<b>Natural riffle-pool sequences</b>	AZ	Sycamore Creek	Nitrate uptake	(Fisher et al., 1998; Valett et al., 1994)
	AZ	Sycamore Creek	Nitrification	(Jones Jr. et al., 1995)
	Brittany	Many	Nitrification	(Lefebvre et al., 2006)
	Ontario	Brougham Creek	Nitrate uptake	(Hill et al., 1998a)
	Ontario	Speed River	Nitrate concentrations	(Franken et al., 2001)
<b>Debris dams</b>	-	Recirculating chamber	Nitrate uptake	(Aumen et al., 1990)
	GA	Ft. Benning	Ammonium uptake	(Roberts et al., 2007b)
	MD	Baltimore LTER	Denitrification	(Groffman et al., 2005)
	MD	Baltimore LTER	Ammonium uptake	(Claessens et al., 2010)
	MI	Ontonagon River	Nitrate uptake	(Hoellein et al., 2009)
	NC	Coweeta	Nitrate uptake	(Munn and Meyer, 1990)
	OR	H.J. Andrews		
	NC	Coweeta	Nitrate uptake	(Wallace et al., 1995)
	NH	Hubbard Brook	Nitrate flux Nitrate uptake	(Bernhardt et al., 2003; Bernhardt et al., 2005)
	WY	Red Canyon Creek	Nitrification	(Fanelli and Lautz, 2008; Lautz and Fanelli, 2008)
<b>Man-made dams and ponds</b>	PA	Chester County	Nitrate uptake Total nitrogen uptake	(Fairchild and Velinsky, 2006)
	WI	Many	Inorganic nitrogen uptake	(Stanley and Doyle, 2002)
<b>Beaver dams</b>	MD	Anne Arundel County	Total nitrogen flux Nitrate flux Total organic nitrogen flux	(Correll et al., 2000)
	MD	Herrington Creek	Nitrate concentrations	(Margolis et al., 2001)
	PA	Mountain Run		
	NY	Pancake-Hall Creek	Nitrate concentrations	(Cirimo and Driscoll, 1993)
	NY	Homer Gulf Creek	Nitrate concentrations	(Klotz, 2010)
	Ontario	Harp Lake	Total nitrogen flux Nitrate flux	(Devito and Dillon, 1993)
	WY	Currant Creek	Nitrate flux Total Kjeldahl nitrogen flux	(Maret et al., 1987)

### 1.3.2.3 *Biotic controls on nutrient retention*

In addition to geomorphology, temporal and spatial variations of in-stream autotrophic and heterotrophic processes, via production and respiration respectively, critically affect in-stream nitrogen retention. In fact, these microbial processes are so important to in-stream nitrogen uptake that some speculate nutrient retention at geomorphic structures is not just attributable to hyporheic flow as discussed previously, but to biotic growth on the structures themselves [e.g. (Aumen et al., 1990; Roberts et al., 2007b)]. Similarly, nitrogen uptake in restored streams has been attributed not just to geomorphology but to in-stream autotrophy facilitated by newly opened forest canopies (Bukaveckas, 2007; Sudduth et al., 2011). Given the importance of these biotic processes, it is not surprising that light availability – as a predominant factor in the biotic shift between heterotrophy to autotrophy - has been shown to control whether respiration or production drives in-stream nitrogen demand (Hall Jr. and Tank, 2003; Hoellein et al., 2007; Newbold et al., 2006). For instance, heterotrophy drives ammonium uptake in permanently dark cave streams (Simon and Benfield, 2002) while autotrophy drives ammonium and nitrate uptake in concrete canals that lack any hyporheic heterotrophic habitat (Izagirre et al., 2012; Kent et al., 2005; Knapp et al., 2009). Even in streams that experience both processes, temporal variations in light availability drive temporal variations in autotrophic and heterotrophic nitrogen uptake. For instance, some have found that nitrate retention is correlated with respiration when the canopy is closed, and it is correlated with production when the canopy is open, (Valett et al., 2008). Thus, both autotrophic production and heterotrophic respiration critically affect in-stream nitrogen uptake.

In-stream autotrophic nitrogen uptake is directly controlled by seasonal and spatial light availability, typically tied to shading from the canopy cover. Spatially, percent canopy cover is inversely related to ammonium uptake (Arango et al., 2008; Johnson et al., 2009). In other words,

as a canopy becomes more open (or less dense), increased sunlight increases primary production which in-turn increases nutrient uptake. Thus, it is not surprising that the River Continuum Concept hypothesizes that headwater streams are net-heterotrophic, only transitioning to net autotrophic at larger order (>3) reaches as shading becomes less prevalent (Vannote et al., 1980). However, even net heterotrophic headwater streams can experience substantial autotrophy [e.g. (Minshall, 1978)]. In fact, autotrophy is so significant in headwater streams that nitrate uptake across many biomes has been shown to correlate primarily with production, not respiration (Hall Jr. and Tank, 2003; Mulholland et al., 2008). Furthermore, across many biomes, biotic assimilation can account for 12-80% of in-stream ammonium uptake (Table 11) and 60%-100% of nitrate uptake (Arango et al., 2008; Bernhardt and Likens, 2002; Sobczak et al., 2003). Temporally, however, the effects of autotrophy on nutrient uptake can vary daily or seasonally (Webster et al., 2003). For instance, leaf emergence in forested streams can suppress algal growth and primary production from spring to summer (Hill et al., 2001; Sabater et al., 2006) causing declines in ammonium and nitrate demand [e.g. (Hoellein et al., 2007; Roberts and Mulholland, 2007)]. Thus, autotrophic uptake of nitrogen varies both spatially and temporally due to the effects of shading on primary producers.

**Table 11. Percent contribution of ammonium uptake via assimilation to total in-stream ammonium uptake.**

State	Basin	% Ammonium uptake via assimilation	Reference
<b>Meta-analysis</b>	Many	70-80%	(Peterson et al., 2001)
<b>KS</b>	Kings Creek	23%	(Dodds et al., 2000)
<b>NC</b>	Upper Ball Creek	12%	(Tank et al., 2000)
<b>MI</b>	Kalamazoo River	47%	(Arango et al., 2008)
<b>OR</b>	Mack Creek	32%	(Ashkenas et al., 2004)
<b>TN</b>	Walker Branch	33-48%	(Mulholland et al., 2000)

While in-stream autotrophic nitrogen uptake correlates with canopy cover and shading, respiration-based nitrogen uptake is associated with heterotrophic lotic food webs (a.k.a. the

“microbial loop”) primarily controlled by seasonal cycles of dissolved organic matter (DOM) inputs (Meyer, 1994). In the dormant season, DOM originates from leaf fall (Meyer et al., 1998; Wetzel and Manny, 1972) which in-turn increases respiration (Gibson and O'Reilly, 2012; Roberts and Mulholland, 2007) and inorganic nitrogen uptake [e.g. (Gulis and Suberkropp, 2003; Mulholland et al., 1997)]. While previous studies have shown that allochthonous leaf-fall alone drives in-stream heterotrophy (Fisher and Likens, 1973; Meyer, 1994; Vannote et al., 1980), autochthonous organic matter from vernal algal growth can also stimulate respiration [e.g. (Haack and McFeters, 1982; Rusanov et al., 2009)] and heterotrophic nitrogen uptake [e.g. (McMillan et al., 2010; Paerl, 1984)]. Overall though, less than 50% of in-stream DOC has been shown to be biologically available or labile (BDOC), meaning less than half of DOC can be readily metabolized by microbes (Table 12), with lability varying by source such as species of tree leaves (Tank and Webster, 1998). Therefore the effects of allochthonous and autochthonous organic matter on in-stream heterotrophic nitrogen uptake vary with temporal and spatial variations in organic matter source.

**Table 12. Percent contribution of biologically available DOC to total in-stream DOC.**

State	Basin	% BDOC in DOC	Reference
<b>Australia</b>	Swan-Canning Estuary	1-17%	(Petronne et al., 2009)
<b>Belgium</b>	Meuse & Scheldt Rivers	17-41%	(Servais et al., 1987)
<b>CO</b>	Blue River	0-30%	(Kaushal and Lewis, 2005)
<b>GA &amp; NC</b>	Many	0-50%	(Meyer, 1994)
<b>PA</b>	White Clay Creek	25%	(Volk et al., 1997)
	White Clay Creek	8.6%	(Kaplan et al., 2008)
	White Clay Creek	26-31%	(Cory and Kaplan, 2012)
<b>VA</b>	Paine Run	3-7%	(Buffam et al., 2001)

Driven by light and organic matter availability, seasonal autotrophic and heterotrophic nutrient retention can drive stream-wide nutrient dynamics. Spatially, when in-stream uptake exceeds inputs, nutrient concentrations decrease longitudinally from upstream to downstream (Brookshire

et al., 2009). This process has been observed in Tennessee streams where organic inputs and nitrate uptake in the spring and fall – driven by vernal algal growth and autumnal leaf-fall respectively – caused DOC concentrations to increase upstream to downstream, while concurrently causing nitrate concentrations to decrease upstream to downstream [e.g. (Roberts and Mulholland, 2007)]. In this manner, predominant seasonal in-stream processes can be deduced by analyzing in-stream biogeochemistry. For instance, nitrate concentrations in a New York stream were observed decreasing longitudinally in the fall due to leaf-litter driving nitrogen uptake; however, nitrate concentrations in the same stream failed to decrease longitudinally in the spring, possibly indicating insignificant vernal autotrophy due to its more northern location (Goodale et al., 2009). Likewise, in some desert streams, nitrate concentrations have been observed decreasing longitudinally throughout the summer indicating unshaded, uninterrupted summer-long autotrophic demand (Grimm, 1987; Grimm et al., 1981; Valett, 1993). While these streams illustrate in-stream nitrogen concentrations controlled by in-stream processes, inorganic nutrient concentrations in 85% of streams in one meta-analysis failed to decrease longitudinally in any season, indicating that inputs, not in-stream retention, typically drive in-stream concentrations (Brookshire et al., 2009). For this reason, as discussed previously, watershed processes controlling nitrate export (Figure 1) are fairly typical (Table 7). However, in-stream nitrogen retention has been shown to control nitrogen export in some streams within the Chesapeake Bay region (Table 13), resulting in yearly bi-modal nitrate concentrations with troughs in the spring and fall characteristic of nitrate retention driven by algal growth and leaf-fall, respectively (Figure 2). Thus, spatial and temporal nitrate variations shed light on the underlying processes - autotrophic or heterotrophic - dominating net in-stream nutrient retention, in addition to the net processes – in-stream or landscape-wide - that dominate nitrogen export from headwater catchments.

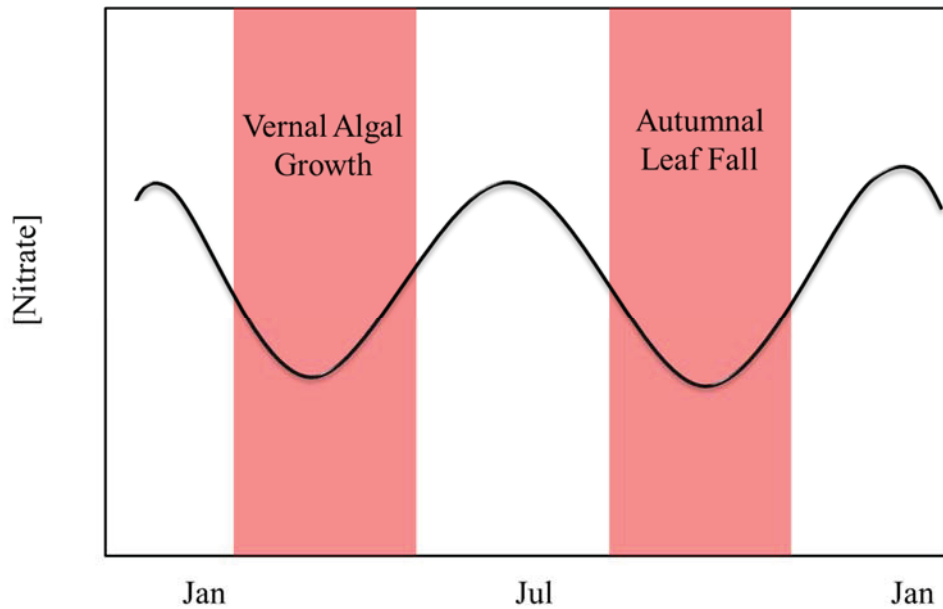


**Figure 2. Typical yearly pattern of in-stream nitrate concentrations in lotic systems dominated by in-stream nitrogen retention in the spring and fall.**

**Table 13: Watersheds in and near the Chesapeake Bay region that experience bi-modal peak nitrate export during the summer and winter.**

<b>Physiographic province</b>	<b>State</b>	<b>Basin/Location</b>	<b>Reference</b>
<b>Allegheny Plateau</b>	NY	Upper Susquehanna	(Goodale et al., 2009)
	PA	River	
<b>Blue Ridge</b>	NC	Coweeta	(Starry et al., 2005; Swank and Vose, 1997)
	VA	Pain Run	(Buffam et al., 2001)
<b>Catskills</b>	NY	Neversink River	(Burns, 1998)
<b>Piedmont</b>	MD	Pond Branch	(Band et al., 2001)
<b>Ridge and Valley</b>	TN	Walker Branch	(Hill et al., 2001; Mulholland, 1992, 2004; Mulholland and Hill, 1997; Roberts and Mulholland, 2007)
	TN	White Oak Creek	(Hill et al., 2001; Mulholland and Hill, 1997)



## 2 OBJECTIVES

This purpose of this study was to elucidate the seasonal effects of temperature, shading, and dissolved organic matter dynamics on baseflow nitrogen retention and export from a headwater, forested catchment in the Piedmont physiographic province of the Chesapeake Bay watershed. These baseflow dynamics were investigated within the 79 ha. forested watershed at Fair Hill Natural Resources Management Area (Fair Hill), located in northeast Maryland, where baseflow annually contributes 24-47% of total discharge (Dhillon and Inamdar, 2013). Six sampling campaigns were conducted throughout the year to capture seasonal variations of shading, temperature, and organic matter dynamics, allowing for short-term temporal comparisons (spring prior to and after leaf-out) in addition to longer term annual comparisons (spring versus fall). Specifically, each campaign included three investigations: 24-hour in-stream environmental data collected with multi-meter probes; continuous drip co-injection experiments of dextrose and ammonium chloride; and a synoptic sampling of surface water every 30-90m along the reach from source to outlet. Due this longitudinal sampling campaign, additional temporal insights were provided by analyzing seasonally varying upstream-to-downstream dynamics.

The headwater, forested stream at Fair Hill was predicted to be net-heterotrophic in-line with the River Continuum Concept (RCC) (Vannote et al., 1980). Additionally, watershed processes at Fair Hill were expected to be similar to other temperate forests. In particular, nitrate concentrations were expected to be lower than regional norms because forested streams in the Piedmont typically export less nitrate than other land-uses (Jordan et al., 1997a, b) and because riparian buffers across the region typically reduce nitrate inputs from shallow groundwater (Table 6). Additionally, shading from canopy growth in summer was expected to reduce in-stream nitrate uptake (Hill et al., 2001; Sabater et al., 2006), while leaf-litter in the fall was expected to increase nitrate uptake

(Fisher and Likens, 1973; Meyer, 1994; Vannote et al., 1980).

The net role of in-stream processes on nutrient export, however, was not clear before the experiment. In most headwater catchments, watershed processes exert a predominant role over in-stream processes in controlling nutrient export; while in the minority of streams, in-stream processes predominate (Brookshire et al., 2009; Goodale et al., 2009). By analyzing temporal in-stream biogeochemistry, it was expected that the stream at Fair Hill would follow one of these two common patterns (Figure 1 and Figure 2). Seasonal nutrient dynamics would therefore help to indicate if vernal algal growth and fall leaf-fall drive in-stream nutrient uptake and reduce nitrate exports (Roberts and Mulholland, 2007). Likewise, it was uncertain if inputs along the stream would exceed in-stream processes; thus a longitudinal sampling regime and uptake experiments were employed to analyze upstream to downstream variations in nutrient concentrations to gain insight on inputs versus in-stream retention (Brookshire et al., 2009).

Using these methods, the drought in September 2010 also provided a unique opportunity to analyze temporal in-stream dynamics within larger seasonal trends. It was unknown if short-term drought-induced processes, seasonal processes, or some combination thereof would have an observable effect on the in-stream biogeochemical patterns analyzed above.

In sum, the purpose of this study is to determine which catchment and in-stream controls at Fair Hill play a predominant role in buffering nitrogen export to the Chesapeake Bay watershed. This study shifts focus from previous stormflow studies at Fair Hill by analyzing baseflow dynamics and in-stream processes, with an additional examination of drought-induced in-stream biogeochemical processes. As such, determinations can be made whether baseflow biogeochemistry at Fair Hill varies spatially or temporally along the reach in response to seasonal variations of shading, temperature, and organic matter dynamics.

### 3 STUDY AREA

This study is located at a forested watershed in Fair Hill Natural Resources Management Area (Fair Hill) (39°42' N, 75°50' W). Fair Hill is located in the Piedmont physiographic province in Cecil County of northeast Maryland (Figure 3 and Figure 4). Elevations at Fair Hill range from 77m to 108m above mean sea level, with gentle slopes from 0.16 to 24 degrees (Inamdar et al., 2013). The 79 ha. watershed at Fair Hill is approximately 50% forest, encircled by actively managed hay/grass fields (Inamdar et al., 2013). The mature forest consists of about 50% American beech (*Fagus grandifolia* Ehrh.) and 25% yellow poplar (*Liriodendron tulipifera* L.). The remaining 25% consists of black oak (*Quercus velutina* Lam.), red maple (*Acer rubrum* L.) and silver maple (*Acer saccharinum* L.) (Klingaman et al., 2007). Mean diameter breadth height is approximately 40cm and mean crest height is 27.8m (Klingaman et al., 2007; Levia et al., 2010; Van Stan II et al., 2011). Leaf-fall at Fair Hill typically begins the first week of November and lasts until the end of April (Levia et al., 2011; Van Stan II et al., 2011) though it can begin as early as the last weeks of September during drought (Inamdar et al., 2013).

The substrate at Fair Hill contains clay, sand, muscovite and biotite – the muscovite gives it a slight “sparkle” (Bascom, 1902), and it is considered part of the deep and well-drained Glenelg series (Inamdar et al., 2013; Inamdar et al., 2011a; Inamdar et al., 2011b). The hillslope soils tend to be coarse and loamy while the valley soils are shaped by frequent saturation (Inamdar et al., 2013; Inamdar et al., 2011a; Inamdar et al., 2011b). The area is underlain by fractured, weathered crystalline rocks (mica-gneiss) from the Mt. Cuba Wissahickon formation interspersed with veins of pegmatite and quartz (Bascom, 1902; Sloto, 2002). This bedrock outcrops across the stream near its confluence with Big Elk Creek.

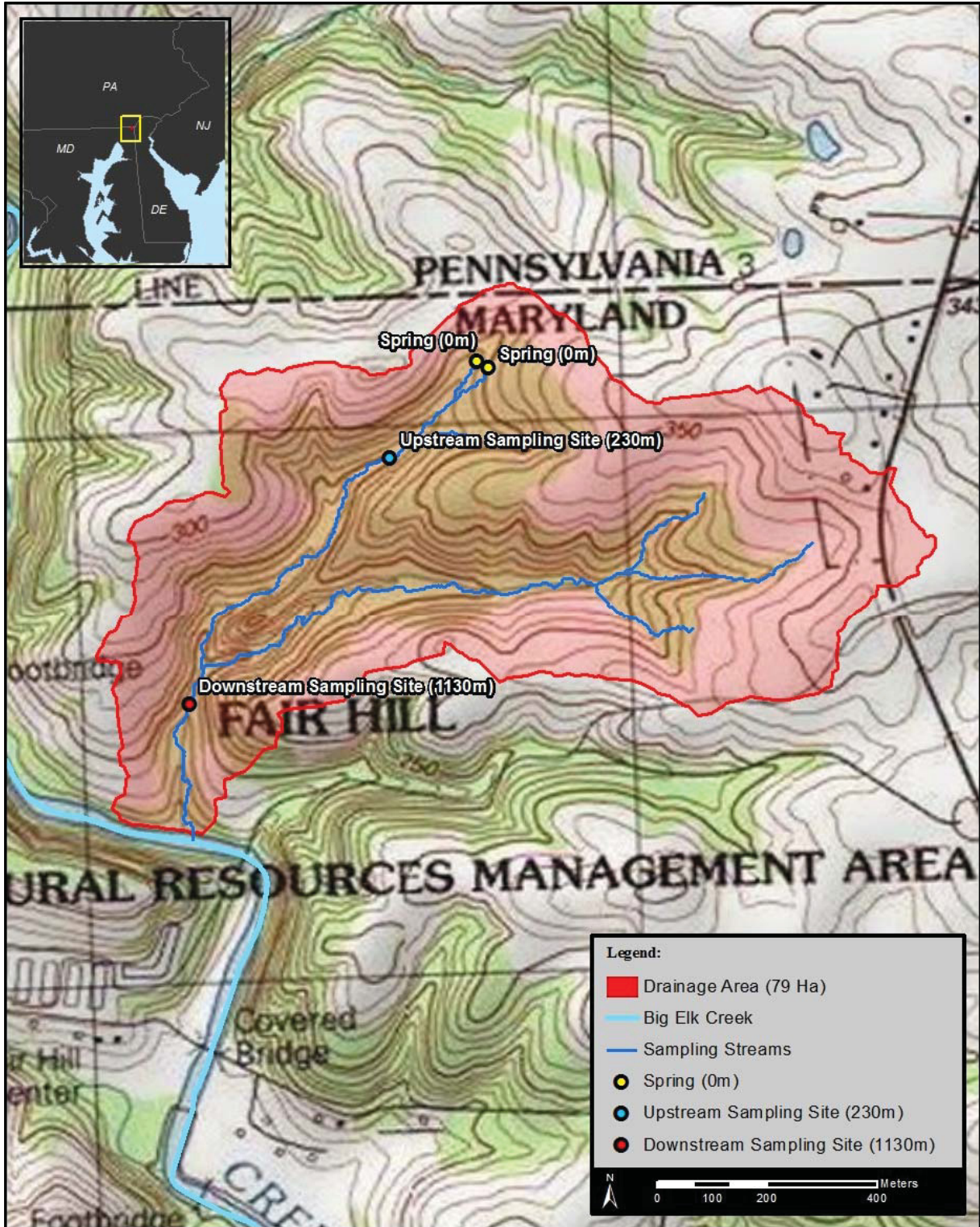


Figure 3. Fair Hill Natural Resource Management Area topographic map.

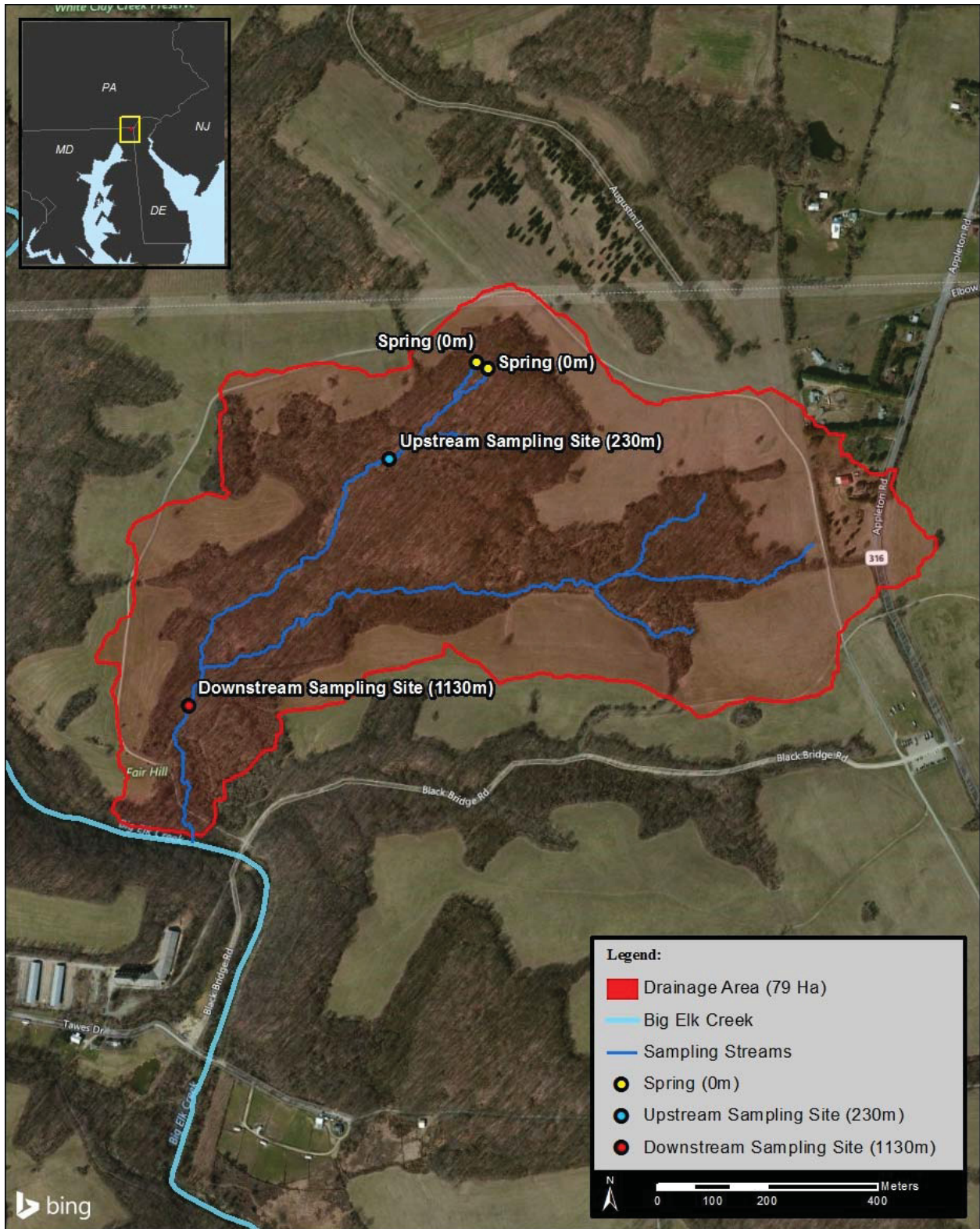
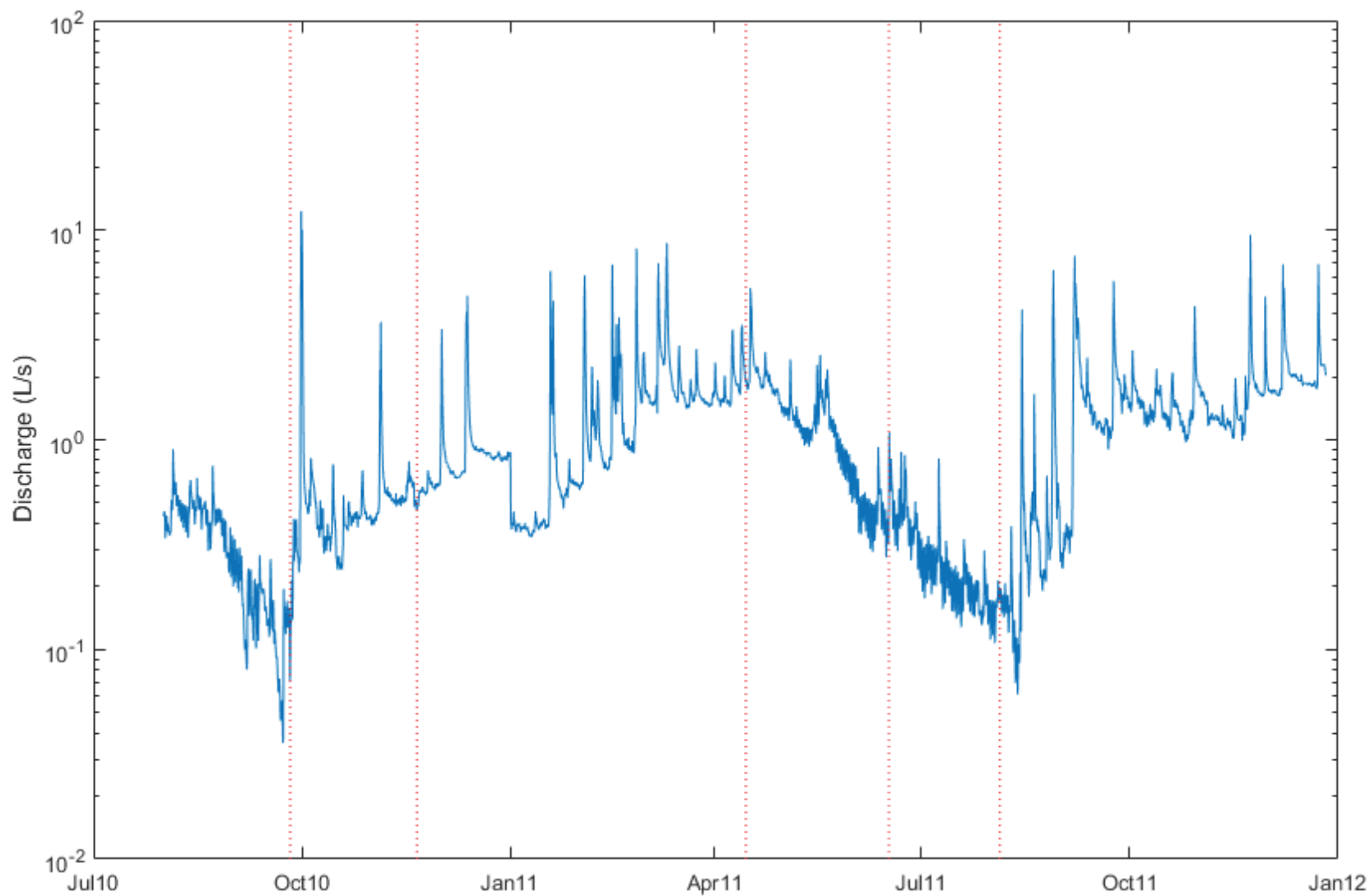


Figure 4. Fair Hill Natural Resource Management Area aerial imagery.

The study catchment has a total drainage area of 79 ha., and it contains two first order spring-fed perennial streams that primarily flow to the southwest to Big Elk Creek. Big Elk Creek is tributary to the Elk River, which joins the Chesapeake Bay near Elkton, MD. The humid, temperate climate at Fair Hill is influenced by the Atlantic Ocean, and the watershed experiences approximately 114cm of rain a year resulting in 27cm (63%) of groundwater discharge and 16cm (37%) of surface runoff (Sloto, 2002). The streams at Fair Hill experience peak flow in late spring and occasionally dry up in late summer (Inamdar et al., 2013; Inamdar et al., 2011a; Inamdar et al., 2011b). A Parshall flume at the upstream sampling site (Figure 3 and Figure 4) recorded discharge every 15 minutes during the two-year study until December 2011 when it stopped due to operational problems (Figure 5).



**Figure 5. 15 minute discharge at Fair Hill, measured via a Parshall flume at the upstream sampling site.** Red lines indicate dates of the two-day sampling campaigns. The last sampling campaign (Feb 2012) is omitted because flows were not recorded after December 2011 due to operational problems with the flume.

Studies took place exclusively on the northern first-order tributary at Fair Hill (Figure 3 and Figure 4). At its source, two springs feed parallel channels that combine approximately 70m downstream of the springs. The reach transitions from first-order to second-order approximately 1130m downstream of the springs with the addition of the eastern first-order tributary (not studied). Along the study reach, two detailed stream sampling sites - the “upstream” and “downstream” sites - were used consistently among the sampling campaigns (Figure 3 and Figure 4). The upstream site is located within the first-order reach approximately 230m downstream from the springs. It has a 12 ha. drainage area. Average stream width and depth at the upstream site are 97cm and 4cm, respectively (Table 14). The downstream site is located below the transition to a second-order reach, approximately 1130m downstream from the springs. It has a drainage area of 78 ha. Average stream width and depth at the downstream site are 130cm and 6cm, respectively (Table 14). For 900m between the two sampling sites, there are no observable springs or tributaries contributing to the study reach.

**Table 14. Stream discharge, width, and depth at the sampling locations.**

Year	Month	Sampling location	Discharge (L/s)	Average width (cm)	Average depth (cm)
2012	February	Upstream	2.64	92.5	5.7
		Downstream	8.56	165	7.0
2011	April	Upstream	1.46	123	4.5
		Downstream	16.8	154	7.8
2011	June	Upstream	0.95	103	2.4
		Downstream	9.88	130	5.4
2011	August	Upstream	0.37	82.5	2.4
		Downstream	2.03	106	3.9
2010	September	Upstream	0.14	72.5	2.8
		Downstream	0.06	50.8	2.0
2010	November	Upstream	0.36	111	5.4
		Downstream	2.56	186	11.9



## 4 FIELD METHODS

Between the fall of 2010 and early 2012, a series of six sampling campaigns were conducted at Fair Hill during six representative seasonal periods (Table 15). Each campaign included three investigations: 24-hour in-stream environmental data collected with multi-meter probes; continuous drip co-injection experiments of dextrose, ammonium chloride and sodium chloride; and a synoptic collection of surface water samples at 30-90m intervals along the reach.

**Table 15. Sampling dates at Fair Hill.**

Year	Month	Dates	Season
2010	September	25 & 26	Fall pre-leaf-fall
2010	November	20 & 21	Fall post-leaf-fall
2011	April	14 & 15	Spring pre-leaf-out
2011	June	16 & 17	Spring post-leaf-out
2011	August	4 & 5	Summer
2012	February	3 & 4	Winter

### 4.1 24-HOUR IN-STREAM ENVIRONMENTAL DATA

During each sampling campaign, YSI multi-meter probes were secured underwater at both the upstream and downstream sampling sites (Figure 3 and Figure 4) to record conductance ( $\mu\text{S}/\text{cm}$ ), specific conductance ( $\mu\text{S}/\text{cm}$ ), pH, dissolved oxygen ( $\text{mg}/\text{L}$ ), dissolved oxygen saturation (%), temperature ( $^{\circ}\text{C}$ ), and pressure (kPa). Each probe collected data at least every five minutes for 24 hours. Before each sampling campaign, probes were lab-calibrated for pH and conductivity, and new dissolved oxygen (DO) membrane caps were installed on each steady-state polarographic DO sensor. Probes were field-calibrated for DO saturation prior to deployment. Data was processed with MATLAB using methods for in-situ single station DO change (Bott, 2006) (Appendix G) to calculate net ecosystem metabolism (NEM), respiration (R), gross primary production (GPP), P/R, average temperature, and pH (Appendix K).

## 4.2 CONTINUOUS NUTRIENT ADDITION EXPERIMENTS

During each sampling campaign, continuous drip co-injections of dextrose, ammonium chloride and sodium chloride were performed at both sampling sites following standard procedures (Webster and Valett, 2006; Workshop, 1990). A nutrient addition experiment was conducted at the downstream site on the first day of each study, and then repeated at the upstream site the next day (Figure 3 and Figure 4) such that the former did not affect the latter. A diaphragm pump powered by a marine battery pumped solutes from 7 or 22L carboys, which were pre-mixed in the lab a day before each investigation. In September 2010, dextrose and ammonium chloride were mixed separately from the sodium chloride solution; for the other experiments all three solutes were mixed together. To determine desired pump speeds, stream discharge was estimated using the Parshall flume, slug-test dilution tracers, and velocity-area measurements. Pump rates were determined before and after the injections using a graduated cylinder and a stopwatch. Injectate concentrations (Table 16) were chosen to produce increases of 5 mg/L of dextrose, 0.05 mg-N/L of ammonium and 5 mg/L of chloride. Chloride concentrations, reported as salt equivalents (Table 16), were summed from ammonium chloride and sodium chloride.

**Table 16. Continuous flow injection set-up including solute concentrations and pump rates.**

<b>Year</b>	<b>Month</b>	<b>Location</b>	<b>Stream discharge* (L/s)</b>	<b>Pump rate (mL/min)</b>	<b>Dextrose (g C<sub>6</sub>H<sub>12</sub>O<sub>6</sub>/L)</b>	<b>Ammonium chloride (g NH<sub>4</sub>Cl/L)</b>	<b>Equivalent salt concentration (g NaCl/L)</b>
2010	September	Upstream	0.14	14.9/14.4**	6.51	0.10	4.15
		Downstream	0.06	15.8/15.2**	6.51	0.10	4.15
2010	November	Upstream	0.36	15.4	23.6	0.36	15.9
		Downstream	2.56	14.8	19.3	1.43	14.5
2011	April	Upstream	1.46	53.0	12.0	0.47	20.5
		Downstream	16.8	67.9	75.0	2.92	117
2011	June	Upstream	0.95	27.4	12.5	0.50	19.8
		Downstream	9.88	20.2	75.0	3.00	102
2011	August	Upstream	0.37	11.9	12.5	0.50	20.4
		Downstream	2.03	9.9	75.0	3.00	107
2012	February	Upstream	2.64	39.1	75.2	3.02	126
		Downstream	8.56	41.8	75.2	3.02	126

\* Stream discharge determined after-the-fact from the injection experiments

\*\* Salt solution injection rate/nutrient solution injection rate

Injection experiments occurred at constrictions in the stream to promote full turbulent mixing. Experiments were 20-40m in length and typically extended downstream until reaching an obstruction (e.g. log-jam). Five sampling stations were spaced roughly equally downstream of each injection site (Table 17 and Table 18). Distance from injection site and stream geometry were measured at each station. During each experiment, spot checks with a YSI multi-meter conductivity probe were used to verify that the first sampling station was located far enough downstream from the injection site such that in-stream solute concentrations (using conductance as a surrogate) were fully-mixed (Figure 6). Additionally, spot checks were taken laterally across the stream to ensure that each cross-section was also fully mixed. A YSI probe at the most downstream station was used to determine when in-stream conductivity levels reached a steady-state plateau, typically 1-3 hours into the experiment. When conductivity plateaued, samples were collected at each station, downstream to upstream, including background samples collected upstream of the injection site (Station 0).

Samples were filtered during collection through a 0.45 $\mu$ m filter using a peristaltic Geopump. The tubing and the filter were continuously rinsed for at least one minute with stream water from the sampling location prior to collection. Dissolved organic carbon (DOC) and biologically available DOC (BDOC) samples were collected in triplicate in amber glass bottles with no head space. Anion, nutrient, and a back-up set of samples were collected in triplicate in plastic scintillation vials with headspace. All samples were immediately refrigerated on ice, and the nutrient samples (for measuring ammonium and phosphate) were frozen on dry-ice within 12-hours and stored in a freezer within 24-hours. All other samples were transferred from ice to a 4°C cooler within 24-hours of collection until analysis.

**Table 17. Station distance from injection site: Upstream experimental site.**

Year	Month	Station 1 (m)	Station 2 (m)	Station 3 (m)	Station 4 (m)	Station 5 (m)
2010	September	3.3	6	8.5	12.3	17.4
2010	November	6	11	16	21	25
2011	April	4	8	12	17	23
2011	June	8	15	26	31	38
2011	August	9	15.5	24.5	32.5	42
2012	February	7	13	20	29	38.5

**Table 18. Station distance from injection site: Downstream experimental site.**

Year	Month	Station 1 (m)	Station 2 (m)	Station 3 (m)	Station 4 (m)	Station 5 (m)
2010	September	2	4	6	8	10
2010	November	18	26	41	56	68
2011	April	6	10	16	20	24.5
2011	June	8	16	23	31	40
2011	August	8	16	24	32	40.5
2012	February	8	16	24	32	42

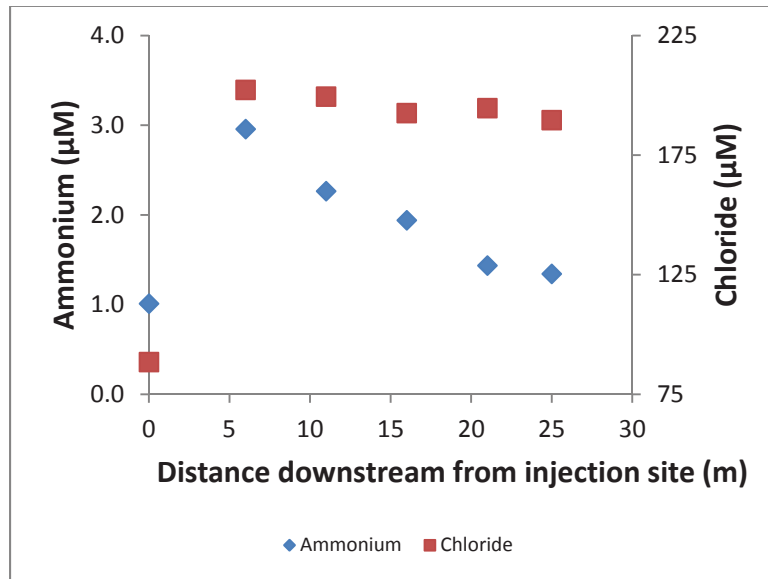


**Figure 6. Typical results from a well-mixed nutrient injection experiment.**  
*Solute concentrations peak before the first sampling location (November 2010, downstream experimental site).*

Stream flow and nutrient uptake parameters were calculated for each station and overall for each experiment using data from the injection experiments. Discharge at each station was calculated using chloride dilution (Appendix H) (Webster and Valett, 2006; Workshop, 1990). Average discharge for each experiment was calculated by averaging discharge from each station. Velocities were determined by dividing discharge by width and average depth at each station. Nutrient uptake length, uptake velocity, and areal uptake were calculated for DOC and ammonium at each station following standard procedures (Appendix I) (Webster and Valett, 2006; Workshop, 1990).

### **4.3 SURFACE WATER LONGITUDINAL SURVEY**

On the first day of each sampling campaign, a longitudinal water quality survey of the stream was conducted by collecting surface water samples at 30-90m intervals along the reach. Sampling began at the downstream experiment site and proceeded upstream to the springs (Figure 3 and Figure 4). Samples near the downstream injection site were collected before initiating the injection experiment. Time and location were recorded at each sampling location. All samples were collected with a peristaltic Geopump and were immediately filtered through a 0.45 $\mu$ m filter. The tubing and filter were rinsed for at least one minute with stream water from each sampling location prior to collection.

At each longitudinal sampling location, individual samples of dissolved organic carbon (DOC) and biologically available DOC (BDOC) were collected in glass amber bottles with no headspace, nutrient and anion samples were collected in plastic scintillation vials with headspace, and isotope samples were collected in clear glass bottles with no headspace. All samples were immediately refrigerated on ice, and nutrient samples (for measuring ammonium and phosphate) were frozen on dry-ice within 12-hours and stored in a freezer within 24-hours. All other samples were transferred from ice to a 4°C cooler within 24-hours of collection until analysis.

## 5 LAB METHODS

Oxygen and hydrogen isotopes ( $\delta^{18}\text{O}$  and  $\delta\text{D}$ ) were analyzed on a Picarro isotope analyzer using cavity ring-down mass spectrometry with a precision of 0.10‰ and 0.50‰ respectively. DOC (MDL = 0.33  $\mu\text{M}$ ) and TDN (MDL = 0.36  $\mu\text{M}$ ) were analyzed with oxidative combustion in a Shimadzu TOC-V CPH using infrared analysis and chemiluminescence, respectively. DIC was analyzed on the Shimadzu TOC-V CPH using acidification with phosphoric acid and sparging, followed by infrared analysis. Ammonium (MDL = 0.04  $\mu\text{M}$ ) and phosphate (MDL = 0.02  $\mu\text{M}$ ) were analyzed on a SEAL Analytical AA3 using continuous segmented flow analysis. Ammonium concentrations were determined using a Berthelot reaction and phosphate concentrations were determined using the Murphy and Riley method. Nitrate (MDL = 1.61  $\mu\text{M}$ ), sulfate (MDL = 2.82  $\mu\text{M}$ ), and chloride (MDL = 1.04  $\mu\text{M}$ ) were analyzed on a Dionex ICS-3000 using ion chromatography. Dissolved organic nitrogen concentrations were determined by subtracting concentrations of nitrate and ammonium from total dissolved nitrogen (1).

Adapting typical methods for determining biologically available dissolved organic carbon (BDOC) (Kaushal and Lewis, 2005; Petrone et al., 2009; Servais et al., 1987; Wiegner et al., 2006), a slurry of sediment from the injection site was mixed with de-ionized water and was filtered through a gravity filter with 1.5 $\mu\text{m}$  filter paper to create an inoculum devoid of large particles and protozoan. Field-filtered samples (0.45 $\mu\text{m}$  filter; stored in 40 mL amber glass vials) were inoculated with 1 mL of inoculum and left in the dark at room temperature for 10 days, covered but not sealed. Blanks of de-ionized water were also inoculated to determine the amount of DOC added with the inoculum. Samples were filtered with a 0.02 $\mu\text{m}$  syringe filter before analysis. BDOC concentration was determined by subtracting the 10-day inoculated DOC concentration from the original raw DOC concentration, corrected for DOC added with the inoculum (2).

$$\text{BDOC} = \text{DOC} + \text{DOC}_1 - \text{DOC}_{10\text{d}} \quad (2)$$

Where:

BDOC = final calculated concentration of biodegradable dissolved organic carbon,

DOC = original, unaltered concentration of dissolved organic carbon,

DOC<sub>1</sub> = concentration of DOC added with the inoculum,

DOC<sub>10d</sub> = concentration of DOC in the sample 10 days after inoculation.



## 6 STATISTICAL ANALYSIS

Samples collected during the longitudinal sampling regime were analyzed in MATLAB (Appendix K) to compare rates and magnitudes of longitudinal changes in solute concentrations, equality of median analyte concentrations among the seasons, and correlations between the median analyte concentrations and environmental factors. Samples taken at the source springs were removed from analysis because they more closely resembled groundwater than surface water. Likewise, samples below the transition from first order to second order were removed due to the influence of the additional non-studied tributary. The remaining data represent a 900m reach devoid of any observable surficial inflows. Analytes investigated include dissolved inorganic carbon (DIC), dissolved organic carbon (DOC), biodegradable/labile dissolved organic carbon (BDOC), refractory dissolved organic carbon (RDOC), total dissolved nitrogen (TDN), dissolved organic nitrogen (DON), nitrate ( $\text{NO}_3^-$ ), ammonium ( $\text{NH}_4^+$ ), phosphate ( $\text{PO}_4^{3-}$ ), sulfate ( $\text{SO}_4^{2-}$ ), chloride ( $\text{Cl}^-$ ), oxygen isotopes ( $\delta^{18}\text{O}$ ), hydrogen isotopes ( $\delta\text{D}$ ), deuterium excess (d-excess), and ratios of  $\text{DOC}/\text{DON}$ ,  $\text{DOC}/\text{PO}_4^{3-}$ , and  $\text{TDN}/\text{PO}_4^{3-}$ . D-excess (3) was used as a measure of variation from the global meteoric water line (GMWL) to determine variations in isotopic fractionalization (Dawson and Simonin, 2011).

$$d - excess = \delta D - 8 * \delta^{18}O \quad (3)$$

In order to compare rates and magnitudes of longitudinal changes in analytes among the seasons, analyte concentrations were plotted by sampling period and distance downstream from the springs (Appendix A). Changes in concentration over distance (slope) were calculated from the springs to the first detailed experiment site (0 – 230m), from the first experiment site to the outlet (230 – 1130m), and the total reach length from springs to outlet (0 – 1130m) (Appendix B). This segmentation of the reach allows for analysis of rapid changes from the springs (<230 m),

changes after the stream reaches a more stable steady-state, and net overall dynamics.

In order to evaluate seasonal differences among the analytes, median values of the seventeen analytes or derived parameters were analyzed in MATLAB for normality and equal variance, which were ultimately used to test equality of median concentrations over the seasons (Appendix C and Appendix K). Each analyte was tested for normality using a non-parametric Shapiro-Wilk test at a significance level of  $p=0.05$ . Analytes were then tested for equal variance at a significance level of  $p=0.05$  using a parametric Bartlett test for normally-distributed analytes, and a non-parametric Levene test for the others. In order to specify if there were significant differences among the seasonal medians, the analytes were analyzed using a non-parametric, multi-way Kruskal-Wallis analysis of equal medians at a significance level of  $p=0.05$ . A non-parametric test was used because no analyte was shown to have equal variance. Lastly, because the Kruskal-Wallis test showed significant differences among all seasonal medians, a non-parametric Dunn-Sidak multiple comparison pair-wise test was performed for each analyte to specify individual differences among the six sampling periods at a significance level of  $p=0.05$ .

Single and multiple linear regressions were used to evaluate if external environmental variables significantly correlated with median analyte concentrations among the six sampling periods. Four independent environmental variables were analyzed, including average analyte concentration at the springs, discharge at the first-order reach, average daily in-stream temperature at the upstream experimental site, and a categorical, binary canopy variable (leaves on or off) (Appendix D). Average analyte concentrations at the spring were used to represent a groundwater input end-member, and hence they were used to test the influence of groundwater versus terrestrial inputs on in-stream concentrations. Upstream discharge was used to analyze if the solutes became diluted with baseflow, testing the influence of baseflow on in-stream concentrations. Canopy cover and

in-stream temperature and were used to evaluate the role of light and temperature on in-stream processes affecting in-stream solutes. Regressions were performed for each analyte and any combination of one, two, three, or four independent variables. Regression equations and coefficients were tested at a significance level of  $p=0.05$ . Due to the low number of data-points and degrees of freedom (6 sampling periods, 4 independent variables), many significant multi-variable relationships ( $p<0.05$ ) resulted, but most of these relationships failed to have significant coefficients ( $p<0.05$ ) and were eliminated from analysis. Multiple-variable regressions that included coefficients that were not independently significantly correlated were also eliminated from analysis.

## 7 RESULTS

### 7.1 HYDROLOGY

The highest baseflow discharge (17 L/s) occurred in the spring (April), and the lowest baseflow discharge ( $< 0.1$  L/s) occurred in the fall (September) during a drought (Figure 7). Discharge typically increased in the downstream direction (gaining stream) except during the September 2010 drought when upstream discharge exceeded downstream (losing stream).

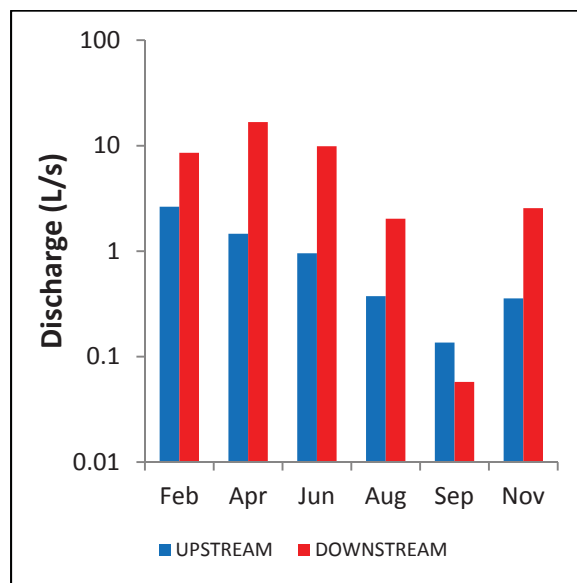


**Figure 7. Seasonal variations in discharge.**

*“Upstream” refers to values at the upstream sampling location.*

*“Downstream” refers to values at the downstream sampling location.*

In September 2010, the northeast climate region - which comprises all states northeast of West Virginia, Maryland, and Delaware - was at the tail-end of a summer-long drought preceded by three months of below normal precipitation (NRCC, 2010). This period was marked by several drought declarations including a drought warning (9/24/2010 to 10/31/2010) in the nearby lower basin of the Delaware River Basin (Rupert and O'Hara, 2010a, b), a drought watch (9/16/2010 to 11/10/2010) in numerous Pennsylvania Counties including Chester County adjacent to Fair Hill (Rathbun, 2010; Smith, 2010), and a streamflow drought watch (9/15/2010 to 9/30/2010) in the

Northern Central Climate Division 6 of Maryland where Fair Hill is located (MDE, 2017). Concurrently, reduced crop yields, local water restrictions, increased fire risks, and boat ramp closures from low water were reported across the region (NRCC, 2010).

The impact of drought on in-stream hydrology was analyzed using the Palmer Hydrological Drought Index (PHDI) (Figure 8). PHDI measures hydrological drought, as opposed to meteorological drought indices like the Palmer Drought Severity Index (PDSI) (Heim Jr., 2002). The PHDI thus illustrates the impacts of drought on stream flow (Heim Jr., 2002). As evidenced by the PHDI, stream flows in the region experienced a three month “moderate drought” during the summer of 2010 directly preceding the September 2010 sampling campaign (Figure 8). In fact, the drought concluded with a record amount of rainfall from the remnants of Tropical Storm Nicole on September 30<sup>th</sup>, 2010, four days after the sampling campaign, thus skewing the monthly PHDI in September 2010 to non-drought status (NOAA, 2010; NRCC, 2010).

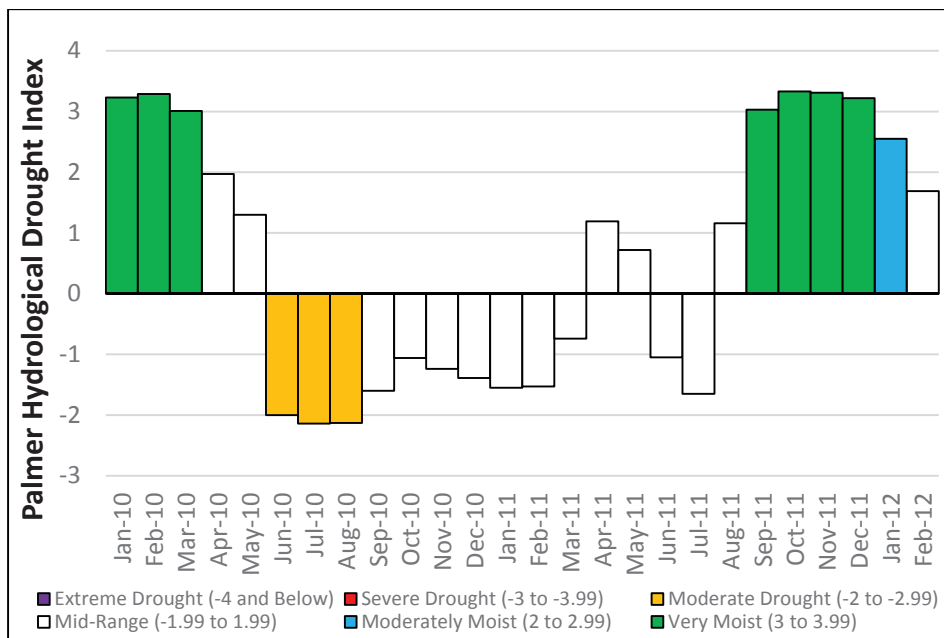


**Figure 8. Palmer Hydrological Drought Index (PHDI) in the Northern Central Climate Division 6 of Maryland.**  
*Data from NOAA (2012).*

## 7.2 CONSERVATIVE SOLUTES & TRACERS

Conservative natural tracers (chloride and both isotopes of water) were relatively constant both spatially and temporally across all sampling periods, with the exception of chloride concentrations downstream of the confluence with the adjacent first-order tributary. Temporally, isotopic compositions experienced little variation among the seasonal sampling periods. For instance, baseflow compositions of  $\delta^{18}\text{O}$  varied seasonally in a sine-wave distribution with an amplitude of only 0.32‰ (Figure 9), similar to other catchments in the Chesapeake Bay region (Table 19). In-stream seasonal variations clearly mirrored variations at the source springs (Figure 9), which is unsurprising given that in-stream compositions of both  $\delta^{18}\text{O}$  and  $\delta\text{D}$  were both strongly correlated with compositions at the source (adjusted  $R^2=92\%$  and  $82\%$ , respectively) (Appendix D).

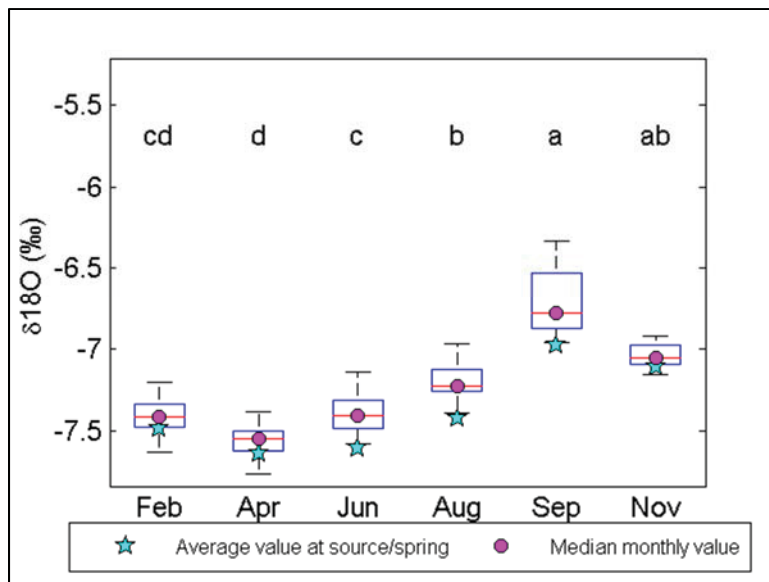


**Figure 9. Seasonal variations in  $\delta^{18}\text{O}$ .**

**Table 19. Annual amplitudes of  $\delta^{18}\text{O}$  in precipitation and baseflow in Chesapeake Bay region watersheds.**

State	Basin	$\delta^{18}\text{O}$ amplitude in precipitation (‰)	$\delta^{18}\text{O}$ amplitude in groundwater /baseflow (‰)	Reference
<b>MD</b>	Fair Hill	-	0.32	This study
<b>PA</b>	Shale Hills Critical Zone	37.8	7.0	(Jin et al., 2011)
	Benner Run	3.41	~0	(DeWalle et al., 1997)
	Mahantango: Brown WS	1.84	0.21	(McGuire et al., 2002)
	Leading Ridge WS1	1.52	0.52	(McGuire et al., 2002)
<b>WV</b>	Fernow WS3	3.15	0.31	(DeWalle et al., 1997)
	Fernow WS4	3.15	0.34	(DeWalle et al., 1997)
<b>VA</b>	Shenandoah Nat'l Park	9.6	0.1	(Plummer et al., 2001)
	Shelter Run	7	1.2	(Böhlke and Michel, 2009)
	Mill Run	7	2.4	(Böhlke and Michel, 2009)

Spatially, conservative tracers were relatively constant upstream to downstream, though chloride concentrations changed dramatically downstream of the confluence with another first order stream. Looking at isotopic compositions,  $\delta^{18}\text{O}$ ,  $\delta\text{D}$ , and d-excess compositions experienced minor longitudinal variations once emerging from the springs (Figure 10 and Appendix A). Net upstream to downstream changes in  $\delta^{18}\text{O}$  values were between -0.05 ‰/km (negative indicates longitudinal decline) and +0.44 ‰/km (positive indicates longitudinal increase) (Appendix B). Likewise,  $\delta\text{D}$  values varied between -0.41 ‰/km and +2.3 ‰/km among the sampling periods (Appendix B). Even with the addition of another first-order stream 1130m below the springs, isotopic compositions remained relatively unchanged (Figure 10). Chloride concentrations, however, were clearly affected by the additional tributary, with concentrations spiking below the confluence (Figure 11). Therefore, due to this significant - and unpredictable - influence of the unstudied tributary on the biogeochemistry of the study reach, analyses excluded all samples (conservative and otherwise) downstream of the confluence.

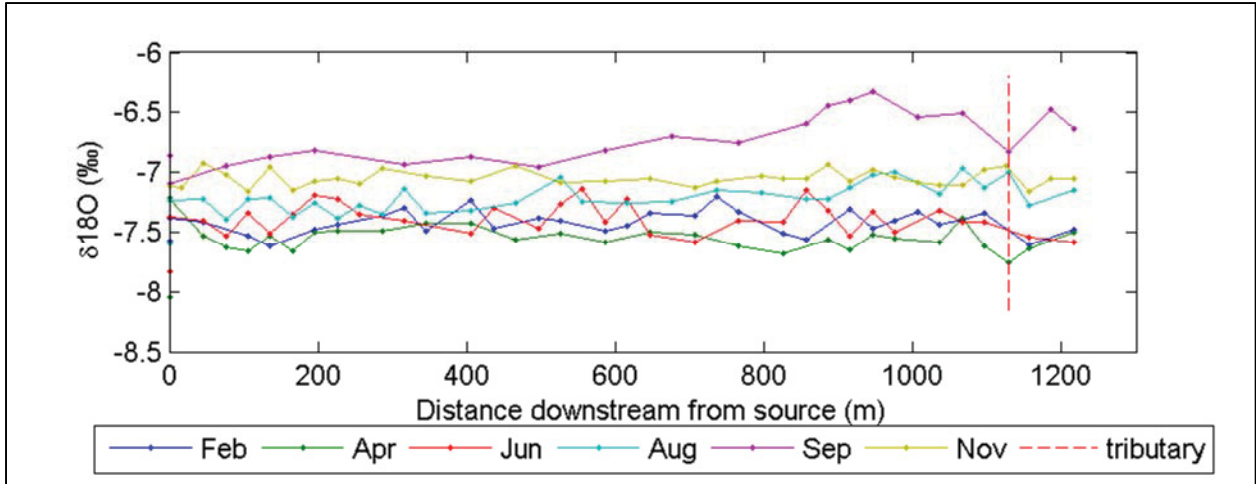


Figure 10. Longitudinal variations in  $\delta^{18}\text{O}$ .

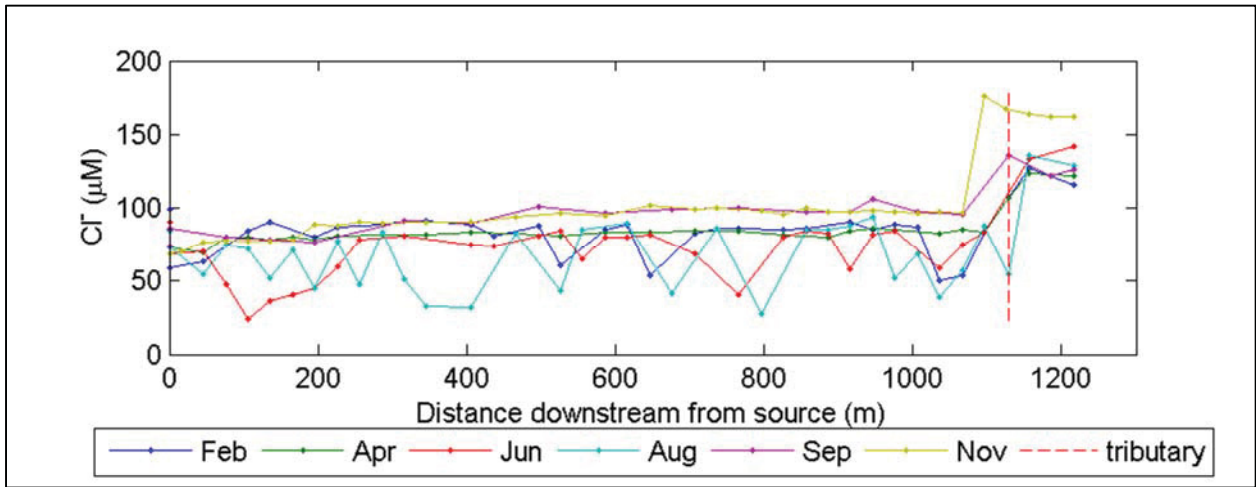


Figure 11. Longitudinal variations in chloride.

### 7.3 ECOSYSTEM METABOLISM

The stream at Fair Hill was net heterotrophic during all sampling periods with negative net ecosystem metabolism (NEM) (Figure 12) and P/R ratios much lower than unity (Table 20). GPP was typically insignificant, with the largest values in April and June each totaling less than one fifth of respiration (Figure 12 and Table 20). NEM correlated with temperature ( $R^2 = 76\%$ ) and canopy cover ( $R^2 = 74\%$ ), with temperature and NEM peaking in the summer when the canopy was closed (negative NEM values indicate respiration). Unlike temperature and ecosystem



metabolism, pH was relatively static throughout the year, only dipping slightly in September and November (Figure 12).

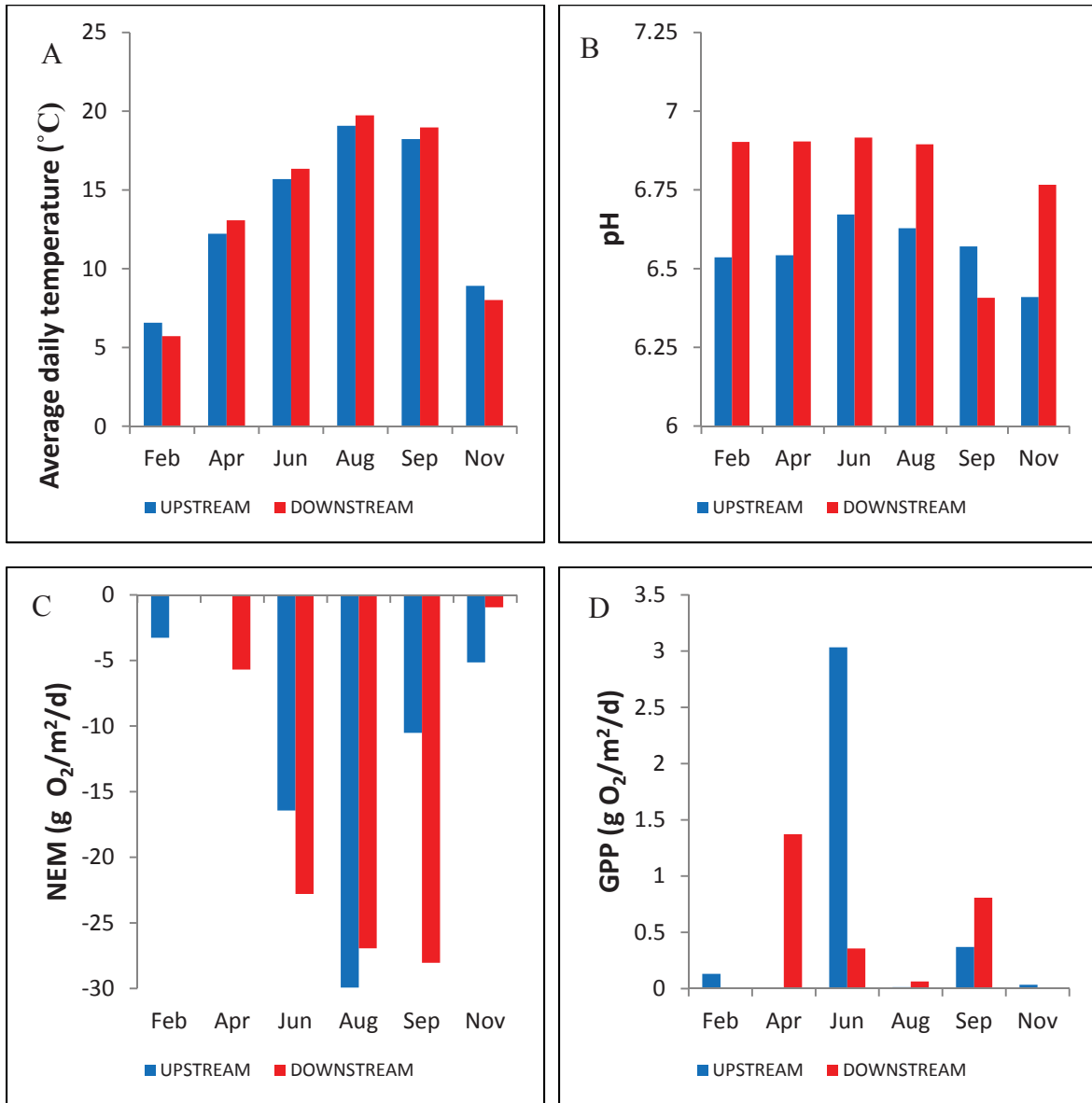


**Figure 12. Seasonal variations in average daily temperature (A), pH (B), net ecosystem metabolism (NEM) (C), and gross primary production (GPP) (D).**

*“Upstream” refers to values at the upstream sampling location.*

*“Downstream” refers to values at the downstream sampling location.*

**Table 20. Ecosystem metabolism at the upstream and downstream experimental sites measured over a 24 hr. period.**

Year	Month	Location	Net ecosystem metabolism (gO <sub>2</sub> /m <sup>2</sup> /d)	Respiration (g O <sub>2</sub> /m <sup>2</sup> /d)	Gross primary production (g O <sub>2</sub> /m <sup>2</sup> /d)	P/R	Average daily temperature (°C)	pH
2012	Feb	Upstream	-3.26	-3.38	0.13	0.039	6.57	6.54
		Downstream	*	*	*	*	5.71	6.90
2011	Apr	Upstream	*	*	*	*	12.2	6.54
		Downstream	-5.70	-6.92	1.37	0.198	13.1	6.90
2011	Jun	Upstream	-16.4	-19.5	3.03	0.156	15.7	6.67
		Downstream	-22.8	-22.6	0.36	0.016	16.3	6.92
2011	Aug	Upstream	-29.9	-23.4	0.01	0.001	19.1	6.63
		Downstream	-26.9	-26.0	0.06	0.002	19.7	6.90
2010	Sep	Upstream	-10.5	-10.7	0.37	0.035	18.2	6.57
		Downstream	-28.0	-28.7	0.81	0.028	19.0	6.41
2010	Nov	Upstream	-5.14	-5.12	0.03	0.007	8.91	6.41
		Downstream	-0.95	-0.82	0.004	0.005	8.01	6.77

\*Instrument malfunction prevented NEM from being calculated.

## 7.4 DISSOLVED ORGANIC MATTER

Dissolved organic matter dynamics appear to vary both spatial and temporally at Fair Hill. As a result, three patterns emerged: 1) although concentrations of dissolved organic matter were typically lower in periods of higher flows, and vice versa, dissolved organic matter concentrations increased from upstream to downstream during all sampling periods; 2) dissolved organic matter was largely refractory in nature; and 3) during the September 2010 drought, the conversion of biologically available organic matter to refractory was particularly pronounced.

Although median in-stream DOC concentrations were lower in the spring when baseflows were higher and were higher in fall when baseflows were lowest, organic matter concentrations consistently increased from source to outlet across all sampling periods. Seasonally, among the sampling periods, the six median in-stream DOC concentrations were inversely correlated to their respective discharges measured at the Parshall flume (adjusted  $R^2$  value of 58%) (Appendix D). In other words, DOC concentrations were generally lower during periods of higher discharge (spring), and concentrations were higher during periods of low baseflow discharge (fall) (Appendix C and Appendix F). Spatially however, DOC concentrations increased from upstream to downstream during all sampling periods, with the largest gains consistency made along the first 230m of the reach after emerging from the springs (Figure 13 and Appendix B). Similarly, dissolved organic nitrogen (DON) dynamics mirrored DOC: as DON concentrations increased downstream of the springs (Appendix A), total dissolved nitrogen (TDN) transitioned from primarily inorganic to proportionally more organic (Table 21). Consequentially, dissolved organic matter concentrations increased with distance downstream from the source springs during all sampling periods, even though dissolved organic matter concentrations were generally higher in periods of lower flow.

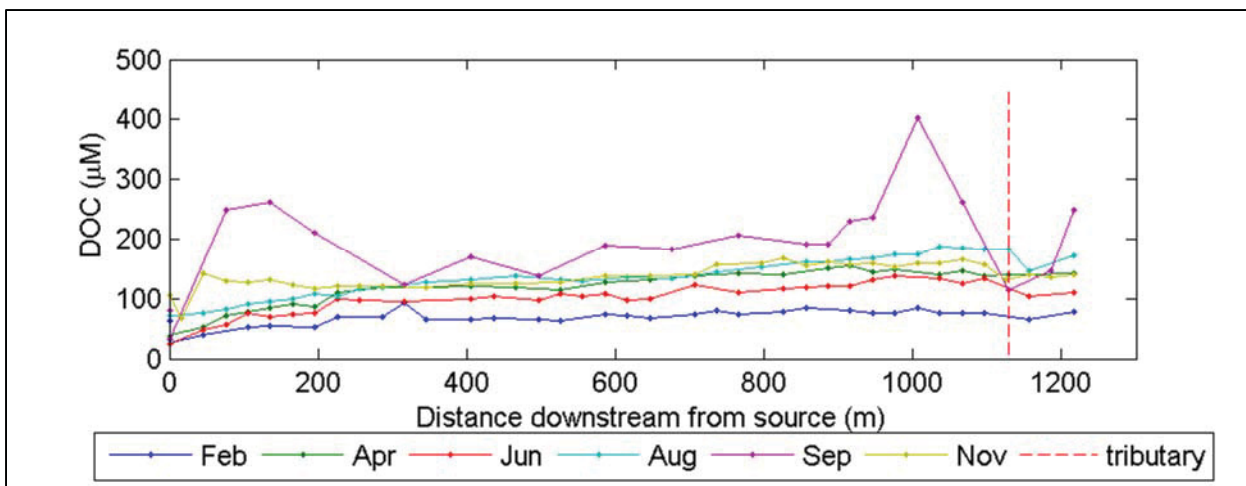


**Figure 13. Longitudinal variations in DOC concentrations.**

**Table 21. Percent contribution of DON to TDN.**

Location	Feb	Apr	Jun	Aug	Sep	Nov	Total
<b>Springs (mean)</b>	22%	39%	0%	7%	11%	0%	12%
<b>In-stream (median)</b>	30%	46%	29%	29%	55%	72%	41%

These organic inputs to the stream at Fair Hill were refractory and nitrogen-poor. Throughout the study, with the exception of the September sampling period, DOC concentrations mirrored refractory DOC concentrations (RDOC), co-increasing together along the length of the stream. In other words, for all sampling periods except September, longitudinal increases in DOC and RDOC concentrations were within 20% of each other, showing that increases in total DOC concentrations simply reflected increases in refractory DOC and vice versa (Appendix B). Closer examination showed that DOC was primarily refractory (85%) with labile BDOC accounting for just 15% of DOC (Table 26). Similarly, in-stream dissolved organic matter was also nitrogen-poor, with median in-stream DOC:DON ratios typically above 15:1 (Appendix C), exceeding the Redfield ratio of approximately 7:1 (Redfield, 1958). Therefore, in-stream dissolved organic matter at Fair Hill was both nitrogen-limited and predominantly refractory.

**Table 22. Percent contribution of BDOC to DOC.**

<b>Location</b>	<b>Feb</b>	<b>Apr</b>	<b>Jun</b>	<b>Aug</b>	<b>Sep</b>	<b>Nov</b>	<b>Total</b>
<b>Springs (mean)</b>	24%	51%	75%	36%	73%	34%	50%
<b>In-stream (median)</b>	15%	14%	28%	7%	22%	8%	15%

Unlike most sampling periods, longitudinal increases in concentrations of RDOC and DOC diverged during the September 2010 drought instead of mirroring each other. Overall, this sampling period experienced the highest in-stream dissolved organic matter concentrations, including concentrations of DOC, RDOC, biologically available DOC (BDOC), and dissolved organic nitrogen (DON) (Appendix F). Spatially, in-stream DOC concentrations in September increased by 28  $\mu\text{M}/\text{km}$  longitudinally while RDOC concentrations increased about three times more at 97  $\mu\text{M}/\text{km}$ . The 69  $\mu\text{M}/\text{km}$  difference is remarkably similar to the concurrent -76  $\mu\text{M}/\text{km}$  decrease in biologically available DOC concentrations (BDOC). Moreover, this longitudinal decrease in BDOC concentrations during September was far greater in magnitude than the longitudinal changes observed in the other sampling periods, which fell between -11 and +11  $\mu\text{M}/\text{km}$ . Therefore, while a portion of the net increase in RDOC concentrations in September can be attributed to the typical pattern of DOC and RDOC concentrations increasing together due to refractory organic inputs, the remainder of the large RDOC increase in September appears to result from BDOC cycling to more refractory forms.

## **7.5 DISSOLVED INORGANIC NUTRIENTS**

Analyses of in-stream inorganic nutrients - including phosphate, nitrate, ammonium, and total dissolved nitrogen (TDN) - revealed that while the stream at Fair Hill was always phosphorus- and nitrogen-limited, their spatial and temporal dynamics were controlled by seasonal biological processes. Across all study periods, in-stream carbon-to-nitrogen (C:N) and carbon-to-phosphorus (C:P) ratios always exceeded their respective Redfield ratios of 106:16 and 106:1 (Appendix F),

indicating that in-stream conditions were constantly both nitrogen- and phosphorus-limited (Redfield, 1958). Additionally, TDN-to-phosphate (N:P) ratios always exceeded the Redfield ratio of 16:1 showing that phosphorus was more limiting than nitrogen. Upon closer examination though, both in-stream nitrogen and phosphate dynamics varied seasonally and spatially. Specifically, nitrate concentrations declined in the fall but not in the spring, while ammonium and phosphate concentrations increased during the growing season.

Looking at seasonal nitrate dynamics, median in-stream concentrations were relatively stable across most sampling periods except in the falls months of September and November when nitrate concentrations decreased both overall and longitudinally, driving similar trends in total dissolved nitrogen (TDN). For example, longitudinal decreases in nitrate concentrations in September and November ( $-9.3 \mu\text{M}/\text{km}$  and  $-5.8 \mu\text{M}/\text{km}$ ) were more than twice the other sampling periods - which were between  $-2.6$  and  $+0.10 \mu\text{M}/\text{km}$  (Appendix B). Similarly, TDN concentrations decreased about  $-6.6 \mu\text{M}/\text{km}$  and  $-5.4 \mu\text{M}/\text{km}$  longitudinally during September and November respectively, largely reflective of losses in nitrate (Appendix B). Median in-stream nitrate concentrations were also significantly lowest in September and November (Figure 14), and unsurprisingly, the lowest median TDN concentrations also occurred in November (Appendix C). Interestingly, there were no other exaggerated declines in nitrate and TDN, either overall or longitudinally, during the winter, spring, or summer sampling periods. Therefore, the fall sampling periods of September and November uniquely experienced the largest in-stream declines in nitrate and TDN concentrations.

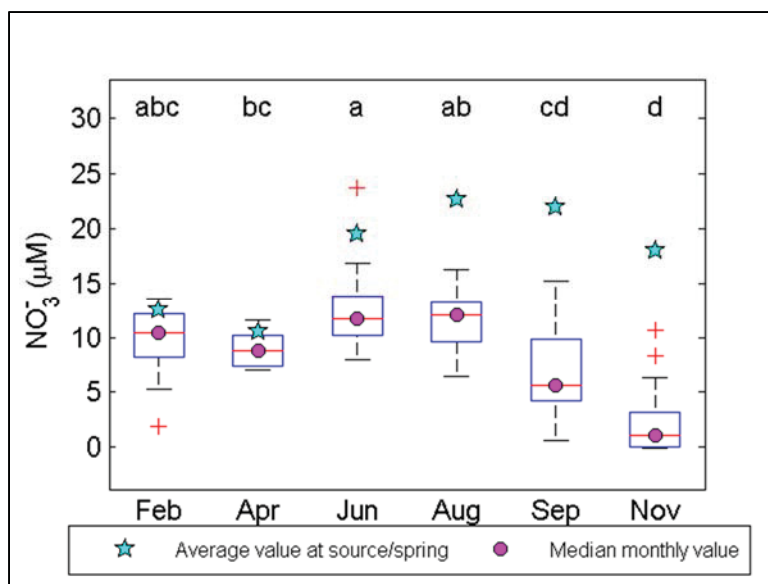


**Figure 14. Seasonal variations in nitrate concentrations.**

Unlike nitrate and TDN concentrations, in-stream ammonium and phosphate concentrations both experienced distinct seasonal peaks when the stream was shaded during growing season. In fact, canopy cover was significantly correlated to both nutrients with adjusted  $R^2$  values over 80% (ammonium= $0.40\mu\text{M}$  without canopy,  $1.3\mu\text{M}$  with; phosphate= $0.32\mu\text{M}$  without canopy,  $0.63\mu\text{M}$  with) (Appendix D). Thus, ammonium and phosphate concentrations were lower when the canopy was bare, and both doubled or more when shaded. In fact, during June, August and September, ammonium and phosphate concentrations were significantly greater than the other sampling periods (Figure 15 and Figure 16). However, in the months with the lowest ammonium concentrations - April and November - in-stream ammonium areal uptake rates were diametrically different, indicating that low concentrations were not predominantly driven by uptake (Appendix J)<sup>2</sup>. Thus while ammonium uptake experiments were inconclusive, stream-wide dynamics show that ammonium and phosphate concentrations were highest during the growing season.

<sup>2</sup> An areal uptake rate of  $0.03 \mu\text{mol}/\text{m}^2/\text{s}$  indicates that a square meter of stream bed removes  $0.03 \mu\text{mol}$  of ammonium from the water column per second, or about  $2600 \mu\text{mol}$  per day.

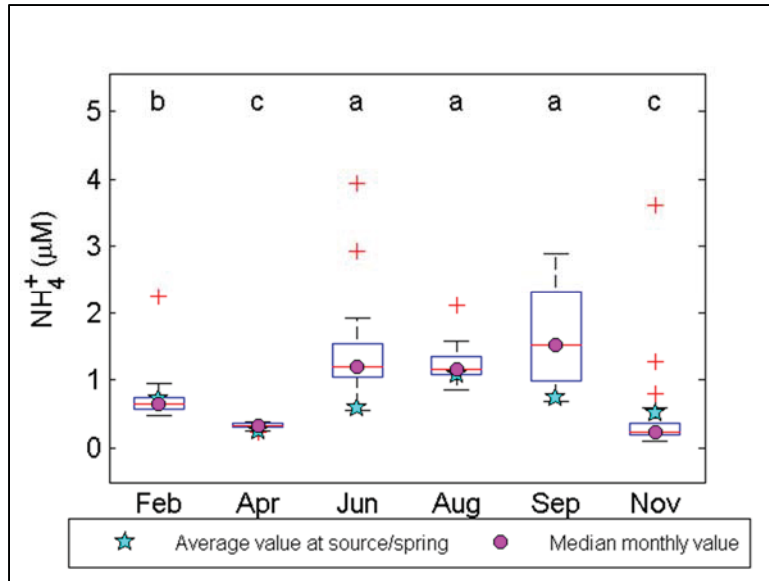


Figure 15: Seasonal variations in ammonium concentrations.

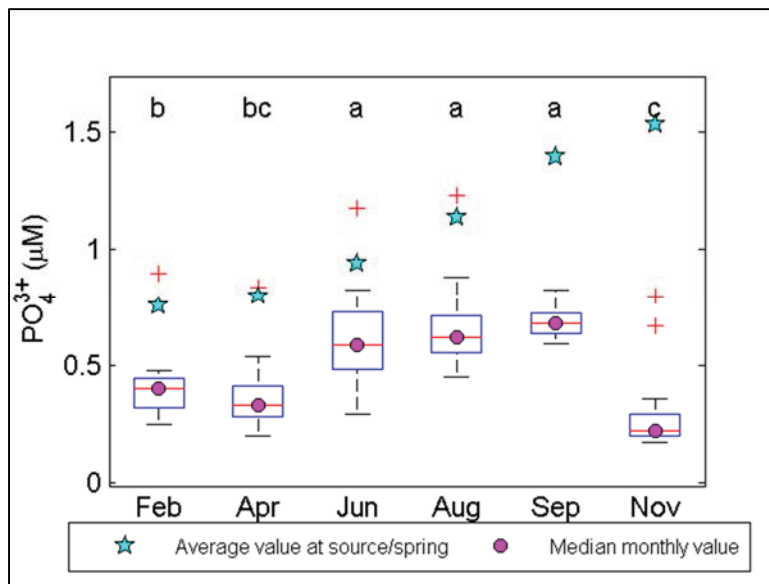


Figure 16: Seasonal variations in phosphate concentrations.



## **8 DISCUSSION**

The purpose of this study was to elucidate catchment and in-stream controls on carbon and nitrogen export and retention during baseflow in a headwater, forested catchment in the Piedmont physiographic province of the Chesapeake Bay watershed. Environmental factors of light availability and temperature, in addition to inorganic and organic in-stream nutrient dynamics, were analyzed to determine seasonal and spatial variations of in-stream processes throughout the watershed. The results add to previous studies at Fair Hill by shifting focus from stormflow to baseflow dynamics and in-stream processes, with an additional examination of in-stream biogeochemistry during a drought in 2010. Through these studies, it was shown that catchment inputs via groundwater and allochthonous organic matter set the foundation lotic biogeochemistry at Fair Hill, creating a nutrient-limited, heterotrophic reach. Within this setting, three temporal “hot-moments” of in-stream nutrient processes were observed: the release of ammonium and phosphate during the warm – but shaded – summer months; nitrate retention in the fall driven by leaf-litter; and a unique moment of nitrate uptake and respiration induced degradation of labile organic matter during a drought. As a result, baseflow biogeochemistry at Fair Hill is neither homogenous among the seasons nor along the reach, but rather varies constantly throughout the year in response to light availability, temperature, and in-stream organic matter dynamics.

### **8.1 CATCHMENT INPUTS TO THE STREAM**

Catchment-wide inputs underlie in-stream baseflow biogeochemistry at Fair Hill. At the most fundamental level, groundwater-fed baseflow provides a relatively constant and unvarying input along the entire stream reach. However, this groundwater source is nutrient-limited, resulting in a similarly nutrient-limited lotic environment, with phosphorus particularly in demand. Moreover, groundwater - along with autotrophy - appear to be minor sources of organic matter to the stream;

as such, refractory terrestrial sources predominate organic inputs, driving in-stream respiration and organic matter dynamics. In sum, nutrient-limited groundwater and terrestrial organic matter set the foundation for in-stream biogeochemistry and processes at Fair Hill, creating a nutrient-limited, heterotrophic reach.

### ***8.1.1 Groundwater hydrologic inputs***

Spring-fed baseflow is the underlying source for relatively unvarying in-stream biogeochemistry at Fair Hill. While previous studies have found that not only is baseflow discharge at Fair Hill correlated with depth to groundwater (Inamdar et al., 2013; Inamdar et al., 2011b), in-stream baseflow chemistry also, unsurprisingly, was found to correlate with the chemistry of deep groundwater and groundwater seeps feeding the stream (Inamdar et al., 2013). Similarly, this study found that median in-stream  $\delta^{18}\text{O}$  and  $\delta\text{D}$  isotopic compositions were positively correlated to their compositions at the source springs with adjusted  $R^2$  values of 92% and 82%, respectively (Appendix D). In other words, previous studies and isotopic analyses in this study confirm that baseflow at Fair Hill is nearly entirely groundwater-based instead of originating from surficial runoff, soil water, or shallow groundwater. Moreover, the biogeochemistry of this groundwater source is notably constant, both seasonally and spatially along the reach. For example, even though the range of baseflow discharges at Fair Hill spanned several orders of magnitude across the seasons (Figure 5 and Figure 7), baseflow isotopic compositions of  $\delta^{18}\text{O}$  experienced minimal seasonal variation (Figure 9). This annual consistency pales in comparison to the in-stream variation observed at Fair Hill during a single storm (1.5‰) (Inamdar et al., 2011b). Spatial variations were similarly minor, with  $\delta^{18}\text{O}$  values changing between -0.05 and 0.24 ‰/km upstream to downstream,  $\delta\text{D}$  values changing between -0.41 and 0.80 ‰/km, and d-excess values changing between -1.1 and 0.31 ‰/km (Appendix B). This lack of longitudinal variation also

demonstrates that there were no observable inflows of water with distinctly different isotopic signatures between the source and the downstream adjoining tributary. Therefore, because the groundwater source was so constant, both temporally and spatially, any significant in-stream biogeochemical variations likely occurred due to surficial – not subsurface - sources and processes.

### ***8.1.2 Groundwater nutrient inputs***

As a result of nutrient-limited groundwater, baseflow at Fair Hill was also nutrient-limited, with phosphorus more limiting than nitrogen. For example, in-stream phosphate concentrations peaked at the source springs (averaging 1.05  $\mu\text{M}$ ) and then declined along the reach (Appendix A and Appendix F). Low phosphate concentrations (Appendix F) in-turn caused carbon-to-phosphorus ratios and nitrogen-to-phosphorus ratios to exceed the Redfield ratios of 106:1 and 16:1, respectively, during all sampling periods (Redfield, 1958). In other words, the stream was phosphorus-limited relative to both carbon and nitrogen. Given that Piedmont streams are typically phosphorus-limited (Miller et al., 1997), it is not surprising that low phosphate concentrations observed at Fair Hill also resemble in-stream concentrations found throughout the region (Table 23). Similarly, the average nitrate concentration at the source springs in Fair Hill was only 17.5  $\mu\text{M}$  (Appendix F) compared to typical groundwater values of 257  $\mu\text{M}$  in the Big Elk Creek basin (Sloto, 2002). With a median concentration of 9.50  $\mu\text{M}$ , in-stream nitrate concentrations (and consequentially TDN concentrations) at Fair Hill were much lower than regional norms (Table 23), causing nitrogen to be either limiting or close to limiting during all sampling periods. Like phosphate, low nitrate concentrations at Fair Hill were not entirely unexpected, as forested streams in the Piedmont typically export less nitrate than agricultural streams (Jordan et al., 1997a, b), and riparian buffers greatly reduce nitrate inputs from shallow groundwater across the region (Table 6). Given that Fair Hill is predominantly forested with a mature riparian buffer and shallow

groundwater (Inamdar et al., 2011b), nitrate concentrations were likely reduced substantially before reaching the stream channel. Nutrient-deficient groundwater inputs at Fair Hill therefore set the stage for nitrogen and phosphate limited in-stream conditions.

**Table 23. In-stream nutrient concentrations of select basins near Fair Hill.**

Basin	Nitrate ( $\mu\text{M}$ )	TDN ( $\mu\text{M}$ )	Ammonium ( $\mu\text{M}$ )	Phosphate ( $\mu\text{M}$ )	Reference
<b>Piedmont</b>		166			(Morgan II et al., 2013)
<b>Piedmont</b>	111		1.4	0.65	(Miller et al., 1997)
<b>Piedmont</b>	243	243	6.4	1.14	(Liu et al., 2000)
<b>Elk River</b>	106	144	2		(Morgan II and Kline, 2011)

### ***8.1.3 Catchment-wide organic inputs***

Even though in-stream respiration was experimentally confirmed during all sampling periods at Fair Hill, in-stream DOC concentrations increased longitudinally from source to outlet during all sampling periods clearly demonstrating that organic inputs far exceeded demand (Brookshire et al., 2009). However, seasonal and spatial variations were closely studied in order to disentangle the various environmental, in-stream, and qualitative influences on in-stream organic matter dynamics. Accordingly, this study has found that while both groundwater and autotrophy are minor sources of lotic organic matter, most in-stream organic matter originates from surficial, refractory sources driving in-stream heterotrophic respiration.

Investigations of both dissolved organic carbon (DOC) and organic nitrogen (DON) in this study find that groundwater was a minor source of dissolved organic matter to the stream. Previous wet weather studies at Fair Hill first examined this trend, finding that DOC concentrations were lower during baseflow, but increased substantially during stormflow (Inamdar et al., 2011a; Inamdar et al., 2011b). Consequentially, baseflow was found to contribute 43% of exported DOC in 2010 and 24% in 2011 at Fair Hill (Dhillon and Inamdar, 2013), similar to contributions of 34% observed in

nearby White Clay Creek (Newbold et al., 1997). These results were confirmed in this study, finding that baseflow discharge and DOC concentrations were inversely related. In other words, dissolved organic matter concentrations were generally lower during periods of higher baseflow. This inverse relationship is consistent with observations of 10 other Piedmont streams, for the same reason that groundwater (as compared to other hydrologic sources such as shallow flow or surface runoff) is not typically a predominant source of dissolved organic matter to Piedmont streams (Jordan et al., 1997b). Accordingly, groundwater inputs in this study were exceeded by other sources, as the average DOC concentration at the source springs (50  $\mu\text{M}$ ) was much lower than the in-stream median (122  $\mu\text{M}$ ). Likewise, average DON concentrations were also lower at the source springs than the in-stream median. This increase in organic matter from groundwater to the stream channel is similar to previous grab samples at Fair Hill which found DOC concentrations of about 63-92  $\mu\text{M}$  in seeps, deep groundwater, and riparian groundwater, and higher concentrations of about 139  $\mu\text{M}$  in baseflow (Inamdar et al., 2011b). Likewise at nearby White Clay Creek, mean in-stream DOC concentrations of 178  $\mu\text{M}$  (Kaplan et al., 1980) were higher than groundwater concentrations of 57  $\mu\text{M}$  (Newbold et al., 1997). Therefore, this study shows that groundwater was a persistent, though minor, source of organic matter at Fair Hill, indicating that most in-stream baseflow organic matter originated from surficial sources instead.

Like groundwater, further observations also reveal that autotrophy was not a significant source of organic matter to the stream at Fair Hill, nor did in-stream production substantially affect in-stream ecosystem metabolism. Examining production values, some GPP was recorded at Fair Hill during each sampling period, peaking in April and June (Figure 12). These seasonal bursts of GPP corresponded with observations at several nearby Piedmont streams, peaking with peak solar radiation in mid-April and declining throughout the rest of the year [e.g. (Bott et al., 1985; Bott et

al., 2006)]. Production at Fair Hill, however, never predominated, failing to exceed 20% of respiration during any sampling period. Moreover, while in-stream DOC concentrations varied seasonally, there were no significant differences in DOC concentrations between April and June (canopy off and on), as would be expected if algal growth peaked in the spring prior to shading from leaf-out (Appendix C). In other words, vernal production, or production during any other season, failed to create an observable release of autochthonous organic matter to the stream. Therefore, in-stream biogeochemistry at Fair Hill appears to be little influenced by autochthonous organic matter in contrast to other forested headwater streams in the Piedmont (Kaplan et al., 1980) and elsewhere (Roberts et al., 2007a; Roberts and Mulholland, 2007).

Given that autotrophy and groundwater were both minor sources of organic matter at Fair Hill, in-stream organic matter was predominated by terrestrial inputs, influencing in-stream biogeochemistry and metabolism. Consistent with this study, previous end-member mixing analyses showed that most in-stream organic matter at Fair Hill originated not from groundwater or autotrophy, but from surficial sources such as precipitation, throughfall, stemflow, leaf leachate, and soil water (Inamdar et al., 2011a; Inamdar et al., 2011b). Spatially, this study finds that these inputs were most pronounced in the first 230m of the stream, where longitudinal increases in DOC concentrations were greatest. In other words, the uppermost reach at Fair Hill was a “hotspot” of organic matter inputs, perhaps originating from organic matter-rich soil water from nearby valley-bottom wetlands (Inamdar et al., 2011a). Similarly in nearby White Clay Creek basin, a hotspot of significant increases in DOC concentrations were observed within the first 100m of the stream, likely due to similar environmental and topographic conditions (Kaplan et al., 1980; Kuserk et al., 1984). At all locations in Fair Hill though, during all sampling periods except September, longitudinal increases in DOC and RDOC concentrations mirrored each other indicating that

refractory inputs were driving in-stream DOC concentrations. Closer examination reveals that in-stream DOC was overwhelming refractory (about 85%), with contributions from BDOC only amounting to about 15%, similar to White Clay Creek where about 9-31% of DOC was biologically available (Table 12). With these predominantly allochthonous inputs, it is not surprising that the stream at Fair Hill was net heterotrophic with consistently negative net ecosystem metabolism and P/R ratios much lower than unity (Table 24), as predicted by the River Continuum Concept (Vannote et al., 1980). This outsized role of heterotrophy within headwater streams is commonly observed across many biomes (Bott et al., 1985; Mulholland et al., 2001), as was clearly the case at Fair Hill. Therefore, this study shows that refractory, organic terrestrial inputs drove in-stream metabolism at Fair Hill, with inputs exceeding demand along the entire reach, especially within the “hot spot” headwater wetland along the first 230m of the reach.

## 8.2 HOT MOMENTS OF IN-STREAM PROCESSES

Though catchment-wide inputs set the foundation for baseflow nutrient dynamics at Fair Hill, temporal in-stream processes ultimately played a significant role in regulating in-stream biogeochemistry. During the growing season, shading and warm temperatures led to the mobilization of ammonium and phosphorus to the stream; in the fall, increased organic inputs led to increased nitrogen uptake; and during the September drought, increased respiration rates led to a unique moment of nutrient processing, decreasing biologically available carbon and nitrate.

### *8.2.1 Nutrient export in the growing season*

During the growing season at Fair Hill, warm-temperature driven respiration released ammonium and phosphate to the lotic system, while shading concurrently prevented autotrophy and the retention of those mobilized nutrients. Trending together across all sampling periods, ammonium and phosphate concentrations were significantly highest during the growing season months of June, August, and September (Figure 15 and Figure 16). As a result, both nutrients were correlated with canopy cover (on/off), as well as temperature and NEM. In other words, when the canopy was full during the growing season, in-stream temperatures, NEM, and concentrations of ammonium and phosphate were highest. This dynamic mirrors other studies that observed respiration peaking with temperatures in the growing season in the Piedmont (Bott et al., 1985; Bott et al., 2006) as well as meta-analyses of headwater streams in many biomes (Hill et al., 2002; Hill et al., 1998b; Sinsabaugh, 1997). Additionally, warm-weather respiration is indicative of organic matter mineralization (i.e. decomposition), which has been shown to release ammonium [e.g. (Roberts and Mulholland, 2007)] and phosphate (Dodds, 2003; Reddy et al., 1999; Withers and Jarvie, 2008) to lotic systems. While ammonium and phosphate concentrations peaked at Fair Hill (Figure 14), nitrate concentrations, however, remained static indicating that released



ammonium was not substantially nitrified. This pattern has been observed in heterotrophic systems where in-stream respiration reduces lotic oxygen concentrations, thereby inhibiting oxic nitrification (Baker et al., 1999; Hedin et al., 1998); whereas in autotrophic systems, oxygen from primary production drives the opposite effect, stimulating nitrification [e.g. (Roberts and Mulholland, 2007)]. Therefore, shading and warm temperatures during the growing season at Fair Hill caused respiration to exceed production (Figure 12), stagnating nitrate concentrations as ammonium concentrations peaked. Perhaps, this prominence of ammonium mobilization over nitrification at Fair Hill also explains why ammonium concentrations correlated with temperature and NEM but not uptake. Thus, driven by warm temperatures and in-stream respiration, a hot moment of ammonium and phosphate export occurred when the stream at Fair Hill was shaded during the growing season.

### ***8.2.2 Fall nutrient retention***

While the growing season was a hot-moment of ammonium and phosphate release, the fall months were, collectively, a hot-moment of in-stream nitrate retention stimulated by organic matter inputs. In the fall sampling periods of September and November, total dissolved nitrogen (TDN) and nitrate concentrations experienced their greatest longitudinal decreases from upstream to downstream (Appendix A and Appendix B), and both of their median in-stream concentrations were lowest in November after leaf-fall (Figure 14 and Appendix C). These decreases are consistent with seasonal nitrogen retention in heterotrophic streams, whereby organic inputs from leaf-litter drive in-stream nitrate retention (Figure 2 and Table 13). In the Piedmont, similar carbon-driven nitrogen uptake has been observed (Band et al., 2001), in addition to denitrification increasing with in-stream carbon content and quality (Newcomer et al., 2012). For similar reasons in other headwater streams, inorganic nitrogen concentrations also decrease in the spring,

attributable to algal assimilation and denitrification induced by autochthonous organic matter (Figure 2 and Table 13). At Fair Hill, however, vernal nitrate concentrations remained static due to a lack of a spring-time algal bloom, as evidenced by low GPP rates (Figure 12) and no significant increase in DOC concentrations (Appendix B). Therefore, a hot moment of in-stream nitrogen uptake only occurred at Fair Hill in the fall, driven by organic inputs from leaf-fall, and a hot-moment of nitrogen uptake failed to materialize in the spring due to a lack of vernal autotrophy.

### ***8.2.3 Biogeochemical cycling during drought***

Like other hot-moments of nutrient cycling in this study, temperature and carbon dynamics formed the basis of in-stream processes during the drought at Fair Hill: organic matter trapped in disconnected pools combined with warm temperatures drove in-stream respiration, increasing nitrate uptake and decreasing organic matter quality. While some have observed that reduced surficial inputs and groundwater dilution during droughts decrease in-stream organic matter concentrations (Dahm et al., 2003), others have observed the opposite, with organic matter building up in hydrologically disconnected pools (Acuña et al., 2005; Lake, 2003; Vazquez et al., 2011; Wall et al., 1998). At Fair Hill, it appears that the latter occurred. Hydrologically, the September sampling period experienced the only losing stream scenario during this study (Figure 7), causing surficially disconnected pools to form along the reach. As a result, organic matter collected in these pools, producing the highest dissolved organic matter concentrations of dissolved organic carbon (DOC) and dissolved organic nitrogen (DON) observed in this study (Appendix C). This trapped organic matter, in conjunction with warm in-stream temperatures (Figure 12), stimulated increased rates of in-stream respiration (negative NEM) (Figure 12). Elevated respiration rates also caused the lowest pH (Figure 12) and highest dissolved inorganic carbon (DIC) concentrations observed (Appendix C), likely resulting from increased CO<sub>2</sub>

production (Nimick et al., 2011). With the downstream transport of organic matter inhibited by fragmented pools, in-stream metabolism utilized trapped organic matter, recycling biologically available carbon to lower quality refractory forms. This drought-induced reduction in carbon quality was evidenced by refractory dissolved organic carbon (RDOC) concentrations increasing at three times the rate of net DOC concentrations, concurrent with the largest longitudinal decrease in biologically available DOC (BDOC) concentrations observed in this study. In other words, new inputs alone did not account for the increase in refractory fractions along the reach, but rather biologically available carbon (BDOC) was cycling to more refractory forms. While studies of arid streams during drought have observed the opposite, with biologically available fractions increasing due to autotrophy (Dahm et al., 1998; Vazquez et al., 2011), autotrophy at Fair Hill was insignificant, particularly during the drought in the fall (Figure 12). Moreover, while heterotrophic streams typically experience increased nitrate export during the growing season due to a lack of autotrophic uptake (Figure 2 and Table 13), nitrate concentrations during the drought at Fair Hill declined both on average (Figure 14) and longitudinally (Appendix A), similar to the in-stream response to leaf-fall. This pattern of drought-induced in-stream nutrient limitations has also been observed across many biomes [e.g. (Acuña et al., 2005; Dahm et al., 2003; Wall et al., 1998)]. Therefore, warm temperatures and drought-trapped organic matter at Fair Hill induced a hot-moment of respiration, which concurrently increased in-stream nitrate uptake and the cycling of biologically available organic matter to more refractory forms.

## 9 CONCLUSION

The purpose of this study was to elucidate catchment and in-stream controls on carbon and nitrogen export and retention during baseflow in a headwater, forested catchment in the Piedmont physiographic province of the Chesapeake Bay watershed. Environmental factors of light availability and temperature, in addition to inorganic and organic in-stream nutrient dynamics, were analyzed to determine seasonal and spatial variations of in-stream processes throughout the watershed.

Catchment-wide inputs set the underlying foundation for baseflow dynamics at Fair Hill. From season to season, the water quality of the groundwater-fed springs was relatively stable in composition, providing a relatively stable foundation for baseflow biogeochemistry. This source was nutrient-limited, resulting in nutrient limitations along the reach, with phosphorus particularly in demand. Groundwater – along with autotrophy – were also poor sources of organic-matter to the lotic system; instead, organic inputs were predominated by refractory, surficial sources. As a result, in-stream organic matter concentrations were elevated at hot-spots within the catchment (such as at headwater wetlands), and organic matter dynamics largely followed the seasonal dynamics (shading and leaf-fall) of the forested, hardwood Piedmont catchment. Therefore, catchment-wide inputs of groundwater and allochthonous matter played a significant role in setting the underlying, nutrient-limited, heterotrophic lotic environment at Fair Hill.

While catchment inputs set the foundation for baseflow dynamics at Fair Hill, three temporal “hot-moments” of in-stream nutrient processes were observed controlling in-stream biogeochemistry: the release of ammonium and phosphate during the warm – but shaded – growing season; nitrate retention in the fall driven by leaf-litter; and a unique moment of nitrate uptake and respiration induced degradation of labile organic matter during a drought. Warm temperatures

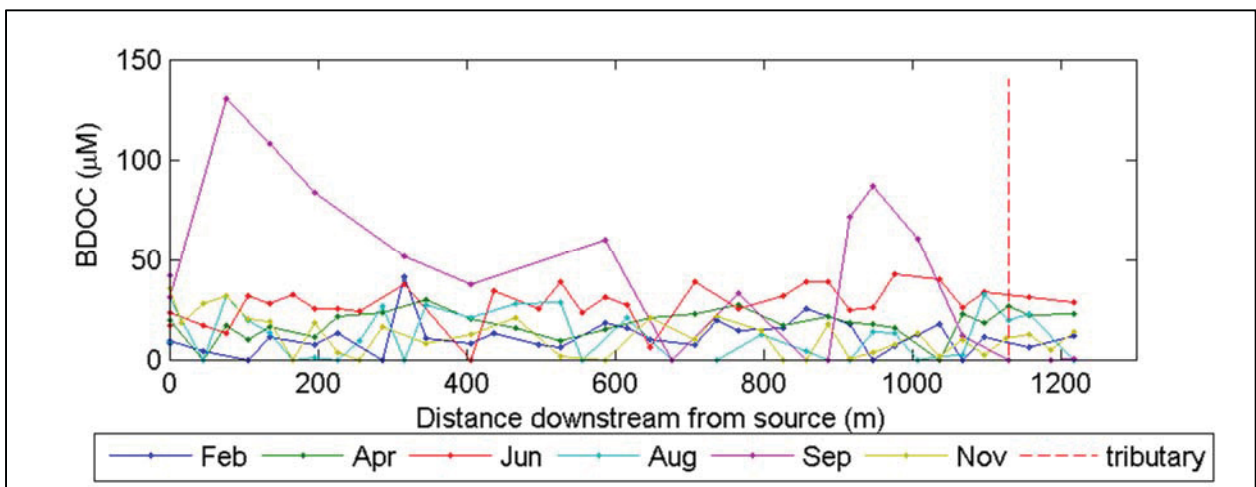
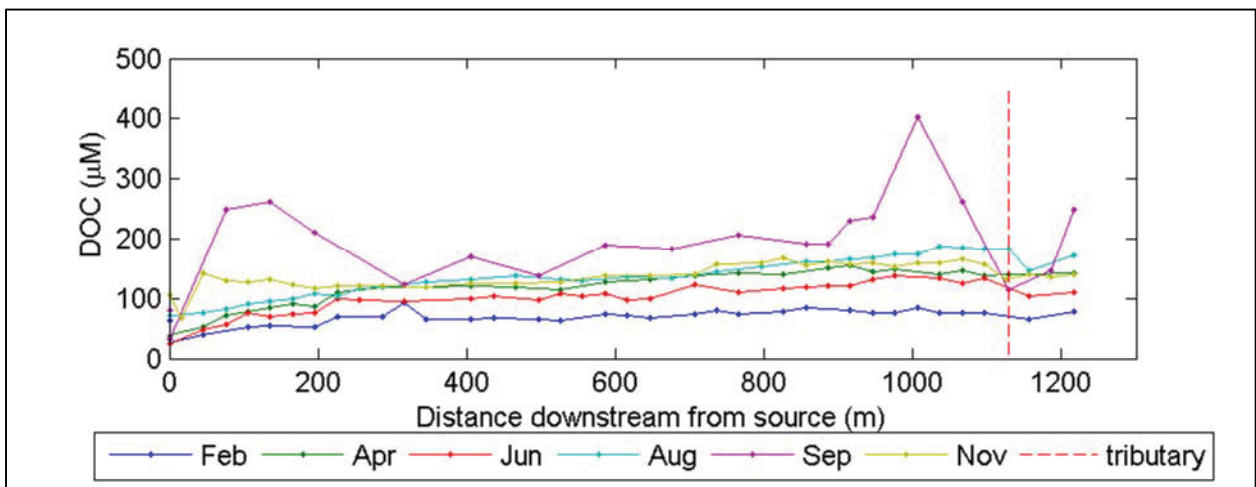
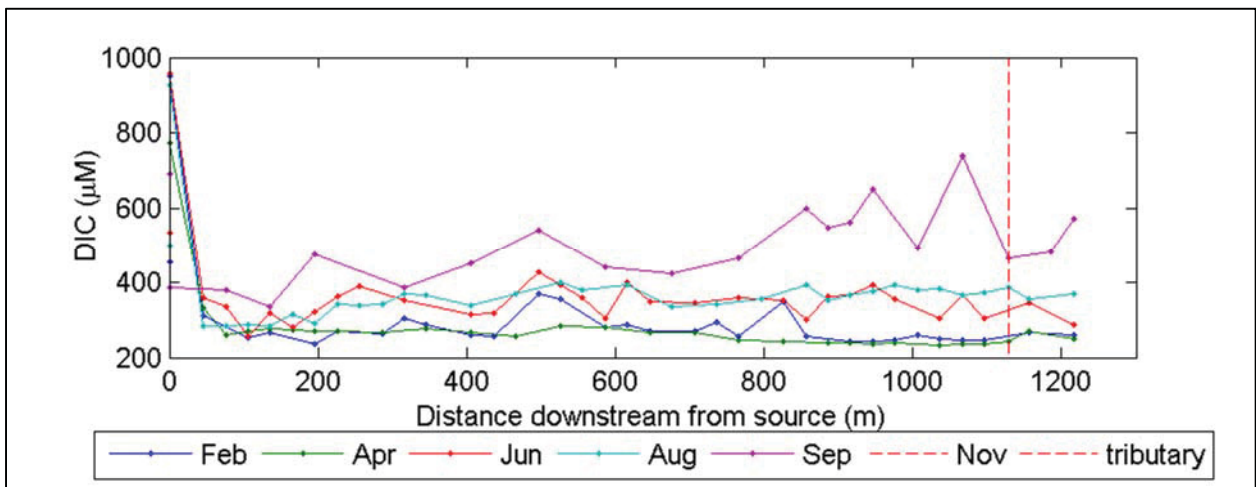
during the growing season stimulated in-stream respiration causing the release of ammonium and phosphate to the water column, while shading concurrently suppressed their autotrophic in-stream uptake. As a result, a hot-moment of in-stream ammonium and phosphate release occurred throughout the warm, shaded growing season. During the fall months, organic detritus from leaf fall drove a hot-moment of in-stream nitrate retention, decreasing in-stream concentrations. A similar hot-moment of nitrate uptake failed to materialize in the spring, however, indicating that vernal in-stream production, unlike leaf fall, did not significantly affect in-stream nutrient dynamics. Lastly, and most unique to this study, a drought in September 2010 affected in-stream dynamics independently of these seasonal processes. As the stream dried, organic matter became trapped in surficial pools, which - combined with warm temperatures - stimulated in-stream respiration. As a result, the stream experienced a hot-moment of nitrate uptake in conjunction with the cycling of biologically available organic carbon to more refractory forms. Thus, seasonal and drought-dependent hot-moments of in-stream dynamics actively created hot-moments of nutrient export and uptake at Fair Hill.

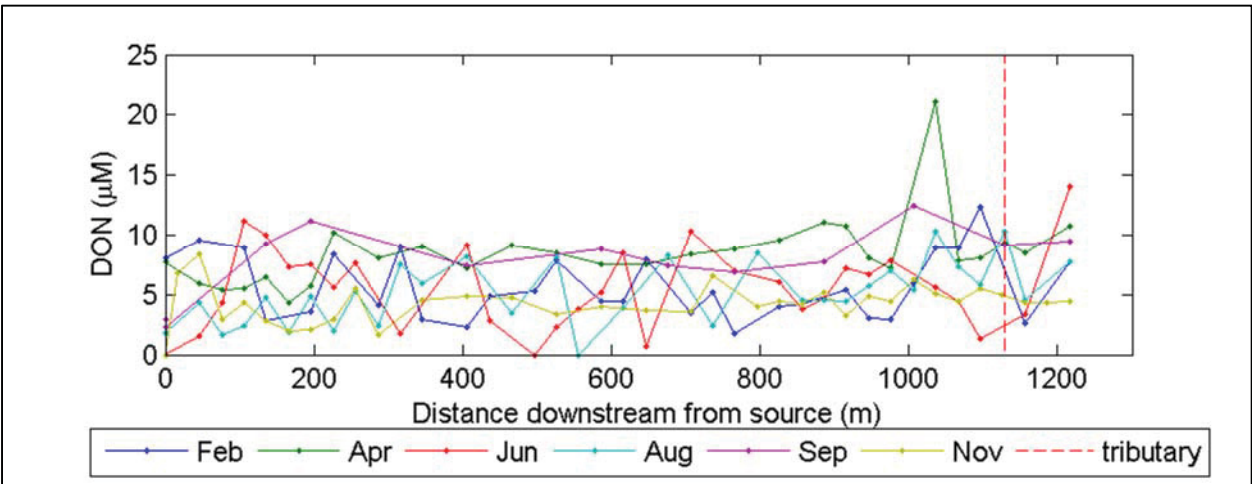
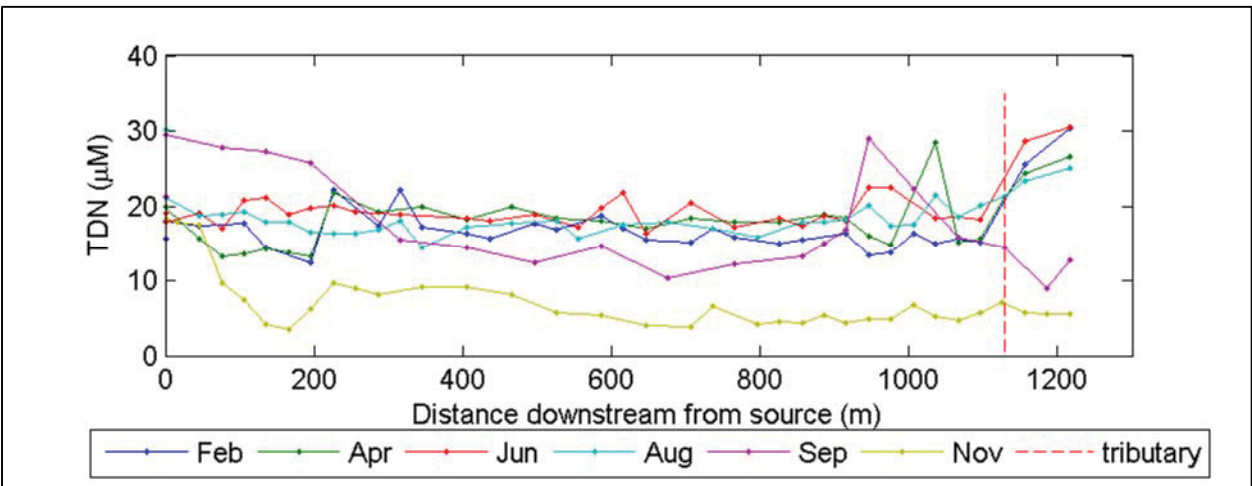
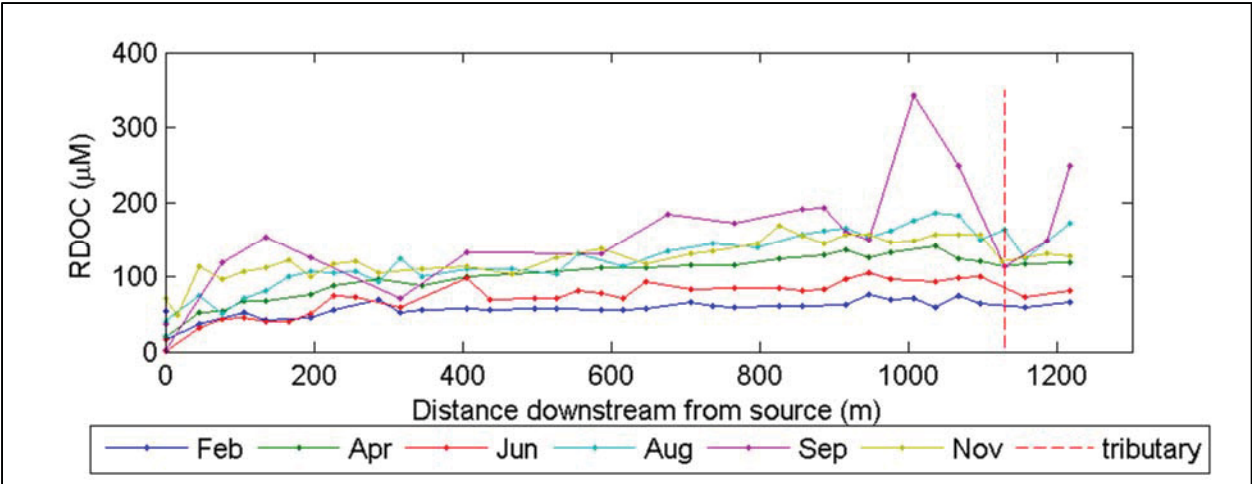
Underlain by baseflow hydrology and allochthonous inputs, and accented by temporal in-stream processes, baseflow biogeochemical dynamics at Fair Hill were therefore neither spatially nor temporally homogenous. Rather, the lotic environment resulted from a complex mix of environmental variables outside of and within the stream itself. Consequently, the capacity of this first-order, headwater, Piedmont stream to buffer nutrient exports to the Chesapeake Bay during baseflow varies temporally throughout the year in response to light availability, temperature, and in-stream organic matter dynamics.

This study provides insight to potential water quality trends in the Chesapeake Bay with a warming climate, and it provides additional insights to evidence-based nutrient management

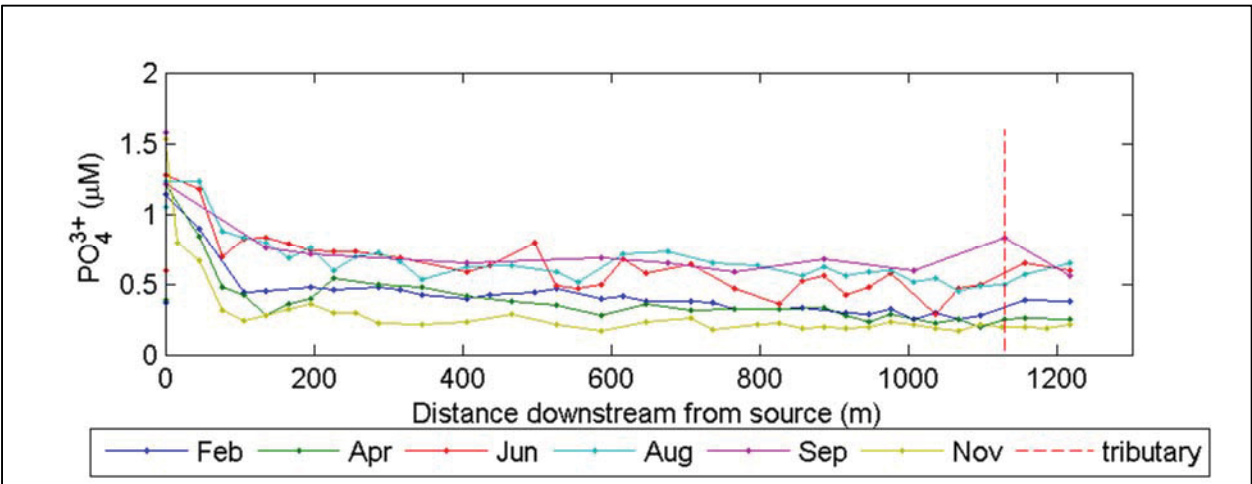
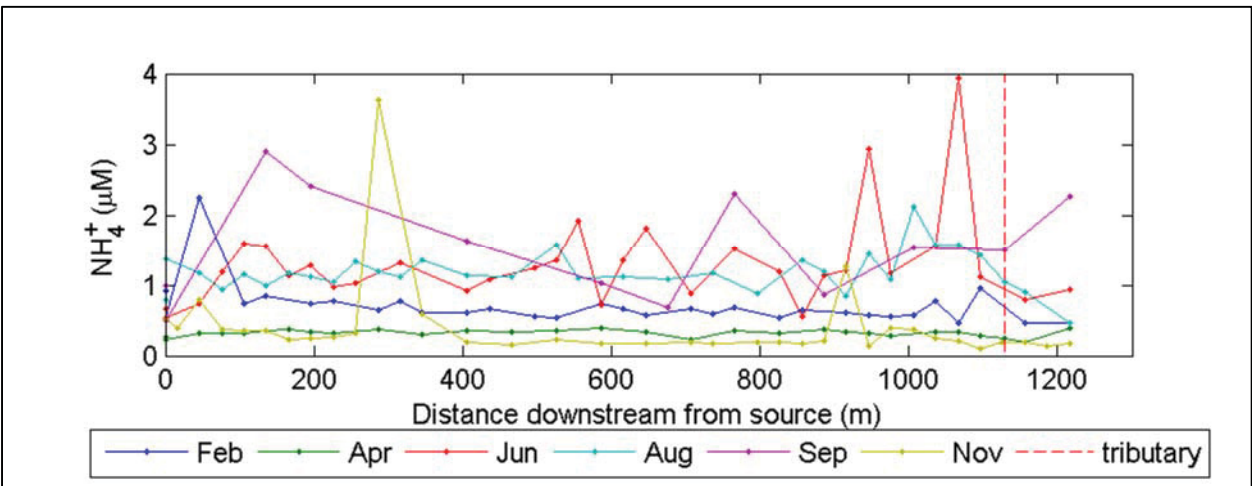
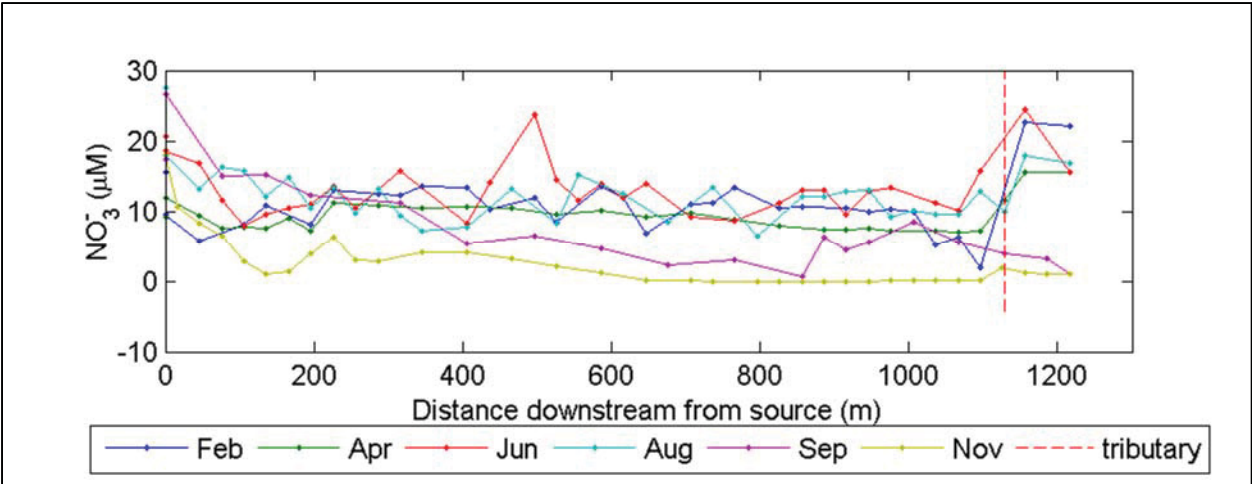
strategies for headwater catchments in the Chesapeake Bay region and elsewhere. In general, climate change models predict greater variability in stream flow in the Chesapeake Bay region, including more frequent and intense flows from tropical storms and longer, more frequent droughts from warmer summer temperatures (Hayhoe et al., 2007; Najjar et al., 2010). Thus, with a changing climate, the drought-induced in-stream nutrient uptake observed in this study may play a greater role in regulating future nitrogen export to the Chesapeake Bay. This study also provides further evidence that forested watersheds in the Chesapeake Bay region provide a critical role in regulating nitrogen export to the estuary. Historic studies show that Bay-wide degradation is associated with widespread deforestation (Brush, 2009), and that forest disturbance increases nitrogen export from headwater catchments (Table 2). Moreover, watershed nitrogen retention is positively correlated with percent forest cover (Correll and Weller, 1997; Zheng et al., 2008), and riparian forests have been shown to decrease nitrogen export from watersheds in the Chesapeake Bay region (Table 6). This study adds nuance to these observations, demonstrating that seasonal, forest processes impact in-stream water quality both spatially and temporally. In particular, organic carbon dynamics linked to leaf-fall at Fair Hill played a critical role in regulating nutrient export, adding support to proposals to amend headwater streams with organic matter to manage nutrient export (Craig et al., 2008; Hester and Gooseff, 2010; Passeport et al., 2013). Most importantly, this study demonstrates that future investigations and models examining nutrient export to the Chesapeake Bay should consider incorporating temporal and spatial impacts of drought and organic matter dynamics on in-stream nutrient processes.

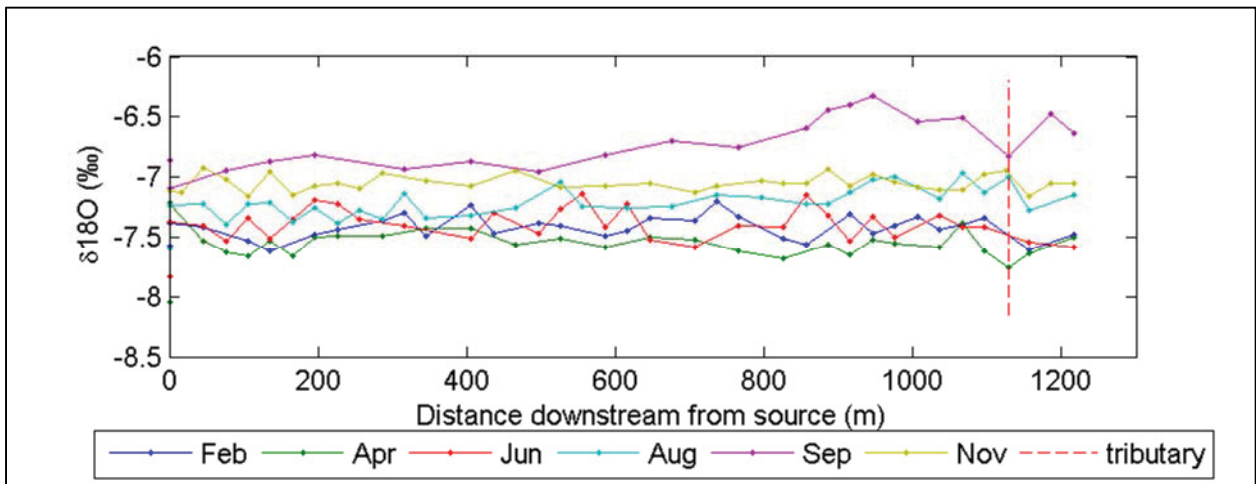
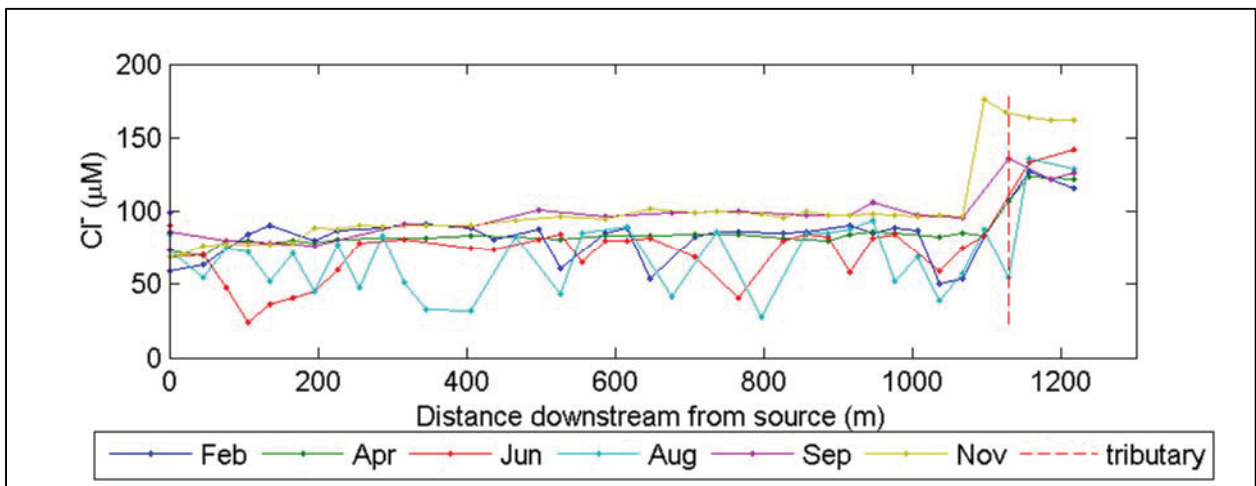
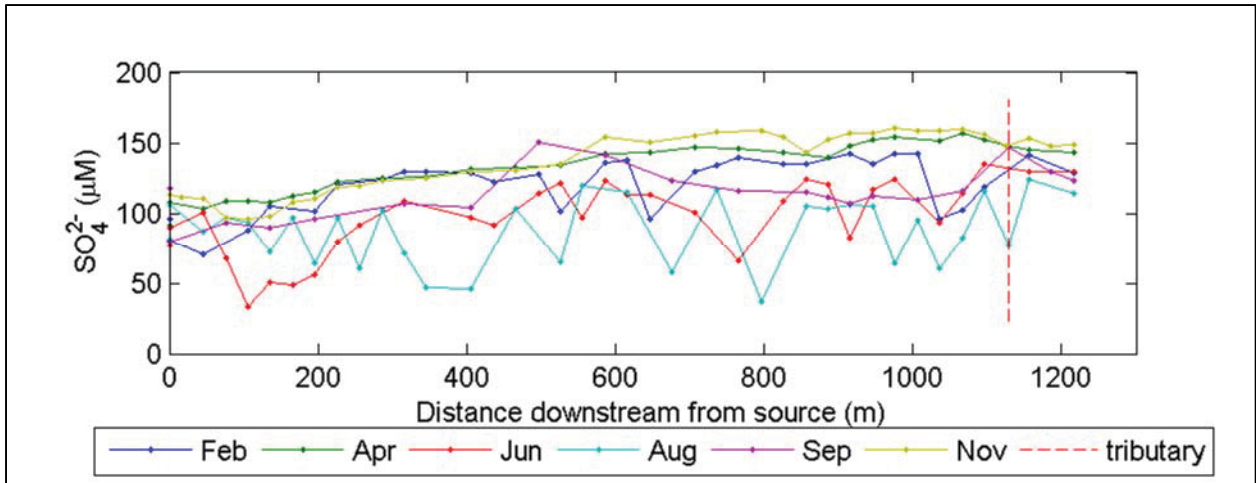
## APPENDIX A: LONGITUDINAL GRAPHS

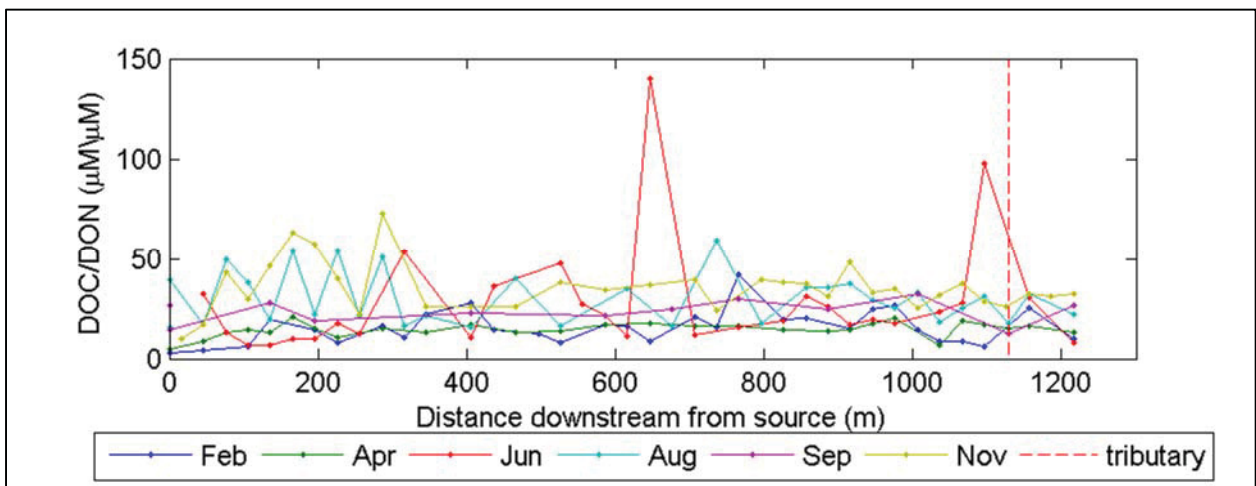
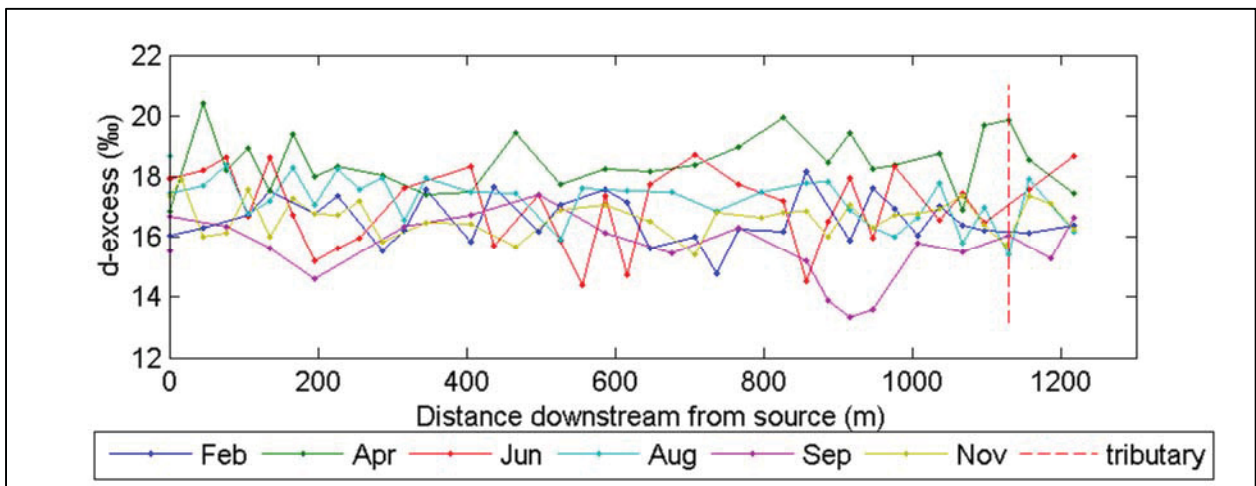
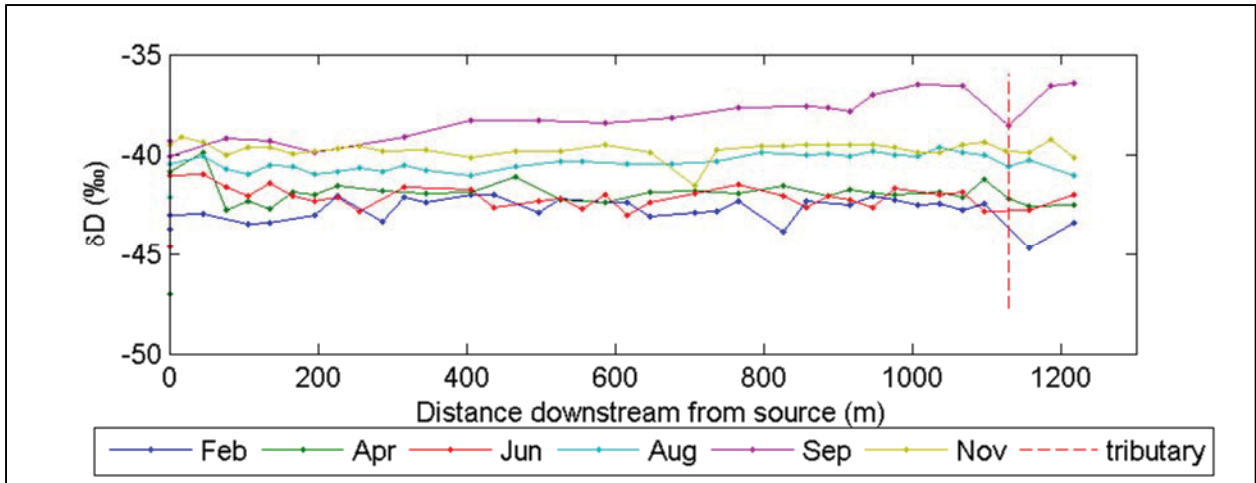


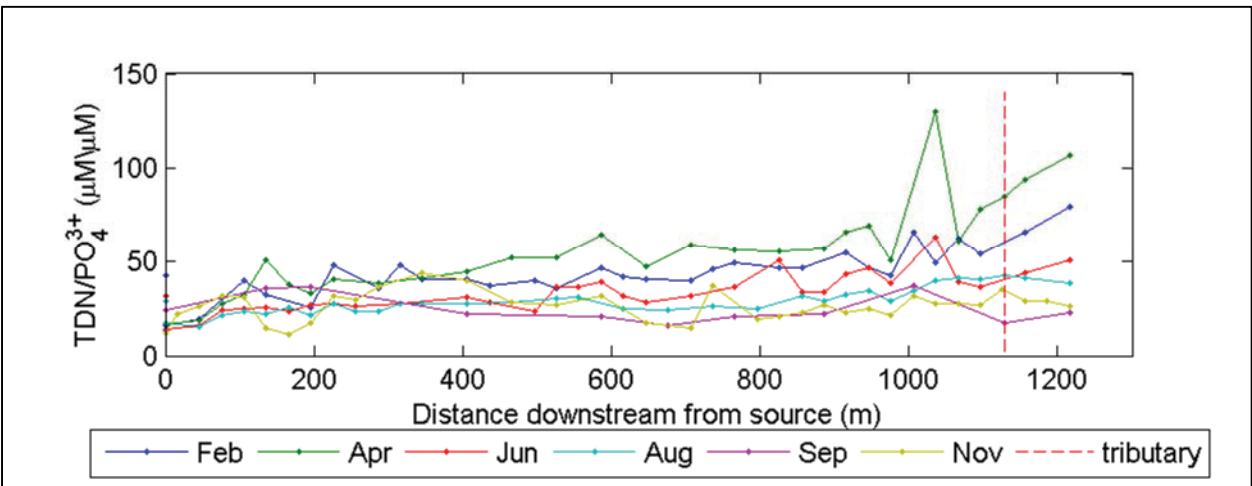
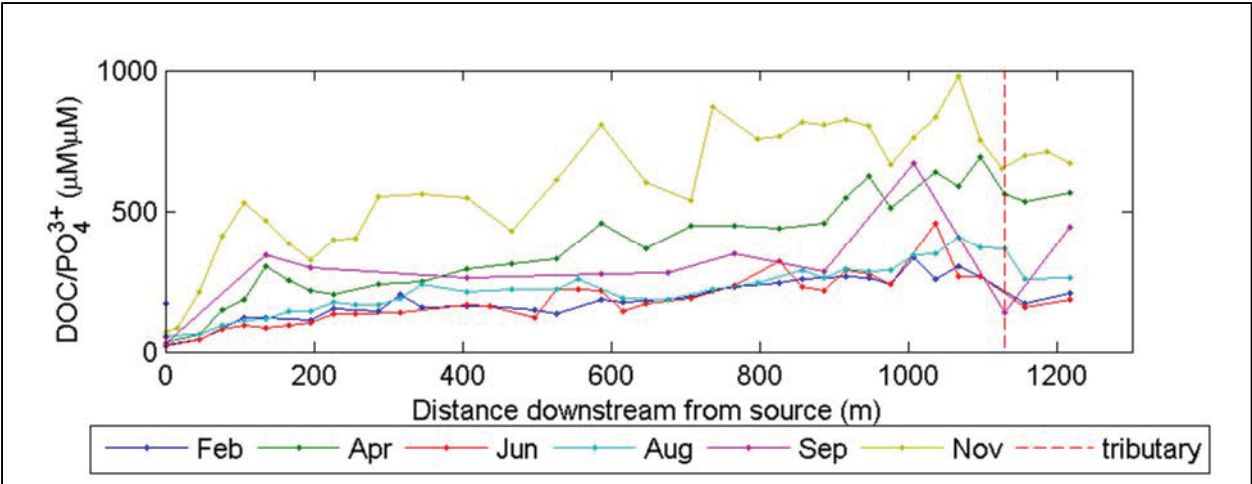












**APPENDIX B: DOWNSTREAM CONCENTRATION CHANGES WITH DISTANCE**

Analyte	Slope	Feb	Apr	Jun	Aug	Sep	Nov
DIC	0-1130m ( $\mu\text{M}/\text{km}$ )	-24.7	-47.6	20.5	76.0	210	-
	0-230m ( $\mu\text{M}/\text{km}$ )	-244	-200	7.60	259	784	-
	230-1130m ( $\mu\text{M}/\text{km}$ )	-60.9	-52.8	-31.1	28.3	225	-

Analyte	Slope	Feb	Apr	Jun	Aug	Sep	Nov
DOC	0-1130m ( $\mu\text{M}/\text{km}$ )	23.8	68.8	64.5	89.2	28.3	45.1
	0-230m ( $\mu\text{M}/\text{km}$ )	125	254	224	176	-319	91.9
	230-1130m ( $\mu\text{M}/\text{km}$ )	10.9	38.8	49.4	78.7	138	49.7

Analyte	Slope	Feb	Apr	Jun	Aug	Sep	Nov
BDOC	0-1130m ( $\mu\text{M}/\text{km}$ )	2.50	4.40	10.6	-3.70	-75.6	-10.9
	0-230m ( $\mu\text{M}/\text{km}$ )	50.4	67.4	58.6	-96.3	-386	-100
	230-1130m ( $\mu\text{M}/\text{km}$ )	-4.70	-4.80	13.2	-10.7	-21.4	-4.60

Analyte	Slope	Feb	Apr	Jun	Aug	Sep	Nov
RDOC	0-1130m ( $\mu\text{M}/\text{km}$ )	21.3	64.3	53.9	92.9	97.4	56.0
	0-230m ( $\mu\text{M}/\text{km}$ )	74.7	185	165	272	66.6	192
	230-1130m ( $\mu\text{M}/\text{km}$ )	15.6	43.5	36.2	89.3	148	54.3

Analyte	Slope	Feb	Apr	Jun	Aug	Sep	Nov
TDN	0-1130m ( $\mu\text{M}/\text{km}$ )	-2.70	3.40	-0.194	1.70	-6.60	-5.40
	0-230m ( $\mu\text{M}/\text{km}$ )	6.80	22.0	7.70	-15.7	-16.4	-53.9
	230-1130m ( $\mu\text{M}/\text{km}$ )	-4.40	-0.37	0.86	3.90	6.90	-4.00

Analyte	Slope	Feb	Apr	Jun	Aug	Sep	Nov
DON	0-1130m ( $\mu\text{M}/\text{km}$ )	0.35	4.50	-1.10	3.70	-0.03	0.71
	0-230m ( $\mu\text{M}/\text{km}$ )	-17.1	14.5	17.6	-1.70	30.9	-25.0
	230-1130m ( $\mu\text{M}/\text{km}$ )	2.90	3.60	1.00	2.80	4.00	1.30

Analyte	Slope	Feb	Apr	Jun	Aug	Sep	Nov
$\text{NO}_3^-$	0-1130m ( $\mu\text{M}/\text{km}$ )	-2.60	-1.10	0.10	-2.30	-9.30	-5.80
	0-230m ( $\mu\text{M}/\text{km}$ )	30.9	7.40	-10.3	-14.0	-22.9	-27.2
	230-1130m ( $\mu\text{M}/\text{km}$ )	-7.30	8.90	-4.90	16.2	23.9	42.7

Analyte	Slope	Feb	Apr	Jun	Aug	Sep	Nov
NH <sub>4</sub> <sup>+</sup>	0-1130m (μM/km)	-0.41	-0.03	0.67	0.26	-1.20	-0.36
	0-230m (μM/km)	-7.00	0.11	0.48	-0.02	-8.20	-1.60
	230-1130m (μM/km)	0.01	-0.07	1.10	0.23	0.16	-0.98

Analyte	Slope	Feb	Apr	Jun	Aug	Sep	Nov
PO <sub>4</sub> <sup>3-</sup>	0-1130m (μM/km)	-0.30	-0.27	-0.43	-0.30	-0.02	-0.23
	0-230m (μM/km)	-2.00	-1.30	-1.50	-2.70	-0.83	-2.00
	230-1130m (μM/km)	-0.25	-0.28	-0.32	-0.17	0.13	-0.06

Analyte	Slope	Feb	Apr	Jun	Aug	Sep	Nov
SO <sub>4</sub> <sup>2-</sup>	0-1130m (μM/km)	26.3	44.5	51.3	7.50	23.5	56.1
	0-230m (μM/km)	246	88.2	-82.2	-37.2	25.4	35.7
	230-1130m (μM/km)	-0.71	32.8	17.1	20.0	0.47	42.6

Analyte	Slope	Feb	Apr	Jun	Aug	Sep	Nov
Cl <sup>-</sup>	0-1130m (μM/km)	-7.00	10.0	26.2	8.40	29.6	40.3
	0-230m (μM/km)	97.8	37.6	-21.2	6.90	-29.0	75.2
	230-1130m (μM/km)	-14.8	8.90	-4.90	16.2	23.9	42.7

Analyte	Slope	Feb	Apr	Jun	Aug	Sep	Nov
δ <sup>18</sup> O	0-1130m (‰/km)	0.08	-0.05	-0.02	0.24	0.44	0.02
	0-230m (‰/km)	0.001	0.46	1.40	-0.41	1.10	-0.17
	230-1130m (‰/km)	-0.02	-0.17	-0.03	0.28	0.57	0.01

Analyte	Slope	Feb	Apr	Jun	Aug	Sep	Nov
δD	0-1130m (‰/km)	0.35	-0.05	-0.41	0.80	2.30	-0.01
	0-230m (‰/km)	4.70	-3.60	-5.70	-2.80	-6.00	-2.40
	230-1130m (‰/km)	-0.11	-0.05	0.15	1.00	2.00	0.32

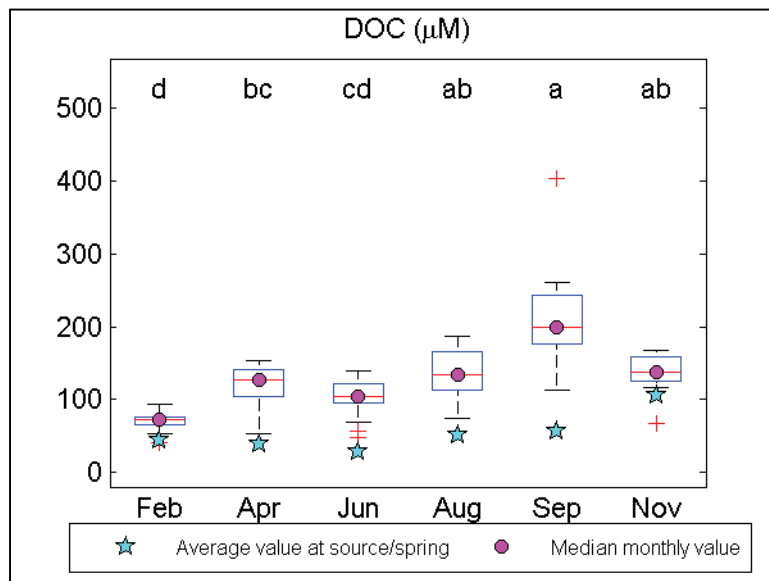
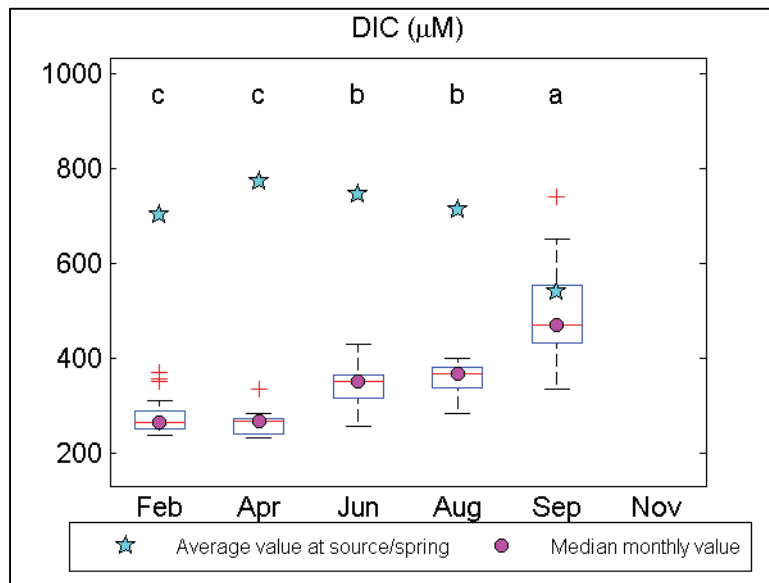
Analyte	Slope	Feb	Apr	Jun	Aug	Sep	Nov
D-excess	0-1130m (‰/km)	-0.25	0.31	-0.27	-1.10	-1.20	-0.17
	0-230m (‰/km)	4.70	-7.30	-17.3	0.53	-14.7	-0.99
	230-1130m (‰/km)	0.08	1.30	0.43	-1.20	-2.60	0.21

Analyte	Slope	Feb	Apr	Jun	Aug	Sep	Nov
DOC/DON	0-1130m ( $\mu\text{M}/\mu\text{M}/\text{km}$ )	4.70	2.20	21.6	-6.20	-1.10	-4.00
	0-230m ( $\mu\text{M}/\mu\text{M}/\text{km}$ )	36.5	19.5	-54.6	84.5	-154	195
	230-1130m ( $\mu\text{M}/\mu\text{M}/\text{km}$ )	-2.20	1.20	5.90	0.22	-3.60	-5.50

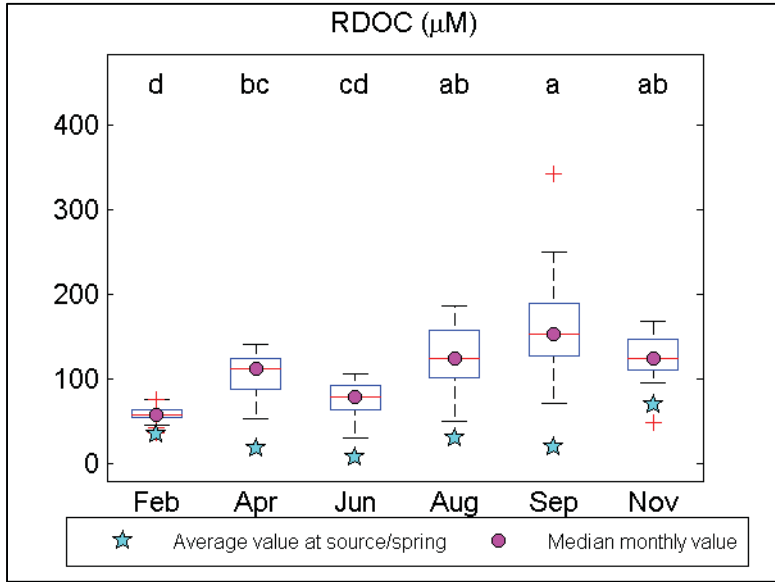
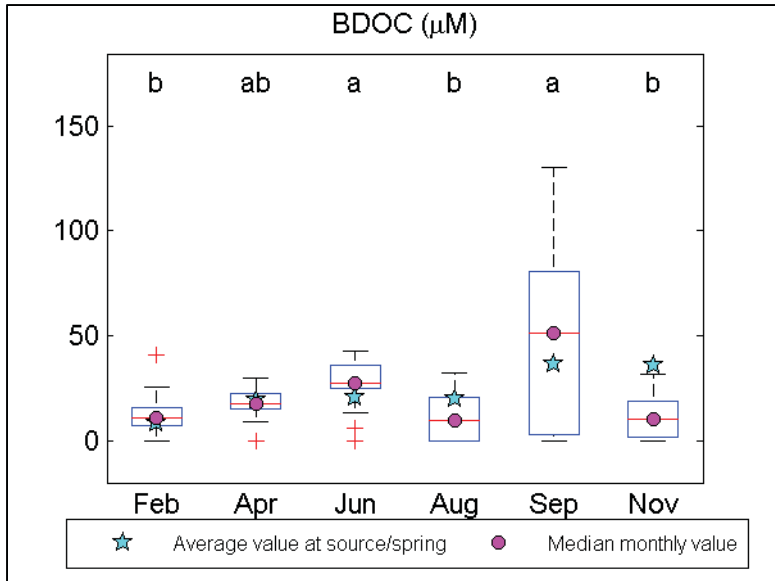
Analyte	Slope	Feb	Apr	Jun	Aug	Sep	Nov
DOC/ $\text{PO}_4^{3-}$	0-1130m ( $\mu\text{M}/\mu\text{M}/\text{km}$ )	188	443	231	229	48.9	494
	0-230m ( $\mu\text{M}/\mu\text{M}/\text{km}$ )	451	740	390	560	-791	1041
	230-1130m ( $\mu\text{M}/\mu\text{M}/\text{km}$ )	186	476	227	212	122	400

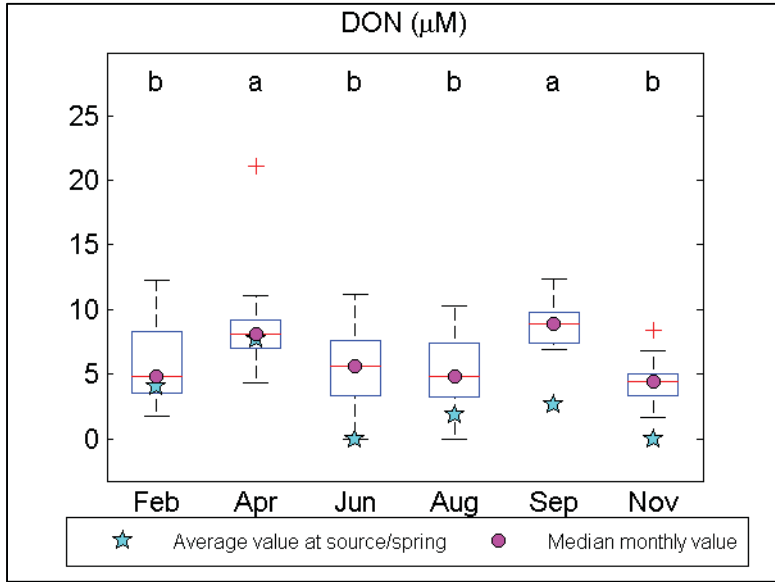
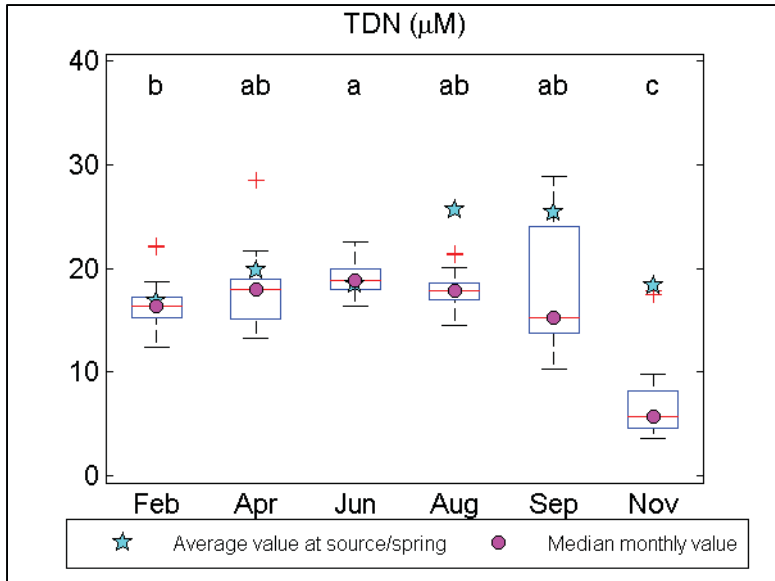
Analyte	Slope	Feb	Apr	Jun	Aug	Sep	Nov
TDN/ $\text{PO}_4^{3-}$	0-1130m ( $\mu\text{M}/\mu\text{M}/\text{km}$ )	22.6	46.7	22.4	15.2	-11.0	0.26
	0-230m ( $\mu\text{M}/\mu\text{M}/\text{km}$ )	95.1	97.3	44.3	47.0	6.50	-21.2
	230-1130m ( $\mu\text{M}/\mu\text{M}/\text{km}$ )	21.5	50.2	23.5	15.9	7.00	-9.90

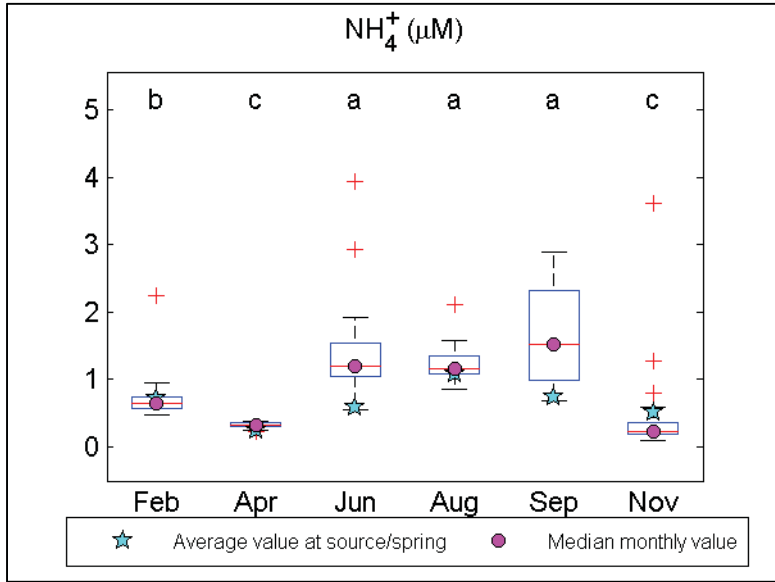
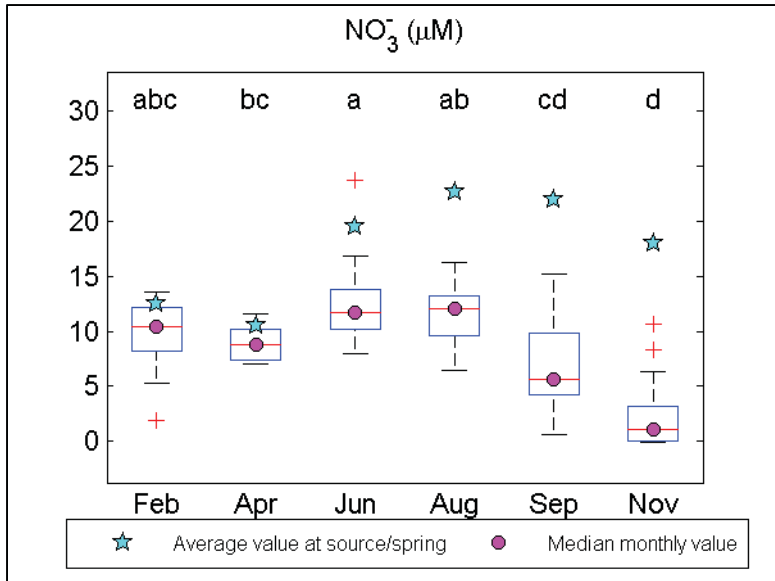
## APPENDIX C: MULTI-WAY PAIR-WISE ANALYSES

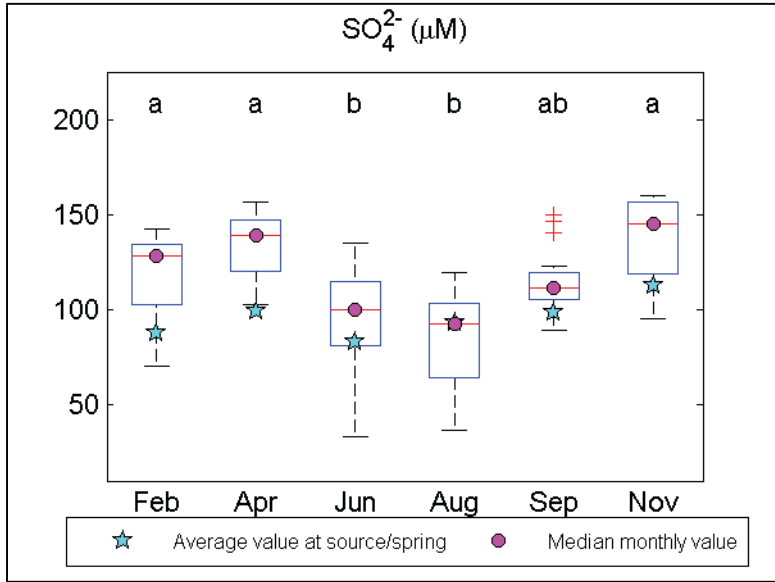
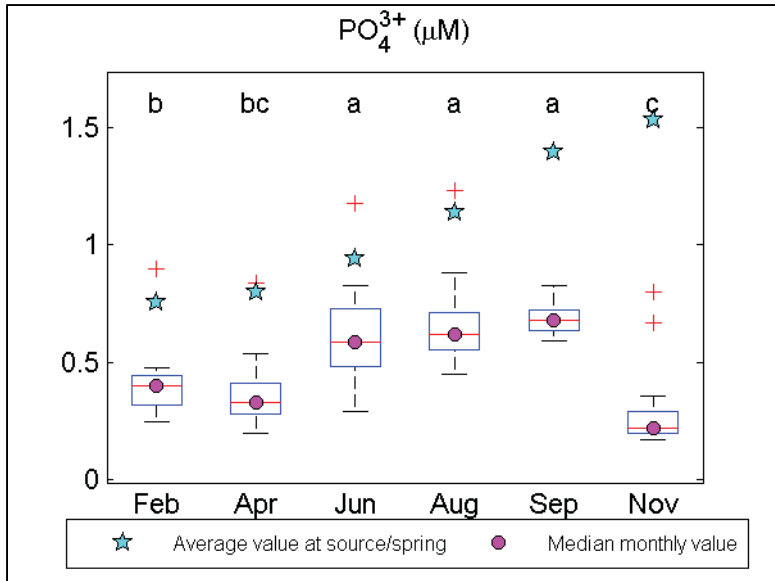


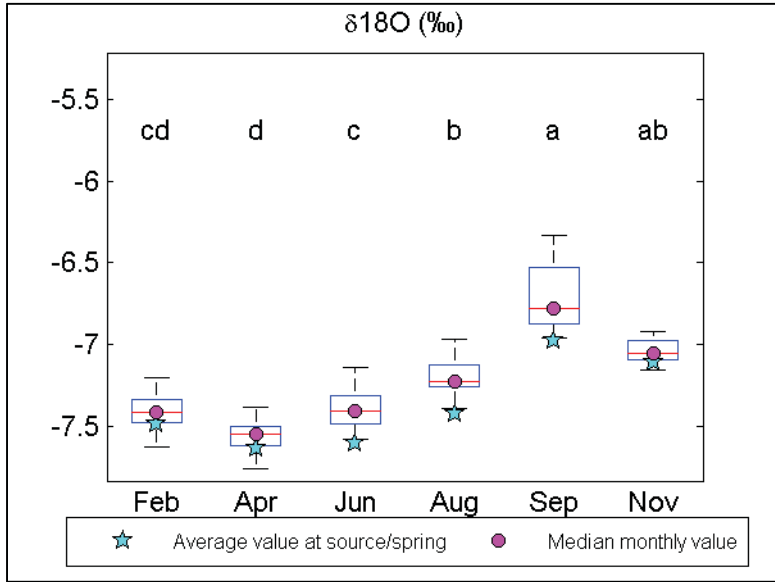
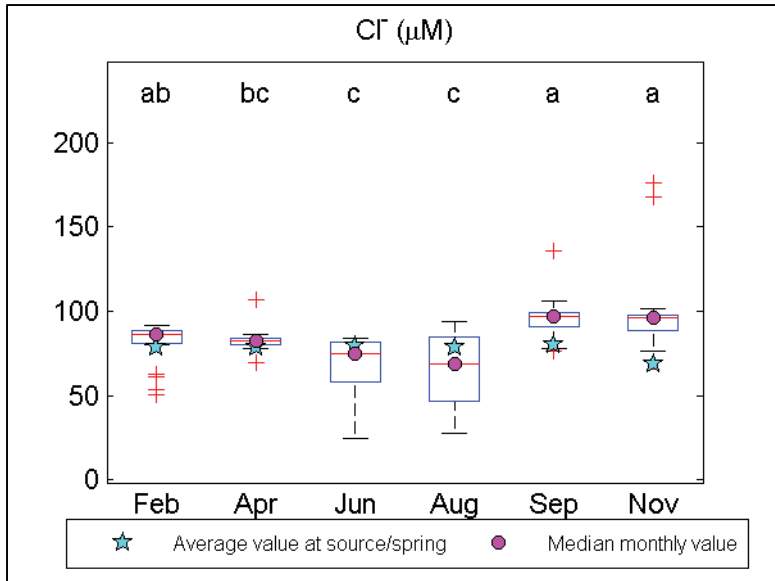


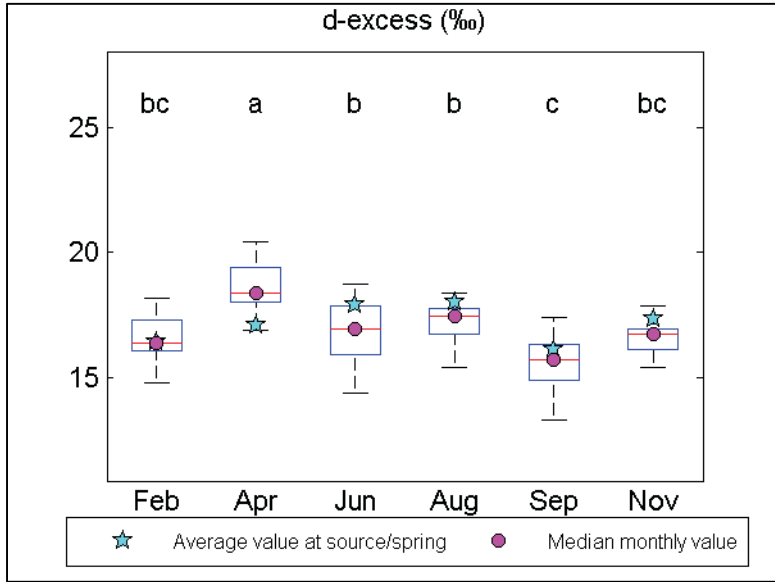
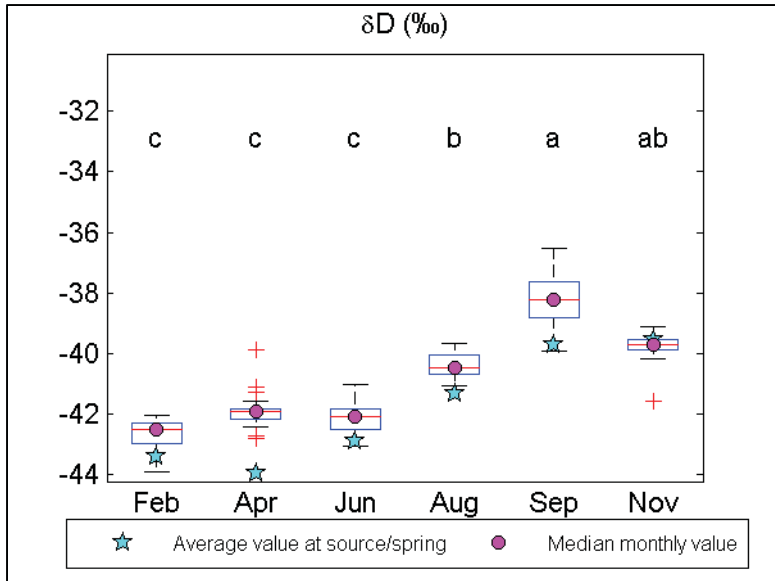


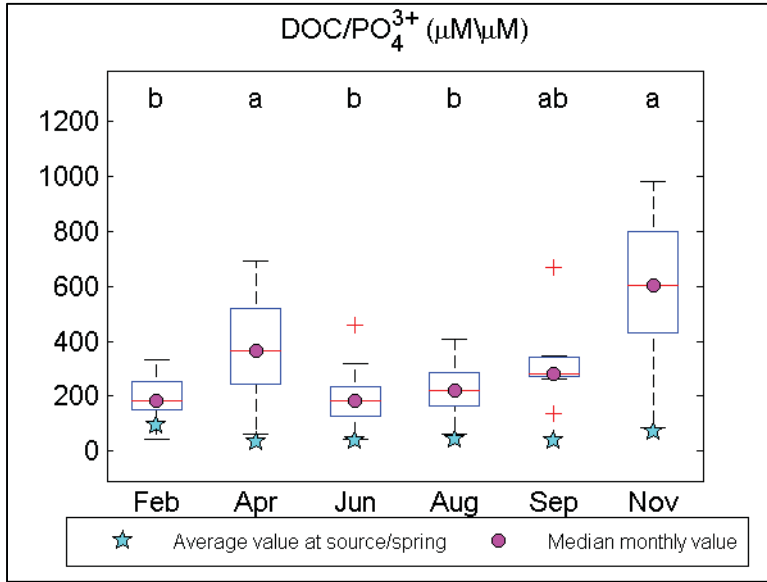
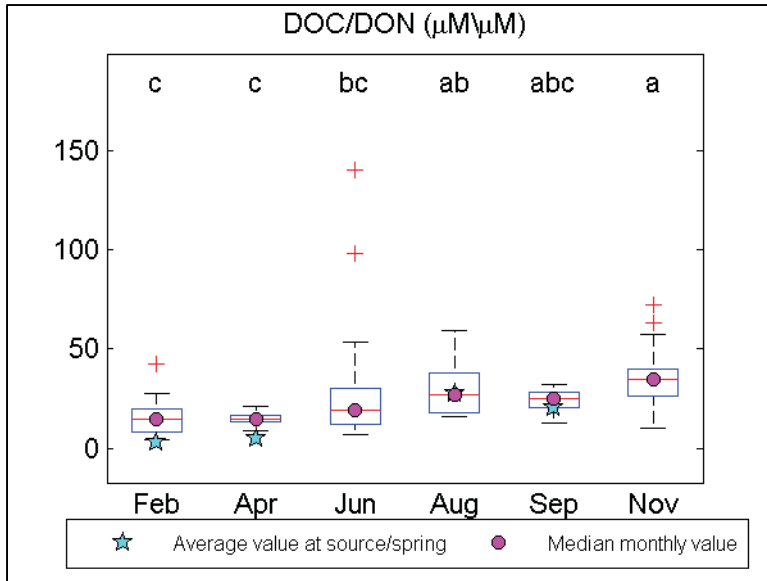


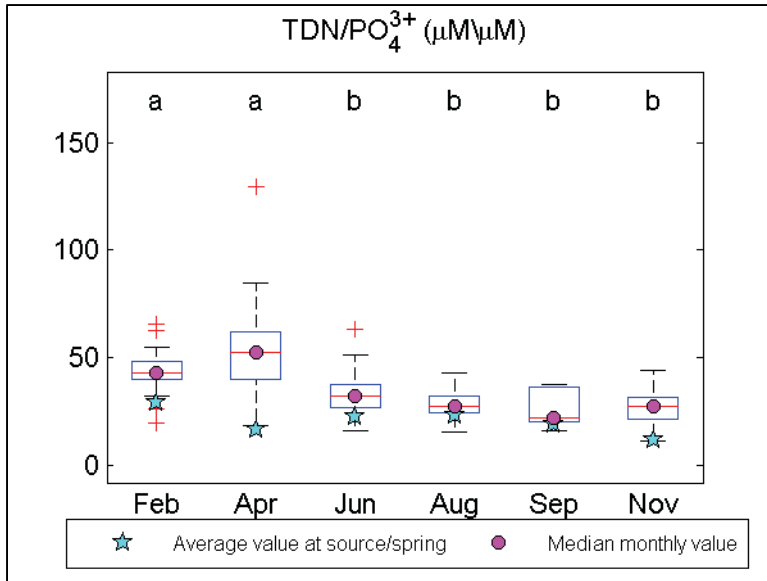














## APPENDIX D: SINGLE-VARIABLE REGRESSION ANALYSES

	Equation			Intercept		Discharge	
	R <sup>2</sup>	Adjusted R <sup>2</sup>	P-value	Intercept	P-value	Coefficient	P-value
DIC	0.73	0.64	0.065	424.6	0.001	-73.05	0.065
DOC	0.66	0.58	0.048	164.7	0.001	-36.18	0.048
BDOC	0.15	-0.06	0.440	27.9	0.055	-6.80	0.440
RDOC	0.73	0.66	0.031	139.0	0.0004	-31.08	0.031
TDN	0.10	-0.12	0.535	13.6	0.013	1.66	0.535
DON	0.04	-0.20	0.715	6.5	0.007	-0.38	0.715
NO <sub>3</sub> <sup>-</sup>	0.17	-0.04	0.420	6.4	0.075	1.85	0.420
NH <sub>4</sub> <sup>+</sup>	0.16	-0.06	0.439	1.1	0.034	-0.22	0.439
PO <sub>4</sub> <sup>3-</sup>	0.12	-0.10	0.501	0.5	0.011	-0.07	0.501
SO <sub>4</sub> <sup>2-</sup>	0.10	-0.13	0.550	112.9	0.001	7.03	0.550
Cl <sup>-</sup>	0.02	-0.23	0.812	85.6	0.0004	-1.52	0.812
δ <sup>18</sup> O	0.50	0.38	0.115	-7.0	0.000001	-0.21	0.115
δD	0.66	0.58	0.048	-39.4	0.0000005	-1.44	0.048
D-excess	0.02	-0.23	0.790	16.8	0.00001	0.14	0.790

	Equation			Intercept		Concentration at source springs	
	R <sup>2</sup>	Adjusted R <sup>2</sup>	P-value	Intercept	P-value	Coefficient	P-value
DIC	0.68	0.57	0.086	878.0	0.026	-0.77	0.086
DOC	0.10	-0.12	0.533	102.3	0.077	0.49	0.533
BDOC	0.26	0.08	0.300	3.2	0.857	0.77	0.300
RDOC	0.02	-0.22	0.782	101.3	0.024	0.23	0.782
TDN	0.05	-0.19	0.677	9.5	0.512	0.28	0.677
DON	0.30	0.12	0.265	5.1	0.007	0.35	0.265
NO <sub>3</sub> <sup>-</sup>	0.001	-0.25	0.953	8.7	0.319	-0.03	0.953
NH <sub>4</sub> <sup>+</sup>	0.39	0.23	0.187	0.1	0.891	1.19	0.187
PO <sub>4</sub> <sup>3-</sup>	0.001	-0.25	0.957	0.5	0.233	0.02	0.957
SO <sub>4</sub> <sup>2-</sup>	0.43	0.29	0.155	-10.5	0.895	1.36	0.155
Cl <sup>-</sup>	0.19	-0.01	0.386	176.5	0.137	-1.19	0.386
δ <sup>18</sup> O	0.94	0.92	0.001	0.3	0.782	1.02	0.001
δD	0.86	0.82	0.008	-7.0	0.371	0.81	0.008
D-excess	0.33	0.16	0.234	5.3	0.563	0.68	0.234

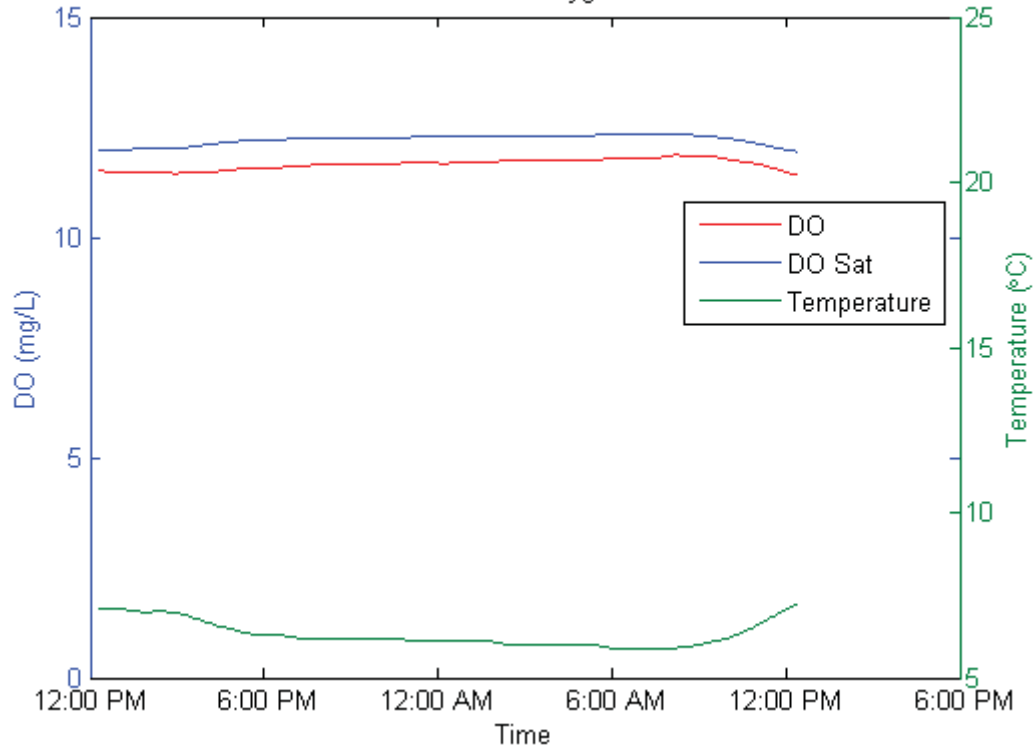
	Equation			Intercept		Temperature	
	R <sup>2</sup>	Adjusted R <sup>2</sup>	P-value	Intercept	P-value	Coefficient	P-value
DIC	0.64	0.52	0.103	151.6	0.179	13.35	0.103
DOC	0.38	0.23	0.192	60.6	0.259	5.09	0.192
BDOC	0.27	0.09	0.290	-1.2	0.952	1.67	0.290
RDOC	0.34	0.17	0.229	55.7	0.228	3.91	0.229
TDN	0.20	-0.003	0.378	9.6	0.194	0.43	0.378
DON	0.16	-0.05	0.428	4.1	0.164	0.15	0.428
NO <sub>3</sub> <sup>-</sup>	0.10	-0.13	0.550	4.8	0.446	0.26	0.550
NH <sub>4</sub> <sup>+</sup>	0.64	0.55	0.056	-0.3	0.577	0.08	0.056
PO <sub>4</sub> <sup>3-</sup>	0.70	0.63	0.037	0.1	0.658	0.03	0.037
SO <sub>4</sub> <sup>2-</sup>	0.64	0.55	0.057	164.9	0.001	-3.35	0.057
Cl <sup>-</sup>	0.15	-0.06	0.451	95.8	0.003	-0.86	0.451
δ <sup>18</sup> O	0.13	-0.08	0.476	-7.5	0.00003	0.02	0.476
δD	0.21	0.01	0.362	-42.8	0.00003	0.15	0.362
D-excess	0.0001	-0.25	0.986	16.9	0.0002	0.002	0.986

	Equation			Intercept		Canopy	
	R <sup>2</sup>	Adjusted R <sup>2</sup>	P-value	Intercept	P-value	Coefficient	P-value
DIC	0.71	0.61	0.073	264.8	0.006	130.85	0.073
DOC	0.19	-0.02	0.393	112.5	0.010	32.98	0.393
BDOC	0.30	0.13	0.258	13.0	0.212	16.38	0.258
RDOC	0.11	-0.12	0.526	98.0	0.009	20.55	0.526
TDN	0.20	-0.002	0.376	13.3	0.009	3.97	0.376
DON	0.04	-0.20	0.705	5.8	0.008	0.68	0.705
NO <sub>3</sub> <sup>-</sup>	0.15	-0.06	0.445	6.7	0.056	3.02	0.445
NH <sub>4</sub> <sup>+</sup>	0.87	0.84	0.006	0.40	0.030	0.90	0.006
PO <sub>4</sub> <sup>3-</sup>	0.87	0.84	0.006	0.32	0.002	0.31	0.006
SO <sub>4</sub> <sup>2-</sup>	0.86	0.82	0.008	137.8	0.00001	-36.05	0.008
Cl <sup>-</sup>	0.15	-0.06	0.447	88.2	0.0002	-8.07	0.447
δ <sup>18</sup> O	0.15	-0.06	0.443	-7.3	0.000002	0.20	0.443
δD	0.13	-0.08	0.476	-41.4	0.000002	1.11	0.476
D-excess	0.07	-0.16	0.611	17.2	0.00001	-0.45	0.611

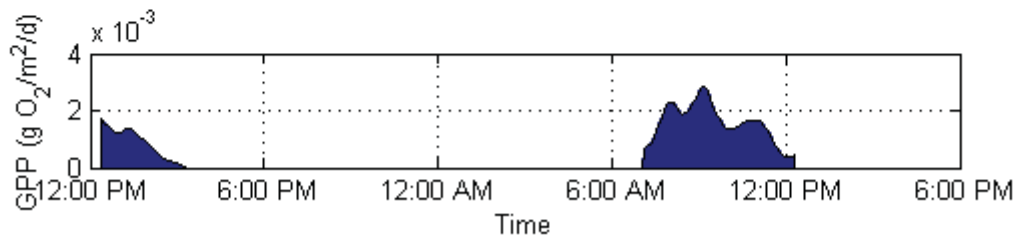
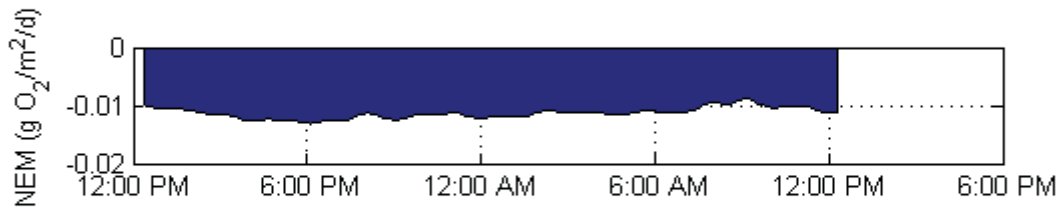
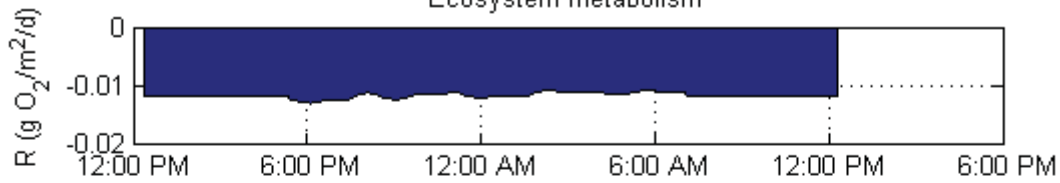
## **APPENDIX E: DAILY VARIATIONS IN TEMPERATURE, DO, AND NEM**

### February 2011, upstream

February: Upstream  
Dissolved oxygen



February: Upstream  
Ecosystem metabolism

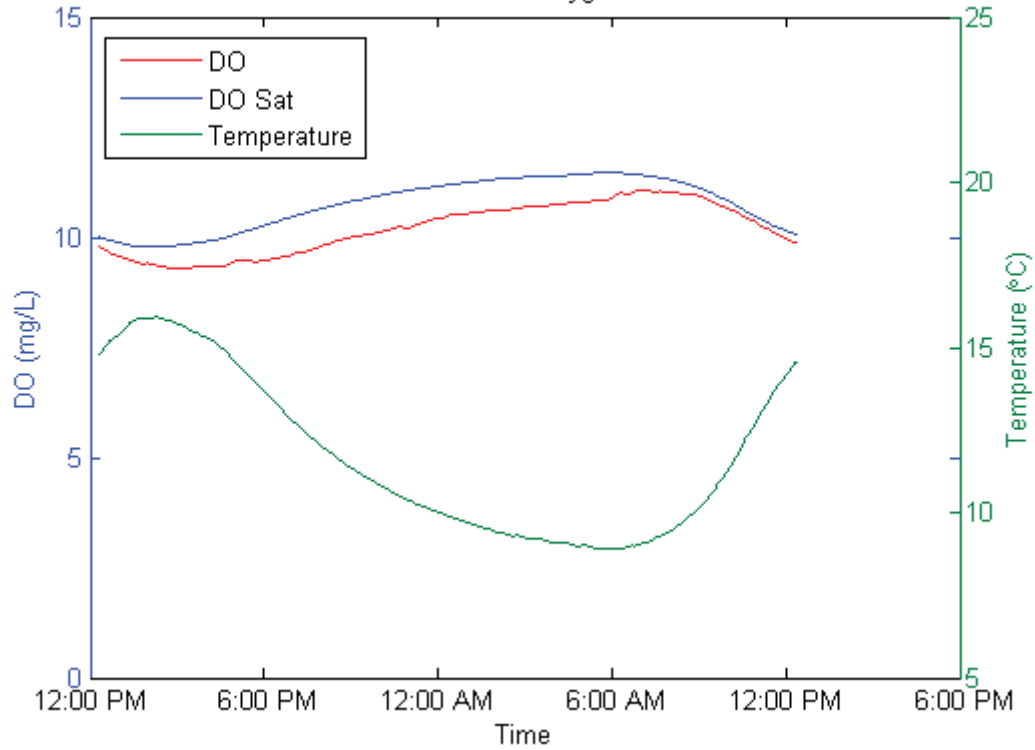


**February 2011, downstream**  
No data; sensor error

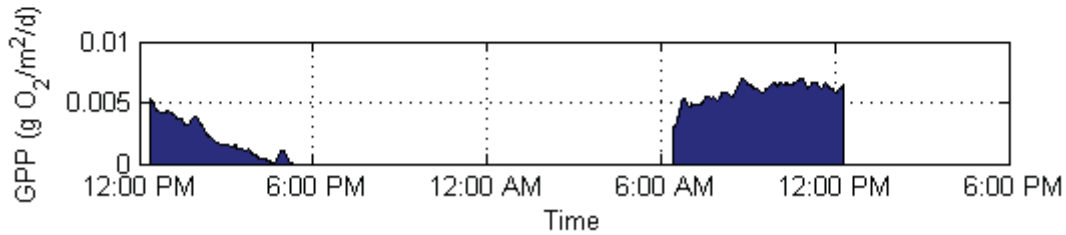
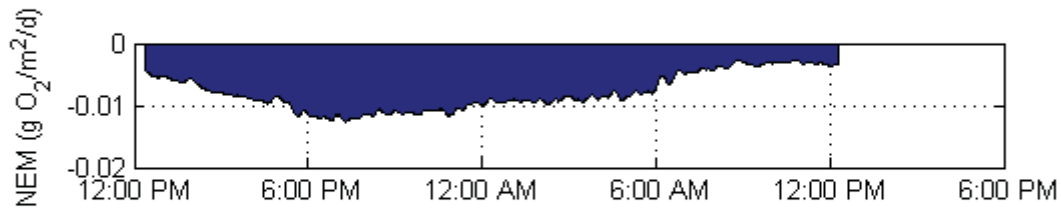
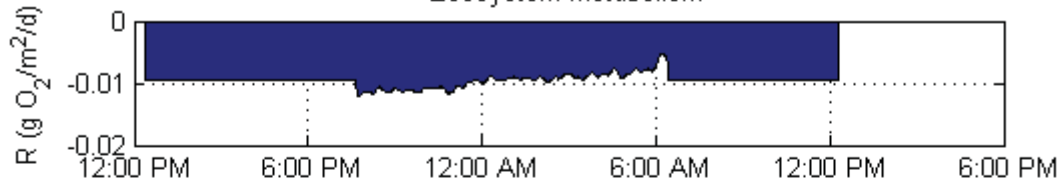
**April 2011, upstream**  
No data, sensor error

### April 2011, downstream

April: Downstream  
Dissolved oxygen

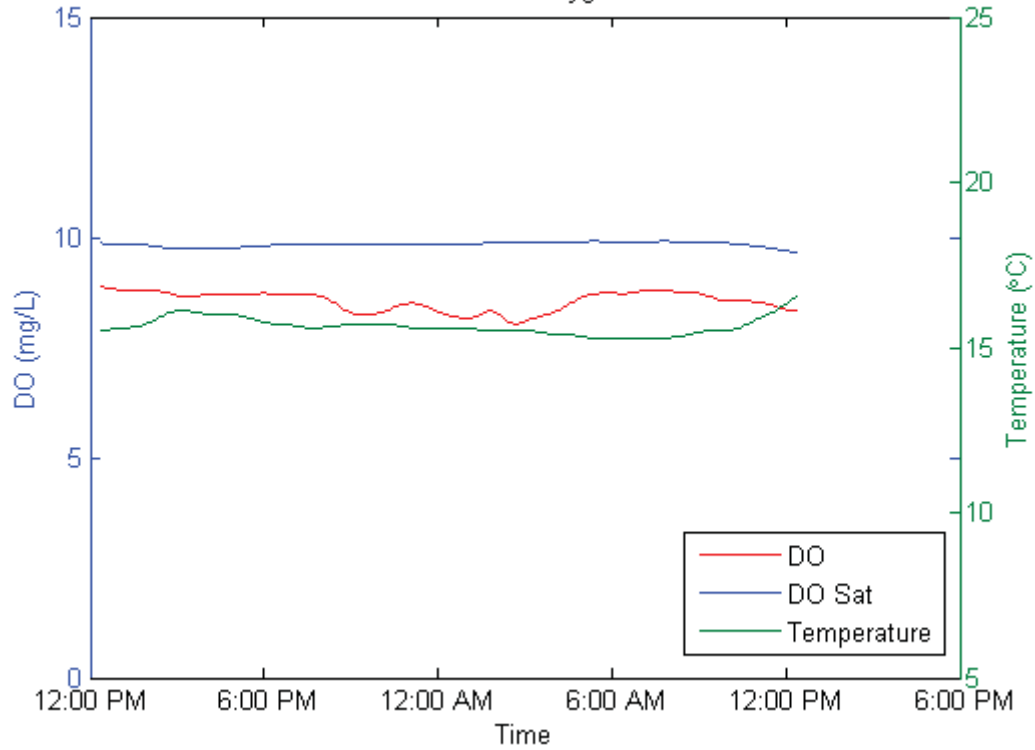


April: Downstream  
Ecosystem metabolism

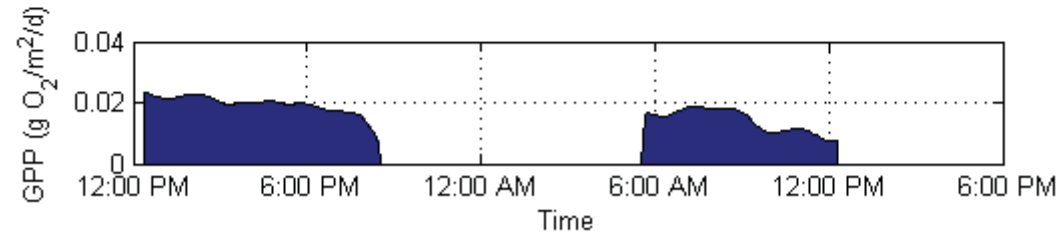
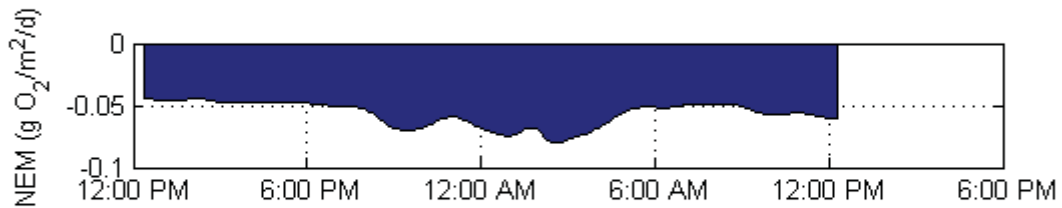
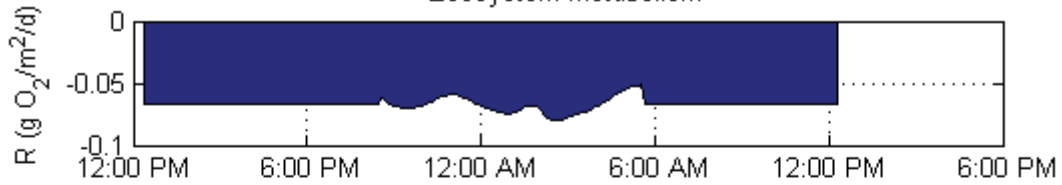


### June 2011, upstream

June: Upstream  
Dissolved oxygen



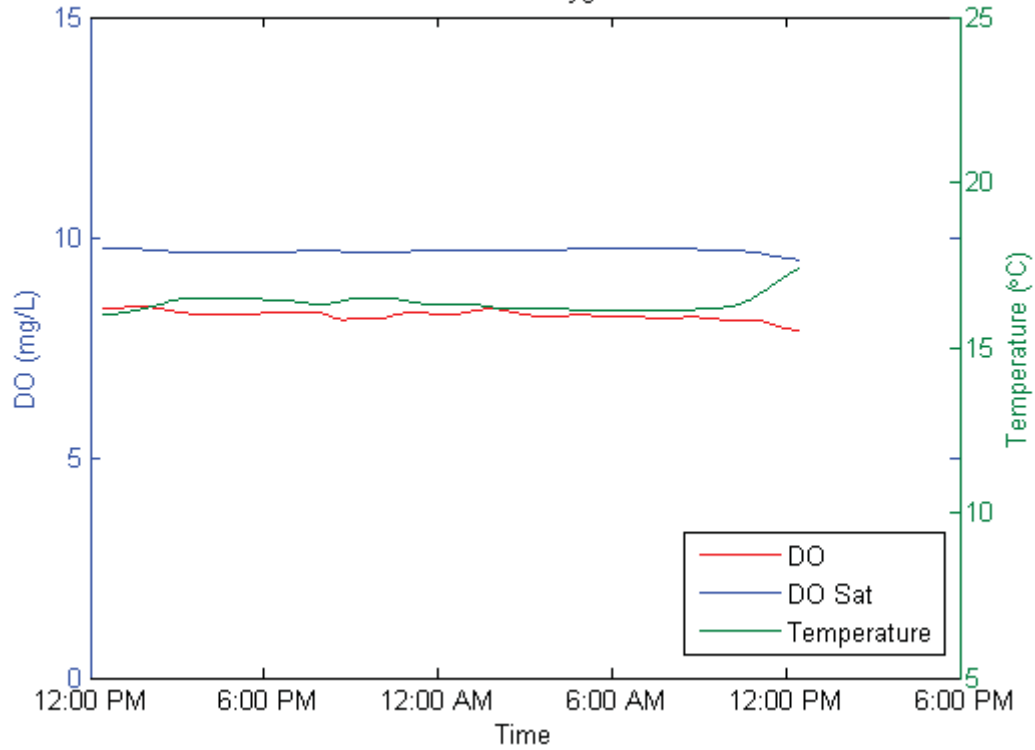
June: Upstream  
Ecosystem metabolism



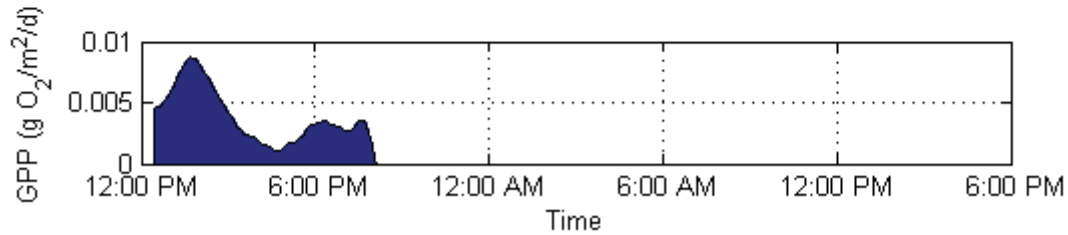
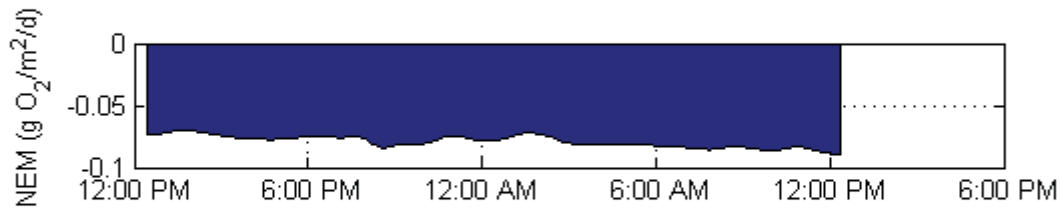
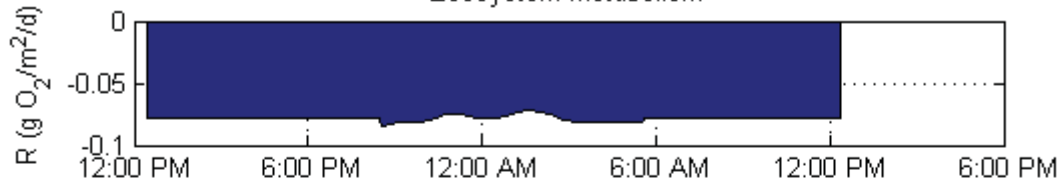


### June 2011, downstream

June: Downstream  
Dissolved oxygen

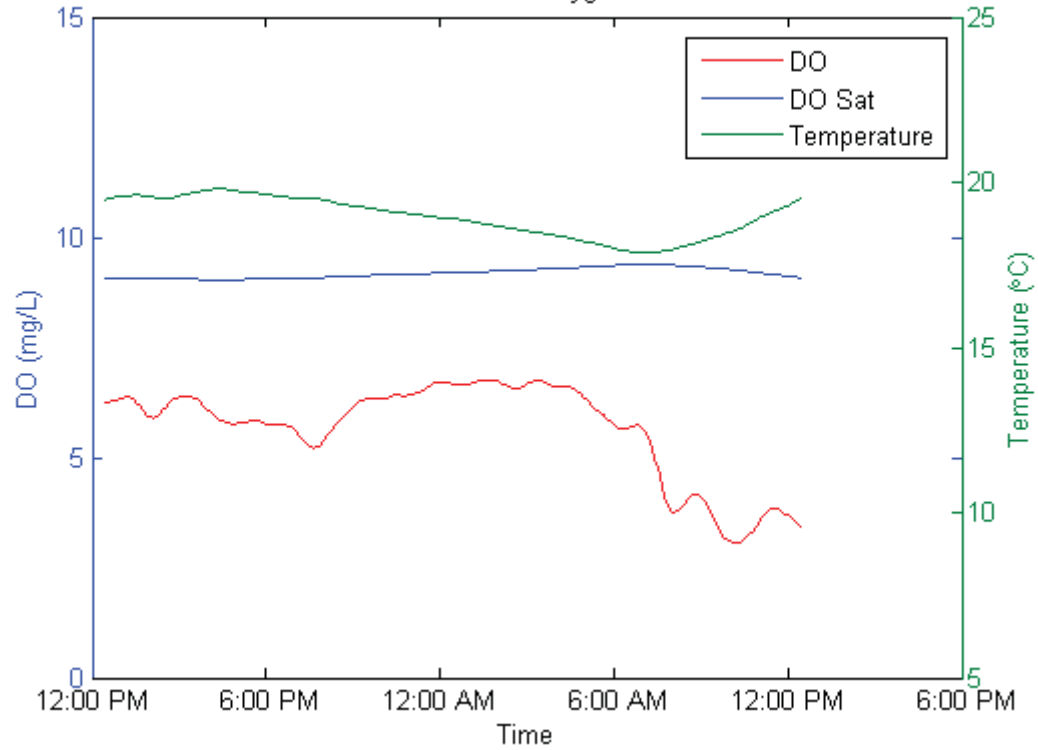


June: Downstream  
Ecosystem metabolism

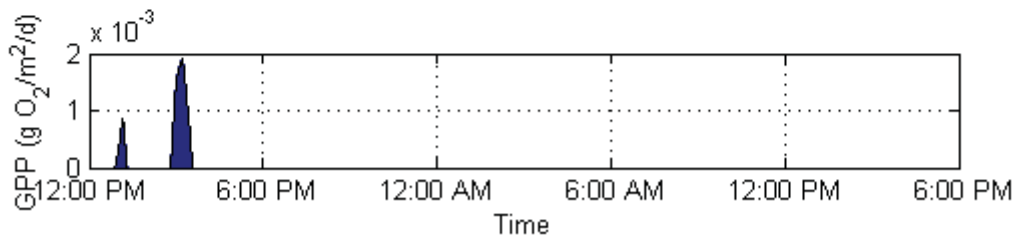
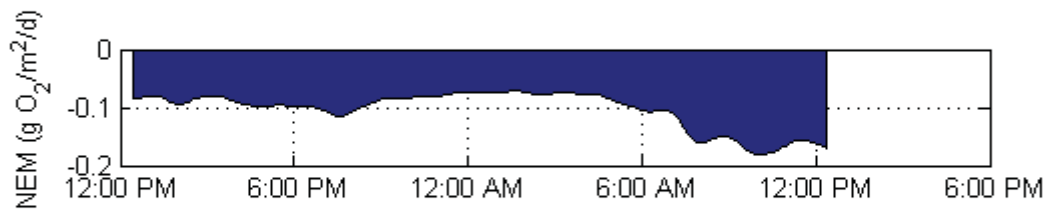
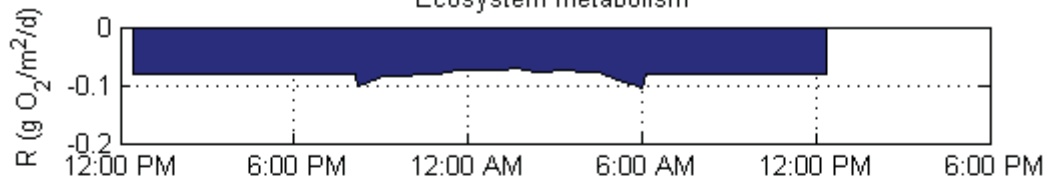


### August 2011, upstream

August: Upstream  
Dissolved oxygen

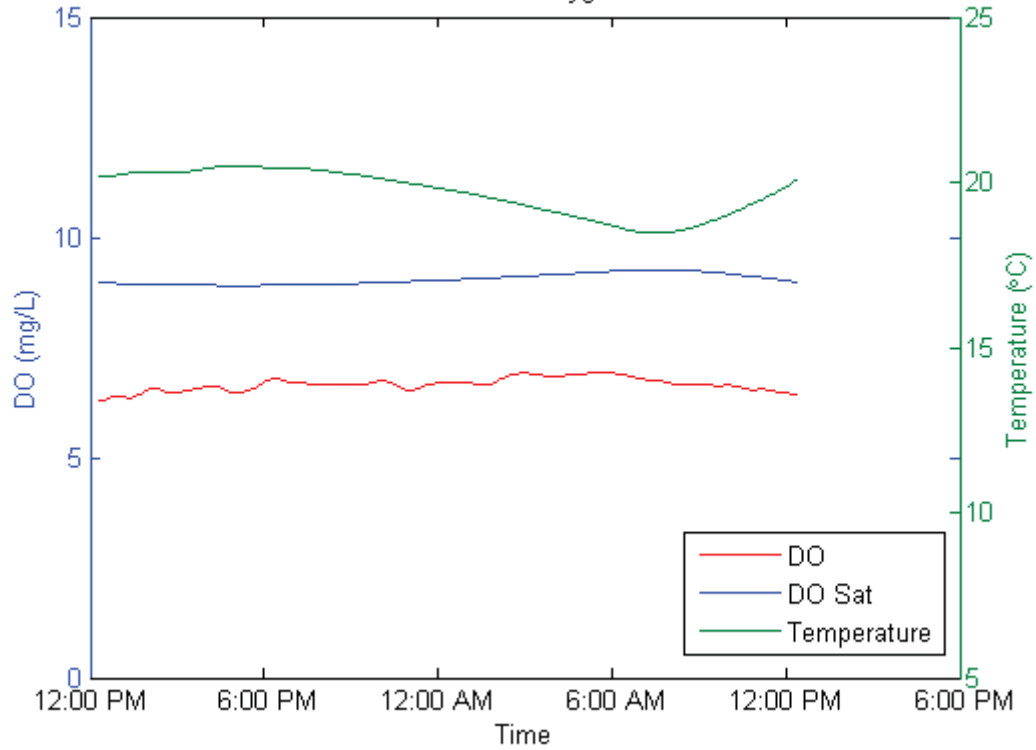


August: Upstream  
Ecosystem metabolism

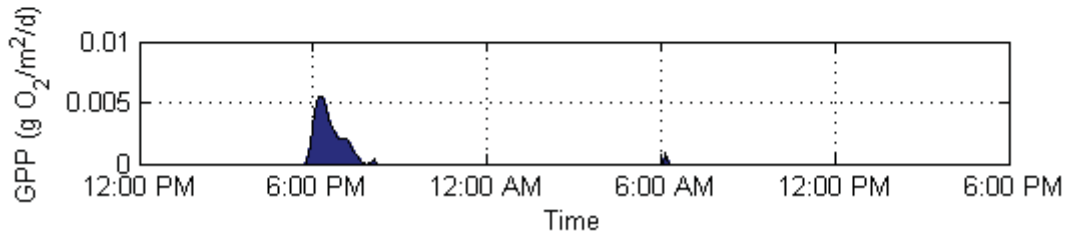
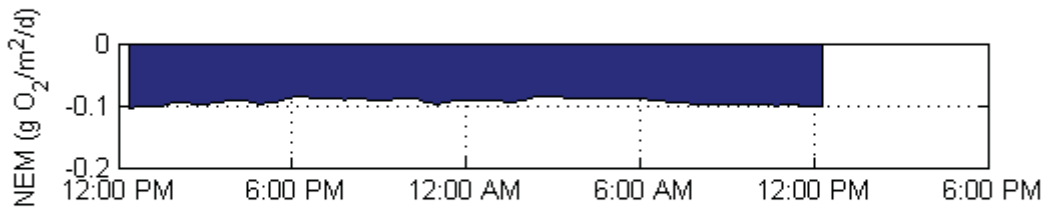
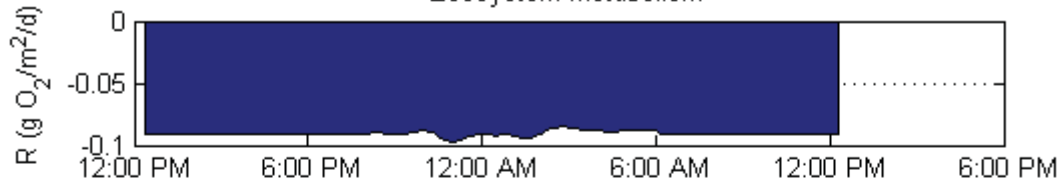


### August 2011, downstream

August: Downstream  
Dissolved oxygen

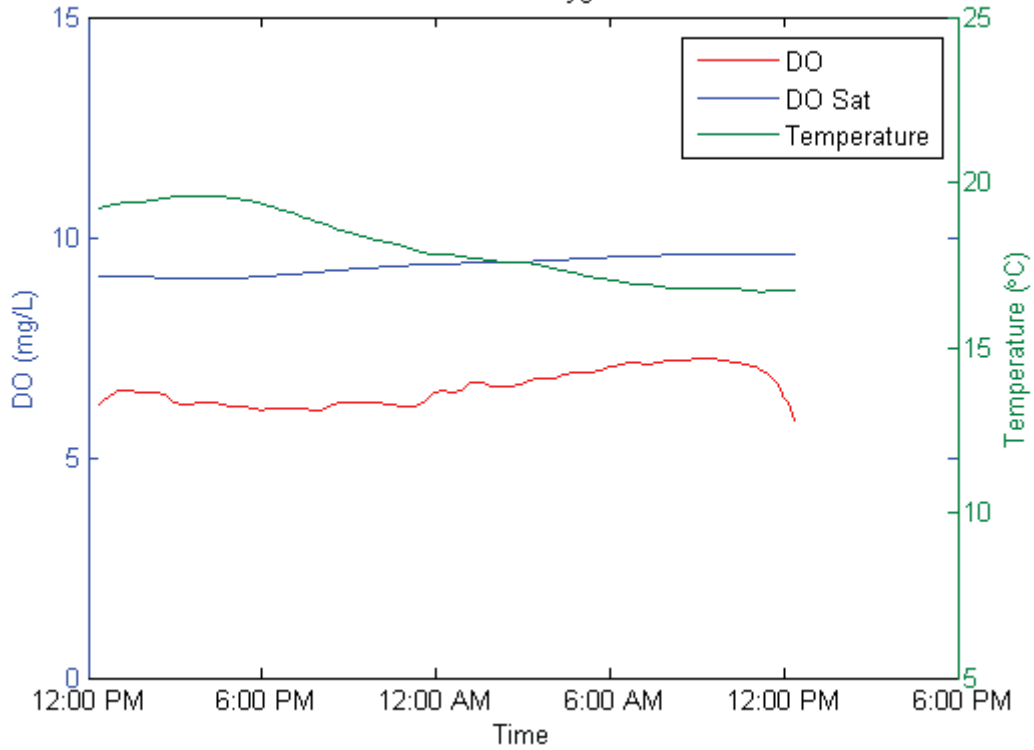


August: Downstream  
Ecosystem metabolism

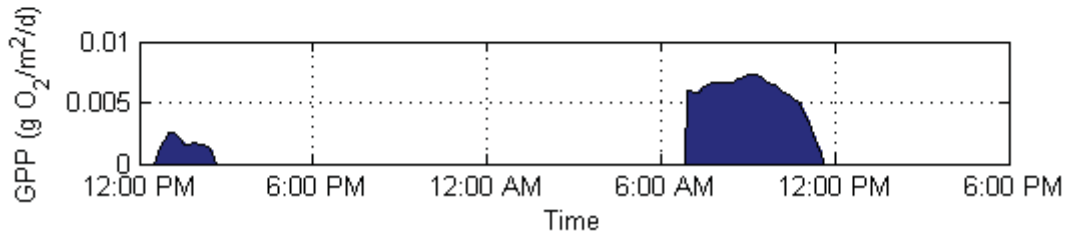
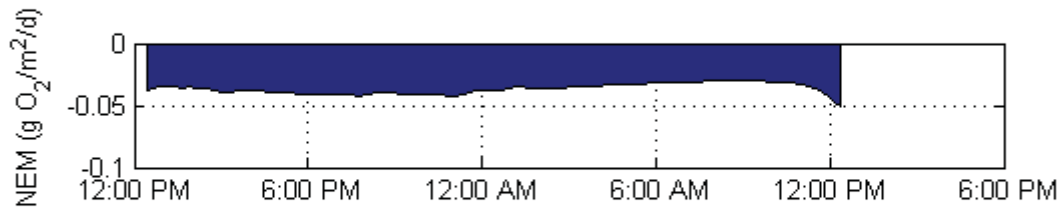
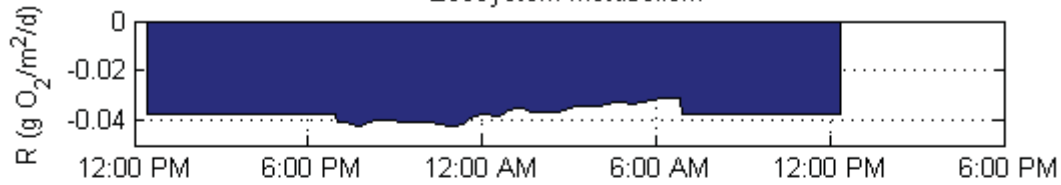


### September 2010, upstream

September: Upstream  
Dissolved oxygen

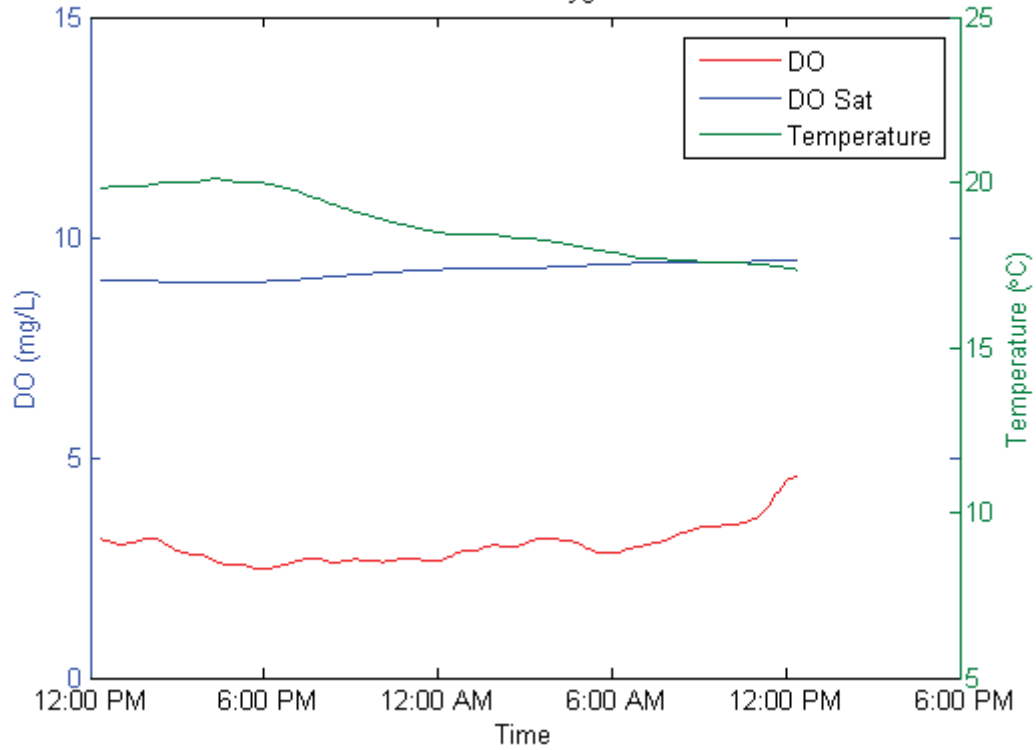


September: Upstream  
Ecosystem metabolism

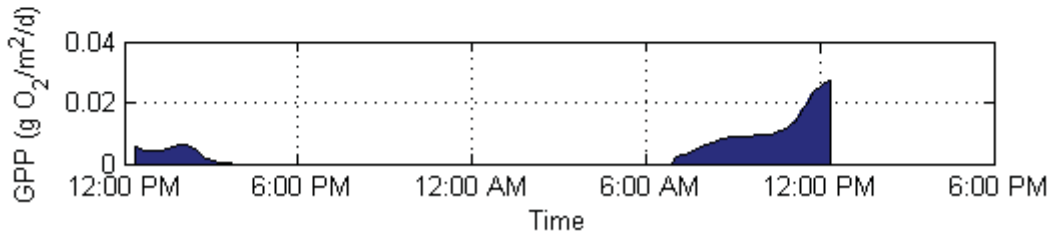
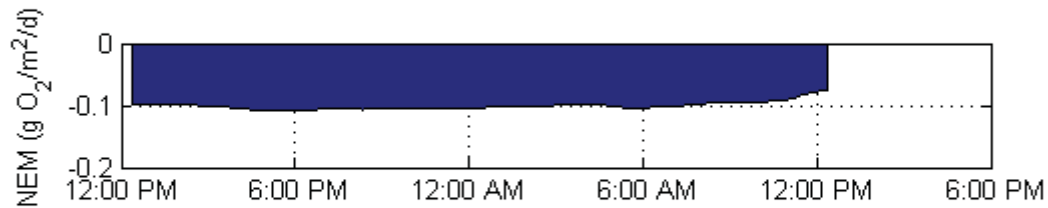
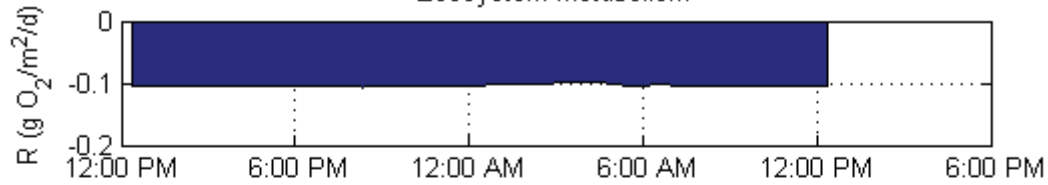


### September 2010, downstream

September: Downstream  
Dissolved oxygen

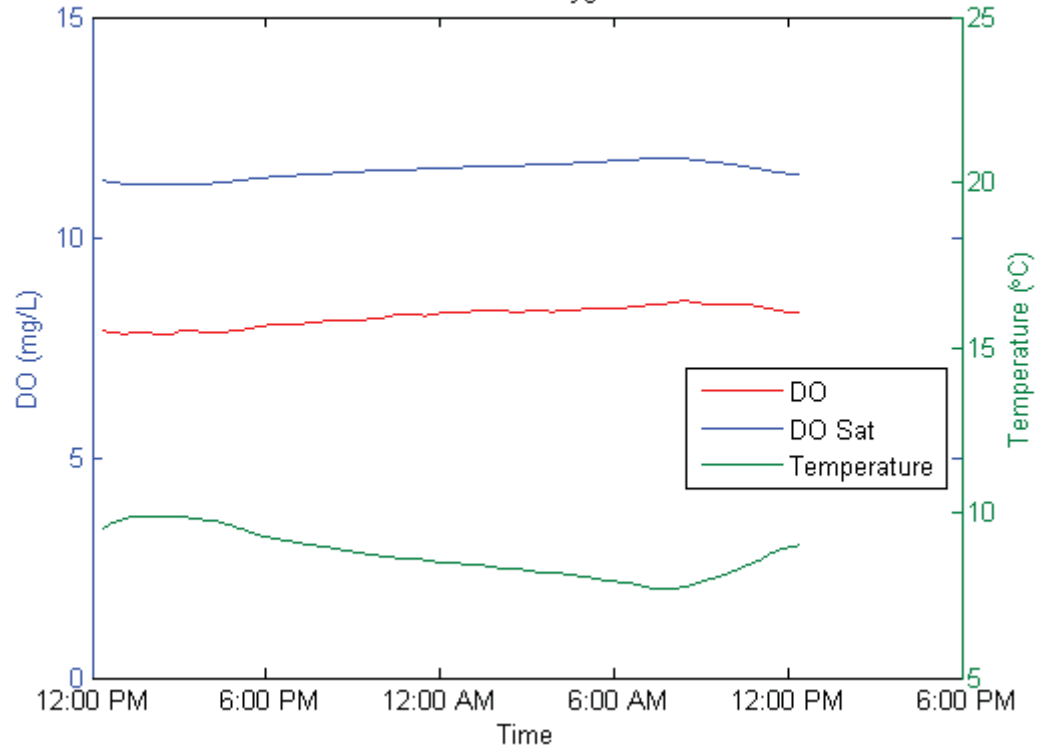


September: Downstream  
Ecosystem metabolism

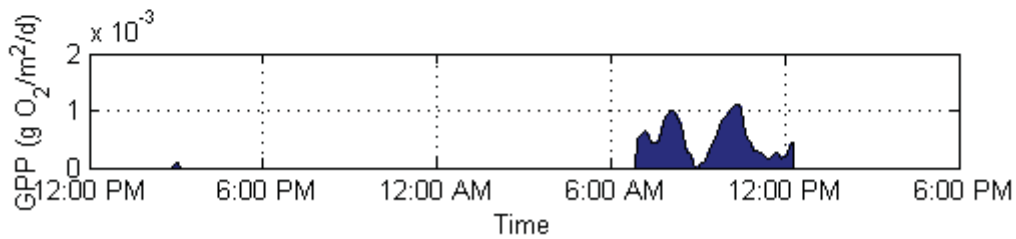
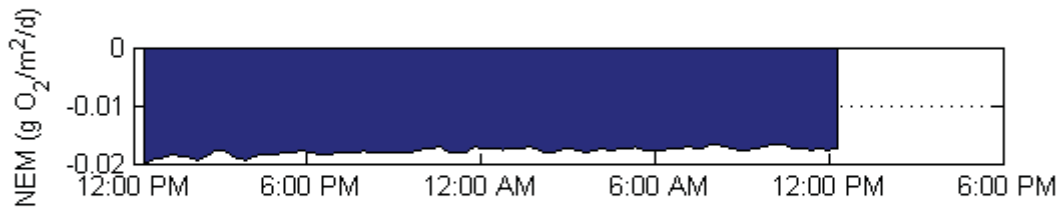
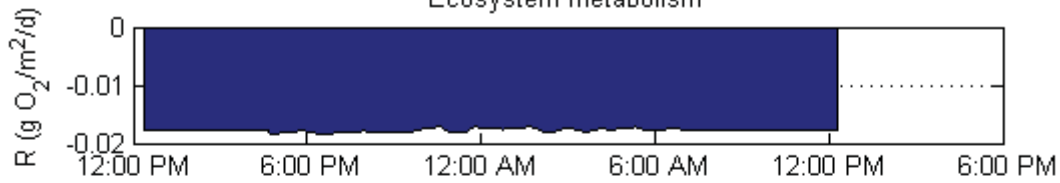


### November 2010, upstream

November: Upstream  
Dissolved oxygen

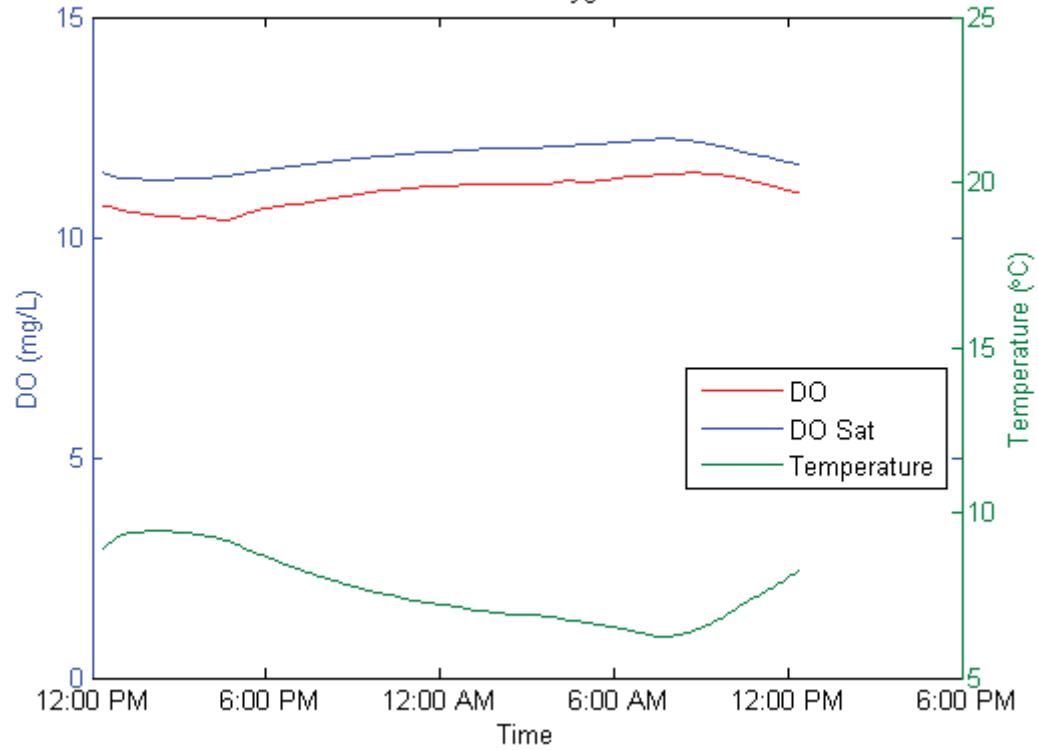


November: Upstream  
Ecosystem metabolism

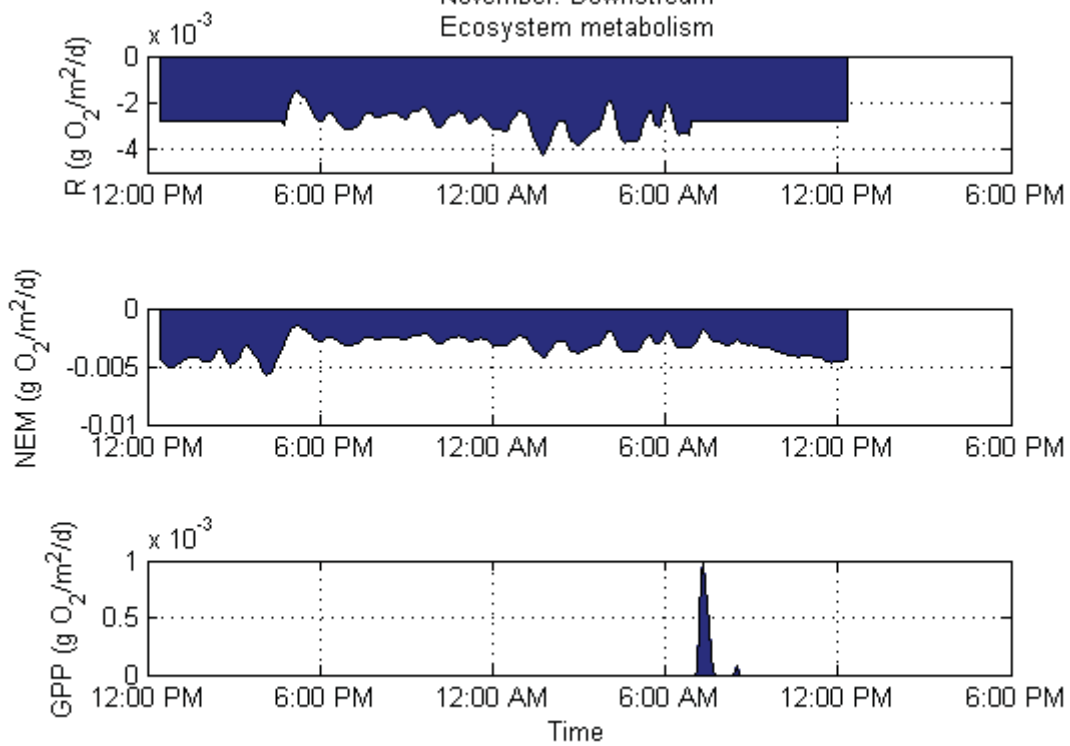


### November 2010, downstream

November: Downstream  
Dissolved oxygen



November: Downstream  
Ecosystem metabolism



## APPENDIX F: IN-STREAM AND SOURCE CONCENTRATIONS

Analyte	Data source	Feb	Apr	Jun	Aug	Sep	Nov	Total
<b>DIC</b> ( $\mu\text{M}$ )	Avg conc. at spring	703	773	746	712	539	-	686
	Med. in-stream conc.	264	266	352	365	470	-	319
<b>DOC</b> ( $\mu\text{M}$ )	Avg conc. at spring	43.9	38.4	28.6	50.7	56.5	106	50.4
	Med. in-stream conc.	72.7	127	104	134	199	138	122
<b>BDOC</b> ( $\mu\text{M}$ )	Avg conc. at spring	8.61	19.6	20.3	19.7	36.6	35.8	22.6
	Med. in-stream conc.	11.0	17.8	27.5	9.33	51.4	10.3	16.6
<b>RDOC</b> ( $\mu\text{M}$ )	Avg conc. at spring	35.3	18.8	8.34	31.0	20.0	70.5	27.8
	Med. in-stream conc.	57.9	112	79.2	124	153	124	104
<b>TDN</b> ( $\mu\text{M}$ )	Avg conc. at spring	16.9	19.9	18.4	25.7	25.4	18.4	21.1
	Med. in-stream conc.	16.3	17.9	18.8	17.8	15.2	5.69	17.1
<b>DON</b> ( $\mu\text{M}$ )	Avg conc. at spring	4.02	7.70	0	1.85	2.64	0	2.47
	Med. in-stream conc.	4.81	8.04	5.62	4.86	8.84	4.41	5.50
<b>NO<sub>3</sub><sup>-</sup></b> ( $\mu\text{M}$ )	Avg conc. at spring	12.5	10.6	19.6	22.7	22.0	18.0	17.5
	Med. in-stream conc.	10.4	8.78	11.7	12.0	5.59	1.04	9.50
<b>NH<sub>4</sub><sup>+</sup></b> ( $\mu\text{M}$ )	Avg conc. at spring	0.73	0.25	0.60	1.08	0.75	0.52	0.66
	Med. in-stream conc.	0.64	0.33	1.21	1.16	1.53	0.225	0.73
<b>PO<sub>4</sub><sup>3-</sup></b> ( $\mu\text{M}$ )	Avg conc. at spring	0.76	0.8	0.94	1.14	1.40	1.53	1.05
	Med. in-stream conc.	0.4	0.33	0.585	0.62	0.68	0.22	0.46
<b>SO<sub>4</sub><sup>2-</sup></b> ( $\mu\text{M}$ )	Avg conc. at spring	88.3	99.5	83.0	93.7	98.6	113	94.5
	Med. in-stream conc.	128	140	101	93.1	112	146	115
<b>Cl<sup>-</sup></b> ( $\mu\text{M}$ )	Avg conc. at spring	78.9	78.8	79.5	78.4	80.0	69.0	78.2
	Med. in-stream conc.	85.9	82.4	74.6	68.8	97.0	96.2	83.4
<b><math>\delta^{18}\text{O}</math></b> (‰)	Avg. value at spring	-7.48	-7.63	-7.60	-7.42	-6.98	-7.11	-7.39
	Med. in-stream value	-7.41	-7.55	-7.40	-7.22	-6.78	-7.05	-7.29
<b><math>\delta\text{D}</math></b> (‰)	Avg. value at spring	-43.4	-43.9	-42.9	-41.3	-39.7	-39.5	-42.0
	Med. in-stream value	-42.5	-41.9	-42.1	-40.5	-38.2	-39.7	-41.3
<b>D-excess</b> (‰)	Avg. value at spring	16.5	17.1	17.9	18.0	16.1	17.4	17.2
	Med. in-stream value	16.4	18.4	17.0	17.5	15.7	16.7	16.9
<b>DOC/DON</b> ( $\mu\text{M}/\mu\text{M}$ )	Avg. ratio at spring	3.17	4.99	-	27.8	20.6	-	17.5
	Med. in-stream ratio	15.0	14.9	19.1	27.1	24.8	34.4	20.6
<b>DOC/ PO<sub>4</sub><sup>3-</sup></b> ( $\mu\text{M}/\mu\text{M}$ )	Avg. ratio at spring	95.3	31.7	37.3	43.3	39.1	69.5	53.1
	Med. in-stream ratio	185	366	181	222	282	605	260
<b>TDN/ PO<sub>4</sub><sup>3-</sup></b> ( $\mu\text{M}/\mu\text{M}$ )	Avg. ratio at spring	29.2	16.4	22.8	23.0	18.9	12.0	21.6
	Med. in-stream ratio	42.9	52.3	32.0	27.4	22.0	27.1	32.4



## APPENDIX G: SINGLE STATION METHOD FOR DETERMINING NEM

Net ecosystem metabolism calculations were calculated using an in-situ single station method of dissolved oxygen (DO) change (Bott, 2006). The code required a data .xls file which had for each time step pH, conductivity ( $\mu\text{S}/\text{cm}$ ), specific conductance ( $\mu\text{S}/\text{cm}$ ), dissolved oxygen (mg/L), dissolved oxygen saturation (%), temperature ( $^{\circ}\text{C}$ ), and pressure (kPa). A generic run name (e.g. “September: Upstream”), average stream velocity (cm/s) (determined from the salt injection), and average stream depth (cm) were inputted manually for each analysis. Additionally, start and end dates and times of the analysis (12:20 pm on the first and second day) and the sunset and sunrise dates and times (at the end of the first day and beginning of the second) were inputted manually. Sunrise and sunset data were obtained for Newark, DE (NOAA, 2012).

All variables were trimmed to a 12:20 pm start and end time for consistency. The midpoints of each time step and the midpoints of each change in DO (4) were calculated, stored, and used for further analysis. Temperatures were converted to Kelvin, and dissolved oxygen saturation concentrations were calculated (5) (Benson and Krause Jr., 1984).

$$\Delta DO_i = DO_{i+1} - DO_i \quad (4)$$

$$DO_{siSTP} = e^{\left(-139.34411 + \frac{1.575701 \times 10^5}{T_i} - \frac{6.642308 \times 10^7}{T_i^2} + \frac{1.243800 \times 10^{10}}{T_i^3} - \frac{8.621949 \times 10^{11}}{T_i^4}\right)} \quad (5)$$

Where:

$\Delta DO_i$  = change in dissolved oxygen concentration at time step  $i$  (mg/L/time step),

$DO_i$  = dissolved oxygen concentration at time step  $i$  (mg/L)

$DO_{siSTP}$  = dissolved oxygen saturation concentration (mg/L) at standard temperature and pressure (STP) at time step  $i$ ,

$T_i$  = temperature in Kelvin at time step  $i$ .

After determining the barometric pressure at the average height of the watershed (92.5 m) (6),

dissolved oxygen saturation concentration was corrected for altitude (7)

$$P_h = \frac{101325}{133.322} (1 - 2.25577 \times 10^{-5} h)^{5.25588} \quad (6)$$

$$DO_{si} = DO_{siSTP} \times \frac{P_h}{760} \quad (7)$$

Where:

$P_h$  = pressure (mmHg),

$DO_s$  = dissolved oxygen saturation concentration (mg/L) at elevation  $h$  (m).

$DO_i$  saturation deficit or surplus ( $DO_i - DO_{si}$ ) (mg/L) was calculated by subtracting the corrected dissolved oxygen saturation concentration from the actual dissolved oxygen concentration. Gas exchange coefficients per time-step at 20°C were calculated using the surface renewal model and were corrected for actual temperature (Bott, 2006) (8) and (9).

$$K_{20} = \frac{1}{N - 1} \times 50.8 \times V^{0.67} \times H^{-1.85} \quad (8)$$

$$K_{2i} = K_{20} \times 1.024^{(t_i - 20)} \quad (9)$$

Where:

$K_{20i}$  = the gas exchange coefficient at 20°C (1/time step),

$K_{2i}$  = gas exchange coefficient (1/time step) at a given temperature  $t_i$  (°C) at time step  $i$ ,

$N$  = total number of time steps in a day,

$V$  = average velocity of the stream (cm/s),

$H$  = average depth of the reach (cm).

Gas exchange rates for each time step were calculated (10), and the averaged value between time steps was used for analysis. The rate of oxygen change corrected for gas exchange (corrected re-aeration) was calculated by adding the gas exchange rate and the dissolved oxygen saturation deficit or surplus at each time step (11). This corrected oxygen change was multiplied by depth to obtain net ecosystem metabolism (NEM) per area per time step (12).

$$E_i = (DO_i - DO_{si}) \times K_{2i} \quad (10)$$

$$CR_i = E_i + \Delta DO_i \quad (11)$$

$$NEM_i = CR_i * \left(\frac{H}{100}\right) \quad (12)$$

Where:

$E_i$  = gas exchange rate (mg/L/time step) at time step  $i$ ,

$CR_i$  = corrected re-aeration rate (mg/L/time step) at time step  $i$ ,

$NEM_i$  = net ecosystem metabolism (g/m<sup>2</sup>/time step) at time step  $i$ .

$NEM_i$  values between sunset and sunrise were averaged to obtain average nighttime NEM ( $NEM_{night}$ ), which was assumed to be equal to the respiration rate at each time step during the day ( $R_{dayi}$ ). This average daily respiration was subtracted from all daytime  $NEM_i$  values (between sunrise and sunset) to determine primary production at each daytime time step ( $P_i$ ) (assuming no nighttime primary production between sunset and sunrise). In cases when daytime  $NEM_i$  values were more negative than average nighttime respiration values - indicating greater daytime respiration than nighttime - subtracting the average nighttime respiration value from  $NEM_i$  values yielded negative primary production values at some time steps - which are implausible. During these time steps, primary production is functionally below the detection limit and was assumed to be operationally equal to 0 (13). Respiration rates at each time step were calculated by subtracting production ( $P_i$ ) values from  $NEM_i$  (14).

*For all timesteps between sunrise and sunset:*

$$\begin{aligned} & \text{if } NEM_i - R_{dayi} > 0, \text{ then } P_i = NEM_i - R_{dayi} \\ & \text{else } P_i = 0 \end{aligned} \quad (13)$$

*For all timesteps between sunset and sunrise:*

$$\begin{aligned} & P_i = 0 \\ & R_i = NEM_i - P_i \end{aligned} \quad (14)$$

Where:

$R_i$  = respiration rate ( $\text{g}/\text{m}^2/\text{time step}$ ) at time step  $i$ ,

$P_i$  = production rate ( $\text{g}/\text{m}^2/\text{time step}$ ) at time step  $i$ .

Metabolism ( $\text{NEM}_i$ ), respiration ( $R_i$ ), and primary production ( $P_i$ ) values at each time step during the 24-hour period were summed to obtain net ecosystem metabolism, respiration, and gross primary production. Additionally, summary statistics of P/R, average daily temperature, and average pH were calculated.

## APPENDIX H: CONSTRAINED-RATE NUTRIENT INJECTION CALCULATIONS

Discharge at each sample station was calculated using chloride dilution using upstream chloride concentrations (Station 0) as background (15).

$$Q = \frac{(C_R - C_0) \times Q_R}{C_i - C_0} \quad (15)$$

Where:

$Q$  = in-stream discharge (L/s),

$i$  = station number,

$C_R$  = chloride concentration of the injectate ( $\mu\text{M}$ ),

$C_0$  = background in-stream chloride concentration at Station 0 ( $\mu\text{M}$ ),

$C_i$  = plateau chloride concentration at station  $i$  ( $\mu\text{M}$ ),

$Q_R$  = discharge rate of the injection pump (L/s).

DOC and ammonium data were normalized for chloride (16), and were log-transformed and plotted with station distance (17). Uptake parameters were calculated by solving a least squares equation for slope ( $k_w$ ). (18) was used to determine uptake distance, (19) was used to determine uptake velocity, and (20) was used to determine areal uptake (example calculations in Appendix I).

$$CN_i = \frac{N_i - N_0}{C_i - C_0} \quad (16)$$

$$\ln(CN_x) = \ln(CN_0) - k_w x \quad (17)$$

$$S_w = \frac{1}{k_w} \quad (18)$$

$$v_f = \frac{Vd}{S_w} \quad (19)$$

$$U = v_f N_0 \quad (20)$$

Where:

$CN_i$  = normalized nutrient (DOC or ammonium) concentration at Station  $i$  ( $\mu\text{M}/\mu\text{M}$ ),

$N_i$  = plateau nutrient concentration at station  $i$  ( $\mu\text{M}$ ),

$N_0$  = background in-stream nutrient concentration at Station 0 ( $\mu\text{M}$ ),

$C_i$  = plateau chloride concentration at station  $i$  ( $\mu\text{M}$ ),

$C_0$  = background in-stream chloride concentration at Station 0 ( $\mu\text{M}$ ),

$CN_x$  = modeled normalized nutrient concentration ( $\mu\text{M}/\mu\text{M}$ ) at distance  $x$  (m) downstream from the injection site,

$CN_0$  = calculated normalized nutrient concentration at Station 0 ( $\mu\text{M}/\mu\text{M}$ ),

$k_w$  = calculated slope ( $1/\text{m}$ ) for the least squares regression between the log-normalized normalized nutrient concentrations and station distances,

$S_w$  = nutrient uptake length (m),

$v_f$  = nutrient uptake velocity (m/s),

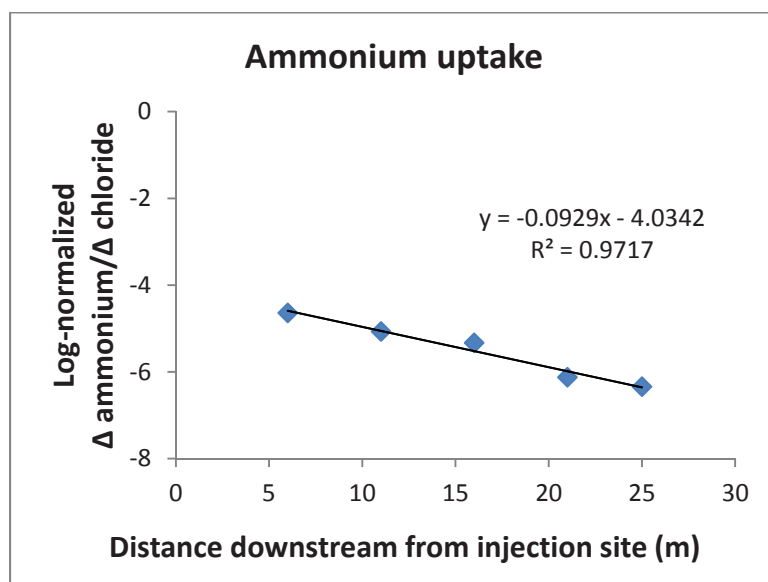
$V$  = average stream velocity of the reach (m/s),

$d$  = average stream depth of the reach (m),

$U$  = areal nutrient uptake rate ( $\mu\text{M m/s}$ ).

## APPENDIX I: EXAMPLE CALCULATIONS FOR AMMONIUM UPTAKE

Note: This example is for the November 2010, upstream injection experiment.



$CN_i$  ( $\Delta$  ammonium /  $\Delta$  chloride) at each station is found using (16), where the change in concentration (e.g.  $\Delta$  ammonium) is the difference between the concentrations at Station  $i$  and the background concentration at Station 0. A linear regression between  $CN_i$  and distance ( $x$ ) yields a slope of  $k_w = -0.09$  (1/m).

Uptake distance ( $S_w$ ) is determined using (17).  $S_w = 1/(0.09 \text{ /m})$ .  $S_w = 10.8 \text{ m}$ .

Uptake velocity is determined Using (18), given a stream velocity ( $V$ ) of 0.006 m/s and a depth ( $d$ ) of 0.05 m.  $v_f = 0.006 \text{ m/s} * 0.05 \text{ m}/10.8\text{m} * (100 \text{ cm}/1 \text{ m})$ .  $v_f = 0.003 \text{ cm/s}$ .

Areal uptake rate is determined using (19), given a background in-stream ammonium concentration ( $N_0$ ) of 1.01  $\mu\text{M}$ .  $U = 0.003 \text{ cm/s} * 1.01 \mu\text{M} * (1 \text{ m}/100 \text{ cm}) * (1 \text{ M}/1000 \mu\text{M}) * (1000 \text{ mol}/1 \text{ m}^3) * (1000 \mu\text{mol}/1 \text{ mol})$ .  $U = 0.03 \mu\text{mol}/\text{m}^2/\text{s}$ .

## APPENDIX J: CARBON AND AMMONIUM UPTAKE VALUES

### DOC uptake – Upstream location

	Feb	Apr	Jun	Aug	Sep	Nov
Uptake length ( $S_w$ ) (m)	0.0	26.7	129.6	62.6	13.9	275.5
Uptake velocity ( $V_f$ ) (cm/s)	0.0	0.004	0.001	0.001	0.001	0.0
Areal uptake (U) ( $\mu\text{M}/\text{m}^2/\text{s}$ )	0.0	4.82	0.93	0.76	2.10	0.14

### DOC uptake – Downstream location

	Feb	Apr	Jun	Aug	Sep	Nov
Uptake length ( $S_w$ ) (m)	29.0	18.9	8.5	92.7	14.5	0.0
Uptake velocity ( $V_f$ ) (cm/s)	0.018	0.058	0.090	0.002	0.001	0.000
Areal uptake (U) ( $\mu\text{M}/\text{m}^2/\text{s}$ )	12.43	74.35	96.17	2.89	0.87	0.00

### Ammonium uptake – Upstream location

	Feb	Apr	Jun	Aug	Sep	Nov
Uptake length ( $S_w$ ) (m)	156.5	121.9	33.0	29.8	7.8	10.8
Uptake velocity ( $V_f$ ) (cm/s)	0.002	0.001	0.003	0.002	0.002	0.003
Areal uptake (U) ( $\mu\text{M}/\text{m}^2/\text{s}$ )	0.013	0.003	0.038	0.022	0.031	0.030

### Ammonium uptake – Downstream location

	Feb	Apr	Jun	Aug	Sep	Nov
Uptake length ( $S_w$ ) (m)	0.0	0.0	216.2	41.0	3.2	25.4
Uptake velocity ( $V_f$ ) (cm/s)	0.0	0.0	0.004	0.005	0.004	0.005
Areal uptake (U) ( $\mu\text{M}/\text{m}^2/\text{s}$ )	0.0	0.0	0.032	0.051	0.020	0.047



## **APPENDIX K: MATLAB CODE**

## K.1 NEM: FEBRUARY 2012, UPSTREAM

```
%Luke Wildfire
%NEM_calculations
%
%10/2/2013

%Clean up
clear all
clc
close all

%-----

%Import csv file (I'll be working with DO data that has ppm - not %
[num txt] = xlsread('D6_upstream.xls');

%-----

%ENTER VARIABLES SPECIFIC TO EACH RUN

%Give run a name
NAME = 'February: Upstream';
%Stream Velocity in (cm/s)
V = 4.97071870057113;
%Stream Height in (cm)
H = 5.73333333;

%-----

%Define dates and times

%12:20pm (20 past noon) on first day of measurement
RoughStartTime = datenum('February 4, 2012 12:20:00000 PM');
%12:20pm (half past noon) on next day of measurement
RoughEndTime = datenum('February 5, 2012 12:20:00000 PM');
%Sunset on first day of measurement
SUNSET = datenum('February 4, 2012 5:26:00.000 PM');
%Sunrise on next day of measurement
SUNRISE = datenum('February 5, 2012 7:07:00.000 AM');

%-----

%Give each variable a name and then smooth
%Graph all variables on one plot vs time
```

```

%TIME is originally (mm/dd/yyyy h:mm:ss PM)
TIME = txt((2:end),1);
%Convert TIME to a number
TIME = datenum(TIME);
%Smooth the data
TIME = smooth(TIME, 25, 'rloess');

%Pressure (kPa)
BARO = num(:,1);
BARO = smooth(BARO, 25, 'rloess');
subplot(2,3,1); plot(TIME,BARO); datetick('x',16); axis tight;
xlabel('Pressure (kPa)');

%Conductance and Specific Conductance (uS/cm)
COND = num(:,2);
COND = smooth(COND, 25, 'rloess');
subplot(2,3,2); plot(TIME,COND); datetick('x',16); axis tight;
xlabel('Conductivity (uS/cm)');
title({NAME ;'All data (untrimmed)'});

SPECCOND = num(:,3);
SPECCOND = smooth(SPECCOND, 25, 'rloess');
subplot(2,3,3); plot(TIME,SPECCOND); datetick('x',16); axis tight;
xlabel('Specific Conductance (uS/cm)');

%Dissolved Oxygen (mg/L, ppm, or g/m^3)
DOPPM = num(:,4);
DOPPM = smooth(DOPPM, 25, 'rloess');
subplot(2,3,4); plot(TIME,DOPPM); datetick('x',16); axis tight;
xlabel('DO (ppm)');

%pH
PH = num(:,5);
PH = smooth(PH, 25, 'rloess');
subplot(2,3,5);plot(TIME,PH); datetick('x',16); axis tight;
xlabel('pH');

%Temperature (deg C)
TEMP = num(:,6);
TEMP = smooth(TEMP, 25, 'rloess');
subplot(2,3,6);plot(TIME,TEMP);datetick('x',16); axis tight;
xlabel('Temperature (deg. C)');

%-----

%Determine time step, and adjust the RoughEndTime up one time step

```

```

TIME_STEP = TIME(2)-TIME(1);
RoughEndTime = RoughEndTime + TIME_STEP;

%-----

%Trim all data to appropriate time frame
%Graph each variable as before

%Create a new figure
figure('Position',[300,300,800,500]);

%Time
TIME_trim1 = TIME(RoughStartTime<TIME);
TIME_trim = TIME_trim1(TIME_trim1<RoughEndTime);
N = length(TIME_trim);
disp(['The number of time increments is: ' num2str(N)]);

%Pressure (kPa)
BARO_trim1 = BARO(RoughStartTime<TIME);
BARO_trim = BARO_trim1(TIME_trim1<RoughEndTime);
subplot(2,3,1); plot(TIME_trim,BARO_trim);
datetick('x','HH');
xlim([RoughStartTime-.05 RoughEndTime+.05]);
xlabel('Time of day (hr)');
ylabel('Pressure (kPa)');
vline([SUNSET SUNRISE]);

%Conductance and Specific Conductance (uS/cm)
COND_trim1 = COND(RoughStartTime<TIME);
COND_trim = COND_trim1(TIME_trim1<RoughEndTime);
subplot(2,3,2); plot(TIME_trim,COND_trim);
datetick('x','HH');
xlim([RoughStartTime-.05 RoughEndTime+.05]);
xlabel('Time of day (hr)');
ylabel('Conductivity (uS/cm)');
vline([SUNSET SUNRISE]);
title({'NAME ;'All data (trimmed)'});

SPECCOND_trim1 = SPECCOND(RoughStartTime<TIME);
SPECCOND_trim = SPECCOND_trim1(TIME_trim1<RoughEndTime);
subplot(2,3,3); plot(TIME_trim,SPECCOND_trim);
datetick('x','HH');
xlim([RoughStartTime-.05 RoughEndTime+.05]);
xlabel('Time of day (hr)');
ylabel('Specific Conductance (uS/cm)');
vline([SUNSET SUNRISE]);

```

```

%Dissolved Oxygen (mg/L, ppm, or g/m^3)
DOPPM_trim1 = DOPPM(RoughStartTime<TIME);
DOPPM_trim = DOPPM_trim1(TIME_trim1<RoughEndTime);
subplot(2,3,4); plot(TIME_trim,DOPPM_trim);
datetick('x','HH');
xlim([RoughStartTime-.05 RoughEndTime+.05]);
xlabel('Time of day (hr)');
ylabel('DO (ppm)');
vline([SUNSET SUNRISE]);

```

```

%pH
PH_trim1 = PH(RoughStartTime<TIME);
PH_trim = PH_trim1(TIME_trim1<RoughEndTime);
subplot(2,3,5);plot(TIME_trim,PH_trim);
datetick('x','HH');
xlim([RoughStartTime-.05 RoughEndTime+.05]);
xlabel('Time of day (hr)');
ylabel('pH');
vline([SUNSET SUNRISE]);

```

```

%Temperature (deg C)
TEMP_trim1 = TEMP(RoughStartTime<TIME);
TEMP_trim = TEMP_trim1(TIME_trim1<RoughEndTime);
subplot(2,3,6);plot(TIME_trim,TEMP_trim);
datetick('x','HH');
xlim([RoughStartTime-.05 RoughEndTime+.05]);
xlabel('Time of day (hr)');
ylabel('Temperature (deg. C)');
vline([SUNSET SUNRISE]);

```

```

%-----

```

```

%Create a vector of time-stamps as the midpoint of each sampling time
%aka Column "D"

```

```

for i=1:(N-1)
    TIME_stamp(i) = (TIME_trim(i) + TIME_trim(i+1))./2;
end
TIME_stamp = TIME_stamp';

```

```

%-----

```

```

%Calculate a vector of Delta DO (column "E")

```

```

for i=1:(N-1)

```

```

    DELTA_DO(i) = (DOPPM_trim(i+1)-DOPPM_trim(i));
end
DELTA_DO = DELTA_DO';

%-----

%Calculate DO Saturation concentration (mg/L)
%Column "F"

%convert temperature to Kelvin
TEMP_Kelvin = TEMP_trim+273.15;

%Use this code to determine DO sat (mg/L)
vp1 = -139.34411;
vp2 = 1.575701e5;
vp3 = -6.642308e7;
vp4 = 1.2438e10;
vp5 = -8.621949e11;
lndo =
vp1+vp2./TEMP_Kelvin+vp3./TEMP_Kelvin.^2+vp4./TEMP_Kelvin.^3+vp5./TEMP_Kelvin.^
4;
DO_SAT = exp(lndo);

%-----

%Correct DO_SAT for altitude (mg/L)
%Column "G"

DO_SAT = .989*DO_SAT;

%-----

%Calculate Oxygen Surplus/Deficit (mg/L)
%Column "H"

DO_DEFICIT = DOPPM_trim - DO_SAT;

%-----

%Calculate K constant
%Column "J"

%First calculate K at 20 deg C (1/hr)
K20 = 50.8 * (V^.67)*(H^-1.85);

%Adjust K for the number of timesteps in 1 day

```

```

K20 = (K20*24)/(N-1);

%Adjust K for temperature
K_Adjust = K20.*(1.024.^(TEMP_trim-20));

%-----

%Calculate gas exchagng per time step (mg/L/TIME_STEP)
%Column "K"

GAS_EXCHANGE = K_Adjust.*DO_DEFICIT;

%-----

%Calculate avg gas exchange per time stamp (mg/L/TIME_STEP)
%Column "L"

for i=1:(N-1)
    AVG_GXCH(i) = (GAS_EXCHANGE(i) + GAS_EXCHANGE(i+1))./2;
end
AVG_GXCH = AVG_GXCH';

%-----

%Calculate corrected reparation (mg/L/Time_step)
%Column "M"

CR = AVG_GXCH+DELTA_DO;

%-----

%Find areal reparation rate (g/m^2/Time_step)
%Column "N"

CR_area = CR.*(H/100);

%-----

%Determine Night-Time hours
TIME_night1 = TIME_stamp(TIME_stamp>SUNSET);
TIME_night = TIME_night1(TIME_night1<SUNRISE);

%Calculate nighttime respiration
R_Night1 = CR_area(TIME_stamp>SUNSET);
R_Night = R_Night1(TIME_night1<SUNRISE);
R_AVG = mean(R_Night);

```

```

%Substitute Night-time average of R for daily CR
R = CR_area;
for i=1:(N-1)
    for j=1:(length(TIME_night))
        if TIME_stamp(i) == TIME_night(j)
            R(i) = CR_area(i);
            break
        else
            R(i)=R_AVG;
        end
    end
end
end

%-----

%Determine PP
for i=1:(N-1)
    PP(i) = CR_area(i)-R(i);
    if PP(i)<0
        PP(i)=0;
    end
end
end
PP = PP';

%-----

%Calculate Average Daily Temperature
TEMP_day1 = TEMP_trim(TIME_trim<SUNSET);
TEMP_day2 = TEMP_trim(TIME_trim>SUNRISE);
TEMP_day = [TEMP_day1; TEMP_day2];
AVG_DAILY_TEMP = mean(TEMP_day);

%-----

%Calculate average pH
PH_avg = mean(PH_trim);

%-----

%Calculate NEM (g/m^2/d)
NEM = sum(CR_area);
Resp = sum(R);
GPP = sum(PP);
PoverR = abs(GPP/Resp);
OUTPUT = [{'AVG_DAILY_TEMP'; 'NEM'; 'Resp'; 'GPP'; 'P/R'; 'Avg pH'}]...

```



```
{AVG_DAILY_TEMP; NEM; Resp; GPP; PoverR; PH_avg}]
Answers = [AVG_DAILY_TEMP; NEM; Resp; GPP; PoverR; PH_avg]
```

```
%-----
```

```
%Plot R, NEM, GPP
figure
```

```
%R
subplot(3,1,1); area(TIME_stamp,R); datetick('x',16);
grid on;
ylabel('R (g O2/m2/d)');
```

```
%Give graph title
title({NAME ;'Ecosystem metabolism'});
```

```
%NEM
subplot(3,1,2); area(TIME_stamp,CR_area); datetick('x',16);
grid on;
ylabel('NEM (g O2/m2/d)');
```

```
%GPP
subplot(3,1,3); area(TIME_stamp, PP); datetick('x',16);
grid on;
ylabel('GPP (g O2/m2/d)');
```

```
%Label axes
xlabel('Time');
```

```
%-----
```

```
%Plot DO, DO Sat & Temp
figure
```

```
%DO
plot(TIME_trim,DOPPM_trim, 'r');
H1 = gca;
hold on;
```

```
%DO Sat & Temp
[A2,H2,H3] = plotyy(TIME_trim,DO_SAT,TIME_trim,TEMP_trim);
```

```
%Manipulate Axes and Plot
F = title({NAME ;'Dissolved oxygen'});
linkaxes(A2, 'x');
xlabel('Time');
```

```
set(A2(2),'xtick',[]);
datetick(A2(1),'x',16);
set(A2(2),'ylim', [5 25], 'ytick', 5:5:25);
set(A2(1),'ylim', [0 15], 'ytick', 0:5:15);
ylabel(A2(1),'DO (mg/L)');
ylabel(A2(2),'Temperature (\circC)');
legend('DO','DO Sat','Temperature','Location', 'Best');
axpos = get(gca,'pos');
extent = get(F,'extent');
set(gca,'pos',[axpos(1) axpos(2) axpos(3) axpos(4)-.02*extent(4)]);
hold off;
```

## K.2 NEM: FEBRUARY 2012, DOWNSTREAM

```
%Luke Wildfire
%NEM_calculations
%
%10/2/2013

%Clean up
clear all
clc
close all

%-----

%Import csv file (I'll be working with DO data that has ppm - not %
[num txt] = xlsread('D6_downstream.xls');

%-----

%ENTER VARIABLES SPECIFIC TO EACH RUN

%Give run a name
NAME = 'February: Downstream';
%Stream Velocity in (cm/s)
V = 7.41122909502021;
%Stream Height in (cm)
H = 7.0;

%-----

%Define dates and times

%12:20pm (20 past noon) on first day of measurement
RoughStartTime = datenum('February 4, 2012 12:20:00000 PM');
%12:20pm (half past noon) on next day of measurement
RoughEndTime = datenum('February 5, 2012 12:20:00000 PM');
%Sunset on first day of measurement
SUNSET = datenum('February 4, 2012 5:26:00.000 PM');
%Sunrise on next day of measurement
SUNRISE = datenum('February 5, 2012 7:07:00.000 AM');

%-----

%Give each variable a name and then smooth
%Graph all variables on one plot vs time
```

```

%TIME is originally (mm/dd/yyyy h:mm:ss PM)
TIME = txt((2:end),1);
%Convert TIME to a number
TIME = datenum(TIME);
%Smooth the data
TIME = smooth(TIME, 25, 'rloess');

%Pressure (kPa)
BARO = num(:,1);
BARO = smooth(BARO, 25, 'rloess');
subplot(2,3,1); plot(TIME,BARO); datetick('x',16); axis tight;
xlabel('Pressure (kPa)');

%Conductance and Specific Conductance (uS/cm)
COND = num(:,2);
COND = smooth(COND, 25, 'rloess');
subplot(2,3,2); plot(TIME,COND); datetick('x',16); axis tight;
xlabel('Conductivity (uS/cm)');
title({NAME ;'All data (untrimmed)'});

SPECCOND = num(:,3);
SPECCOND = smooth(SPECCOND, 25, 'rloess');
subplot(2,3,3); plot(TIME,SPECCOND); datetick('x',16); axis tight;
xlabel('Specific Conductance (uS/cm)');

%Dissolved Oxygen (mg/L, ppm, or g/m^3)
DOPPM = num(:,4);
DOPPM = smooth(DOPPM, 25, 'rloess');
subplot(2,3,4); plot(TIME,DOPPM); datetick('x',16); axis tight;
xlabel('DO (ppm)');

%pH
PH = num(:,5);
PH = smooth(PH, 25, 'rloess');
subplot(2,3,5);plot(TIME,PH); datetick('x',16); axis tight;
xlabel('pH');

%Temperature (deg C)
TEMP = num(:,6);
TEMP = smooth(TEMP, 25, 'rloess');
subplot(2,3,6);plot(TIME,TEMP);datetick('x',16); axis tight;
xlabel('Temperature (deg. C)');

%-----

%Determine time step, and adjust the RoughEndTime up one time step

```

```

TIME_STEP = TIME(2)-TIME(1);
RoughEndTime = RoughEndTime + TIME_STEP;

%-----

%Trim all data to appropriate time frame
%Graph each variable as before

%Create a new figure
figure('Position',[300,300,800,500]);

%Time
TIME_trim1 = TIME(RoughStartTime<TIME);
TIME_trim = TIME_trim1(TIME_trim1<RoughEndTime);
N = length(TIME_trim);
disp(['The number of time increments is: ' num2str(N)]);

%Pressure (kPa)
BARO_trim1 = BARO(RoughStartTime<TIME);
BARO_trim = BARO_trim1(TIME_trim1<RoughEndTime);
subplot(2,3,1); plot(TIME_trim,BARO_trim);
datetick('x','HH');
xlim([RoughStartTime-.05 RoughEndTime+.05]);
xlabel('Time of day (hr)');
ylabel('Pressure (kPa)');
vline([SUNSET SUNRISE]);

%Conductance and Specific Conductance (uS/cm)
COND_trim1 = COND(RoughStartTime<TIME);
COND_trim = COND_trim1(TIME_trim1<RoughEndTime);
subplot(2,3,2); plot(TIME_trim,COND_trim);
datetick('x','HH');
xlim([RoughStartTime-.05 RoughEndTime+.05]);
xlabel('Time of day (hr)');
ylabel('Conductivity (uS/cm)');
vline([SUNSET SUNRISE]);
title({'NAME ';'All data (trimmed)'});

SPECCOND_trim1 = SPECCOND(RoughStartTime<TIME);
SPECCOND_trim = SPECCOND_trim1(TIME_trim1<RoughEndTime);
subplot(2,3,3); plot(TIME_trim,SPECCOND_trim);
datetick('x','HH');
xlim([RoughStartTime-.05 RoughEndTime+.05]);
xlabel('Time of day (hr)');
ylabel('Specific Conductance (uS/cm)');
vline([SUNSET SUNRISE]);

```

```

%Dissolved Oxygen (mg/L, ppm, or g/m^3)
DOPPM_trim1 = DOPPM(RoughStartTime<TIME);
DOPPM_trim = DOPPM_trim1(TIME_trim1<RoughEndTime);
subplot(2,3,4); plot(TIME_trim,DOPPM_trim);
datetick('x','HH');
xlim([RoughStartTime-.05 RoughEndTime+.05]);
xlabel('Time of day (hr)');
ylabel('DO (ppm)');
vline([SUNSET SUNRISE]);

```

```

%pH
PH_trim1 = PH(RoughStartTime<TIME);
PH_trim = PH_trim1(TIME_trim1<RoughEndTime);
subplot(2,3,5);plot(TIME_trim,PH_trim);
datetick('x','HH');
xlim([RoughStartTime-.05 RoughEndTime+.05]);
xlabel('Time of day (hr)');
ylabel('pH');
vline([SUNSET SUNRISE]);

```

```

%Temperature (deg C)
TEMP_trim1 = TEMP(RoughStartTime<TIME);
TEMP_trim = TEMP_trim1(TIME_trim1<RoughEndTime);
subplot(2,3,6);plot(TIME_trim,TEMP_trim);
datetick('x','HH');
xlim([RoughStartTime-.05 RoughEndTime+.05]);
xlabel('Time of day (hr)');
ylabel('Temperature (deg. C)');
vline([SUNSET SUNRISE]);

```

```

%-----

```

```

%Create a vector of time-stamps as the midpoint of each sampling time
%aka Column "D"

```

```

for i=1:(N-1)
    TIME_stamp(i) = (TIME_trim(i) + TIME_trim(i+1))./2;
end
TIME_stamp = TIME_stamp';

```

```

%-----

```

```

%Calculate a vector of Delta DO (column "E")

```

```

for i=1:(N-1)

```

```

    DELTA_DO(i) = (DOPPM_trim(i+1)-DOPPM_trim(i));
end
DELTA_DO = DELTA_DO';

%-----

%Calculate DO Saturation concentration (mg/L)
%Column "F"

%convert temperature to Kelvin
TEMP_Kelvin = TEMP_trim+273.15;

%Use this code to determine DO sat (mg/L)
vp1 = -139.34411;
vp2 = 1.575701e5;
vp3 = -6.642308e7;
vp4 = 1.2438e10;
vp5 = -8.621949e11;
lndo =
vp1+vp2./TEMP_Kelvin+vp3./TEMP_Kelvin.^2+vp4./TEMP_Kelvin.^3+vp5./TEMP_Kelvin.^
4;
DO_SAT = exp(lndo);

%-----

%Correct DO_SAT for altitude (mg/L)
%Column "G"

DO_SAT = .989*DO_SAT;

%-----

%Calculate Oxygen Surplus/Deficit (mg/L)
%Column "H"

DO_DEFICIT = DOPPM_trim - DO_SAT;

%-----

%Calculate K constant
%Column "J"

%First calculate K at 20 deg C (1/hr)
K20 = 50.8 * (V^.67)*(H^-1.85);

%Adjust K for the number of timesteps in 1 day

```

```

K20 = (K20*24)/(N-1);

%Adjust K for temperature
K_Adjust = K20.*(1.024.^(TEMP_trim-20));

%-----

%Calculate gas exchagng per time step (mg/L/TIME_STEP)
%Column "K"

GAS_EXCHANGE = K_Adjust.*DO_DEFICIT;

%-----

%Calculate avg gas exchange per time stamp (mg/L/TIME_STEP)
%Column "L"

for i=1:(N-1)
    AVG_GXCH(i) = (GAS_EXCHANGE(i) + GAS_EXCHANGE(i+1))./2;
end
AVG_GXCH = AVG_GXCH';

%-----

%Calculate corrected reparation (mg/L/Time_step)
%Column "M"

CR = AVG_GXCH+DELTA_DO;

%-----

%Find areal reparation rate (g/m^2/Time_step)
%Column "N"

CR_area = CR.*(H/100);

%-----

%Determine Night-Time hours
TIME_night1 = TIME_stamp(TIME_stamp>SUNSET);
TIME_night = TIME_night1(TIME_night1<SUNRISE);

%Calculate nighttime respiration
R_Night1 = CR_area(TIME_stamp>SUNSET);
R_Night = R_Night1(TIME_night1<SUNRISE);
R_AVG = mean(R_Night);

```



```

%Substitute Night-time average of R for daily CR
R = CR_area;
for i=1:(N-1)
    for j=1:(length(TIME_night))
        if TIME_stamp(i) == TIME_night(j)
            R(i) = CR_area(i);
            break
        else
            R(i)=R_AVG;
        end
    end
end
end

%-----

%Determine PP
for i=1:(N-1)
    PP(i) = CR_area(i)-R(i);
    if PP(i)<0
        PP(i)=0;
    end
end
end
PP = PP';

%-----

%Caluculate Average Daily Temperature
TEMP_day1 = TEMP_trim(TIME_trim<SUNSET);
TEMP_day2 = TEMP_trim(TIME_trim>SUNRISE);
TEMP_day = [TEMP_day1; TEMP_day2];
AVG_DAILY_TEMP = mean(TEMP_day);

%-----

%Calculate average pH
PH_avg = mean(PH_trim);

%-----

%Calculate NEM (g/m^2/d)
NEM = sum(CR_area);
Resp = sum(R);
GPP = sum(PP);
PoverR = abs(GPP/Resp);
OUTPUT = [{'AVG_DAILY_TEMP'; 'NEM'; 'Resp'; 'GPP'; 'P/R'; 'Avg pH'}]...

```

```
{AVG_DAILY_TEMP; NEM; Resp; GPP; PoverR; PH_avg}]
Answers = [AVG_DAILY_TEMP; NEM; Resp; GPP; PoverR; PH_avg]
```

```
%-----
```

```
%Plot R, NEM, GPP
figure
```

```
%R
subplot(3,1,1); area(TIME_stamp,R); datetick('x',16);
grid on;
ylabel('R (g O2/m2/d)');
```

```
%Give graph title
title({NAME ;'Ecosystem metabolism'});
```

```
%NEM
subplot(3,1,2); area(TIME_stamp,CR_area); datetick('x',16);
grid on;
ylabel('NEM (g O2/m2/d)');
```

```
%GPP
subplot(3,1,3); area(TIME_stamp, PP); datetick('x',16);
grid on;
ylabel('GPP (g O2/m2/d)');
```

```
%Label axes
xlabel('Time');
```

```
%-----
```

```
%Plot DO, DO Sat & Temp
figure
```

```
%DO
plot(TIME_trim,DOPPM_trim, 'r');
H1 = gca;
hold on;
```

```
%DO Sat & Temp
[A2,H2,H3] = plotyy(TIME_trim,DO_SAT,TIME_trim,TEMP_trim);
```

```
%Manipulate Axes and Plot
F = title({NAME ;'Dissolved oxygen'});
linkaxes(A2, 'x');
xlabel('Time');
```

```
set(A2(2),'xtick',[]);
datetick(A2(1),'x',16);
set(A2(2),'ylim', [5 25], 'ytick', 5:5:25);
set(A2(1),'ylim', [0 15], 'ytick', 0:5:15);
ylabel(A2(1),'DO (mg/L)');
ylabel(A2(2),'Temperature (\circC)');
legend('DO','DO Sat','Temperature','Location', 'Best');
axpos = get(gca,'pos');
extent = get(F,'extent');
set(gca,'pos',[axpos(1) axpos(2) axpos(3) axpos(4)-.02*extent(4)]);
hold off;
```

### K.3 NEM: APRIL 2011, UPSTREAM

```
%Luke Wildfire
%NEM_calculations
%
%10/2/2013

%Clean up
clear all
clc
close all

%-----

%Import csv file (I'll be working with DO data that has ppm - not %
[num txt] = xlsread('D3_upstream.xls');

%-----

%ENTER VARIABLES SPECIFIC TO EACH RUN

%Give run a name
NAME = 'April: Upstream';
%Stream Velocity in (cm/s)
V = 2.6679;
%Stream Height in (cm)
H = 4.4667;

%-----

%Define dates and times

%12:20pm (20 past noon) on first day of measurement
RoughStartTime = datenum('April 14, 2010 12:20:00000 PM');
%12:20pm (half past noon) on next day of measurement
RoughEndTime = datenum('April 15, 2010 12:20:00000 PM');
%Sunset on first day of measurement
SUNSET = datenum('April 14, 2010 7:40:00.000 PM');
%Sunrise on next day of measurement
SUNRISE = datenum('April 15, 2010 6:26:00.000 AM');

%-----

%Give each variable a name and then smooth
%Graph all variables on one plot vs time
```

```

%TIME is originally (mm/dd/yyyy h:mm:ss PM)
TIME = txt((2:end),1);
%Convert TIME to a number
TIME = datenum(TIME);
%Smooth the data
TIME = smooth(TIME, 25, 'rloess');

%Pressure (kPa)
BARO = num(:,1);
BARO = smooth(BARO, 25, 'rloess');
subplot(2,3,1); plot(TIME,BARO); datetick('x',16); axis tight;
xlabel('Pressure (kPa)');

%Conductance and Specific Conductance (uS/cm)
COND = num(:,2);
COND = smooth(COND, 25, 'rloess');
subplot(2,3,2); plot(TIME,COND); datetick('x',16); axis tight;
xlabel('Conductivity (uS/cm)');
title({NAME ;'All data (untrimmed)'});

SPECCOND = num(:,3);
SPECCOND = smooth(SPECCOND, 25, 'rloess');
subplot(2,3,3); plot(TIME,SPECCOND); datetick('x',16); axis tight;
xlabel('Specific Conductance (uS/cm)');

%Dissolved Oxygen (mg/L, ppm, or g/m^3)
DOPPM = num(:,4);
DOPPM = smooth(DOPPM, 25, 'rloess');
subplot(2,3,4); plot(TIME,DOPPM); datetick('x',16); axis tight;
xlabel('DO (ppm)');

%pH
PH = num(:,5);
PH = smooth(PH, 25, 'rloess');
subplot(2,3,5);plot(TIME,PH); datetick('x',16); axis tight;
xlabel('pH');

%Temperature (deg C)
TEMP = num(:,6);
TEMP = smooth(TEMP, 25, 'rloess');
subplot(2,3,6);plot(TIME,TEMP);datetick('x',16); axis tight;
xlabel('Temperature (deg. C)');

%-----

%Determine time step, and adjust the RoughEndTime up one time step

```

```

TIME_STEP = TIME(2)-TIME(1);
RoughEndTime = RoughEndTime + TIME_STEP;

%-----

%Trim all data to appropriate time frame
%Graph each variable as before

%Create a new figure
figure('Position',[300,300,800,500]);

%Time
TIME_trim1 = TIME(RoughStartTime<TIME);
TIME_trim = TIME_trim1(TIME_trim1<RoughEndTime);
N = length(TIME_trim);
disp(['The number of time increments is: ' num2str(N)]);

%Pressure (kPa)
BARO_trim1 = BARO(RoughStartTime<TIME);
BARO_trim = BARO_trim1(TIME_trim1<RoughEndTime);
subplot(2,3,1); plot(TIME_trim,BARO_trim);
datetick('x','HH');
xlim([RoughStartTime-.05 RoughEndTime+.05]);
xlabel('Time of day (hr)');
ylabel('Pressure (kPa)');
vline([SUNSET SUNRISE]);

%Conductance and Specific Conductance (uS/cm)
COND_trim1 = COND(RoughStartTime<TIME);
COND_trim = COND_trim1(TIME_trim1<RoughEndTime);
subplot(2,3,2); plot(TIME_trim,COND_trim);
datetick('x','HH');
xlim([RoughStartTime-.05 RoughEndTime+.05]);
xlabel('Time of day (hr)');
ylabel('Conductivity (uS/cm)');
vline([SUNSET SUNRISE]);
title({'NAME ';'All data (trimmed)'});

SPECCOND_trim1 = SPECCOND(RoughStartTime<TIME);
SPECCOND_trim = SPECCOND_trim1(TIME_trim1<RoughEndTime);
subplot(2,3,3); plot(TIME_trim,SPECCOND_trim);
datetick('x','HH');
xlim([RoughStartTime-.05 RoughEndTime+.05]);
xlabel('Time of day (hr)');
ylabel('Specific Conductance (uS/cm)');
vline([SUNSET SUNRISE]);

```

```

%Dissolved Oxygen (mg/L, ppm, or g/m^3)
DOPPM_trim1 = DOPPM(RoughStartTime<TIME);
DOPPM_trim = DOPPM_trim1(TIME_trim1<RoughEndTime);
subplot(2,3,4); plot(TIME_trim,DOPPM_trim);
datetick('x','HH');
xlim([RoughStartTime-.05 RoughEndTime+.05]);
xlabel('Time of day (hr)');
ylabel('DO (ppm)');
vline([SUNSET SUNRISE]);

```

```

%pH
PH_trim1 = PH(RoughStartTime<TIME);
PH_trim = PH_trim1(TIME_trim1<RoughEndTime);
subplot(2,3,5);plot(TIME_trim,PH_trim);
datetick('x','HH');
xlim([RoughStartTime-.05 RoughEndTime+.05]);
xlabel('Time of day (hr)');
ylabel('pH');
vline([SUNSET SUNRISE]);

```

```

%Temperature (deg C)
TEMP_trim1 = TEMP(RoughStartTime<TIME);
TEMP_trim = TEMP_trim1(TIME_trim1<RoughEndTime);
subplot(2,3,6);plot(TIME_trim,TEMP_trim);
datetick('x','HH');
xlim([RoughStartTime-.05 RoughEndTime+.05]);
xlabel('Time of day (hr)');
ylabel('Temperature (deg. C)');
vline([SUNSET SUNRISE]);

```

```

%-----

```

```

%Create a vector of time-stamps as the midpoint of each sampling time
%aka Column "D"

```

```

for i=1:(N-1)
    TIME_stamp(i) = (TIME_trim(i) + TIME_trim(i+1))./2;
end
TIME_stamp = TIME_stamp';

```

```

%-----

```

```

%Calculate a vector of Delta DO (column "E")

```

```

for i=1:(N-1)

```

```

    DELTA_DO(i) = (DOPPM_trim(i+1)-DOPPM_trim(i));
end
DELTA_DO = DELTA_DO';

%-----

%Calculate DO Saturation concentration (mg/L)
%Column "F"

%convert temperature to Kelvin
TEMP_Kelvin = TEMP_trim+273.15;

%Use this code to determine DO sat (mg/L)
vp1 = -139.34411;
vp2 = 1.575701e5;
vp3 = -6.642308e7;
vp4 = 1.2438e10;
vp5 = -8.621949e11;
lndo =
vp1+vp2./TEMP_Kelvin+vp3./TEMP_Kelvin.^2+vp4./TEMP_Kelvin.^3+vp5./TEMP_Kelvin.^
4;
DO_SAT = exp(lndo);

%-----

%Correct DO_SAT for altitude (mg/L)
%Column "G"

DO_SAT = .989*DO_SAT;

%-----

%Calculate Oxygen Surplus/Deficit (mg/L)
%Column "H"

DO_DEFICIT = DOPPM_trim - DO_SAT;

%-----

%Calculate K constant
%Column "J"

%First calculate K at 20 deg C (1/hr)
K20 = 50.8 * (V^.67)*(H^-1.85);

%Adjust K for the number of timesteps in 1 day

```



```

K20 = (K20*24)/(N-1);

%Adjust K for temperature
K_Adjust = K20.*(1.024.^(TEMP_trim-20));

%-----

%Calculate gas exchagng per time step (mg/L/TIME_STEP)
%Column "K"

GAS_EXCHANGE = K_Adjust.*DO_DEFICIT;

%-----

%Calculate avg gas exchange per time stamp (mg/L/TIME_STEP)
%Column "L"

for i=1:(N-1)
    AVG_GXCH(i) = (GAS_EXCHANGE(i) + GAS_EXCHANGE(i+1))./2;
end
AVG_GXCH = AVG_GXCH';

%-----

%Calculate corrected reparation (mg/L/Time_step)
%Column "M"

CR = AVG_GXCH+DELTA_DO;

%-----

%Find areal reparation rate (g/m^2/Time_step)
%Column "N"

CR_area = CR.*(H/100);

%-----

%Determine Night-Time hours
TIME_night1 = TIME_stamp(TIME_stamp>SUNSET);
TIME_night = TIME_night1(TIME_night1<SUNRISE);

%Calculate nighttime respiration
R_Night1 = CR_area(TIME_stamp>SUNSET);
R_Night = R_Night1(TIME_night1<SUNRISE);
R_AVG = mean(R_Night);

```

```

%Substitute Night-time average of R for daily CR
R = CR_area;
for i=1:(N-1)
    for j=1:(length(TIME_night))
        if TIME_stamp(i) == TIME_night(j)
            R(i) = CR_area(i);
            break
        else
            R(i)=R_AVG;
        end
    end
end
end

%-----

%Determine PP
for i=1:(N-1)
    PP(i) = CR_area(i)-R(i);
    if PP(i)<0
        PP(i)=0;
    end
end
end
PP = PP';

%-----

%Caluculate Average Daily Temperature
TEMP_day1 = TEMP_trim(TIME_trim<SUNSET);
TEMP_day2 = TEMP_trim(TIME_trim>SUNRISE);
TEMP_day = [TEMP_day1; TEMP_day2];
AVG_DAILY_TEMP = mean(TEMP_day);

%-----

%Calculate average pH
PH_avg = mean(PH_trim);

%-----

%Calculate NEM (g/m^2/d)
NEM = sum(CR_area);
Resp = sum(R);
GPP = sum(PP);
PoverR = abs(GPP/Resp);
OUTPUT = [{'AVG_DAILY_TEMP'; 'NEM'; 'Resp'; 'GPP'; 'P/R'; 'Avg pH'}]...

```

```
{AVG_DAILY_TEMP; NEM; Resp; GPP; PoverR; PH_avg}]
Answers = [AVG_DAILY_TEMP; NEM; Resp; GPP; PoverR; PH_avg]
```

```
%-----
```

```
%Plot R, NEM, GPP
figure
```

```
%R
subplot(3,1,1); area(TIME_stamp,R); datetick('x',16);
grid on;
ylabel('R (g O2/m2/d)');
```

```
%Give graph title
title({NAME ;'Ecosystem metabolism'});
```

```
%NEM
subplot(3,1,2); area(TIME_stamp,CR_area); datetick('x',16);
grid on;
ylabel('NEM (g O2/m2/d)');
```

```
%GPP
subplot(3,1,3); area(TIME_stamp, PP); datetick('x',16);
grid on;
ylabel('GPP (g O2/m2/d)');
```

```
%Label axes
xlabel('Time');
```

```
%-----
```

```
%Plot DO, DO Sat & Temp
figure
```

```
%DO
plot(TIME_trim,DOPPM_trim, 'r');
H1 = gca;
hold on;
```

```
%DO Sat & Temp
[A2,H2,H3] = plotyy(TIME_trim,DO_SAT,TIME_trim,TEMP_trim);
```

```
%Manipulate Axes and Plot
F = title({NAME ;'Dissolved oxygen'});
linkaxes(A2, 'x');
xlabel('Time');
```

```
set(A2(2),'xtick',[]);
datetick(A2(1),'x',16);
set(A2(2),'ylim', [5 25], 'ytick', 5:5:25);
set(A2(1),'ylim', [0 15], 'ytick', 0:5:15);
ylabel(A2(1),'DO (mg/L)');
ylabel(A2(2),'Temperature (\circC)');
legend('DO','DO Sat','Temperature','Location', 'Best');
axpos = get(gca,'pos');
extent = get(F,'extent');
set(gca,'pos',[axpos(1) axpos(2) axpos(3) axpos(4)-.02*extent(4)]);
hold off;
```

## K.4 NEM: APRIL 2011, DOWNSTREAM

```
%Luke Wildfire
%NEM_calculations
%
%10/2/2013

%Clean up
clear all
clc
close all

%-----

%Import csv file (I'll be working with DO data that has ppm - not %
[num txt] = xlsread('D3_downstream.xls');

%-----

%ENTER VARIABLES SPECIFIC TO EACH RUN

%Give run a name
NAME = 'April: Downstream';
%Stream Velocity in (cm/s)
V = 13.9740;
%Stream Height in (cm)
H = 7.7833;

%-----

%Define dates and times

%12:20pm (20 past noon) on first day of measurement
RoughStartTime = datenum('April 14, 2011 12:20:00000 PM');
%12:20pm (half past noon) on next day of measurement
RoughEndTime = datenum('April 15, 2011 12:20:00000 PM');
%Sunset on first day of measurement
SUNSET = datenum('April 14, 2011 7:40:00.000 PM');
%Sunrise on next day of measurement
SUNRISE = datenum('April 15, 2011 6:26:00.000 AM');

%-----

%Give each variable a name and then smooth
%Graph all variables on one plot vs time
```

```

%TIME is originally (mm/dd/yyyy h:mm:ss PM)
TIME = txt((2:end),1);
%Convert TIME to a number
TIME = datenum(TIME);
%Smooth the data
TIME = smooth(TIME, 25, 'rloess');

%Pressure (kPa)
BARO = num(:,1);
BARO = smooth(BARO, 25, 'rloess');
subplot(2,3,1); plot(TIME,BARO); datetick('x',16); axis tight;
xlabel('Pressure (kPa)');

%Conductance and Specific Conductance (uS/cm)
COND = num(:,2);
COND = smooth(COND, 25, 'rloess');
subplot(2,3,2); plot(TIME,COND); datetick('x',16); axis tight;
xlabel('Conductivity (uS/cm)');
title({NAME ;'All data (untrimmed)'});

SPECCOND = num(:,3);
SPECCOND = smooth(SPECCOND, 25, 'rloess');
subplot(2,3,3); plot(TIME,SPECCOND); datetick('x',16); axis tight;
xlabel('Specific Conductance (uS/cm)');

%Dissolved Oxygen (mg/L, ppm, or g/m^3)
DOPPM = num(:,4);
DOPPM = smooth(DOPPM, 25, 'rloess');
subplot(2,3,4); plot(TIME,DOPPM); datetick('x',16); axis tight;
xlabel('DO (ppm)');

%pH
PH = num(:,5);
PH = smooth(PH, 25, 'rloess');
subplot(2,3,5);plot(TIME,PH); datetick('x',16); axis tight;
xlabel('pH');

%Temperature (deg C)
TEMP = num(:,6);
TEMP = smooth(TEMP, 25, 'rloess');
subplot(2,3,6);plot(TIME,TEMP);datetick('x',16); axis tight;
xlabel('Temperature (deg. C)');

%-----

%Determine time step, and adjust the RoughEndTime up one time step

```

```

TIME_STEP = TIME(2)-TIME(1);
RoughEndTime = RoughEndTime + TIME_STEP;

%-----

%Trim all data to appropriate time frame
%Graph each variable as before

%Create a new figure
figure('Position',[300,300,800,500]);

%Time
TIME_trim1 = TIME(RoughStartTime<TIME);
TIME_trim = TIME_trim1(TIME_trim1<RoughEndTime);
N = length(TIME_trim);
disp(['The number of time increments is: ' num2str(N)]);

%Pressure (kPa)
BARO_trim1 = BARO(RoughStartTime<TIME);
BARO_trim = BARO_trim1(TIME_trim1<RoughEndTime);
subplot(2,3,1); plot(TIME_trim,BARO_trim);
datetick('x','HH');
xlim([RoughStartTime-.05 RoughEndTime+.05]);
xlabel('Time of day (hr)');
ylabel('Pressure (kPa)');
vline([SUNSET SUNRISE]);

%Conductance and Specific Conductance (uS/cm)
COND_trim1 = COND(RoughStartTime<TIME);
COND_trim = COND_trim1(TIME_trim1<RoughEndTime);
subplot(2,3,2); plot(TIME_trim,COND_trim);
datetick('x','HH');
xlim([RoughStartTime-.05 RoughEndTime+.05]);
xlabel('Time of day (hr)');
ylabel('Conductivity (uS/cm)');
vline([SUNSET SUNRISE]);
title({'NAME ;'All data (trimmed)'});

SPECCOND_trim1 = SPECCOND(RoughStartTime<TIME);
SPECCOND_trim = SPECCOND_trim1(TIME_trim1<RoughEndTime);
subplot(2,3,3); plot(TIME_trim,SPECCOND_trim);
datetick('x','HH');
xlim([RoughStartTime-.05 RoughEndTime+.05]);
xlabel('Time of day (hr)');
ylabel('Specific Conductance (uS/cm)');
vline([SUNSET SUNRISE]);

```

```

%Dissolved Oxygen (mg/L, ppm, or g/m^3)
DOPPM_trim1 = DOPPM(RoughStartTime<TIME);
DOPPM_trim = DOPPM_trim1(TIME_trim1<RoughEndTime);
subplot(2,3,4); plot(TIME_trim,DOPPM_trim);
datetick('x','HH');
xlim([RoughStartTime-.05 RoughEndTime+.05]);
xlabel('Time of day (hr)');
ylabel('DO (ppm)');
vline([SUNSET SUNRISE]);

```

```

%pH
PH_trim1 = PH(RoughStartTime<TIME);
PH_trim = PH_trim1(TIME_trim1<RoughEndTime);
subplot(2,3,5);plot(TIME_trim,PH_trim);
datetick('x','HH');
xlim([RoughStartTime-.05 RoughEndTime+.05]);
xlabel('Time of day (hr)');
ylabel('pH');
vline([SUNSET SUNRISE]);

```

```

%Temperature (deg C)
TEMP_trim1 = TEMP(RoughStartTime<TIME);
TEMP_trim = TEMP_trim1(TIME_trim1<RoughEndTime);
subplot(2,3,6);plot(TIME_trim,TEMP_trim);
datetick('x','HH');
xlim([RoughStartTime-.05 RoughEndTime+.05]);
xlabel('Time of day (hr)');
ylabel('Temperature (deg. C)');
vline([SUNSET SUNRISE]);

```

```

%-----

```

```

%Create a vector of time-stamps as the midpoint of each sampling time
%aka Column "D"

```

```

for i=1:(N-1)
    TIME_stamp(i) = (TIME_trim(i) + TIME_trim(i+1))./2;
end
TIME_stamp = TIME_stamp';

```

```

%-----

```

```

%Calculate a vector of Delta DO (column "E")

```

```

for i=1:(N-1)

```



```

    DELTA_DO(i) = (DOPPM_trim(i+1)-DOPPM_trim(i));
end
DELTA_DO = DELTA_DO';

%-----

%Calculate DO Saturation concentration (mg/L)
%Column "F"

%convert temperature to Kelvin
TEMP_Kelvin = TEMP_trim+273.15;

%Use this code to determine DO sat (mg/L)
vp1 = -139.34411;
vp2 = 1.575701e5;
vp3 = -6.642308e7;
vp4 = 1.2438e10;
vp5 = -8.621949e11;
lnDO =
vp1+vp2./TEMP_Kelvin+vp3./TEMP_Kelvin.^2+vp4./TEMP_Kelvin.^3+vp5./TEMP_Kelvin.^
4;
DO_SAT = exp(lnDO);

%-----

%Correct DO_SAT for altitude (mg/L)
%Column "G"

DO_SAT = .989*DO_SAT;

%-----

%Calculate Oxygen Surplus/Deficit (mg/L)
%Column "H"

DO_DEFICIT = DOPPM_trim - DO_SAT;

%-----

%Calculate K constant
%Column "J"

%First calculate K at 20 deg C (1/hr)
K20 = 50.8 * (V^.67)*(H^-1.85);

%Adjust K for the number of timesteps in 1 day

```

```

K20 = (K20*24)/(N-1);

%Adjust K for temperature
K_Adjust = K20.*(1.024.^(TEMP_trim-20));

%-----

%Calculate gas exchagng per time step (mg/L/TIME_STEP)
%Column "K"

GAS_EXCHANGE = K_Adjust.*DO_DEFICIT;

%-----

%Calculate avg gas exchange per time stamp (mg/L/TIME_STEP)
%Column "L"

for i=1:(N-1)
    AVG_GXCH(i) = (GAS_EXCHANGE(i) + GAS_EXCHANGE(i+1))./2;
end
AVG_GXCH = AVG_GXCH';

%-----

%Calculate corrected reparation (mg/L/Time_step)
%Column "M"

CR = AVG_GXCH+DELTA_DO;

%-----

%Find areal reparation rate (g/m^2/Time_step)
%Column "N"

CR_area = CR.*(H/100);

%-----

%Determine Night-Time hours
TIME_night1 = TIME_stamp(TIME_stamp>SUNSET);
TIME_night = TIME_night1(TIME_night1<SUNRISE);

%Calculate nighttime respiration
R_Night1 = CR_area(TIME_stamp>SUNSET);
R_Night = R_Night1(TIME_night1<SUNRISE);
R_AVG = mean(R_Night);

```

```

%Substitute Night-time average of R for daily CR
R = CR_area;
for i=1:(N-1)
    for j=1:(length(TIME_night))
        if TIME_stamp(i) == TIME_night(j)
            R(i) = CR_area(i);
            break
        else
            R(i)=R_AVG;
        end
    end
end
end

%-----

%Determine PP
for i=1:(N-1)
    PP(i) = CR_area(i)-R(i);
    if PP(i)<0
        PP(i)=0;
    end
end
end
PP = PP';

%-----

%Caluculate Average Daily Temperature
TEMP_day1 = TEMP_trim(TIME_trim<SUNSET);
TEMP_day2 = TEMP_trim(TIME_trim>SUNRISE);
TEMP_day = [TEMP_day1; TEMP_day2];
AVG_DAILY_TEMP = mean(TEMP_day);

%-----

%Calculate average pH
PH_avg = mean(PH_trim);

%-----

%Calculate NEM (g/m^2/d)
NEM = sum(CR_area);
Resp = sum(R);
GPP = sum(PP);
PoverR = abs(GPP/Resp);
OUTPUT = [{'AVG_DAILY_TEMP'; 'NEM'; 'Resp'; 'GPP'; 'P/R'; 'Avg pH'}]...

```

```
{AVG_DAILY_TEMP; NEM; Resp; GPP; PoverR; PH_avg}]
Answers = [AVG_DAILY_TEMP; NEM; Resp; GPP; PoverR; PH_avg]
```

```
%-----
```

```
%Plot R, NEM, GPP
figure
```

```
%R
subplot(3,1,1); area(TIME_stamp,R); datetick('x',16);
grid on;
ylabel('R (g O2/m2/d)');
```

```
%Give graph title
title({NAME ;'Ecosystem metabolism'});
```

```
%NEM
subplot(3,1,2); area(TIME_stamp,CR_area); datetick('x',16);
grid on;
ylabel('NEM (g O2/m2/d)');
```

```
%GPP
subplot(3,1,3); area(TIME_stamp, PP); datetick('x',16);
grid on;
ylabel('GPP (g O2/m2/d)');
```

```
%Label axes
xlabel('Time');
```

```
%-----
```

```
%Plot DO, DO Sat & Temp
figure
```

```
%DO
plot(TIME_trim,DOPPM_trim, 'r');
H1 = gca;
hold on;
```

```
%DO Sat & Temp
[A2,H2,H3] = plotyy(TIME_trim,DO_SAT,TIME_trim,TEMP_trim);
```

```
%Manipulate Axes and Plot
F = title({NAME ;'Dissolved oxygen'});
linkaxes(A2, 'x');
xlabel('Time');
```

```
set(A2(2),'xtick',[]);
datetick(A2(1),'x',16);
set(A2(2),'ylim', [5 25], 'ytick', 5:5:25);
set(A2(1),'ylim', [0 15], 'ytick', 0:5:15);
ylabel(A2(1),'DO (mg/L)');
ylabel(A2(2),'Temperature (\circC)');
legend('DO','DO Sat','Temperature','Location', 'Best');
axpos = get(gca,'pos');
extent = get(F,'extent');
set(gca,'pos',[axpos(1) axpos(2) axpos(3) axpos(4)-.02*extent(4)]);
hold off;
```

## K.5 NEM: JUNE 2011, UPSTREAM

```
%Luke Wildfire
%NEM_calculations
%
%10/2/2013

%Clean up
clear all
clc
close all

%-----

%Import csv file (I'll be working with DO data that has ppm - not %
[num txt] = xlsread('D4_upstream.xls');

%-----

%ENTER VARIABLES SPECIFIC TO EACH RUN

%Give run a name
NAME = 'June: Upstream';
%Stream Velocity in (cm/s)
V = 3.8169;
%Stream Height in (cm)
H = 2.4167;

%-----

%Define dates and times

%12:20pm (20 past noon) on first day of measurement
RoughStartTime = datenum('June 16, 2011 12:20:00000 PM');
%12:20pm (half past noon) on next day of measurement
RoughEndTime = datenum('June 17, 2011 12:20:00000 PM');
%Sunset on first day of measurement
SUNSET = datenum('June 16, 2011 8:32:00.000 PM');
%Sunrise on next day of measurement
SUNRISE = datenum('June 17, 2011 5:34:00.000 AM');

%-----

%Give each variable a name and then smooth
%Graph all variables on one plot vs time
```

```

%TIME is originally (mm/dd/yyyy h:mm:ss PM)
TIME = txt((2:end),1);
%Convert TIME to a number
TIME = datenum(TIME);
%Smooth the data
TIME = smooth(TIME, 25, 'rloess');

%Pressure (kPa)
BARO = num(:,1);
BARO = smooth(BARO, 25, 'rloess');
subplot(2,3,1); plot(TIME,BARO); datetick('x',16); axis tight;
xlabel('Pressure (kPa)');

%Conductance and Specific Conductance (uS/cm)
COND = num(:,2);
COND = smooth(COND, 25, 'rloess');
subplot(2,3,2); plot(TIME,COND); datetick('x',16); axis tight;
xlabel('Conductivity (uS/cm)');
title({NAME ;'All data (untrimmed)'});

SPECCOND = num(:,3);
SPECCOND = smooth(SPECCOND, 25, 'rloess');
subplot(2,3,3); plot(TIME,SPECCOND); datetick('x',16); axis tight;
xlabel('Specific Conductance (uS/cm)');

%Dissolved Oxygen (mg/L, ppm, or g/m^3)
DOPPM = num(:,4);
DOPPM = smooth(DOPPM, 25, 'rloess');
subplot(2,3,4); plot(TIME,DOPPM); datetick('x',16); axis tight;
xlabel('DO (ppm)');

%pH
PH = num(:,5);
PH = smooth(PH, 25, 'rloess');
subplot(2,3,5);plot(TIME,PH); datetick('x',16); axis tight;
xlabel('pH');

%Temperature (deg C)
TEMP = num(:,6);
TEMP = smooth(TEMP, 25, 'rloess');
subplot(2,3,6);plot(TIME,TEMP);datetick('x',16); axis tight;
xlabel('Temperature (deg. C)');

%-----

%Determine time step, and adjust the RoughEndTime up one time step

```

```

TIME_STEP = TIME(2)-TIME(1);
RoughEndTime = RoughEndTime + TIME_STEP;

%-----

%Trim all data to appropriate time frame
%Graph each variable as before

%Create a new figure
figure('Position',[300,300,800,500]);

%Time
TIME_trim1 = TIME(RoughStartTime<TIME);
TIME_trim = TIME_trim1(TIME_trim1<RoughEndTime);
N = length(TIME_trim);
disp(['The number of time increments is: ' num2str(N)]);

%Pressure (kPa)
BARO_trim1 = BARO(RoughStartTime<TIME);
BARO_trim = BARO_trim1(TIME_trim1<RoughEndTime);
subplot(2,3,1); plot(TIME_trim,BARO_trim);
datetick('x','HH');
xlim([RoughStartTime-.05 RoughEndTime+.05]);
xlabel('Time of day (hr)');
ylabel('Pressure (kPa)');
vline([SUNSET SUNRISE]);

%Conductance and Specific Conductance (uS/cm)
COND_trim1 = COND(RoughStartTime<TIME);
COND_trim = COND_trim1(TIME_trim1<RoughEndTime);
subplot(2,3,2); plot(TIME_trim,COND_trim);
datetick('x','HH');
xlim([RoughStartTime-.05 RoughEndTime+.05]);
xlabel('Time of day (hr)');
ylabel('Conductivity (uS/cm)');
vline([SUNSET SUNRISE]);
title({'NAME ;'All data (trimmed)'});

SPECCOND_trim1 = SPECCOND(RoughStartTime<TIME);
SPECCOND_trim = SPECCOND_trim1(TIME_trim1<RoughEndTime);
subplot(2,3,3); plot(TIME_trim,SPECCOND_trim);
datetick('x','HH');
xlim([RoughStartTime-.05 RoughEndTime+.05]);
xlabel('Time of day (hr)');
ylabel('Specific Conductance (uS/cm)');
vline([SUNSET SUNRISE]);

```



```

%Dissolved Oxygen (mg/L, ppm, or g/m^3)
DOPPM_trim1 = DOPPM(RoughStartTime<TIME);
DOPPM_trim = DOPPM_trim1(TIME_trim1<RoughEndTime);
subplot(2,3,4); plot(TIME_trim,DOPPM_trim);
datetick('x','HH');
xlim([RoughStartTime-.05 RoughEndTime+.05]);
xlabel('Time of day (hr)');
ylabel('DO (ppm)');
vline([SUNSET SUNRISE]);

```

```

%pH
PH_trim1 = PH(RoughStartTime<TIME);
PH_trim = PH_trim1(TIME_trim1<RoughEndTime);
subplot(2,3,5);plot(TIME_trim,PH_trim);
datetick('x','HH');
xlim([RoughStartTime-.05 RoughEndTime+.05]);
xlabel('Time of day (hr)');
ylabel('pH');
vline([SUNSET SUNRISE]);

```

```

%Temperature (deg C)
TEMP_trim1 = TEMP(RoughStartTime<TIME);
TEMP_trim = TEMP_trim1(TIME_trim1<RoughEndTime);
subplot(2,3,6);plot(TIME_trim,TEMP_trim);
datetick('x','HH');
xlim([RoughStartTime-.05 RoughEndTime+.05]);
xlabel('Time of day (hr)');
ylabel('Temperature (deg. C)');
vline([SUNSET SUNRISE]);

```

```

%-----

```

```

%Create a vector of time-stamps as the midpoint of each sampling time
%aka Column "D"

```

```

for i=1:(N-1)
    TIME_stamp(i) = (TIME_trim(i) + TIME_trim(i+1))./2;
end
TIME_stamp = TIME_stamp';

```

```

%-----

```

```

%Calculate a vector of Delta DO (column "E")

```

```

for i=1:(N-1)

```

```

    DELTA_DO(i) = (DOPPM_trim(i+1)-DOPPM_trim(i));
end
DELTA_DO = DELTA_DO';

%-----

%Calculate DO Saturation concentration (mg/L)
%Column "F"

%convert temperature to Kelvin
TEMP_Kelvin = TEMP_trim+273.15;

%Use this code to determine DO sat (mg/L)
vp1 = -139.34411;
vp2 = 1.575701e5;
vp3 = -6.642308e7;
vp4 = 1.2438e10;
vp5 = -8.621949e11;
lndo =
vp1+vp2./TEMP_Kelvin+vp3./TEMP_Kelvin.^2+vp4./TEMP_Kelvin.^3+vp5./TEMP_Kelvin.^
4;
DO_SAT = exp(lndo);

%-----

%Correct DO_SAT for altitude (mg/L)
%Column "G"

DO_SAT = .989*DO_SAT;

%-----

%Calculate Oxygen Surplus/Deficit (mg/L)
%Column "H"

DO_DEFICIT = DOPPM_trim - DO_SAT;

%-----

%Calculate K constant
%Column "J"

%First calculate K at 20 deg C (1/hr)
K20 = 50.8 * (V^.67)*(H^-1.85);

%Adjust K for the number of timesteps in 1 day

```

```

K20 = (K20*24)/(N-1);

%Adjust K for temperature
K_Adjust = K20.*(1.024.^(TEMP_trim-20));

%-----

%Calculate gas exchagng per time step (mg/L/TIME_STEP)
%Column "K"

GAS_EXCHANGE = K_Adjust.*DO_DEFICIT;

%-----

%Calculate avg gas exchange per time stamp (mg/L/TIME_STEP)
%Column "L"

for i=1:(N-1)
    AVG_GXCH(i) = (GAS_EXCHANGE(i) + GAS_EXCHANGE(i+1))./2;
end
AVG_GXCH = AVG_GXCH';

%-----

%Calculate corrected reparation (mg/L/Time_step)
%Column "M"

CR = AVG_GXCH+DELTA_DO;

%-----

%Find areal reparation rate (g/m^2/Time_step)
%Column "N"

CR_area = CR.*(H/100);

%-----

%Determine Night-Time hours
TIME_night1 = TIME_stamp(TIME_stamp>SUNSET);
TIME_night = TIME_night1(TIME_night1<SUNRISE);

%Calculate nighttime respiration
R_Night1 = CR_area(TIME_stamp>SUNSET);
R_Night = R_Night1(TIME_night1<SUNRISE);
R_AVG = mean(R_Night);

```

```

%Substitute Night-time average of R for daily CR
R = CR_area;
for i=1:(N-1)
    for j=1:(length(TIME_night))
        if TIME_stamp(i) == TIME_night(j)
            R(i) = CR_area(i);
            break
        else
            R(i)=R_AVG;
        end
    end
end
end

%-----

%Determine PP
for i=1:(N-1)
    PP(i) = CR_area(i)-R(i);
    if PP(i)<0
        PP(i)=0;
    end
end
PP = PP';

%-----

%Calculate Average Daily Temperature
TEMP_day1 = TEMP_trim(TIME_trim<SUNSET);
TEMP_day2 = TEMP_trim(TIME_trim>SUNRISE);
TEMP_day = [TEMP_day1; TEMP_day2];
AVG_DAILY_TEMP = mean(TEMP_day);

%-----

%Calculate average pH
PH_avg = mean(PH_trim);

%-----

%Calculate NEM (g/m^2/d)
NEM = sum(CR_area);
Resp = sum(R);
GPP = sum(PP);
PoverR = abs(GPP/Resp);
OUTPUT = [{'AVG_DAILY_TEMP'; 'NEM'; 'Resp'; 'GPP'; 'P/R'; 'Avg pH'}]...

```

```
{AVG_DAILY_TEMP; NEM; Resp; GPP; PoverR; PH_avg}]
Answers = [AVG_DAILY_TEMP; NEM; Resp; GPP; PoverR; PH_avg]
```

```
%-----
```

```
%Plot R, NEM, GPP
figure
```

```
%R
subplot(3,1,1); area(TIME_stamp,R); datetick('x',16);
grid on;
ylabel('R (g O2/m2/d)');
```

```
%Give graph title
title({NAME ;'Ecosystem metabolism'});
```

```
%NEM
subplot(3,1,2); area(TIME_stamp,CR_area); datetick('x',16);
grid on;
ylabel('NEM (g O2/m2/d)');
```

```
%GPP
subplot(3,1,3); area(TIME_stamp, PP); datetick('x',16);
grid on;
ylabel('GPP (g O2/m2/d)');
```

```
%Label axes
xlabel('Time');
```

```
%-----
```

```
%Plot DO, DO Sat & Temp
figure
```

```
%DO
plot(TIME_trim,DOPPM_trim, 'r');
H1 = gca;
hold on;
```

```
%DO Sat & Temp
[A2,H2,H3] = plotyy(TIME_trim,DO_SAT,TIME_trim,TEMP_trim);
```

```
%Manipulate Axes and Plot
F = title({NAME ;'Dissolved oxygen'});
linkaxes(A2, 'x');
xlabel('Time');
```

```
set(A2(2),'xtick',[]);
datetick(A2(1),'x',16);
set(A2(2),'ylim', [5 25], 'ytick', 5:5:25);
set(A2(1),'ylim', [0 15], 'ytick', 0:5:15);
ylabel(A2(1),'DO (mg/L)');
ylabel(A2(2),'Temperature (\circC)');
legend('DO','DO Sat','Temperature','Location', 'Best');
axpos = get(gca,'pos');
extent = get(F,'extent');
set(gca,'pos',[axpos(1) axpos(2) axpos(3) axpos(4)-.02*extent(4)]);
hold off;
```

## K.6 NEM: JUNE 2011, DOWNSTREAM

```
%Luke Wildfire
%NEM_calculations
%
%10/2/2013

%Clean up
clear all
clc
close all

%-----

%Import csv file (I'll be working with DO data that has ppm - not %
[num txt] = xlsread('D4_downstream.xls');

%-----

%ENTER VARIABLES SPECIFIC TO EACH RUN

%Give run a name
NAME = 'June: Downstream';
%Stream Velocity in (cm/s)
V = 14.0248;
%Stream Height in (cm)
H = 5.4167;

%-----

%Define dates and times

%12:20pm (20 past noon) on first day of measurement
RoughStartTime = datenum('June 16, 2011 12:20:00000 PM');
%12:20pm (half past noon) on next day of measurement
RoughEndTime = datenum('June 17, 2011 12:20:00000 PM');
%Sunset on first day of measurement
SUNSET = datenum('June 16, 2011 8:32:00.000 PM');
%Sunrise on next day of measurement
SUNRISE = datenum('June 17, 2011 5:34:00.000 AM');

%-----

%Give each variable a name and then smooth
%Graph all variables on one plot vs time
```

```

%TIME is originally (mm/dd/yyyy h:mm:ss PM)
TIME = txt((2:end),1);
%Convert TIME to a number
TIME = datenum(TIME);
%Smooth the data
TIME = smooth(TIME, 25, 'rloess');

%Pressure (kPa)
BARO = num(:,1);
BARO = smooth(BARO, 25, 'rloess');
subplot(2,3,1); plot(TIME,BARO); datetick('x',16); axis tight;
xlabel('Pressure (kPa)');

%Conductance and Specific Conductance (uS/cm)
COND = num(:,2);
COND = smooth(COND, 25, 'rloess');
subplot(2,3,2); plot(TIME,COND); datetick('x',16); axis tight;
xlabel('Conductivity (uS/cm)');
title({NAME ;'All data (untrimmed)'});

SPECCOND = num(:,3);
SPECCOND = smooth(SPECCOND, 25, 'rloess');
subplot(2,3,3); plot(TIME,SPECCOND); datetick('x',16); axis tight;
xlabel('Specific Conductance (uS/cm)');

%Dissolved Oxygen (mg/L, ppm, or g/m^3)
DOPPM = num(:,4);
DOPPM = smooth(DOPPM, 25, 'rloess');
subplot(2,3,4); plot(TIME,DOPPM); datetick('x',16); axis tight;
xlabel('DO (ppm)');

%pH
PH = num(:,5);
PH = smooth(PH, 25, 'rloess');
subplot(2,3,5);plot(TIME,PH); datetick('x',16); axis tight;
xlabel('pH');

%Temperature (deg C)
TEMP = num(:,6);
TEMP = smooth(TEMP, 25, 'rloess');
subplot(2,3,6);plot(TIME,TEMP);datetick('x',16); axis tight;
xlabel('Temperature (deg. C)');

%-----

%Determine time step, and adjust the RoughEndTime up one time step

```



```

TIME_STEP = TIME(2)-TIME(1);
RoughEndTime = RoughEndTime + TIME_STEP;

%-----

%Trim all data to appropriate time frame
%Graph each variable as before

%Create a new figure
figure('Position',[300,300,800,500]);

%Time
TIME_trim1 = TIME(RoughStartTime<TIME);
TIME_trim = TIME_trim1(TIME_trim1<RoughEndTime);
N = length(TIME_trim);
disp(['The number of time increments is: ' num2str(N)]);

%Pressure (kPa)
BARO_trim1 = BARO(RoughStartTime<TIME);
BARO_trim = BARO_trim1(TIME_trim1<RoughEndTime);
subplot(2,3,1); plot(TIME_trim,BARO_trim);
datetick('x','HH');
xlim([RoughStartTime-.05 RoughEndTime+.05]);
xlabel('Time of day (hr)');
ylabel('Pressure (kPa)');
vline([SUNSET SUNRISE]);

%Conductance and Specific Conductance (uS/cm)
COND_trim1 = COND(RoughStartTime<TIME);
COND_trim = COND_trim1(TIME_trim1<RoughEndTime);
subplot(2,3,2); plot(TIME_trim,COND_trim);
datetick('x','HH');
xlim([RoughStartTime-.05 RoughEndTime+.05]);
xlabel('Time of day (hr)');
ylabel('Conductivity (uS/cm)');
vline([SUNSET SUNRISE]);
title({'NAME ;'All data (trimmed)'});

SPECCOND_trim1 = SPECCOND(RoughStartTime<TIME);
SPECCOND_trim = SPECCOND_trim1(TIME_trim1<RoughEndTime);
subplot(2,3,3); plot(TIME_trim,SPECCOND_trim);
datetick('x','HH');
xlim([RoughStartTime-.05 RoughEndTime+.05]);
xlabel('Time of day (hr)');
ylabel('Specific Conductance (uS/cm)');
vline([SUNSET SUNRISE]);

```

```

%Dissolved Oxygen (mg/L, ppm, or g/m^3)
DOPPM_trim1 = DOPPM(RoughStartTime<TIME);
DOPPM_trim = DOPPM_trim1(TIME_trim1<RoughEndTime);
subplot(2,3,4); plot(TIME_trim,DOPPM_trim);
datetick('x','HH');
xlim([RoughStartTime-.05 RoughEndTime+.05]);
xlabel('Time of day (hr)');
ylabel('DO (ppm)');
vline([SUNSET SUNRISE]);

```

```

%pH
PH_trim1 = PH(RoughStartTime<TIME);
PH_trim = PH_trim1(TIME_trim1<RoughEndTime);
subplot(2,3,5);plot(TIME_trim,PH_trim);
datetick('x','HH');
xlim([RoughStartTime-.05 RoughEndTime+.05]);
xlabel('Time of day (hr)');
ylabel('pH');
vline([SUNSET SUNRISE]);

```

```

%Temperature (deg C)
TEMP_trim1 = TEMP(RoughStartTime<TIME);
TEMP_trim = TEMP_trim1(TIME_trim1<RoughEndTime);
subplot(2,3,6);plot(TIME_trim,TEMP_trim);
datetick('x','HH');
xlim([RoughStartTime-.05 RoughEndTime+.05]);
xlabel('Time of day (hr)');
ylabel('Temperature (deg. C)');
vline([SUNSET SUNRISE]);

```

```

%-----

```

```

%Create a vector of time-stamps as the midpoint of each sampling time
%aka Column "D"

```

```

for i=1:(N-1)
    TIME_stamp(i) = (TIME_trim(i) + TIME_trim(i+1))./2;
end
TIME_stamp = TIME_stamp';

```

```

%-----

```

```

%Calculate a vector of Delta DO (column "E")

```

```

for i=1:(N-1)

```

```

    DELTA_DO(i) = (DOPPM_trim(i+1)-DOPPM_trim(i));
end
DELTA_DO = DELTA_DO';

%-----

%Calculate DO Saturation concentration (mg/L)
%Column "F"

%convert temperature to Kelvin
TEMP_Kelvin = TEMP_trim+273.15;

%Use this code to determine DO sat (mg/L)
vp1 = -139.34411;
vp2 = 1.575701e5;
vp3 = -6.642308e7;
vp4 = 1.2438e10;
vp5 = -8.621949e11;
lnDO =
vp1+vp2./TEMP_Kelvin+vp3./TEMP_Kelvin.^2+vp4./TEMP_Kelvin.^3+vp5./TEMP_Kelvin.^
4;
DO_SAT = exp(lnDO);

%-----

%Correct DO_SAT for altitude (mg/L)
%Column "G"

DO_SAT = .989*DO_SAT;

%-----

%Calculate Oxygen Surplus/Deficit (mg/L)
%Column "H"

DO_DEFICIT = DOPPM_trim - DO_SAT;

%-----

%Calculate K constant
%Column "J"

%First calculate K at 20 deg C (1/hr)
K20 = 50.8 * (V^.67)*(H^-1.85);

%Adjust K for the number of timesteps in 1 day

```

```

K20 = (K20*24)/(N-1);

%Adjust K for temperature
K_Adjust = K20.*(1.024.^(TEMP_trim-20));

%-----

%Calculate gas exchagng per time step (mg/L/TIME_STEP)
%Column "K"

GAS_EXCHANGE = K_Adjust.*DO_DEFICIT;

%-----

%Calculate avg gas exchange per time stamp (mg/L/TIME_STEP)
%Column "L"

for i=1:(N-1)
    AVG_GXCH(i) = (GAS_EXCHANGE(i) + GAS_EXCHANGE(i+1))./2;
end
AVG_GXCH = AVG_GXCH';

%-----

%Calculate corrected reparation (mg/L/Time_step)
%Column "M"

CR = AVG_GXCH+DELTA_DO;

%-----

%Find areal reparation rate (g/m^2/Time_step)
%Column "N"

CR_area = CR.*(H/100);

%-----

%Determine Night-Time hours
TIME_night1 = TIME_stamp(TIME_stamp>SUNSET);
TIME_night = TIME_night1(TIME_night1<SUNRISE);

%Calculate nighttime respiration
R_Night1 = CR_area(TIME_stamp>SUNSET);
R_Night = R_Night1(TIME_night1<SUNRISE);
R_AVG = mean(R_Night);

```

```

%Substitute Night-time average of R for daily CR
R = CR_area;
for i=1:(N-1)
    for j=1:(length(TIME_night))
        if TIME_stamp(i) == TIME_night(j)
            R(i) = CR_area(i);
            break
        else
            R(i)=R_AVG;
        end
    end
end
end

%-----

%Determine PP
for i=1:(N-1)
    PP(i) = CR_area(i)-R(i);
    if PP(i)<0
        PP(i)=0;
    end
end
end
PP = PP';

%-----

%Calculate Average Daily Temperature
TEMP_day1 = TEMP_trim(TIME_trim<SUNSET);
TEMP_day2 = TEMP_trim(TIME_trim>SUNRISE);
TEMP_day = [TEMP_day1; TEMP_day2];
AVG_DAILY_TEMP = mean(TEMP_day);

%-----

%Calculate average pH
PH_avg = mean(PH_trim);

%-----

%Calculate NEM (g/m^2/d)
NEM = sum(CR_area);
Resp = sum(R);
GPP = sum(PP);
PoverR = abs(GPP/Resp);
OUTPUT = [{'AVG_DAILY_TEMP'; 'NEM'; 'Resp'; 'GPP'; 'P/R'; 'Avg pH'}]...

```

```
{AVG_DAILY_TEMP; NEM; Resp; GPP; PoverR; PH_avg}]
Answers = [AVG_DAILY_TEMP; NEM; Resp; GPP; PoverR; PH_avg]
```

```
%-----
```

```
%Plot R, NEM, GPP
figure
```

```
%R
subplot(3,1,1); area(TIME_stamp,R); datetick('x',16);
grid on;
ylabel('R (g O2/m2/d)');
```

```
%Give graph title
title({NAME ;'Ecosystem metabolism'});
```

```
%NEM
subplot(3,1,2); area(TIME_stamp,CR_area); datetick('x',16);
grid on;
ylabel('NEM (g O2/m2/d)');
```

```
%GPP
subplot(3,1,3); area(TIME_stamp, PP); datetick('x',16);
grid on;
ylabel('GPP (g O2/m2/d)');
```

```
%Label axes
xlabel('Time');
```

```
%-----
```

```
%Plot DO, DO Sat & Temp
figure
```

```
%DO
plot(TIME_trim,DOPPM_trim, 'r');
H1 = gca;
hold on;
```

```
%DO Sat & Temp
[A2,H2,H3] = plotyy(TIME_trim,DO_SAT,TIME_trim,TEMP_trim);
```

```
%Manipulate Axes and Plot
F = title({NAME ;'Dissolved oxygen'});
linkaxes(A2, 'x');
xlabel('Time');
```

```
set(A2(2),'xtick',[]);
datetick(A2(1),'x',16);
set(A2(2),'ylim', [5 25], 'ytick', 5:5:25);
set(A2(1),'ylim', [0 15], 'ytick', 0:5:15);
ylabel(A2(1),'DO (mg/L)');
ylabel(A2(2),'Temperature (\circC)');
legend('DO','DO Sat','Temperature','Location', 'Best');
axpos = get(gca,'pos');
extent = get(F,'extent');
set(gca,'pos',[axpos(1) axpos(2) axpos(3) axpos(4)-.02*extent(4)]);
hold off;
```

## K.7 NEM: AUGUST 2011, UPSTREAM

```
%Luke Wildfire
%NEM_calculations
%
%10/2/2013

%Clean up
clear all
clc
close all

%-----

%Import csv file (I'll be working with DO data that has ppm - not %
[num txt] = xlsread('D5_upstream.xls');

%-----

%ENTER VARIABLES SPECIFIC TO EACH RUN

%Give run a name
NAME = 'August: Upstream';
%Stream Velocity in (cm/s)
V = 1.8670;
%Stream Height in (cm)
H = 2.4333;

%-----

%Define dates and times

%12:20pm (20 past noon) on first day of measurement
RoughStartTime = datenum('August 4, 2011 12:20:00000 PM');
%12:20pm (half past noon) on next day of measurement
RoughEndTime = datenum('August 5, 2011 12:20:00000 PM');
%Sunset on first day of measurement
SUNSET = datenum('August 4, 2011 8:12:00.000 PM');
%Sunrise on next day of measurement
SUNRISE = datenum('August 5, 2011 6:04:00.000 AM');

%-----

%Give each variable a name and then smooth
%Graph all variables on one plot vs time
```



```

%TIME is originally (mm/dd/yyyy h:mm:ss PM)
TIME = txt((2:end),1);
%Convert TIME to a number
TIME = datenum(TIME);
%Smooth the data
TIME = smooth(TIME, 25, 'rloess');

%Pressure (kPa)
BARO = num(:,1);
BARO = smooth(BARO, 25, 'rloess');
subplot(2,3,1); plot(TIME,BARO); datetick('x',16); axis tight;
xlabel('Pressure (kPa)');

%Conductance and Specific Conductance (uS/cm)
COND = num(:,2);
COND = smooth(COND, 25, 'rloess');
subplot(2,3,2); plot(TIME,COND); datetick('x',16); axis tight;
xlabel('Conductivity (uS/cm)');
title({NAME ;'All data (untrimmed)'});

SPECCOND = num(:,3);
SPECCOND = smooth(SPECCOND, 25, 'rloess');
subplot(2,3,3); plot(TIME,SPECCOND); datetick('x',16); axis tight;
xlabel('Specific Conductance (uS/cm)');

%Dissolved Oxygen (mg/L, ppm, or g/m^3)
DOPPM = num(:,4);
DOPPM = smooth(DOPPM, 25, 'rloess');
subplot(2,3,4); plot(TIME,DOPPM); datetick('x',16); axis tight;
xlabel('DO (ppm)');

%pH
PH = num(:,5);
PH = smooth(PH, 25, 'rloess');
subplot(2,3,5);plot(TIME,PH); datetick('x',16); axis tight;
xlabel('pH');

%Temperature (deg C)
TEMP = num(:,6);
TEMP = smooth(TEMP, 25, 'rloess');
subplot(2,3,6);plot(TIME,TEMP);datetick('x',16); axis tight;
xlabel('Temperature (deg. C)');

%-----

%Determine time step, and adjust the RoughEndTime up one time step

```

```

TIME_STEP = TIME(2)-TIME(1);
RoughEndTime = RoughEndTime + TIME_STEP;

%-----

%Trim all data to appropriate time frame
%Graph each variable as before

%Create a new figure
figure('Position',[300,300,800,500]);

%Time
TIME_trim1 = TIME(RoughStartTime<TIME);
TIME_trim = TIME_trim1(TIME_trim1<RoughEndTime);
N = length(TIME_trim);
disp(['The number of time increments is: ' num2str(N)]);

%Pressure (kPa)
BARO_trim1 = BARO(RoughStartTime<TIME);
BARO_trim = BARO_trim1(TIME_trim1<RoughEndTime);
subplot(2,3,1); plot(TIME_trim,BARO_trim);
datetick('x','HH');
xlim([RoughStartTime-.05 RoughEndTime+.05]);
xlabel('Time of day (hr)');
ylabel('Pressure (kPa)');
vline([SUNSET SUNRISE]);

%Conductance and Specific Conductance (uS/cm)
COND_trim1 = COND(RoughStartTime<TIME);
COND_trim = COND_trim1(TIME_trim1<RoughEndTime);
subplot(2,3,2); plot(TIME_trim,COND_trim);
datetick('x','HH');
xlim([RoughStartTime-.05 RoughEndTime+.05]);
xlabel('Time of day (hr)');
ylabel('Conductivity (uS/cm)');
vline([SUNSET SUNRISE]);
title({'NAME ;'All data (trimmed)'});

SPECCOND_trim1 = SPECCOND(RoughStartTime<TIME);
SPECCOND_trim = SPECCOND_trim1(TIME_trim1<RoughEndTime);
subplot(2,3,3); plot(TIME_trim,SPECCOND_trim);
datetick('x','HH');
xlim([RoughStartTime-.05 RoughEndTime+.05]);
xlabel('Time of day (hr)');
ylabel('Specific Conductance (uS/cm)');
vline([SUNSET SUNRISE]);

```

```

%Dissolved Oxygen (mg/L, ppm, or g/m^3)
DOPPM_trim1 = DOPPM(RoughStartTime<TIME);
DOPPM_trim = DOPPM_trim1(TIME_trim1<RoughEndTime);
subplot(2,3,4); plot(TIME_trim,DOPPM_trim);
datetick('x','HH');
xlim([RoughStartTime-.05 RoughEndTime+.05]);
xlabel('Time of day (hr)');
ylabel('DO (ppm)');
vline([SUNSET SUNRISE]);

```

```

%pH
PH_trim1 = PH(RoughStartTime<TIME);
PH_trim = PH_trim1(TIME_trim1<RoughEndTime);
subplot(2,3,5);plot(TIME_trim,PH_trim);
datetick('x','HH');
xlim([RoughStartTime-.05 RoughEndTime+.05]);
xlabel('Time of day (hr)');
ylabel('pH');
vline([SUNSET SUNRISE]);

```

```

%Temperature (deg C)
TEMP_trim1 = TEMP(RoughStartTime<TIME);
TEMP_trim = TEMP_trim1(TIME_trim1<RoughEndTime);
subplot(2,3,6);plot(TIME_trim,TEMP_trim);
datetick('x','HH');
xlim([RoughStartTime-.05 RoughEndTime+.05]);
xlabel('Time of day (hr)');
ylabel('Temperature (deg. C)');
vline([SUNSET SUNRISE]);

```

```

%-----

```

```

%Create a vector of time-stamps as the midpoint of each sampling time
%aka Column "D"

```

```

for i=1:(N-1)
    TIME_stamp(i) = (TIME_trim(i) + TIME_trim(i+1))./2;
end
TIME_stamp = TIME_stamp';

```

```

%-----

```

```

%Calculate a vector of Delta DO (column "E")

```

```

for i=1:(N-1)

```

```

    DELTA_DO(i) = (DOPPM_trim(i+1)-DOPPM_trim(i));
end
DELTA_DO = DELTA_DO';

%-----

%Calculate DO Saturation concentration (mg/L)
%Column "F"

%convert temperature to Kelvin
TEMP_Kelvin = TEMP_trim+273.15;

%Use this code to determine DO sat (mg/L)
vp1 = -139.34411;
vp2 = 1.575701e5;
vp3 = -6.642308e7;
vp4 = 1.2438e10;
vp5 = -8.621949e11;
lnDO =
vp1+vp2./TEMP_Kelvin+vp3./TEMP_Kelvin.^2+vp4./TEMP_Kelvin.^3+vp5./TEMP_Kelvin.^
4;
DO_SAT = exp(lnDO);

%-----

%Correct DO_SAT for altitude (mg/L)
%Column "G"

DO_SAT = .989*DO_SAT;

%-----

%Calculate Oxygen Surplus/Deficit (mg/L)
%Column "H"

DO_DEFICIT = DOPPM_trim - DO_SAT;

%-----

%Calculate K constant
%Column "J"

%First calculate K at 20 deg C (1/hr)
K20 = 50.8 * (V^.67)*(H^-1.85);

%Adjust K for the number of timesteps in 1 day

```

```

K20 = (K20*24)/(N-1);

%Adjust K for temperature
K_Adjust = K20.*(1.024.^(TEMP_trim-20));

%-----

%Calculate gas exchagng per time step (mg/L/TIME_STEP)
%Column "K"

GAS_EXCHANGE = K_Adjust.*DO_DEFICIT;

%-----

%Calculate avg gas exchange per time stamp (mg/L/TIME_STEP)
%Column "L"

for i=1:(N-1)
    AVG_GXCH(i) = (GAS_EXCHANGE(i) + GAS_EXCHANGE(i+1))./2;
end
AVG_GXCH = AVG_GXCH';

%-----

%Calculate corrected reparation (mg/L/Time_step)
%Column "M"

CR = AVG_GXCH+DELTA_DO;

%-----

%Find areal reparation rate (g/m^2/Time_step)
%Column "N"

CR_area = CR.*(H/100);

%-----

%Determine Night-Time hours
TIME_night1 = TIME_stamp(TIME_stamp>SUNSET);
TIME_night = TIME_night1(TIME_night1<SUNRISE);

%Calculate nighttime respiration
R_Night1 = CR_area(TIME_stamp>SUNSET);
R_Night = R_Night1(TIME_night1<SUNRISE);
R_AVG = mean(R_Night);

```

```

%Substitute Night-time average of R for daily CR
R = CR_area;
for i=1:(N-1)
    for j=1:(length(TIME_night))
        if TIME_stamp(i) == TIME_night(j)
            R(i) = CR_area(i);
            break
        else
            R(i)=R_AVG;
        end
    end
end
end

%-----

%Determine PP
for i=1:(N-1)
    PP(i) = CR_area(i)-R(i);
    if PP(i)<0
        PP(i)=0;
    end
end
end
PP = PP';

%-----

%Caluculate Average Daily Temperature
TEMP_day1 = TEMP_trim(TIME_trim<SUNSET);
TEMP_day2 = TEMP_trim(TIME_trim>SUNRISE);
TEMP_day = [TEMP_day1; TEMP_day2];
AVG_DAILY_TEMP = mean(TEMP_day);

%-----

%Calculate average pH
PH_avg = mean(PH_trim);

%-----

%Calculate NEM (g/m^2/d)
NEM = sum(CR_area);
Resp = sum(R);
GPP = sum(PP);
PoverR = abs(GPP/Resp);
OUTPUT = [{'AVG_DAILY_TEMP'; 'NEM'; 'Resp'; 'GPP'; 'P/R'; 'Avg pH'}]...

```

```
{AVG_DAILY_TEMP; NEM; Resp; GPP; PoverR; PH_avg}]
Answers = [AVG_DAILY_TEMP; NEM; Resp; GPP; PoverR; PH_avg]
```

```
%-----
```

```
%Plot R, NEM, GPP
figure
```

```
%R
subplot(3,1,1); area(TIME_stamp,R); datetick('x',16);
grid on;
ylabel('R (g O2/m2/d)');
```

```
%Give graph title
title({NAME ;'Ecosystem metabolism'});
```

```
%NEM
subplot(3,1,2); area(TIME_stamp,CR_area); datetick('x',16);
grid on;
ylabel('NEM (g O2/m2/d)');
```

```
%GPP
subplot(3,1,3); area(TIME_stamp, PP); datetick('x',16);
grid on;
ylabel('GPP (g O2/m2/d)');
```

```
%Label axes
xlabel('Time');
```

```
%-----
```

```
%Plot DO, DO Sat & Temp
figure
```

```
%DO
plot(TIME_trim,DOPPM_trim, 'r');
H1 = gca;
hold on;
```

```
%DO Sat & Temp
[A2,H2,H3] = plotyy(TIME_trim,DO_SAT,TIME_trim,TEMP_trim);
```

```
%Manipulate Axes and Plot
F = title({NAME ;'Dissolved oxygen'});
linkaxes(A2, 'x');
xlabel('Time');
```

```
set(A2(2),'xtick',[]);
datetick(A2(1),'x',16);
set(A2(2),'ylim', [5 25], 'ytick', 5:5:25);
set(A2(1),'ylim', [0 15], 'ytick', 0:5:15);
ylabel(A2(1),'DO (mg/L)');
ylabel(A2(2),'Temperature (\circC)');
legend('DO','DO Sat','Temperature','Location', 'Best');
axpos = get(gca,'pos');
extent = get(F,'extent');
set(gca,'pos',[axpos(1) axpos(2) axpos(3) axpos(4)-.02*extent(4)]);
hold off;
```



## K.8 NEM: AUGUST 2011, DOWNSTREAM

```
%Luke Wildfire
%NEM_calculations
%
%10/2/2013

%Clean up
clear all
clc
close all

%-----

%Import csv file (I'll be working with DO data that has ppm - not %
[num txt] = xlsread('D5_downstream.xls');

%-----

%ENTER VARIABLES SPECIFIC TO EACH RUN

%Give run a name
NAME = 'August: Downstream';
%Stream Velocity in (cm/s)
V = 4.9831;
%Stream Height in (cm)
H = 3.850;

%-----

%Define dates and times

%12:20pm (20 past noon) on first day of measurement
RoughStartTime = datenum('August 4, 2011 12:20:00000 PM');
%12:20pm (half past noon) on next day of measurement
RoughEndTime = datenum('August 5, 2011 12:20:00000 PM');
%Sunset on first day of measurement
SUNSET = datenum('August 4, 2011 8:12:00.000 PM');
%Sunrise on next day of measurement
SUNRISE = datenum('August 5, 2011 6:04:00.000 AM');

%-----

%Give each variable a name and then smooth
%Graph all variables on one plot vs time
```

```

%TIME is originally (mm/dd/yyyy h:mm:ss PM)
TIME = txt((2:end),1);
%Convert TIME to a number
TIME = datenum(TIME);
%Smooth the data
TIME = smooth(TIME, 25, 'rloess');

%Pressure (kPa)
BARO = num(:,1);
BARO = smooth(BARO, 25, 'rloess');
subplot(2,3,1); plot(TIME,BARO); datetick('x',16); axis tight;
xlabel('Pressure (kPa)');

%Conductance and Specific Conductance (uS/cm)
COND = num(:,2);
COND = smooth(COND, 25, 'rloess');
subplot(2,3,2); plot(TIME,COND); datetick('x',16); axis tight;
xlabel('Conductivity (uS/cm)');
title({NAME ;'All data (untrimmed)'});

SPECCOND = num(:,3);
SPECCOND = smooth(SPECCOND, 25, 'rloess');
subplot(2,3,3); plot(TIME,SPECCOND); datetick('x',16); axis tight;
xlabel('Specific Conductance (uS/cm)');

%Dissolved Oxygen (mg/L, ppm, or g/m^3)
DOPPM = num(:,4);
DOPPM = smooth(DOPPM, 25, 'rloess');
subplot(2,3,4); plot(TIME,DOPPM); datetick('x',16); axis tight;
xlabel('DO (ppm)');

%pH
PH = num(:,5);
PH = smooth(PH, 25, 'rloess');
subplot(2,3,5);plot(TIME,PH); datetick('x',16); axis tight;
xlabel('pH');

%Temperature (deg C)
TEMP = num(:,6);
TEMP = smooth(TEMP, 25, 'rloess');
subplot(2,3,6);plot(TIME,TEMP);datetick('x',16); axis tight;
xlabel('Temperature (deg. C)');

%-----

%Determine time step, and adjust the RoughEndTime up one time step

```

```

TIME_STEP = TIME(2)-TIME(1);
RoughEndTime = RoughEndTime + TIME_STEP;

%-----

%Trim all data to appropriate time frame
%Graph each variable as before

%Create a new figure
figure('Position',[300,300,800,500]);

%Time
TIME_trim1 = TIME(RoughStartTime<TIME);
TIME_trim = TIME_trim1(TIME_trim1<RoughEndTime);
N = length(TIME_trim);
disp(['The number of time increments is: ' num2str(N)]);

%Pressure (kPa)
BARO_trim1 = BARO(RoughStartTime<TIME);
BARO_trim = BARO_trim1(TIME_trim1<RoughEndTime);
subplot(2,3,1); plot(TIME_trim,BARO_trim);
datetick('x','HH');
xlim([RoughStartTime-.05 RoughEndTime+.05]);
xlabel('Time of day (hr)');
ylabel('Pressure (kPa)');
vline([SUNSET SUNRISE]);

%Conductance and Specific Conductance (uS/cm)
COND_trim1 = COND(RoughStartTime<TIME);
COND_trim = COND_trim1(TIME_trim1<RoughEndTime);
subplot(2,3,2); plot(TIME_trim,COND_trim);
datetick('x','HH');
xlim([RoughStartTime-.05 RoughEndTime+.05]);
xlabel('Time of day (hr)');
ylabel('Conductivity (uS/cm)');
vline([SUNSET SUNRISE]);
title({'NAME ;'All data (trimmed)'});

SPECCOND_trim1 = SPECCOND(RoughStartTime<TIME);
SPECCOND_trim = SPECCOND_trim1(TIME_trim1<RoughEndTime);
subplot(2,3,3); plot(TIME_trim,SPECCOND_trim);
datetick('x','HH');
xlim([RoughStartTime-.05 RoughEndTime+.05]);
xlabel('Time of day (hr)');
ylabel('Specific Conductance (uS/cm)');
vline([SUNSET SUNRISE]);

```

```

%Dissolved Oxygen (mg/L, ppm, or g/m^3)
DOPPM_trim1 = DOPPM(RoughStartTime<TIME);
DOPPM_trim = DOPPM_trim1(TIME_trim1<RoughEndTime);
subplot(2,3,4); plot(TIME_trim,DOPPM_trim);
datetick('x','HH');
xlim([RoughStartTime-.05 RoughEndTime+.05]);
xlabel('Time of day (hr)');
ylabel('DO (ppm)');
vline([SUNSET SUNRISE]);

```

```

%pH
PH_trim1 = PH(RoughStartTime<TIME);
PH_trim = PH_trim1(TIME_trim1<RoughEndTime);
subplot(2,3,5);plot(TIME_trim,PH_trim);
datetick('x','HH');
xlim([RoughStartTime-.05 RoughEndTime+.05]);
xlabel('Time of day (hr)');
ylabel('pH');
vline([SUNSET SUNRISE]);

```

```

%Temperature (deg C)
TEMP_trim1 = TEMP(RoughStartTime<TIME);
TEMP_trim = TEMP_trim1(TIME_trim1<RoughEndTime);
subplot(2,3,6);plot(TIME_trim,TEMP_trim);
datetick('x','HH');
xlim([RoughStartTime-.05 RoughEndTime+.05]);
xlabel('Time of day (hr)');
ylabel('Temperature (deg. C)');
vline([SUNSET SUNRISE]);

```

```

%-----

```

```

%Create a vector of time-stamps as the midpoint of each sampling time
%aka Column "D"

```

```

for i=1:(N-1)
    TIME_stamp(i) = (TIME_trim(i) + TIME_trim(i+1))./2;
end
TIME_stamp = TIME_stamp';

```

```

%-----

```

```

%Calculate a vector of Delta DO (column "E")

```

```

for i=1:(N-1)

```

```

    DELTA_DO(i) = (DOPPM_trim(i+1)-DOPPM_trim(i));
end
DELTA_DO = DELTA_DO';

%-----

%Calculate DO Saturation concentration (mg/L)
%Column "F"

%convert temperature to Kelvin
TEMP_Kelvin = TEMP_trim+273.15;

%Use this code to determine DO sat (mg/L)
vp1 = -139.34411;
vp2 = 1.575701e5;
vp3 = -6.642308e7;
vp4 = 1.2438e10;
vp5 = -8.621949e11;
lndo =
vp1+vp2./TEMP_Kelvin+vp3./TEMP_Kelvin.^2+vp4./TEMP_Kelvin.^3+vp5./TEMP_Kelvin.^
4;
DO_SAT = exp(lndo);

%-----

%Correct DO_SAT for altitude (mg/L)
%Column "G"

DO_SAT = .989*DO_SAT;

%-----

%Calculate Oxygen Surplus/Deficit (mg/L)
%Column "H"

DO_DEFICIT = DOPPM_trim - DO_SAT;

%-----

%Calculate K constant
%Column "J"

%First calculate K at 20 deg C (1/hr)
K20 = 50.8 * (V^.67)*(H^-1.85);

%Adjust K for the number of timesteps in 1 day

```

```

K20 = (K20*24)/(N-1);

%Adjust K for temperature
K_Adjust = K20.*(1.024.^(TEMP_trim-20));

%-----

%Calculate gas exchagng per time step (mg/L/TIME_STEP)
%Column "K"

GAS_EXCHANGE = K_Adjust.*DO_DEFICIT;

%-----

%Calculate avg gas exchange per time stamp (mg/L/TIME_STEP)
%Column "L"

for i=1:(N-1)
    AVG_GXCH(i) = (GAS_EXCHANGE(i) + GAS_EXCHANGE(i+1))./2;
end
AVG_GXCH = AVG_GXCH';

%-----

%Calculate corrected reparation (mg/L/Time_step)
%Column "M"

CR = AVG_GXCH+DELTA_DO;

%-----

%Find areal reparation rate (g/m^2/Time_step)
%Column "N"

CR_area = CR.*(H/100);

%-----

%Determine Night-Time hours
TIME_night1 = TIME_stamp(TIME_stamp>SUNSET);
TIME_night = TIME_night1(TIME_night1<SUNRISE);

%Calculate nighttime respiration
R_Night1 = CR_area(TIME_stamp>SUNSET);
R_Night = R_Night1(TIME_night1<SUNRISE);
R_AVG = mean(R_Night);

```

```

%Substitute Night-time average of R for daily CR
R = CR_area;
for i=1:(N-1)
    for j=1:(length(TIME_night))
        if TIME_stamp(i) == TIME_night(j)
            R(i) = CR_area(i);
            break
        else
            R(i)=R_AVG;
        end
    end
end
end

%-----

%Determine PP
for i=1:(N-1)
    PP(i) = CR_area(i)-R(i);
    if PP(i)<0
        PP(i)=0;
    end
end
end
PP = PP';

%-----

%Calculate Average Daily Temperature
TEMP_day1 = TEMP_trim(TIME_trim<SUNSET);
TEMP_day2 = TEMP_trim(TIME_trim>SUNRISE);
TEMP_day = [TEMP_day1; TEMP_day2];
AVG_DAILY_TEMP = mean(TEMP_day);

%-----

%Calculate average pH
PH_avg = mean(PH_trim);

%-----

%Calculate NEM (g/m^2/d)
NEM = sum(CR_area);
Resp = sum(R);
GPP = sum(PP);
PoverR = abs(GPP/Resp);
OUTPUT = [{'AVG_DAILY_TEMP'; 'NEM'; 'Resp'; 'GPP'; 'P/R'; 'Avg pH'}]...

```

```
{AVG_DAILY_TEMP; NEM; Resp; GPP; PoverR; PH_avg}]
Answers = [AVG_DAILY_TEMP; NEM; Resp; GPP; PoverR; PH_avg]
```

```
%-----
```

```
%Plot R, NEM, GPP
figure
```

```
%R
subplot(3,1,1); area(TIME_stamp,R); datetick('x',16);
grid on;
ylabel('R (g O2/m2/d)');
```

```
%Give graph title
title({NAME ;'Ecosystem metabolism'});
```

```
%NEM
subplot(3,1,2); area(TIME_stamp,CR_area); datetick('x',16);
grid on;
ylabel('NEM (g O2/m2/d)');
```

```
%GPP
subplot(3,1,3); area(TIME_stamp, PP); datetick('x',16);
grid on;
ylabel('GPP (g O2/m2/d)');
```

```
%Label axes
xlabel('Time');
```

```
%-----
```

```
%Plot DO, DO Sat & Temp
figure
```

```
%DO
plot(TIME_trim,DOPPM_trim, 'r');
H1 = gca;
hold on;
```

```
%DO Sat & Temp
[A2,H2,H3] = plotyy(TIME_trim,DO_SAT,TIME_trim,TEMP_trim);
```

```
%Manipulate Axes and Plot
F = title({NAME ;'Dissolved oxygen'});
linkaxes(A2, 'x');
xlabel('Time');
```



```
set(A2(2),'xtick',[]);
datetick(A2(1),'x',16);
set(A2(2),'ylim', [5 25], 'ytick', 5:5:25);
set(A2(1),'ylim', [0 15], 'ytick', 0:5:15);
ylabel(A2(1),'DO (mg/L)');
ylabel(A2(2),'Temperature (\circC)');
legend('DO','DO Sat','Temperature','Location', 'Best');
axpos = get(gca,'pos');
extent = get(F,'extent');
set(gca,'pos',[axpos(1) axpos(2) axpos(3) axpos(4)-.02*extent(4)]);
hold off;
```

## K.9 NEM: SEPTEMBER 2010, UPSTREAM

```
%Luke Wildfire
%NEM_calculations
%
%10/2/2013

%Clean up
clear all
clc
close all

%-----

%Import csv file (I'll be working with DO data that has ppm - not %
[num txt] = xlsread('D1_upstream.xls');

%-----

%ENTER VARIABLES SPECIFIC TO EACH RUN

%Give run a name
NAME = 'September: Upstream';
%Stream Velocity in (cm/s)
V = .6776;
%Stream Height in (cm)
H = 2.7667;

%-----

%Define dates and times

%12:20pm (20 past noon) on first day of measurement
RoughStartTime = datenum('September 25, 2010 12:20:00000 PM');
%12:20pm (half past noon) on next day of measurement
RoughEndTime = datenum('September 26, 2010 12:20:00000 PM');
%Sunset on first day of measurement
SUNSET = datenum('September 25, 2010 6:56:00.000 PM');
%Sunrise on next day of measurement
SUNRISE = datenum('September 26, 2010 6:54:00.000 AM');

%-----

%Give each variable a name and then smooth
%Graph all variables on one plot vs time
```

```

%TIME is originally (mm/dd/yyyy h:mm:ss PM)
TIME = txt((2:end),1);
%Convert TIME to a number
TIME = datenum(TIME);
%Smooth the data
TIME = smooth(TIME, 25, 'rloess');

%Pressure (kPa)
BARO = num(:,1);
BARO = smooth(BARO, 25, 'rloess');
subplot(2,3,1); plot(TIME,BARO); datetick('x',16); axis tight;
xlabel('Pressure (kPa)');

%Conductance and Specific Conductance (uS/cm)
COND = num(:,2);
COND = smooth(COND, 25, 'rloess');
subplot(2,3,2); plot(TIME,COND); datetick('x',16); axis tight;
xlabel('Conductivity (uS/cm)');
title({NAME ;'All data (untrimmed)'});

SPECCOND = num(:,3);
SPECCOND = smooth(SPECCOND, 25, 'rloess');
subplot(2,3,3); plot(TIME,SPECCOND); datetick('x',16); axis tight;
xlabel('Specific Conductance (uS/cm)');

%Dissolved Oxygen (mg/L, ppm, or g/m^3)
DOPPM = num(:,4);
DOPPM = smooth(DOPPM, 25, 'rloess');
subplot(2,3,4); plot(TIME,DOPPM); datetick('x',16); axis tight;
xlabel('DO (ppm)');

%pH
PH = num(:,5);
PH = smooth(PH, 25, 'rloess');
subplot(2,3,5);plot(TIME,PH); datetick('x',16); axis tight;
xlabel('pH');

%Temperature (deg C)
TEMP = num(:,6);
TEMP = smooth(TEMP, 25, 'rloess');
subplot(2,3,6);plot(TIME,TEMP);datetick('x',16); axis tight;
xlabel('Temperature (deg. C)');

%-----

%Determine time step, and adjust the RoughEndTime up one time step

```

```

TIME_STEP = TIME(2)-TIME(1);
RoughEndTime = RoughEndTime + TIME_STEP;

%-----

%Trim all data to appropriate time frame
%Graph each variable as before

%Create a new figure
figure('Position',[300,300,800,500]);

%Time
TIME_trim1 = TIME(RoughStartTime<TIME);
TIME_trim = TIME_trim1(TIME_trim1<RoughEndTime);
N = length(TIME_trim);
disp(['The number of time increments is: ' num2str(N)]);

%Pressure (kPa)
BARO_trim1 = BARO(RoughStartTime<TIME);
BARO_trim = BARO_trim1(TIME_trim1<RoughEndTime);
subplot(2,3,1); plot(TIME_trim,BARO_trim);
datetick('x','HH');
xlim([RoughStartTime-.05 RoughEndTime+.05]);
xlabel('Time of day (hr)');
ylabel('Pressure (kPa)');
vline([SUNSET SUNRISE]);

%Conductance and Specific Conductance (uS/cm)
COND_trim1 = COND(RoughStartTime<TIME);
COND_trim = COND_trim1(TIME_trim1<RoughEndTime);
subplot(2,3,2); plot(TIME_trim,COND_trim);
datetick('x','HH');
xlim([RoughStartTime-.05 RoughEndTime+.05]);
xlabel('Time of day (hr)');
ylabel('Conductivity (uS/cm)');
vline([SUNSET SUNRISE]);
title({'NAME ;'All data (trimmed)'});

SPECCOND_trim1 = SPECCOND(RoughStartTime<TIME);
SPECCOND_trim = SPECCOND_trim1(TIME_trim1<RoughEndTime);
subplot(2,3,3); plot(TIME_trim,SPECCOND_trim);
datetick('x','HH');
xlim([RoughStartTime-.05 RoughEndTime+.05]);
xlabel('Time of day (hr)');
ylabel('Specific Conductance (uS/cm)');
vline([SUNSET SUNRISE]);

```

```

%Dissolved Oxygen (mg/L, ppm, or g/m^3)
DOPPM_trim1 = DOPPM(RoughStartTime<TIME);
DOPPM_trim = DOPPM_trim1(TIME_trim1<RoughEndTime);
subplot(2,3,4); plot(TIME_trim,DOPPM_trim);
datetick('x','HH');
xlim([RoughStartTime-.05 RoughEndTime+.05]);
xlabel('Time of day (hr)');
ylabel('DO (ppm)');
vline([SUNSET SUNRISE]);

```

```

%pH
PH_trim1 = PH(RoughStartTime<TIME);
PH_trim = PH_trim1(TIME_trim1<RoughEndTime);
subplot(2,3,5);plot(TIME_trim,PH_trim);
datetick('x','HH');
xlim([RoughStartTime-.05 RoughEndTime+.05]);
xlabel('Time of day (hr)');
ylabel('pH');
vline([SUNSET SUNRISE]);

```

```

%Temperature (deg C)
TEMP_trim1 = TEMP(RoughStartTime<TIME);
TEMP_trim = TEMP_trim1(TIME_trim1<RoughEndTime);
subplot(2,3,6);plot(TIME_trim,TEMP_trim);
datetick('x','HH');
xlim([RoughStartTime-.05 RoughEndTime+.05]);
xlabel('Time of day (hr)');
ylabel('Temperature (deg. C)');
vline([SUNSET SUNRISE]);

```

```

%-----

```

```

%Create a vector of time-stamps as the midpoint of each sampling time
%aka Column "D"

```

```

for i=1:(N-1)
    TIME_stamp(i) = (TIME_trim(i) + TIME_trim(i+1))./2;
end
TIME_stamp = TIME_stamp';

```

```

%-----

```

```

%Calculate a vector of Delta DO (column "E")

```

```

for i=1:(N-1)

```

```

    DELTA_DO(i) = (DOPPM_trim(i+1)-DOPPM_trim(i));
end
DELTA_DO = DELTA_DO';

%-----

%Calculate DO Saturation concentration (mg/L)
%Column "F"

%convert temperature to Kelvin
TEMP_Kelvin = TEMP_trim+273.15;

%Use this code to determine DO sat (mg/L)
vp1 = -139.34411;
vp2 = 1.575701e5;
vp3 = -6.642308e7;
vp4 = 1.2438e10;
vp5 = -8.621949e11;
lnDO =
vp1+vp2./TEMP_Kelvin+vp3./TEMP_Kelvin.^2+vp4./TEMP_Kelvin.^3+vp5./TEMP_Kelvin.^
4;
DO_SAT = exp(lnDO);

%-----

%Correct DO_SAT for altitude (mg/L)
%Column "G"

DO_SAT = .989*DO_SAT;

%-----

%Calculate Oxygen Surplus/Deficit (mg/L)
%Column "H"

DO_DEFICIT = DOPPM_trim - DO_SAT;

%-----

%Calculate K constant
%Column "J"

%First calculate K at 20 deg C (1/hr)
K20 = 50.8 * (V^.67)*(H^-1.85);

%Adjust K for the number of timesteps in 1 day

```

```

K20 = (K20*24)/(N-1);

%Adjust K for temperature
K_Adjust = K20.*(1.024.^(TEMP_trim-20));

%-----

%Calculate gas exchagng per time step (mg/L/TIME_STEP)
%Column "K"

GAS_EXCHANGE = K_Adjust.*DO_DEFICIT;

%-----

%Calculate avg gas exchange per time stamp (mg/L/TIME_STEP)
%Column "L"

for i=1:(N-1)
    AVG_GXCH(i) = (GAS_EXCHANGE(i) + GAS_EXCHANGE(i+1))./2;
end
AVG_GXCH = AVG_GXCH';

%-----

%Calculate corrected reparation (mg/L/Time_step)
%Column "M"

CR = AVG_GXCH+DELTA_DO;

%-----

%Find areal reparation rate (g/m^2/Time_step)
%Column "N"

CR_area = CR.*(H/100);

%-----

%Determine Night-Time hours
TIME_night1 = TIME_stamp(TIME_stamp>SUNSET);
TIME_night = TIME_night1(TIME_night1<SUNRISE);

%Calculate nighttime respiration
R_Night1 = CR_area(TIME_stamp>SUNSET);
R_Night = R_Night1(TIME_night1<SUNRISE);
R_AVG = mean(R_Night);

```

```

%Substitute Night-time average of R for daily CR
R = CR_area;
for i=1:(N-1)
    for j=1:(length(TIME_night))
        if TIME_stamp(i) == TIME_night(j)
            R(i) = CR_area(i);
            break
        else
            R(i)=R_AVG;
        end
    end
end
end

%-----

%Determine PP
for i=1:(N-1)
    PP(i) = CR_area(i)-R(i);
    if PP(i)<0
        PP(i)=0;
    end
end
end
PP = PP';

%-----

%Caluculate Average Daily Temperature
TEMP_day1 = TEMP_trim(TIME_trim<SUNSET);
TEMP_day2 = TEMP_trim(TIME_trim>SUNRISE);
TEMP_day = [TEMP_day1; TEMP_day2];
AVG_DAILY_TEMP = mean(TEMP_day);

%-----

%Calculate average pH
PH_avg = mean(PH_trim);

%-----

%Calculate NEM (g/m^2/d)
NEM = sum(CR_area);
Resp = sum(R);
GPP = sum(PP);
PoverR = abs(GPP/Resp);
OUTPUT = [{'AVG_DAILY_TEMP'; 'NEM'; 'Resp'; 'GPP'; 'P/R'; 'Avg pH'}]...

```



```
{AVG_DAILY_TEMP; NEM; Resp; GPP; PoverR; PH_avg}]
Answers = [AVG_DAILY_TEMP; NEM; Resp; GPP; PoverR; PH_avg]
```

```
%-----
```

```
%Plot R, NEM, GPP
figure
```

```
%R
subplot(3,1,1); area(TIME_stamp,R); datetick('x',16);
grid on;
ylabel('R (g O2/m2/d)');
```

```
%Give graph title
title({NAME ;'Ecosystem metabolism'});
```

```
%NEM
subplot(3,1,2); area(TIME_stamp,CR_area); datetick('x',16);
grid on;
ylabel('NEM (g O2/m2/d)');
```

```
%GPP
subplot(3,1,3); area(TIME_stamp, PP); datetick('x',16);
grid on;
ylabel('GPP (g O2/m2/d)');
```

```
%Label axes
xlabel('Time');
```

```
%-----
```

```
%Plot DO, DO Sat & Temp
figure
```

```
%DO
plot(TIME_trim,DOPPM_trim, 'r');
H1 = gca;
hold on;
```

```
%DO Sat & Temp
[A2,H2,H3] = plotyy(TIME_trim,DO_SAT,TIME_trim,TEMP_trim);
```

```
%Manipulate Axes and Plot
F = title({NAME ;'Dissolved oxygen'});
linkaxes(A2, 'x');
xlabel('Time');
```

```
set(A2(2),'xtick',[]);
datetick(A2(1),'x',16);
set(A2(2),'ylim', [5 25], 'ytick', 5:5:25);
set(A2(1),'ylim', [0 15], 'ytick', 0:5:15);
ylabel(A2(1),'DO (mg/L)');
ylabel(A2(2),'Temperature (\circC)');
legend('DO','DO Sat','Temperature','Location', 'Best');
axpos = get(gca,'pos');
extent = get(F,'extent');
set(gca,'pos',[axpos(1) axpos(2) axpos(3) axpos(4)-.02*extent(4)]);
hold off;
```

## K.10 NEM: SEPTEMBER 2010, DOWNSTREAM

```
%Luke Wildfire
%NEM_calculations
%
%10/2/2013

%Clean up
clear all
clc
close all

%-----

%Import csv file (I'll be working with DO data that has ppm - not %
[num txt] = xlsread('D1_downstream.xls');

%-----

%ENTER VARIABLES SPECIFIC TO EACH RUN

%Give run a name
NAME = 'September: Downstream';
%Stream Velocity in (cm/s)
V = .5677;
%Stream Height in (cm)
H = 2;

%-----

%Define dates and times

%12:20pm (20 past noon) on first day of measurement
RoughStartTime = datenum('September 25, 2010 12:20:00000 PM');
%12:20pm (half past noon) on next day of measurement
RoughEndTime = datenum('September 26, 2010 12:20:00000 PM');
%Sunset on first day of measurement
SUNSET = datenum('September 25, 2010 6:56:00.000 PM');
%Sunrise on next day of measurement
SUNRISE = datenum('September 26, 2010 6:54:00.000 AM');

%-----

%Give each variable a name and then smooth
%Graph all variables on one plot vs time
```

```

%TIME is originally (mm/dd/yyyy h:mm:ss PM)
TIME = txt((2:end),1);
%Convert TIME to a number
TIME = datenum(TIME);
%Smooth the data
TIME = smooth(TIME, 25, 'rloess');

%Pressure (kPa)
BARO = num(:,1);
BARO = smooth(BARO, 25, 'rloess');
subplot(2,3,1); plot(TIME,BARO); datetick('x',16); axis tight;
xlabel('Pressure (kPa)');

%Conductance and Specific Conductance (uS/cm)
COND = num(:,2);
COND = smooth(COND, 25, 'rloess');
subplot(2,3,2); plot(TIME,COND); datetick('x',16); axis tight;
xlabel('Conductivity (uS/cm)');
title({NAME ;'All data (untrimmed)'});

SPECCOND = num(:,3);
SPECCOND = smooth(SPECCOND, 25, 'rloess');
subplot(2,3,3); plot(TIME,SPECCOND); datetick('x',16); axis tight;
xlabel('Specific Conductance (uS/cm)');

%Dissolved Oxygen (mg/L, ppm, or g/m^3)
DOPPM = num(:,4);
DOPPM = smooth(DOPPM, 25, 'rloess');
subplot(2,3,4); plot(TIME,DOPPM); datetick('x',16); axis tight;
xlabel('DO (ppm)');

%pH
PH = num(:,5);
PH = smooth(PH, 25, 'rloess');
subplot(2,3,5);plot(TIME,PH); datetick('x',16); axis tight;
xlabel('pH');

%Temperature (deg C)
TEMP = num(:,6);
TEMP = smooth(TEMP, 25, 'rloess');
subplot(2,3,6);plot(TIME,TEMP);datetick('x',16); axis tight;
xlabel('Temperature (deg. C)');

%-----

%Determine time step, and adjust the RoughEndTime up one time step

```

```

TIME_STEP = TIME(2)-TIME(1);
RoughEndTime = RoughEndTime + TIME_STEP;

%-----

%Trim all data to appropriate time frame
%Graph each variable as before

%Create a new figure
figure('Position',[300,300,800,500]);

%Time
TIME_trim1 = TIME(RoughStartTime<TIME);
TIME_trim = TIME_trim1(TIME_trim1<RoughEndTime);
N = length(TIME_trim);
disp(['The number of time increments is: ' num2str(N)]);

%Pressure (kPa)
BARO_trim1 = BARO(RoughStartTime<TIME);
BARO_trim = BARO_trim1(TIME_trim1<RoughEndTime);
subplot(2,3,1); plot(TIME_trim,BARO_trim);
datetick('x','HH');
xlim([RoughStartTime-.05 RoughEndTime+.05]);
xlabel('Time of day (hr)');
ylabel('Pressure (kPa)');
vline([SUNSET SUNRISE]);

%Conductance and Specific Conductance (uS/cm)
COND_trim1 = COND(RoughStartTime<TIME);
COND_trim = COND_trim1(TIME_trim1<RoughEndTime);
subplot(2,3,2); plot(TIME_trim,COND_trim);
datetick('x','HH');
xlim([RoughStartTime-.05 RoughEndTime+.05]);
xlabel('Time of day (hr)');
ylabel('Conductivity (uS/cm)');
vline([SUNSET SUNRISE]);
title({'NAME ;'All data (trimmed)'});

SPECCOND_trim1 = SPECCOND(RoughStartTime<TIME);
SPECCOND_trim = SPECCOND_trim1(TIME_trim1<RoughEndTime);
subplot(2,3,3); plot(TIME_trim,SPECCOND_trim);
datetick('x','HH');
xlim([RoughStartTime-.05 RoughEndTime+.05]);
xlabel('Time of day (hr)');
ylabel('Specific Conductance (uS/cm)');
vline([SUNSET SUNRISE]);

```

```

%Dissolved Oxygen (mg/L, ppm, or g/m^3)
DOPPM_trim1 = DOPPM(RoughStartTime<TIME);
DOPPM_trim = DOPPM_trim1(TIME_trim1<RoughEndTime);
subplot(2,3,4); plot(TIME_trim,DOPPM_trim);
datetick('x','HH');
xlim([RoughStartTime-.05 RoughEndTime+.05]);
xlabel('Time of day (hr)');
ylabel('DO (ppm)');
vline([SUNSET SUNRISE]);

```

```

%pH
PH_trim1 = PH(RoughStartTime<TIME);
PH_trim = PH_trim1(TIME_trim1<RoughEndTime);
subplot(2,3,5);plot(TIME_trim,PH_trim);
datetick('x','HH');
xlim([RoughStartTime-.05 RoughEndTime+.05]);
xlabel('Time of day (hr)');
ylabel('pH');
vline([SUNSET SUNRISE]);

```

```

%Temperature (deg C)
TEMP_trim1 = TEMP(RoughStartTime<TIME);
TEMP_trim = TEMP_trim1(TIME_trim1<RoughEndTime);
subplot(2,3,6);plot(TIME_trim,TEMP_trim);
datetick('x','HH');
xlim([RoughStartTime-.05 RoughEndTime+.05]);
xlabel('Time of day (hr)');
ylabel('Temperature (deg. C)');
vline([SUNSET SUNRISE]);

```

```

%-----

```

```

%Create a vector of time-stamps as the midpoint of each sampling time
%aka Column "D"

```

```

for i=1:(N-1)
    TIME_stamp(i) = (TIME_trim(i) + TIME_trim(i+1))./2;
end
TIME_stamp = TIME_stamp';

```

```

%-----

```

```

%Calculate a vector of Delta DO (column "E")

```

```

for i=1:(N-1)

```

```

    DELTA_DO(i) = (DOPPM_trim(i+1)-DOPPM_trim(i));
end
DELTA_DO = DELTA_DO';

%-----

%Calculate DO Saturation concentration (mg/L)
%Column "F"

%convert temperature to Kelvin
TEMP_Kelvin = TEMP_trim+273.15;

%Use this code to determine DO sat (mg/L)
vp1 = -139.34411;
vp2 = 1.575701e5;
vp3 = -6.642308e7;
vp4 = 1.2438e10;
vp5 = -8.621949e11;
lndo =
vp1+vp2./TEMP_Kelvin+vp3./TEMP_Kelvin.^2+vp4./TEMP_Kelvin.^3+vp5./TEMP_Kelvin.^
4;
DO_SAT = exp(lndo);

%-----

%Correct DO_SAT for altitude (mg/L)
%Column "G"

DO_SAT = .989*DO_SAT;

%-----

%Calculate Oxygen Surplus/Deficit (mg/L)
%Column "H"

DO_DEFICIT = DOPPM_trim - DO_SAT;

%-----

%Calculate K constant
%Column "J"

%First calculate K at 20 deg C (1/hr)
K20 = 50.8 * (V^.67)*(H^-1.85);

%Adjust K for the number of timesteps in 1 day

```

```

K20 = (K20*24)/(N-1);

%Adjust K for temperature
K_Adjust = K20.*(1.024.^(TEMP_trim-20));

%-----

%Calculate gas exchagng per time step (mg/L/TIME_STEP)
%Column "K"

GAS_EXCHANGE = K_Adjust.*DO_DEFICIT;

%-----

%Calculate avg gas exchange per time stamp (mg/L/TIME_STEP)
%Column "L"

for i=1:(N-1)
    AVG_GXCH(i) = (GAS_EXCHANGE(i) + GAS_EXCHANGE(i+1))./2;
end
AVG_GXCH = AVG_GXCH';

%-----

%Calculate corrected reparation (mg/L/Time_step)
%Column "M"

CR = AVG_GXCH+DELTA_DO;

%-----

%Find areal reparation rate (g/m^2/Time_step)
%Column "N"

CR_area = CR.*(H/100);

%-----

%Determine Night-Time hours
TIME_night1 = TIME_stamp(TIME_stamp>SUNSET);
TIME_night = TIME_night1(TIME_night1<SUNRISE);

%Calculate nighttime respiration
R_Night1 = CR_area(TIME_stamp>SUNSET);
R_Night = R_Night1(TIME_night1<SUNRISE);
R_AVG = mean(R_Night);

```



```

%Substitute Night-time average of R for daily CR
R = CR_area;
for i=1:(N-1)
    for j=1:(length(TIME_night))
        if TIME_stamp(i) == TIME_night(j)
            R(i) = CR_area(i);
            break
        else
            R(i)=R_AVG;
        end
    end
end
end

%-----

%Determine PP
for i=1:(N-1)
    PP(i) = CR_area(i)-R(i);
    if PP(i)<0
        PP(i)=0;
    end
end
PP = PP';

%-----

%Calculate Average Daily Temperature
TEMP_day1 = TEMP_trim(TIME_trim<SUNSET);
TEMP_day2 = TEMP_trim(TIME_trim>SUNRISE);
TEMP_day = [TEMP_day1; TEMP_day2];
AVG_DAILY_TEMP = mean(TEMP_day);

%-----

%Calculate average pH
PH_avg = mean(PH_trim);

%-----

%Calculate NEM (g/m^2/d)
NEM = sum(CR_area);
Resp = sum(R);
GPP = sum(PP);
PoverR = abs(GPP/Resp);
OUTPUT = [{'AVG_DAILY_TEMP'; 'NEM'; 'Resp'; 'GPP'; 'P/R'; 'Avg pH'}]...

```

```
{AVG_DAILY_TEMP; NEM; Resp; GPP; PoverR; PH_avg}]
Answers = [AVG_DAILY_TEMP; NEM; Resp; GPP; PoverR; PH_avg]
```

```
%-----
```

```
%Plot R, NEM, GPP
figure
```

```
%R
subplot(3,1,1); area(TIME_stamp,R); datetick('x',16);
grid on;
ylabel('R (g O2/m2/d)');
```

```
%Give graph title
title({NAME ;'Ecosystem metabolism'});
```

```
%NEM
subplot(3,1,2); area(TIME_stamp,CR_area); datetick('x',16);
grid on;
ylabel('NEM (g O2/m2/d)');
```

```
%GPP
subplot(3,1,3); area(TIME_stamp, PP); datetick('x',16);
grid on;
ylabel('GPP (g O2/m2/d)');
```

```
%Label axes
xlabel('Time');
```

```
%-----
```

```
%Plot DO, DO Sat & Temp
figure
```

```
%DO
plot(TIME_trim,DOPPM_trim, 'r');
H1 = gca;
hold on;
```

```
%DO Sat & Temp
[A2,H2,H3] = plotyy(TIME_trim,DO_SAT,TIME_trim,TEMP_trim);
```

```
%Manipulate Axes and Plot
F = title({NAME ;'Dissolved oxygen'});
linkaxes(A2, 'x');
xlabel('Time');
```

```
set(A2(2),'xtick',[]);
datetick(A2(1),'x',16);
set(A2(2),'ylim', [5 25], 'ytick', 5:5:25);
set(A2(1),'ylim', [0 15], 'ytick', 0:5:15);
ylabel(A2(1),'DO (mg/L)');
ylabel(A2(2),'Temperature (\circC)');
legend('DO','DO Sat','Temperature','Location', 'Best');
axpos = get(gca,'pos');
extent = get(F,'extent');
set(gca,'pos',[axpos(1) axpos(2) axpos(3) axpos(4)-.02*extent(4)]);
hold off;
```

## K.11 NEM: NOVEMBER 2010, UPSTREAM

```
%Luke Wildfire
%NEM_calculations
%
%10/2/2013

%Clean up
clear all
clc
close all

%-----

%Import csv file (I'll be working with DO data that has ppm - not %
[num txt] = xlsread('D2_upstream.xls');

%-----

%ENTER VARIABLES SPECIFIC TO EACH RUN

%Give run a name
NAME = 'November: Upstream';
%Stream Velocity in (cm/s)
V = .5923;
%Stream Height in (cm)
H = 5.4333;

%-----

%Define dates and times

%12:20pm (20 past noon) on first day of measurement
RoughStartTime = datenum('November 20, 2010 12:20:00000 PM');
%12:20pm (half past noon) on next day of measurement
RoughEndTime = datenum('November 21, 2010 12:20:00000 PM');
%Sunset on first day of measurement
SUNSET = datenum('November 20, 2010 4:44:00.000 PM');
%Sunrise on next day of measurement
SUNRISE = datenum('November 21, 2010 6:54:00.000 AM');

%-----

%Give each variable a name and then smooth
%Graph all variables on one plot vs time
```

```

%TIME is originally (mm/dd/yyyy h:mm:ss PM)
TIME = txt((2:end),1);
%Convert TIME to a number
TIME = datenum(TIME);
%Smooth the data
TIME = smooth(TIME, 25, 'rloess');

%Pressure (kPa)
BARO = num(:,1);
BARO = smooth(BARO, 25, 'rloess');
subplot(2,3,1); plot(TIME,BARO); datetick('x',16); axis tight;
xlabel('Pressure (kPa)');

%Conductance and Specific Conductance (uS/cm)
COND = num(:,2);
COND = smooth(COND, 25, 'rloess');
subplot(2,3,2); plot(TIME,COND); datetick('x',16); axis tight;
xlabel('Conductivity (uS/cm)');
title({NAME ;'All data (untrimmed)'});

SPECCOND = num(:,3);
SPECCOND = smooth(SPECCOND, 25, 'rloess');
subplot(2,3,3); plot(TIME,SPECCOND); datetick('x',16); axis tight;
xlabel('Specific Conductance (uS/cm)');

%Dissolved Oxygen (mg/L, ppm, or g/m^3)
DOPPM = num(:,4);
DOPPM = smooth(DOPPM, 25, 'rloess');
subplot(2,3,4); plot(TIME,DOPPM); datetick('x',16); axis tight;
xlabel('DO (ppm)');

%pH
PH = num(:,5);
PH = smooth(PH, 25, 'rloess');
subplot(2,3,5);plot(TIME,PH); datetick('x',16); axis tight;
xlabel('pH');

%Temperature (deg C)
TEMP = num(:,6);
TEMP = smooth(TEMP, 25, 'rloess');
subplot(2,3,6);plot(TIME,TEMP);datetick('x',16); axis tight;
xlabel('Temperature (deg. C)');

%-----

%Determine time step, and adjust the RoughEndTime up one time step

```

```

TIME_STEP = TIME(2)-TIME(1);
RoughEndTime = RoughEndTime + TIME_STEP;

%-----

%Trim all data to appropriate time frame
%Graph each variable as before

%Create a new figure
figure('Position',[300,300,800,500]);

%Time
TIME_trim1 = TIME(RoughStartTime<TIME);
TIME_trim = TIME_trim1(TIME_trim1<RoughEndTime);
N = length(TIME_trim);
disp(['The number of time increments is: ' num2str(N)]);

%Pressure (kPa)
BARO_trim1 = BARO(RoughStartTime<TIME);
BARO_trim = BARO_trim1(TIME_trim1<RoughEndTime);
subplot(2,3,1); plot(TIME_trim,BARO_trim);
datetick('x','HH');
xlim([RoughStartTime-.05 RoughEndTime+.05]);
xlabel('Time of day (hr)');
ylabel('Pressure (kPa)');
vline([SUNSET SUNRISE]);

%Conductance and Specific Conductance (uS/cm)
COND_trim1 = COND(RoughStartTime<TIME);
COND_trim = COND_trim1(TIME_trim1<RoughEndTime);
subplot(2,3,2); plot(TIME_trim,COND_trim);
datetick('x','HH');
xlim([RoughStartTime-.05 RoughEndTime+.05]);
xlabel('Time of day (hr)');
ylabel('Conductivity (uS/cm)');
vline([SUNSET SUNRISE]);
title({'NAME ';'All data (trimmed)'});

SPECCOND_trim1 = SPECCOND(RoughStartTime<TIME);
SPECCOND_trim = SPECCOND_trim1(TIME_trim1<RoughEndTime);
subplot(2,3,3); plot(TIME_trim,SPECCOND_trim);
datetick('x','HH');
xlim([RoughStartTime-.05 RoughEndTime+.05]);
xlabel('Time of day (hr)');
ylabel('Specific Conductance (uS/cm)');
vline([SUNSET SUNRISE]);

```

```

%Dissolved Oxygen (mg/L, ppm, or g/m^3)
DOPPM_trim1 = DOPPM(RoughStartTime<TIME);
DOPPM_trim = DOPPM_trim1(TIME_trim1<RoughEndTime);
subplot(2,3,4); plot(TIME_trim,DOPPM_trim);
datetick('x','HH');
xlim([RoughStartTime-.05 RoughEndTime+.05]);
xlabel('Time of day (hr)');
ylabel('DO (ppm)');
vline([SUNSET SUNRISE]);

```

```

%pH
PH_trim1 = PH(RoughStartTime<TIME);
PH_trim = PH_trim1(TIME_trim1<RoughEndTime);
subplot(2,3,5);plot(TIME_trim,PH_trim);
datetick('x','HH');
xlim([RoughStartTime-.05 RoughEndTime+.05]);
xlabel('Time of day (hr)');
ylabel('pH');
vline([SUNSET SUNRISE]);

```

```

%Temperature (deg C)
TEMP_trim1 = TEMP(RoughStartTime<TIME);
TEMP_trim = TEMP_trim1(TIME_trim1<RoughEndTime);
subplot(2,3,6);plot(TIME_trim,TEMP_trim);
datetick('x','HH');
xlim([RoughStartTime-.05 RoughEndTime+.05]);
xlabel('Time of day (hr)');
ylabel('Temperature (deg. C)');
vline([SUNSET SUNRISE]);

```

```

%-----

```

```

%Create a vector of time-stamps as the midpoint of each sampling time
%aka Column "D"

```

```

for i=1:(N-1)
    TIME_stamp(i) = (TIME_trim(i) + TIME_trim(i+1))./2;
end
TIME_stamp = TIME_stamp';

```

```

%-----

```

```

%Calculate a vector of Delta DO (column "E")

```

```

for i=1:(N-1)

```

```

    DELTA_DO(i) = (DOPPM_trim(i+1)-DOPPM_trim(i));
end
DELTA_DO = DELTA_DO';

%-----

%Calculate DO Saturation concentration (mg/L)
%Column "F"

%convert temperature to Kelvin
TEMP_Kelvin = TEMP_trim+273.15;

%Use this code to determine DO sat (mg/L)
vp1 = -139.34411;
vp2 = 1.575701e5;
vp3 = -6.642308e7;
vp4 = 1.2438e10;
vp5 = -8.621949e11;
lnDO =
vp1+vp2./TEMP_Kelvin+vp3./TEMP_Kelvin.^2+vp4./TEMP_Kelvin.^3+vp5./TEMP_Kelvin.^
4;
DO_SAT = exp(lnDO);

%-----

%Correct DO_SAT for altitude (mg/L)
%Column "G"

DO_SAT = .989*DO_SAT;

%-----

%Calculate Oxygen Surplus/Deficit (mg/L)
%Column "H"

DO_DEFICIT = DOPPM_trim - DO_SAT;

%-----

%Calculate K constant
%Column "J"

%First calculate K at 20 deg C (1/hr)
K20 = 50.8 * (V^.67)*(H^-1.85);

%Adjust K for the number of timesteps in 1 day

```



```

K20 = (K20*24)/(N-1);

%Adjust K for temperature
K_Adjust = K20.*(1.024.^(TEMP_trim-20));

%-----

%Calculate gas exchagng per time step (mg/L/TIME_STEP)
%Column "K"

GAS_EXCHANGE = K_Adjust.*DO_DEFICIT;

%-----

%Calculate avg gas exchange per time stamp (mg/L/TIME_STEP)
%Column "L"

for i=1:(N-1)
    AVG_GXCH(i) = (GAS_EXCHANGE(i) + GAS_EXCHANGE(i+1))./2;
end
AVG_GXCH = AVG_GXCH';

%-----

%Calculate corrected reparation (mg/L/Time_step)
%Column "M"

CR = AVG_GXCH+DELTA_DO;

%-----

%Find areal reparation rate (g/m^2/Time_step)
%Column "N"

CR_area = CR.*(H/100);

%-----

%Determine Night-Time hours
TIME_night1 = TIME_stamp(TIME_stamp>SUNSET);
TIME_night = TIME_night1(TIME_night1<SUNRISE);

%Calculate nighttime respiration
R_Night1 = CR_area(TIME_stamp>SUNSET);
R_Night = R_Night1(TIME_night1<SUNRISE);
R_AVG = mean(R_Night);

```

```

%Substitute Night-time average of R for daily CR
R = CR_area;
for i=1:(N-1)
    for j=1:(length(TIME_night))
        if TIME_stamp(i) == TIME_night(j)
            R(i) = CR_area(i);
            break
        else
            R(i)=R_AVG;
        end
    end
end
end

%-----

%Determine PP
for i=1:(N-1)
    PP(i) = CR_area(i)-R(i);
    if PP(i)<0
        PP(i)=0;
    end
end
end
PP = PP';

%-----

%Calculate Average Daily Temperature
TEMP_day1 = TEMP_trim(TIME_trim<SUNSET);
TEMP_day2 = TEMP_trim(TIME_trim>SUNRISE);
TEMP_day = [TEMP_day1; TEMP_day2];
AVG_DAILY_TEMP = mean(TEMP_day);

%-----

%Calculate average pH
PH_avg = mean(PH_trim);

%-----

%Calculate NEM (g/m^2/d)
NEM = sum(CR_area);
Resp = sum(R);
GPP = sum(PP);
PoverR = abs(GPP/Resp);
OUTPUT = [{'AVG_DAILY_TEMP'; 'NEM'; 'Resp'; 'GPP'; 'P/R'; 'Avg pH'}]...

```

```
{AVG_DAILY_TEMP; NEM; Resp; GPP; PoverR; PH_avg}]
Answers = [AVG_DAILY_TEMP; NEM; Resp; GPP; PoverR; PH_avg]
```

```
%-----
```

```
%Plot R, NEM, GPP
figure
```

```
%R
subplot(3,1,1); area(TIME_stamp,R); datetick('x',16);
grid on;
ylabel('R (g O2/m2/d)');
```

```
%Give graph title
title({NAME ;'Ecosystem metabolism'});
```

```
%NEM
subplot(3,1,2); area(TIME_stamp,CR_area); datetick('x',16);
grid on;
ylabel('NEM (g O2/m2/d)');
```

```
%GPP
subplot(3,1,3); area(TIME_stamp, PP); datetick('x',16);
grid on;
ylabel('GPP (g O2/m2/d)');
```

```
%Label axes
xlabel('Time');
```

```
%-----
```

```
%Plot DO, DO Sat & Temp
figure
```

```
%DO
plot(TIME_trim,DOPPM_trim, 'r');
H1 = gca;
hold on;
```

```
%DO Sat & Temp
[A2,H2,H3] = plotyy(TIME_trim,DO_SAT,TIME_trim,TEMP_trim);
```

```
%Manipulate Axes and Plot
F = title({NAME ;'Dissolved oxygen'});
linkaxes(A2, 'x');
xlabel('Time');
```

```
set(A2(2),'xtick',[]);
datetick(A2(1),'x',16);
set(A2(2),'ylim', [5 25], 'ytick', 5:5:25);
set(A2(1),'ylim', [0 15], 'ytick', 0:5:15);
ylabel(A2(1),'DO (mg/L)');
ylabel(A2(2),'Temperature (\circC)');
legend('DO','DO Sat','Temperature','Location', 'Best');
axpos = get(gca,'pos');
extent = get(F,'extent');
set(gca,'pos',[axpos(1) axpos(2) axpos(3) axpos(4)-.02*extent(4)]);
hold off;
```

## K.12 NEM: NOVEMBER 2010, DOWNSTREAM

```
%Luke Wildfire
%NEM_calculations
%
%10/2/2013

%Clean up
clear all
clc
close all

%-----

%Import csv file (I'll be working with DO data that has ppm - not %
[num txt] = xlsread('D2_downstream.xls');

%-----

%ENTER VARIABLES SPECIFIC TO EACH RUN

%Give run a name
NAME = 'November: Downstream';
%Stream Velocity in (cm/s)
V = 1.1594;
%Stream Height in (cm)
H = 11.852;

%-----

%Define dates and times

%12:20pm (20 past noon) on first day of measurement
RoughStartTime = datenum('November 20, 2010 12:20:00000 PM');
%12:20pm (half past noon) on next day of measurement
RoughEndTime = datenum('November 21, 2010 12:20:00000 PM');
%Sunset on first day of measurement
SUNSET = datenum('November 20, 2010 4:44:00.000 PM');
%Sunrise on next day of measurement
SUNRISE = datenum('November 21, 2010 6:54:00.000 AM');

%-----

%Give each variable a name and then smooth
%Graph all variables on one plot vs time
```

```

%TIME is originally (mm/dd/yyyy h:mm:ss PM)
TIME = txt((2:end),1);
%Convert TIME to a number
TIME = datenum(TIME);
%Smooth the data
TIME = smooth(TIME, 25, 'rloess');

%Pressure (kPa)
BARO = num(:,1);
BARO = smooth(BARO, 25, 'rloess');
subplot(2,3,1); plot(TIME,BARO); datetick('x',16); axis tight;
xlabel('Pressure (kPa)');

%Conductance and Specific Conductance (uS/cm)
COND = num(:,2);
COND = smooth(COND, 25, 'rloess');
subplot(2,3,2); plot(TIME,COND); datetick('x',16); axis tight;
xlabel('Conductivity (uS/cm)');
title({NAME ;'All data (untrimmed)'});

SPECCOND = num(:,3);
SPECCOND = smooth(SPECCOND, 25, 'rloess');
subplot(2,3,3); plot(TIME,SPECCOND); datetick('x',16); axis tight;
xlabel('Specific Conductance (uS/cm)');

%Dissolved Oxygen (mg/L, ppm, or g/m^3)
DOPPM = num(:,4);
DOPPM = smooth(DOPPM, 25, 'rloess');
subplot(2,3,4); plot(TIME,DOPPM); datetick('x',16); axis tight;
xlabel('DO (ppm)');

%pH
PH = num(:,5);
PH = smooth(PH, 25, 'rloess');
subplot(2,3,5);plot(TIME,PH); datetick('x',16); axis tight;
xlabel('pH');

%Temperature (deg C)
TEMP = num(:,6);
TEMP = smooth(TEMP, 25, 'rloess');
subplot(2,3,6);plot(TIME,TEMP);datetick('x',16); axis tight;
xlabel('Temperature (deg. C)');

%-----

%Determine time step, and adjust the RoughEndTime up one time step

```

```

TIME_STEP = TIME(2)-TIME(1);
RoughEndTime = RoughEndTime + TIME_STEP;

%-----

%Trim all data to appropriate time frame
%Graph each variable as before

%Create a new figure
figure('Position',[300,300,800,500]);

%Time
TIME_trim1 = TIME(RoughStartTime<TIME);
TIME_trim = TIME_trim1(TIME_trim1<RoughEndTime);
N = length(TIME_trim);
disp(['The number of time increments is: ' num2str(N)]);

%Pressure (kPa)
BARO_trim1 = BARO(RoughStartTime<TIME);
BARO_trim = BARO_trim1(TIME_trim1<RoughEndTime);
subplot(2,3,1); plot(TIME_trim,BARO_trim);
datetick('x','HH');
xlim([RoughStartTime-.05 RoughEndTime+.05]);
xlabel('Time of day (hr)');
ylabel('Pressure (kPa)');
vline([SUNSET SUNRISE]);

%Conductance and Specific Conductance (uS/cm)
COND_trim1 = COND(RoughStartTime<TIME);
COND_trim = COND_trim1(TIME_trim1<RoughEndTime);
subplot(2,3,2); plot(TIME_trim,COND_trim);
datetick('x','HH');
xlim([RoughStartTime-.05 RoughEndTime+.05]);
xlabel('Time of day (hr)');
ylabel('Conductivity (uS/cm)');
vline([SUNSET SUNRISE]);
title({'NAME ';'All data (trimmed)'});

SPECCOND_trim1 = SPECCOND(RoughStartTime<TIME);
SPECCOND_trim = SPECCOND_trim1(TIME_trim1<RoughEndTime);
subplot(2,3,3); plot(TIME_trim,SPECCOND_trim);
datetick('x','HH');
xlim([RoughStartTime-.05 RoughEndTime+.05]);
xlabel('Time of day (hr)');
ylabel('Specific Conductance (uS/cm)');
vline([SUNSET SUNRISE]);

```

```

%Dissolved Oxygen (mg/L, ppm, or g/m^3)
DOPPM_trim1 = DOPPM(RoughStartTime<TIME);
DOPPM_trim = DOPPM_trim1(TIME_trim1<RoughEndTime);
subplot(2,3,4); plot(TIME_trim,DOPPM_trim);
datetick('x','HH');
xlim([RoughStartTime-.05 RoughEndTime+.05]);
xlabel('Time of day (hr)');
ylabel('DO (ppm)');
vline([SUNSET SUNRISE]);

```

```

%pH
PH_trim1 = PH(RoughStartTime<TIME);
PH_trim = PH_trim1(TIME_trim1<RoughEndTime);
subplot(2,3,5);plot(TIME_trim,PH_trim);
datetick('x','HH');
xlim([RoughStartTime-.05 RoughEndTime+.05]);
xlabel('Time of day (hr)');
ylabel('pH');
vline([SUNSET SUNRISE]);

```

```

%Temperature (deg C)
TEMP_trim1 = TEMP(RoughStartTime<TIME);
TEMP_trim = TEMP_trim1(TIME_trim1<RoughEndTime);
subplot(2,3,6);plot(TIME_trim,TEMP_trim);
datetick('x','HH');
xlim([RoughStartTime-.05 RoughEndTime+.05]);
xlabel('Time of day (hr)');
ylabel('Temperature (deg. C)');
vline([SUNSET SUNRISE]);

```

```

%-----

```

```

%Create a vector of time-stamps as the midpoint of each sampling time
%aka Column "D"

```

```

for i=1:(N-1)
    TIME_stamp(i) = (TIME_trim(i) + TIME_trim(i+1))./2;
end
TIME_stamp = TIME_stamp';

```

```

%-----

```

```

%Calculate a vector of Delta DO (column "E")

```

```

for i=1:(N-1)

```



```

    DELTA_DO(i) = (DOPPM_trim(i+1)-DOPPM_trim(i));
end
DELTA_DO = DELTA_DO';

%-----

%Calculate DO Saturation concentration (mg/L)
%Column "F"

%convert temperature to Kelvin
TEMP_Kelvin = TEMP_trim+273.15;

%Use this code to determine DO sat (mg/L)
vp1 = -139.34411;
vp2 = 1.575701e5;
vp3 = -6.642308e7;
vp4 = 1.2438e10;
vp5 = -8.621949e11;
lndo =
vp1+vp2./TEMP_Kelvin+vp3./TEMP_Kelvin.^2+vp4./TEMP_Kelvin.^3+vp5./TEMP_Kelvin.^
4;
DO_SAT = exp(lndo);

%-----

%Correct DO_SAT for altitude (mg/L)
%Column "G"

DO_SAT = .989*DO_SAT;

%-----

%Calculate Oxygen Surplus/Deficit (mg/L)
%Column "H"

DO_DEFICIT = DOPPM_trim - DO_SAT;

%-----

%Calculate K constant
%Column "J"

%First calculate K at 20 deg C (1/hr)
K20 = 50.8 * (V^.67)*(H^-1.85);

%Adjust K for the number of timesteps in 1 day

```

```

K20 = (K20*24)/(N-1);

%Adjust K for temperature
K_Adjust = K20.*(1.024.^(TEMP_trim-20));

%-----

%Calculate gas exchagng per time step (mg/L/TIME_STEP)
%Column "K"

GAS_EXCHANGE = K_Adjust.*DO_DEFICIT;

%-----

%Calculate avg gas exchange per time stamp (mg/L/TIME_STEP)
%Column "L"

for i=1:(N-1)
    AVG_GXCH(i) = (GAS_EXCHANGE(i) + GAS_EXCHANGE(i+1))./2;
end
AVG_GXCH = AVG_GXCH';

%-----

%Calculate corrected reparation (mg/L/Time_step)
%Column "M"

CR = AVG_GXCH+DELTA_DO;

%-----

%Find areal reparation rate (g/m^2/Time_step)
%Column "N"

CR_area = CR.*(H/100);

%-----

%Determine Night-Time hours
TIME_night1 = TIME_stamp(TIME_stamp>SUNSET);
TIME_night = TIME_night1(TIME_night1<SUNRISE);

%Calculate nighttime respiration
R_Night1 = CR_area(TIME_stamp>SUNSET);
R_Night = R_Night1(TIME_night1<SUNRISE);
R_AVG = mean(R_Night);

```

```

%Substitute Night-time average of R for daily CR
R = CR_area;
for i=1:(N-1)
    for j=1:(length(TIME_night))
        if TIME_stamp(i) == TIME_night(j)
            R(i) = CR_area(i);
            break
        else
            R(i)=R_AVG;
        end
    end
end
end

%-----

%Determine PP
for i=1:(N-1)
    PP(i) = CR_area(i)-R(i);
    if PP(i)<0
        PP(i)=0;
    end
end
end
PP = PP';

%-----

%Calculate Average Daily Temperature
TEMP_day1 = TEMP_trim(TIME_trim<SUNSET);
TEMP_day2 = TEMP_trim(TIME_trim>SUNRISE);
TEMP_day = [TEMP_day1; TEMP_day2];
AVG_DAILY_TEMP = mean(TEMP_day);

%-----

%Calculate average pH
PH_avg = mean(PH_trim);

%-----

%Calculate NEM (g/m^2/d)
NEM = sum(CR_area);
Resp = sum(R);
GPP = sum(PP);
PoverR = abs(GPP/Resp);
OUTPUT = [{'AVG_DAILY_TEMP'; 'NEM'; 'Resp'; 'GPP'; 'P/R'; 'Avg pH'}]...

```

```
{AVG_DAILY_TEMP; NEM; Resp; GPP; PoverR; PH_avg}]
Answers = [AVG_DAILY_TEMP; NEM; Resp; GPP; PoverR; PH_avg]
```

```
%-----
```

```
%Plot R, NEM, GPP
figure
```

```
%R
subplot(3,1,1); area(TIME_stamp,R); datetick('x',16);
grid on;
ylabel('R (g O2/m2/d)');
```

```
%Give graph title
title({NAME ;'Ecosystem metabolism'});
```

```
%NEM
subplot(3,1,2); area(TIME_stamp,CR_area); datetick('x',16);
grid on;
ylabel('NEM (g O2/m2/d)');
```

```
%GPP
subplot(3,1,3); area(TIME_stamp, PP); datetick('x',16);
grid on;
ylabel('GPP (g O2/m2/d)');
```

```
%Label axes
xlabel('Time');
```

```
%-----
```

```
%Plot DO, DO Sat & Temp
figure
```

```
%DO
plot(TIME_trim,DOPPM_trim, 'r');
H1 = gca;
hold on;
```

```
%DO Sat & Temp
[A2,H2,H3] = plotyy(TIME_trim,DO_SAT,TIME_trim,TEMP_trim);
```

```
%Manipulate Axes and Plot
F = title({NAME ;'Dissolved oxygen'});
linkaxes(A2, 'x');
xlabel('Time');
```

```
set(A2(2),'xtick',[]);
datetick(A2(1),'x',16);
set(A2(2),'ylim', [5 25], 'ytick', 5:5:25);
set(A2(1),'ylim', [0 15], 'ytick', 0:5:15);
ylabel(A2(1),'DO (mg/L)');
ylabel(A2(2),'Temperature (\circC)');
legend('DO','DO Sat','Temperature','Location', 'Best');
axpos = get(gca,'pos');
extent = get(F,'extent');
set(gca,'pos',[axpos(1) axpos(2) axpos(3) axpos(4)-.02*extent(4)]);
hold off;
```

## K.13 MULTI-VARIABLE STATISTICAL ANALYSIS

```
%% Code for comparing del boxplots
%Luke Wildfire
%July 31, 2013

%% Initialize workspace
clc
close all
clear all

%% Initialize data

[D1,D1_words] = ...
    xlsread('data_for_stats_sans_springs_and_2nd_stream.xls', 'D1_Sep');
[D2,D2_words] = ...
    xlsread('data_for_stats_sans_springs_and_2nd_stream.xls', 'D2_Nov');
[D3,D3_words] = ...
    xlsread('data_for_stats_sans_springs_and_2nd_stream.xls', 'D3_Apr');
[D4,D4_words] = ...
    xlsread('data_for_stats_sans_springs_and_2nd_stream.xls', 'D4_Jun');
[D5,D5_words] = ...
    xlsread('data_for_stats_sans_springs_and_2nd_stream.xls', 'D5_Aug');
[D6,D6_words] = ...
    xlsread('data_for_stats_sans_springs_and_2nd_stream.xls', 'D6_Feb');

[headers,labels] = ...
    xlsread('data_for_stats_sans_springs_and_2nd_stream.xls', 'header');
months = {'Feb', 'Apr', 'Jun', 'Aug', 'Sep', 'Nov'};
group = [repmat({'Feb'}, length(D6(:,1)), 1);...
        repmat({'Apr'}, length(D3(:,1)), 1);...
        repmat({'Jun'}, length(D4(:,1)), 1);...
        repmat({'Aug'}, length(D5(:,1)), 1);...
        repmat({'Sep'}, length(D1(:,1)), 1);...
        repmat({'Nov'}, length(D2(:,1)), 1)];

[spring_data] = ...
    xlsread('data_for_stats_sans_springs_and_2nd_stream.xls', 'springs');

k = [4 6 8 12 14 17 19 21 22 24 25 29 30 31 43 46 51 53];
ccc = char(8240);
label = {...
    ['DOC (\muM)']...
    ['DIC (\muM)']...
    ['TDN (\muM)']...
    ['BDOC (\muM)']...
}
```

```

['RDOC (\muM)']...
['NH_4^{+} (\muM)']...
['PO_4^{3+} (\muM)']...
['Cl^{-} (\muM)']...
['NO_3^{-} (\muM)']...
['SO_4^{2-} (\muM)']...
['DON (\muM)']...
['\delta^{18}O (' ccc ')']...
['\delta D (' ccc ')']...
['d-excess (' ccc ')']...
['DOC/TDN^{\mu M \mu M}']...
['DOC/DON (\mu M \mu M)']...
['DOC/PO_4^{3+} (\mu M \mu M)']...
['TDN/PO_4^{3+} (\mu M \mu M)']...
};

```

significance =...

```

{'d' 'bc' 'cd' 'ab' 'a' 'ab' ;...
'c' 'c' 'b' 'b' 'a' " ;
'b' 'ab' 'a' 'ab' 'ab' 'c' ;
'b' 'ab' 'a' 'b' 'a' 'b' ;
'd' 'bc' 'cd' 'ab' 'a' 'ab' ;
'b' 'c' 'a' 'a' 'a' 'c' ;
'b' 'bc' 'a' 'a' 'a' 'c' ;
'ab' 'bc' 'c' 'c' 'a' 'a' ;
'abc' 'bc' 'a' 'ab' 'cd' 'd' ;
'a' 'a' 'b' 'b' 'ab' 'a' ;
'b' 'a' 'b' 'b' 'a' 'b' ;
'cd' 'd' 'c' 'b' 'a' 'ab' ;
'c' 'c' 'c' 'b' 'a' 'ab' ;
'bc' 'a' 'b' 'b' 'c' 'bc' ;
'e' 'cd' 'de' 'bc' 'ab' 'a' ;
'c' 'c' 'bc' 'ab' 'abc' 'a' ;
'b' 'a' 'b' 'b' 'ab' 'a' ;
'a' 'a' 'b' 'b' 'b' 'b' };

```

%% Group data

```

for i=1:length(k)
    sublabel(i,1) = label(i);
    x(:,i) = [D6(:,k(i)); D3(:,k(i)); D4(:,k(i)); D5(:,k(i));...
            D1(:,k(i)); D2(:,k(i))];
end

```

%% Percent Change analysis

```

slope_ttl = ones(length(k),6);

```

```
slope_us = ones(length(k),6);
slope_ds = ones(length(k),6);
```

```
for i=1:length(k)
```

```
    c = k(i);
```

```
    D1_x_orig = D1(:,1);
    D1_y_orig = D1(:,c);
    D1_y_total = D1_y_orig(~isnan(D1_y_orig));
    D1_x_total = D1_x_orig(~isnan(D1_y_orig));
    D1_y_upstream = D1_y_total(D1_x_total<227);
    D1_x_upstream = D1_x_total(D1_x_total<227);
    D1_y_downstream = D1_y_total(D1_x_total>227);
    D1_x_downstream = D1_x_total(D1_x_total>227);
```

```
    D2_x_orig = D2(:,1);
    D2_y_orig = D2(:,c);
    D2_y_total = D2_y_orig(~isnan(D2_y_orig));
    D2_x_total = D2_x_orig(~isnan(D2_y_orig));
    D2_y_upstream = D2_y_total(D2_x_total<227);
    D2_x_upstream = D2_x_total(D2_x_total<227);
    D2_y_downstream = D2_y_total(D2_x_total>227);
    D2_x_downstream = D2_x_total(D2_x_total>227);
```

```
    D3_x_orig = D3(:,1);
    D3_y_orig = D3(:,c);
    D3_y_total = D3_y_orig(~isnan(D3_y_orig));
    D3_x_total = D3_x_orig(~isnan(D3_y_orig));
    D3_y_upstream = D3_y_total(D3_x_total<227);
    D3_x_upstream = D3_x_total(D3_x_total<227);
    D3_y_downstream = D3_y_total(D3_x_total>227);
    D3_x_downstream = D3_x_total(D3_x_total>227);
```

```
    D4_x_orig = D4(:,1);
    D4_y_orig = D4(:,c);
    D4_y_total = D4_y_orig(~isnan(D4_y_orig));
    D4_x_total = D4_x_orig(~isnan(D4_y_orig));
    D4_y_upstream = D4_y_total(D4_x_total<227);
    D4_x_upstream = D4_x_total(D4_x_total<227);
    D4_y_downstream = D4_y_total(D4_x_total>227);
    D4_x_downstream = D4_x_total(D4_x_total>227);
```

```
    D5_x_orig = D5(:,1);
    D5_y_orig = D5(:,c);
    D5_y_total = D5_y_orig(~isnan(D5_y_orig));
```



```

D5_x_total = D5_x_orig(~isnan(D5_y_orig));
D5_y_upstream = D5_y_total(D5_x_total<227);
D5_x_upstream = D5_x_total(D5_x_total<227);
D5_y_downstream = D5_y_total(D5_x_total>227);
D5_x_downstream = D5_x_total(D5_x_total>227);

D6_x_orig = D6(:,1);
D6_y_orig = D6(:,c);
D6_y_total = D6_y_orig(~isnan(D6_y_orig));
D6_x_total = D6_x_orig(~isnan(D6_y_orig));
D6_y_upstream = D6_y_total(D6_x_total<227);
D6_x_upstream = D6_x_total(D6_x_total<227);
D6_y_downstream = D6_y_total(D6_x_total>227);
D6_x_downstream = D6_x_total(D6_x_total>227);

%% Total slope
D6_slope_total{i} = polyfit(D6_x_total,D6_y_total,1);
slope_ttl(i,1)= D6_slope_total{i}(1);

D3_slope_total{i} = polyfit(D3_x_total,D3_y_total,1);
slope_ttl(i,2)= D3_slope_total{i}(1);

D4_slope_total{i} = polyfit(D4_x_total,D4_y_total,1);
slope_ttl(i,3)= D4_slope_total{i}(1);

D5_slope_total{i} = polyfit(D5_x_total,D5_y_total,1);
slope_ttl(i,4)= D5_slope_total{i}(1);

D1_slope_total{i} = polyfit(D1_x_total,D1_y_total,1);
slope_ttl(i,5)= D1_slope_total{i}(1);

D2_slope_total{i} = polyfit(D2_x_total,D2_y_total,1);
slope_ttl(i,6)= D2_slope_total{i}(1);

%% Upstream slope

D6_slope_upstream{i} = polyfit(D6_x_upstream,D6_y_upstream,1);
slope_us(i,1)= D6_slope_upstream{i}(1);

D3_slope_upstream{i} = polyfit(D3_x_upstream,D3_y_upstream,1);
slope_us(i,2)= D3_slope_upstream{i}(1);

D4_slope_upstream{i} = polyfit(D4_x_upstream,D4_y_upstream,1);
slope_us(i,3)= D4_slope_upstream{i}(1);

D5_slope_upstream{i} = polyfit(D5_x_upstream,D5_y_upstream,1);

```

```

slope_us(i,4)= D5_slope_upstream{i}(1);

D1_slope_upstream{i} = polyfit(D1_x_upstream,D1_y_upstream,1);
slope_us(i,5)= D1_slope_upstream{i}(1);

D2_slope_upstream{i} = polyfit(D2_x_upstream,D2_y_upstream,1);
slope_us(i,6)= D2_slope_upstream{i}(1);

%% Downstream slope

D6_slope_downstream{i} = polyfit(D6_x_downstream,D6_y_downstream,1);
slope_ds(i,1)= D6_slope_downstream{i}(1);

D3_slope_downstream{i} = polyfit(D3_x_downstream,D3_y_downstream,1);
slope_ds(i,2)= D3_slope_downstream{i}(1);

D4_slope_downstream{i} = polyfit(D4_x_downstream,D4_y_downstream,1);
slope_ds(i,3)= D4_slope_downstream{i}(1);

D5_slope_downstream{i} = polyfit(D5_x_downstream,D5_y_downstream,1);
slope_ds(i,4)= D5_slope_downstream{i}(1);

D1_slope_downstream{i} = polyfit(D1_x_downstream,D1_y_downstream,1);
slope_ds(i,5)= D1_slope_downstream{i}(1);

D2_slope_downstream{i} = polyfit(D2_x_downstream,D2_y_downstream,1);
slope_ds(i,6)= D2_slope_downstream{i}(1);

end

slope_ttl_head =...
    {'Total Slope' 'Feb', 'Apr', 'Jun', 'Aug', 'Sep', 'Nov'};
slope_ttl_summary_data = horzcat(sublabel,num2cell(slope_ttl));
slope_ttl_summary = vertcat(slope_ttl_head, slope_ttl_summary_data);
disp(slope_ttl_summary)

slope_us_head =...
    {'Upstream Slope' 'Feb', 'Apr', 'Jun', 'Aug', 'Sep', 'Nov'};
slope_us_summary_data = horzcat(sublabel,num2cell(slope_us));
slope_us_summary = vertcat(slope_us_head, slope_us_summary_data);
disp(slope_us_summary)

slope_ds_head =...
    {'Downstream Slope' 'Feb', 'Apr', 'Jun', 'Aug', 'Sep', 'Nov'};
slope_ds_summary_data = horzcat(sublabel,num2cell(slope_ds));
slope_ds_summary = vertcat(slope_ds_head, slope_ds_summary_data);

```

```

disp(slope_ds_summary)

slope_ttl
slope_us
slope_ds

%% Test normality using Shapiro-Wilk normality test
O_Norm = ones([length(k),1]);
P_Norm = ones([length(k),1]);
Q_Norm = ones([length(k),1]);
for i=1:length(k)
    [O_Norm(i),P_Norm(i), Q_Norm] = swtest(x(:,i));
end
%Reject null-hypothesis of normality if p<.05
%Accept Normal: O_Norm(i)=0
%Reject Not Normal: O_Norm(i)=1
%% Test for equal variance

%use Barlett if normal O_Norm(i)=0. %Use Levene if not-normal O_Norm(i)=1

P_Vars = ones([length(k),1]);
O_Vars = ones([length(k),1]);

for i=1:length(k)
    if O_Norm(i) == 0
        P_Vars(i) = vartestn(x(:,i),group, 'off');
    else
        P_Vars(i) = vartestn(x(:,1),group, 'off', 'robust');
    end

    %Reject null-hypothesis of equal-variance if p<.05
    %Accept Normal: O_Vars(i)=0
    %Reject Not Normal: O_Vars(i)=1

    if P_Vars(i) < .05
        O_Vars(i) = 1;
    else
        O_Vars(i) = 0;
    end
end
end
%% Run Kruskal Wallis test & Dunn-Sidak multiple comparison test

P_Kruskal = ones([length(k),1]);
O_Kruskal = ones([length(k),1]);

```

```

for i=1:length(k)
    [P_Kruskal(i), table, stats] = kruskalwallis(x(:,i),group, 'off');

    %Reject null-hypothesis of similiar means if p<.05
    %Accept Normal: O_Kruskal(i)=0
    %Reject Not Normal: O_Kruskal(i)=1

    if P_Kruskal(i) < .05
        O_Kruskal(i) = 1;
    else
        O_Kruskal(i) = 0;
    end

    %figure
    [d,m,h] = multcompare(stats,'ctype','dunn-sidak','display','off');
    %to display comparison graph, change 'off' to 'on'.
    %And "uncomment" figure in line-141

    e = ones([length(d(:,1)),1]);
    for j=1:length(d(:,1))
        if (0>d(j,3)) && (0<d(j,5))
            e(j) = 1;
        else
            e(j) = 0;
        end
    end

    d = horzcat(d,e);
    table_heading = {'Group 1','Group2','Lower_CI','Mean Difference',...
        'Upper CI', 'P-Value', 'NoSigDif=1'};
    disp(label(i))
    disp(vertcat(table_heading, num2cell(d)))

    [grpMed] = grpstats(x(:,i),group, {'median'});
    month_num = length(grpMed);

    figure
    boxplot(x(:,i),group)
    title(sublabel(i))
    %ylabel(sublabel(i))

    hold on
    plot([1:month_num],spring_data(:,k(i)), 'mp',...
        'MarkerEdgeColor','k','MarkerFaceColor','c',...
        'MarkerSize',8)

```

```
hold off
```

```
hold on
```

```
plot([1:month_num],grpMed,'co',...  
     'MarkerEdgeColor','k','MarkerFaceColor','m',...  
     'MarkerSize',5)
```

```
hold off
```

```
if max(x(:,i)) > 0  
    YL = get(gca,'ylim');  
    set(gca,'ylim',[YL(1)-0.1*YL(2) 1.35*YL(2)])  
    for t=1:length(stats.gnames)  
        text(t,(1.25*YL(2)),significance(i,t),...  
             'HorizontalAlignment','center')  
    end
```

```
else
```

```
    YL = get(gca,'ylim');  
    set(gca,'ylim',[YL(1) (5/6)*YL(2)])  
    for t=1:length(stats.gnames)  
        text(t,(10/11)*YL(2),significance(i,t),...  
             'HorizontalAlignment','center')  
    end
```

```
end
```

```
lgd = legend('Average value at source/spring','Median monthly value',...  
            'location','SouthOutside',...  
            'orientation','horizontal');  
pos = get(lgd,'position');  
set(lgd, 'FontSize',7)  
set(lgd, 'position',[.5 .04 .04 pos(4)])
```

```
set(gcf, 'PaperUnits', 'inches');  
set(gcf, 'PaperSize', [4 3]);  
set(gcf, 'PaperPositionMode', 'manual');  
set(gcf, 'PaperPosition', [0 0 4 3]);  
set(gcf, 'renderer', 'painters');  
print(gcf, '-dpng', ['Boxplots' num2str(i) '.png']);
```

```
end
```

```
test_summary_head = {'analyte' 'normal=0' 'Equal Variance=0'...  
                    'equal_means=0'};  
test_summary_data = horzcat(sublabel,num2cell(O_Norm),...
```

```
    num2cell(O_Vars),num2cell(O_Kruskal));  
test_summary = vertcat(test_summary_head, test_summary_data);  
disp(test_summary)
```

## K.14 LINEAR REGRESSION, 1 VARIABLE

```
%% Multiple linear regression with 1 variable - no interaction
%Luke Wildfire
%May 28, 2012

%% Initialize workspace
clc
close all
clear all

%% Initialize data

[D1,D1_words] = ...
    xlsread('data_for_stats_sans_springs_and_2nd_stream.xls', 'D1_Sep');
[D2,D2_words] = ...
    xlsread('data_for_stats_sans_springs_and_2nd_stream.xls', 'D2_Nov');
[D3,D3_words] = ...
    xlsread('data_for_stats_sans_springs_and_2nd_stream.xls', 'D3_Apr');
[D4,D4_words] = ...
    xlsread('data_for_stats_sans_springs_and_2nd_stream.xls', 'D4_Jun');
[D5,D5_words] = ...
    xlsread('data_for_stats_sans_springs_and_2nd_stream.xls', 'D5_Aug');
[D6,D6_words] = ...
    xlsread('data_for_stats_sans_springs_and_2nd_stream.xls', 'D6_Feb');

[headers,labels] = ...
    xlsread('data_for_stats_sans_springs_and_2nd_stream.xls', 'header');
months = {'Feb', 'Apr', 'Jun', 'Aug', 'Sep', 'Nov'};
group = [repmat({'Feb'}, length(D6(:,1)), 1);...
        repmat({'Apr'}, length(D3(:,1)), 1);...
        repmat({'Jun'}, length(D4(:,1)), 1);...
        repmat({'Aug'}, length(D5(:,1)), 1);...
        repmat({'Sep'}, length(D1(:,1)), 1);...
        repmat({'Nov'}, length(D2(:,1)), 1)];
k = [4 6 8 12 14 17 19 21 22 24 25 29 30 31 43 46 51 53];

[spring_data] = ...
    xlsread('data_for_stats_sans_springs_and_2nd_stream.xls', 'springs');

%% Group data

for i=1:length(k)
    sublabel(i,1) = labels(k(i));
    x(:,i) = [D6(:,k(i)); D3(:,k(i)); D4(:,k(i)); D5(:,k(i));...
            D1(:,k(i)); D2(:,k(i))];
end
```

```

medians {i} = grpstats(x(:,i),group,'median');
end

%% Intialize regression variables

Q_us_injection = [2.636 1.460 0.953 0.375 0.136 0.357];
temp_us = [6.572 12.226 15.691 19.073 18.229 8.911];
%resp_us = [-3.377 6.264 -19.476 -23.413 -10.692 -5.124];
%season: 0=canopy off; 1= canopy on
canopy = [0 0 1 1 1 0];

%nutrient regression variables
toc_vf_us = [0.000000000 0.004466172 0.000711812 0.000726256...
0.001345525 0.000116833];
labile_C_vf_us = [0 0 0.000902615 0.002851436 0.002728440 0];
nh4n_vf_us = [0.001821126 0.000977208 0.002795510 0.001523611 ...
0.002392224 0.002990127];

whichstats = {'rsquare','adjrsquare','tstat', 'fstat'};
display_label = {'Analyte' 'R-squared' 'Adj R-squared' 'P-value'};

%% Multiple regression of Spring conc

cor_variables = {'Intercept' ; 'Conc. at spring'};

for i=1:length(k)
x_regress = [spring_data(:,k(i))];
regstats_stats {i} = regstats(medians {i},x_regress,...
'linear',whichstats);

mreg_Rsqr{i} = regstats_stats {i}.rsquare;
mreg_adjRsqr{i} = regstats_stats {i}.adjrsquare;
mreg_pvalue{i} = regstats_stats {i}.fstat.pval;
mreg_betas {i} = regstats_stats {i}.tstat.beta;
mreg_pbeta {i} = regstats_stats {i}.tstat.pval;

disp(sublabel{i})
display_title{i} = {sublabel{i} mreg_Rsqr{i} mreg_adjRsqr{i}...
mreg_pvalue{i}};
disp(vertcat(display_label, display_title{i}));

mreg_output{i} = horzcat(cor_variables, num2cell(mreg_betas {i}),...
num2cell(mreg_pbeta {i}));
mreg_head = {'Variable' 'Slope' 'P-value'};
disp(vertcat(mreg_head, mreg_output{i}));
end

```



```
%% Multiple regression of Discharge
```

```
cor_variables = {'Intercept' ; 'Discharge (L/s)'};
```

```
for i=1:length(k)
```

```
    x_regress = [Q_us_injection];
```

```
    regstats_stats{i} = regstats(medians{i},x_regress,...  
        'linear',whichstats);
```

```
    mreg_Rsqr{i} = regstats_stats{i}.rsquare;
```

```
    mreg_adjRsqr{i} = regstats_stats{i}.adjrsquare;
```

```
    mreg_pvalue{i} = regstats_stats{i}.fstat.pval;
```

```
    mreg_betas{i} = regstats_stats{i}.tstat.beta;
```

```
    mreg_pbeta{i} = regstats_stats{i}.tstat.pval;
```

```
    disp(sublabel{i})
```

```
    display_title{i} = {sublabel{i} mreg_Rsqr{i} mreg_adjRsqr{i}...  
        mreg_pvalue{i}};
```

```
    disp(vertcat(display_label, display_title{i}));
```

```
    mreg_output{i} = horzcat(cor_variables, num2cell(mreg_betas{i}),...  
        num2cell(mreg_pbeta{i}));
```

```
    mreg_head = {'Variable' 'Slope' 'P-value'};
```

```
    disp(vertcat(mreg_head, mreg_output{i}));
```

```
end
```

```
%% Multiple regression of Temp
```

```
cor_variables = {'Intercept' ; 'Temp (deg. C)'};
```

```
for i=1:length(k)
```

```
    x_regress = [temp_us];
```

```
    regstats_stats{i} = regstats(medians{i},x_regress,...  
        'linear',whichstats);
```

```
    mreg_Rsqr{i} = regstats_stats{i}.rsquare;
```

```
    mreg_adjRsqr{i} = regstats_stats{i}.adjrsquare;
```

```
    mreg_pvalue{i} = regstats_stats{i}.fstat.pval;
```

```
    mreg_betas{i} = regstats_stats{i}.tstat.beta;
```

```
    mreg_pbeta{i} = regstats_stats{i}.tstat.pval;
```

```
    disp(sublabel{i})
```

```
    display_title{i} = {sublabel{i} mreg_Rsqr{i} mreg_adjRsqr{i}...  
        mreg_pvalue{i}};
```

```
    disp(vertcat(display_label, display_title{i}));
```

```

mreg_output{i} = horzcat(cor_variables, num2cell(mreg_betas{i}),...
    num2cell(mreg_pbeta{i}));
mreg_head = {'Variable' 'Slope' 'P-value'};
disp(vertcat(mreg_head, mreg_output{i}));
end

%% Multiple regression of Canopy

cor_variables = {'Intercept'; 'Canopy (on/off)'};

for i=1:length(k)
    x_regress = [canopy'];
    regstats_stats{i} = regstats(medians{i},x_regress,...
        'linear',whichstats);

    mreg_Rsqr{i} = regstats_stats{i}.rsquare;
    mreg_adjRsqr{i} = regstats_stats{i}.adjrsquare;
    mreg_pvalue{i} = regstats_stats{i}.fstat.pval;
    mreg_betas{i} = regstats_stats{i}.tstat.beta;
    mreg_pbeta{i} = regstats_stats{i}.tstat.pval;

    disp(sublabel{i})
    display_title{i} = {sublabel{i} mreg_Rsqr{i} mreg_adjRsqr{i}...
        mreg_pvalue{i}};
    disp(vertcat(display_label, display_title{i}));

    mreg_output{i} = horzcat(cor_variables, num2cell(mreg_betas{i}),...
        num2cell(mreg_pbeta{i}));
    mreg_head = {'Variable' 'Slope' 'P-value'};
    disp(vertcat(mreg_head, mreg_output{i}));
end

```

## K.15 MULTIPLE LINEAR REGRESSION, 2 VARIABLES

```
%% Multiple linear regression with 2 variables - no interaction
%Luke Wildfire
%May 28, 2012

%% Initialize workspace
clc
close all
clear all

%% Initialize data

[D1,D1_words] = ...
    xlsread('data_for_stats_sans_springs_and_2nd_stream.xls', 'D1_Sep');
[D2,D2_words] = ...
    xlsread('data_for_stats_sans_springs_and_2nd_stream.xls', 'D2_Nov');
[D3,D3_words] = ...
    xlsread('data_for_stats_sans_springs_and_2nd_stream.xls', 'D3_Apr');
[D4,D4_words] = ...
    xlsread('data_for_stats_sans_springs_and_2nd_stream.xls', 'D4_Jun');
[D5,D5_words] = ...
    xlsread('data_for_stats_sans_springs_and_2nd_stream.xls', 'D5_Aug');
[D6,D6_words] = ...
    xlsread('data_for_stats_sans_springs_and_2nd_stream.xls', 'D6_Feb');

[headers,labels] = ...
    xlsread('data_for_stats_sans_springs_and_2nd_stream.xls', 'header');
months = {'Feb', 'Apr', 'Jun', 'Aug', 'Sep', 'Nov'};
group = [repmat({'Feb'}, length(D6(:,1)), 1);...
    repmat({'Apr'}, length(D3(:,1)), 1);...
    repmat({'Jun'}, length(D4(:,1)), 1);...
    repmat({'Aug'}, length(D5(:,1)), 1);...
    repmat({'Sep'}, length(D1(:,1)), 1);...
    repmat({'Nov'}, length(D2(:,1)), 1)];
k = [4 6 8 12 14 17 19 21 22 24 25 29 30 31 43 46 51 53];

[spring_data] = ...
    xlsread('data_for_stats_sans_springs_and_2nd_stream.xls', 'springs');

%% Group data

for i=1:length(k)
    sublabel(i,1) = labels(k(i));
    x(:,i) = [D6(:,k(i)); D3(:,k(i)); D4(:,k(i)); D5(:,k(i));...
        D1(:,k(i)); D2(:,k(i))];
```

```

medians {i} = grpstats(x(:,i),group,'median');
end

%% Intialize regression variables

Q_us_injection = [2.636 1.460 0.953 0.375 0.136 0.357];
temp_us = [6.572 12.226 15.691 19.073 18.229 8.911];
%resp_us = [-3.377 6.264 -19.476 -23.413 -10.692 -5.124];
%season: 0=canopy off; 1= canopy on
canopy = [0 0 1 1 1 0];

%nutrient regression variables
toc_vf_us = [0.000000000 0.004466172 0.000711812 0.000726256...
0.001345525 0.000116833];
labile_C_vf_us = [0 0 0.000902615 0.002851436 0.002728440 0];
nh4n_vf_us = [0.001821126 0.000977208 0.002795510 0.001523611 ...
0.002392224 0.002990127];

whichstats = {'rsquare','adjrsquare','tstat', 'fstat'};
display_label = {'Analyte' 'R-squared' 'Adj R-squared' 'P-value'};

%% Multiple regression of Spring conc, Discharge

cor_variables = {'Intercept' ; 'Conc. at spring';'Discharge (L/s)'};

for i=1:length(k)
x_regress = [spring_data(:,k(i)) Q_us_injection];
regstats_stats {i} = regstats(medians {i},x_regress,...
'linear',whichstats);

mreg_Rsqr{i} = regstats_stats {i}.rsquare;
mreg_adjRsqr{i} = regstats_stats {i}.adjrsquare;
mreg_pvalue{i} = regstats_stats {i}.fstat.pval;
mreg_betas {i} = regstats_stats {i}.tstat.beta;
mreg_pbeta {i} = regstats_stats {i}.tstat.pval;

disp(sublabel{i})
display_title{i} = {sublabel{i} mreg_Rsqr{i} mreg_adjRsqr{i}...
mreg_pvalue{i}};
disp(vertcat(display_label, display_title{i}));

mreg_output {i} = horzcat(cor_variables, num2cell(mreg_betas {i}),...
num2cell(mreg_pbeta {i}));
mreg_head = {'Variable' 'Slope' 'P-value'};
disp(vertcat(mreg_head, mreg_output {i}));
end

```

```

%% Multiple regression of Spring conc, Temp

cor_variables = {'Intercept' ; 'Conc. at spring'; 'Temp (deg. C)'};

for i=1:length(k)
    x_regress = [spring_data(:,k(i)) temp_us'];
    regstats_stats{i} = regstats(medians{i},x_regress,...
        'linear',whichstats);

    mreg_Rsqr{i} = regstats_stats{i}.rsquare;
    mreg_adjRsqr{i} = regstats_stats{i}.adjrsquare;
    mreg_pvalue{i} = regstats_stats{i}.fstat.pval;
    mreg_betas{i} = regstats_stats{i}.tstat.beta;
    mreg_pbeta{i} = regstats_stats{i}.tstat.pval;

    disp(sublabel{i})
    display_title{i} = {sublabel{i} mreg_Rsqr{i} mreg_adjRsqr{i}...
        mreg_pvalue{i}};
    disp(vertcat(display_label, display_title{i}));

    mreg_output{i} = horzcat(cor_variables, num2cell(mreg_betas{i}),...
        num2cell(mreg_pbeta{i}));
    mreg_head = {'Variable' 'Slope' 'P-value'};
    disp(vertcat(mreg_head, mreg_output{i}));
end

%% Multiple regression of Spring conc, Canopy

cor_variables = {'Intercept' ; 'Conc. at spring'; 'Canopy (on/off)'};

for i=1:length(k)
    x_regress = [spring_data(:,k(i)) canopy'];
    regstats_stats{i} = regstats(medians{i},x_regress,...
        'linear',whichstats);

    mreg_Rsqr{i} = regstats_stats{i}.rsquare;
    mreg_adjRsqr{i} = regstats_stats{i}.adjrsquare;
    mreg_pvalue{i} = regstats_stats{i}.fstat.pval;
    mreg_betas{i} = regstats_stats{i}.tstat.beta;
    mreg_pbeta{i} = regstats_stats{i}.tstat.pval;

    disp(sublabel{i})
    display_title{i} = {sublabel{i} mreg_Rsqr{i} mreg_adjRsqr{i}...
        mreg_pvalue{i}};
    disp(vertcat(display_label, display_title{i}));

```

```

mreg_output{i} = horzcat(cor_variables, num2cell(mreg_betas{i}),...
    num2cell(mreg_pbeta{i}));
mreg_head = {'Variable' 'Slope' 'P-value'};
disp(vertcat(mreg_head, mreg_output{i}));
end

```

%% Multiple regression of Discharge, Temp

```
cor_variables = {'Intercept' ; 'Discharge (L/s)'; 'Temp (deg. C)'};
```

```
for i=1:length(k)
```

```

x_regress = [Q_us_injection' temp_us'];
regstats_stats{i} = regstats(medians{i},x_regress,...
    'linear',whichstats);

```

```

mreg_Rsqr{i} = regstats_stats{i}.rsquare;
mreg_adjRsqr{i} = regstats_stats{i}.adjrsquare;
mreg_pvalue{i} = regstats_stats{i}.fstat.pval;
mreg_betas{i} = regstats_stats{i}.tstat.beta;
mreg_pbeta{i} = regstats_stats{i}.tstat.pval;

```

```

disp(sublabel{i})
display_title{i} = {sublabel{i} mreg_Rsqr{i} mreg_adjRsqr{i}...
    mreg_pvalue{i}};
disp(vertcat(display_label, display_title{i}));

```

```

mreg_output{i} = horzcat(cor_variables, num2cell(mreg_betas{i}),...
    num2cell(mreg_pbeta{i}));
mreg_head = {'Variable' 'Slope' 'P-value'};
disp(vertcat(mreg_head, mreg_output{i}));
end

```

%% Multiple regression of Discharge, Canopy

```
cor_variables = {'Intercept' ; 'Discharge (L/s)'; 'Canopy (on/off)'};
```

```
for i=1:length(k)
```

```

x_regress = [Q_us_injection' canopy'];
regstats_stats{i} = regstats(medians{i},x_regress,...
    'linear',whichstats);

```

```

mreg_Rsqr{i} = regstats_stats{i}.rsquare;
mreg_adjRsqr{i} = regstats_stats{i}.adjrsquare;
mreg_pvalue{i} = regstats_stats{i}.fstat.pval;
mreg_betas{i} = regstats_stats{i}.tstat.beta;

```

```

mreg_pbeta{i} = regstats_stats{i}.tstat.pval;

disp(sublabel{i})
display_title{i} = {sublabel{i} mreg_Rsqr{i} mreg_adjRsqr{i}...
    mreg_pvalue{i}};
disp(vertcat(display_label, display_title{i}));

mreg_output{i} = horzcat(cor_variables, num2cell(mreg_betas{i}),...
    num2cell(mreg_pbeta{i}));
mreg_head = {'Variable' 'Slope' 'P-value'};
disp(vertcat(mreg_head, mreg_output{i}));
end

%% Multiple regression of Temp, Canopy

cor_variables = {'Intercept' ; 'Temp (deg. C)'; 'Canopy (on/off)'};

for i=1:length(k)
    x_regress = [temp_us' canopy'];
    regstats_stats{i} = regstats(medians{i},x_regress,...
        'linear',whichstats);

    mreg_Rsqr{i} = regstats_stats{i}.rsquare;
    mreg_adjRsqr{i} = regstats_stats{i}.adjrsquare;
    mreg_pvalue{i} = regstats_stats{i}.fstat.pval;
    mreg_betas{i} = regstats_stats{i}.tstat.beta;
    mreg_pbeta{i} = regstats_stats{i}.tstat.pval;

    disp(sublabel{i})
    display_title{i} = {sublabel{i} mreg_Rsqr{i} mreg_adjRsqr{i}...
        mreg_pvalue{i}};
    disp(vertcat(display_label, display_title{i}));

    mreg_output{i} = horzcat(cor_variables, num2cell(mreg_betas{i}),...
        num2cell(mreg_pbeta{i}));
    mreg_head = {'Variable' 'Slope' 'P-value'};
    disp(vertcat(mreg_head, mreg_output{i}));
end

```

## K.16 MULTIPLE LINEAR REGRESSION, 3 VARIABLES

```
%% Multiple linear regression with 3 variables - no interaction
%Luke Wildfire
%May 28, 2012

%% Initialize workspace
clc
close all
clear all

%% Initialize data

[D1,D1_words] = ...
    xlsread('data_for_stats_sans_springs_and_2nd_stream.xls', 'D1_Sep');
[D2,D2_words] = ...
    xlsread('data_for_stats_sans_springs_and_2nd_stream.xls', 'D2_Nov');
[D3,D3_words] = ...
    xlsread('data_for_stats_sans_springs_and_2nd_stream.xls', 'D3_Apr');
[D4,D4_words] = ...
    xlsread('data_for_stats_sans_springs_and_2nd_stream.xls', 'D4_Jun');
[D5,D5_words] = ...
    xlsread('data_for_stats_sans_springs_and_2nd_stream.xls', 'D5_Aug');
[D6,D6_words] = ...
    xlsread('data_for_stats_sans_springs_and_2nd_stream.xls', 'D6_Feb');

[headers,labels] = ...
    xlsread('data_for_stats_sans_springs_and_2nd_stream.xls', 'header');
months = {'Feb', 'Apr', 'Jun', 'Aug', 'Sep', 'Nov'};
group = [repmat({'Feb'}, length(D6(:,1)), 1);...
        repmat({'Apr'}, length(D3(:,1)), 1);...
        repmat({'Jun'}, length(D4(:,1)), 1);...
        repmat({'Aug'}, length(D5(:,1)), 1);...
        repmat({'Sep'}, length(D1(:,1)), 1);...
        repmat({'Nov'}, length(D2(:,1)), 1)];
k = [4 6 8 12 14 17 19 21 22 24 25 29 30 31 43 46 51 53];

[spring_data] = ...
    xlsread('data_for_stats_sans_springs_and_2nd_stream.xls', 'springs');

%% Group data

for i=1:length(k)
    sublabel(i,1) = labels(k(i));
    x(:,i) = [D6(:,k(i)); D3(:,k(i)); D4(:,k(i)); D5(:,k(i));...
            D1(:,k(i)); D2(:,k(i))];
end
```



```

medians {i} = grpstats(x(:,i),group,'median');
end

%% Intialize regression variables

Q_us_injection = [2.636 1.460 0.953 0.375 0.136 0.357];
temp_us = [6.572 12.226 15.691 19.073 18.229 8.911];
%resp_us = [-3.377 6.264 -19.476 -23.413 -10.692 -5.124];
%season: 0=canopy off; 1= canopy on
canopy = [0 0 1 1 1 0];

%nutrient regression variables
toc_vf_us = [0.000000000 0.004466172 0.000711812 0.000726256...
0.001345525 0.000116833];
labile_C_vf_us = [0 0 0.000902615 0.002851436 0.002728440 0];
nh4n_vf_us = [0.001821126 0.000977208 0.002795510 0.001523611 ...
0.002392224 0.002990127];

whichstats = {'rsquare','adjrsquare','tstat', 'fstat'};
display_label = {'Analyte' 'R-squared' 'Adj R-squared' 'P-value'};

%% Multiple regression of Spring conc, Discharge, Temp

cor_variables = {'Intercept'; 'Conc. at spring'; ...
'Discharge (L/s)'; 'Temp (deg. C)'};

for i=1:length(k)
x_regress = [spring_data(:,k(i)) Q_us_injection' ...
temp_us'];
regstats_stats {i} = regstats(medians {i},x_regress,...
'linear',whichstats);

mreg_Rsqr {i} = regstats_stats {i}.rsquare;
mreg_adjRsqr {i} = regstats_stats {i}.adjrsquare;
mreg_pvalue {i} = regstats_stats {i}.fstat.pval;
mreg_betas {i} = regstats_stats {i}.tstat.beta;
mreg_pbeta {i} = regstats_stats {i}.tstat.pval;

disp(sublabel {i})
display_title {i} = {sublabel {i} mreg_Rsqr {i} mreg_adjRsqr {i}...
mreg_pvalue {i}};
disp(vertcat(display_label, display_title {i}));

mreg_output {i} = horzcat(cor_variables, num2cell(mreg_betas {i}),...
num2cell(mreg_pbeta {i}));
mreg_head = {'Variable' 'Slope' 'P-value'};

```

```

disp(vertcat(mreg_head, mreg_output{i}));
end

%% Multiple regression of Spring conc, Discharge, Canopy

cor_variables = {'Intercept' ; 'Conc. at spring'; ...
                'Discharge (L/s)'; 'Canopy (on/off)'};

for i=1:length(k)
    x_regress = [spring_data(:,k(i)) Q_us_injection' ...
                canopy'];
    regstats_stats{i} = regstats(medians{i},x_regress,...
                                'linear',whichstats);

    mreg_Rsqr{i} = regstats_stats{i}.rsquare;
    mreg_adjRsqr{i} = regstats_stats{i}.adjrsquare;
    mreg_pvalue{i} = regstats_stats{i}.fstat.pval;
    mreg_betas{i} = regstats_stats{i}.tstat.beta;
    mreg_pbeta{i} = regstats_stats{i}.tstat.pval;

    disp(sublabel{i})
    display_title{i} = {sublabel{i} mreg_Rsqr{i} mreg_adjRsqr{i}...
                        mreg_pvalue{i}};
    disp(vertcat(display_label, display_title{i}));

    mreg_output{i} = horzcat(cor_variables, num2cell(mreg_betas{i}),...
                            num2cell(mreg_pbeta{i}));
    mreg_head = {'Variable' 'Slope' 'P-value'};
    disp(vertcat(mreg_head, mreg_output{i}));
end

```

```

%% Multiple regression of Spring conc, Temp, Canopy

```

```

cor_variables = {'Intercept' ; 'Conc. at spring'; ...
                'Temp (deg. C)'; 'Canopy (on/off)'};

for i=1:length(k)
    x_regress = [spring_data(:,k(i)) ...
                temp_us' canopy'];
    regstats_stats{i} = regstats(medians{i},x_regress,...
                                'linear',whichstats);

    mreg_Rsqr{i} = regstats_stats{i}.rsquare;
    mreg_adjRsqr{i} = regstats_stats{i}.adjrsquare;
    mreg_pvalue{i} = regstats_stats{i}.fstat.pval;
    mreg_betas{i} = regstats_stats{i}.tstat.beta;

```

```

mreg_pbeta{i} = regstats_stats{i}.tstat.pval;

disp(sublabel{i})
display_title{i} = {sublabel{i} mreg_Rsqr{i} mreg_adjRsqr{i}...
    mreg_pvalue{i}};
disp(vertcat(display_label, display_title{i}));

mreg_output{i} = horzcat(cor_variables, num2cell(mreg_betas{i}),...
    num2cell(mreg_pbeta{i}));
mreg_head = {'Variable' 'Slope' 'P-value'};
disp(vertcat(mreg_head, mreg_output{i}));
end

%% Multiple regression of Discharge, Temp, Canopy

cor_variables = {'Intercept'; ...
    'Discharge (L/s)'; 'Temp (deg. C)'; 'Canopy (on/off)'};

for i=1:length(k)
    x_regress = ['Q_us_injection' ...
        temp_us' canopy'];
    regstats_stats{i} = regstats(medians{i},x_regress,...
        'linear',whichstats);

    mreg_Rsqr{i} = regstats_stats{i}.rsquare;
    mreg_adjRsqr{i} = regstats_stats{i}.adjrsquare;
    mreg_pvalue{i} = regstats_stats{i}.fstat.pval;
    mreg_betas{i} = regstats_stats{i}.tstat.beta;
    mreg_pbeta{i} = regstats_stats{i}.tstat.pval;

    disp(sublabel{i})
    display_title{i} = {sublabel{i} mreg_Rsqr{i} mreg_adjRsqr{i}...
        mreg_pvalue{i}};
    disp(vertcat(display_label, display_title{i}));

    mreg_output{i} = horzcat(cor_variables, num2cell(mreg_betas{i}),...
        num2cell(mreg_pbeta{i}));
    mreg_head = {'Variable' 'Slope' 'P-value'};
    disp(vertcat(mreg_head, mreg_output{i}));
end

```

## K.17 MULTIPLE LINEAR REGRESSION, 4 VARIABLES

```
%% Multiple linear regression with 4 variables - no interaction
%Luke Wildfire
%May 28, 2012

%% Initialize workspace
clc
close all
clear all

%% Initialize data

[D1,D1_words] = ...
    xlsread('data_for_stats_sans_springs_and_2nd_stream.xls', 'D1_Sep');
[D2,D2_words] = ...
    xlsread('data_for_stats_sans_springs_and_2nd_stream.xls', 'D2_Nov');
[D3,D3_words] = ...
    xlsread('data_for_stats_sans_springs_and_2nd_stream.xls', 'D3_Apr');
[D4,D4_words] = ...
    xlsread('data_for_stats_sans_springs_and_2nd_stream.xls', 'D4_Jun');
[D5,D5_words] = ...
    xlsread('data_for_stats_sans_springs_and_2nd_stream.xls', 'D5_Aug');
[D6,D6_words] = ...
    xlsread('data_for_stats_sans_springs_and_2nd_stream.xls', 'D6_Feb');

[headers,labels] = ...
    xlsread('data_for_stats_sans_springs_and_2nd_stream.xls', 'header');
months = {'Feb', 'Apr', 'Jun', 'Aug', 'Sep', 'Nov'};
group = [repmat({'Feb'}, length(D6(:,1)), 1);...
        repmat({'Apr'}, length(D3(:,1)), 1);...
        repmat({'Jun'}, length(D4(:,1)), 1);...
        repmat({'Aug'}, length(D5(:,1)), 1);...
        repmat({'Sep'}, length(D1(:,1)), 1);...
        repmat({'Nov'}, length(D2(:,1)), 1)];
k = [4 6 8 12 14 17 19 21 22 24 25 29 30 31 43 46 51 53];

[spring_data] = ...
    xlsread('data_for_stats_sans_springs_and_2nd_stream.xls', 'springs');

%% Group data

for i=1:length(k)
    sublabel(i,1) = labels(k(i));
    x(:,i) = [D6(:,k(i)); D3(:,k(i)); D4(:,k(i)); D5(:,k(i));...
            D1(:,k(i)); D2(:,k(i))];
end
```

```

medians {i} = grpstats(x(:,i),group,'median');
end

%% Intialize regression variables

Q_us_injection = [2.636 1.460 0.953 0.375 0.136 0.357];
temp_us = [6.572 12.226 15.691 19.073 18.229 8.911];
%resp_us = [-3.377 6.264 -19.476 -23.413 -10.692 -5.124];
%season: 0=canopy off; 1= canopy on
canopy = [0 0 1 1 1 0];

%nutrient regression variables
toc_vf_us = [0.000000000 0.004466172 0.000711812 0.000726256...
0.001345525 0.000116833];
labile_C_vf_us = [0 0 0.000902615 0.002851436 0.002728440 0];
nh4n_vf_us = [0.001821126 0.000977208 0.002795510 0.001523611 ...
0.002392224 0.002990127];

whichstats = {'rsquare','adjrsquare','tstat', 'fstat'};
display_label = {'Analyte' 'R-squared' 'Adj R-squared' 'P-value'};

%% Multiple regression of spring conc, discharge, temp, & canopy

cor_variables = {'Intercept'; 'Conc. at spring'; ...
'Discharge (L/s)'; 'Temp (deg. C)'; 'Canopy (on/off)'};

for i=1:length(k)
x_regress = [spring_data(:,k(i)) Q_us_injection' ...
temp_us' canopy'];
regstats_stats {i} = regstats(medians {i},x_regress,...
'linear',whichstats);

mreg_Rsqr {i} = regstats_stats {i}.rsquare;
mreg_adjRsqr {i} = regstats_stats {i}.adjrsquare;
mreg_pvalue {i} = regstats_stats {i}.fstat.pval;
mreg_betas {i} = regstats_stats {i}.tstat.beta;
mreg_pbeta {i} = regstats_stats {i}.tstat.pval;

disp(sublabel {i})
display_title {i} = {sublabel {i} mreg_Rsqr {i} mreg_adjRsqr {i}...
mreg_pvalue {i}};
disp(vertcat(display_label, display_title {i}));

mreg_output {i} = horzcat(cor_variables, num2cell(mreg_betas {i}),...
num2cell(mreg_pbeta {i}));
mreg_head = {'Variable' 'Slope' 'P-value'};

```

```
    disp(vertcat(mreg_head, mreg_output{i}));  
end
```

## K.18 LONGITUDINAL ANALYTE PLOTS

```
%%Code for making Longitudnal graphs of Delaware data
%Luke Wildfire
%July 31, 2013

%% Initialize workspace
clc
close all
clear all

%% Initialize data

[D1,D1_words] = xlsread('data_for_stats.xls', 'D1_Sep');
[D2,D2_words] = xlsread('data_for_stats.xls', 'D2_Nov');
[D3,D3_words] = xlsread('data_for_stats.xls', 'D3_Apr');
[D4,D4_words] = xlsread('data_for_stats.xls', 'D4_Jun');
[D5,D5_words] = xlsread('data_for_stats.xls', 'D5_Aug');
[D6,D6_words] = xlsread('data_for_stats.xls', 'D6_Feb');

[headers,badlabels] = ...
    xlsread('data_for_stats.xls', 'header');

%% Pull out relevant data. Give them names

k = [4 6 8 12 14 17 19 21 22 24 25 26 29 30 31 33 34 35 36 37 38 39 40 ...
    41 42 43 46 51 53 54 56];
ccc = char(8240);
label = {...
    ['DOC (\muM)']...
    ['DIC (\muM)']...
    ['TDN (\muM)']...
    ['BDOC (\muM)']...
    ['RDOC (\muM)']...
    ['NH_4^+ (\muM)']...
    ['PO_4^3^+ (\muM)']...
    ['Cl^- (\muM)']...
    ['NO_3^- (\muM)']...
    ['SO_4^2^- (\muM)']...
    ['DON (\muM)']...
    ['Percent of TDN as DON (%)']...
    ['\delta18O (' ccc ')']...
    ['\deltaD (' ccc ')']...
    ['d-excess (' ccc ')']...
    ['DIC/Cl^- (\muM\\muM)']...
    ['DOC/Cl^- (\muM\\muM)']...
}
```

```

['BDOC/CI^- (\muM\\muM)']...
['RDOC/CI^- (\muM\\muM)']...
['TDN/CI^- (\muM\\muM)']...
['NH_4^+/CI^- (\muM\\muM)']...
['NO_3^-/CI^- (\muM\\muM)']...
['DON/CI^- (\muM\\muM)']...
['PO_4^3^+/CI^- (\muM\\muM)']...
['SO_4^2^-/CI^- (\muM\\muM)']...
['DOC/TDN^- (\muM\\muM)']...
['DOC/DON (\muM\\muM)']...
['DOC/PO_4^3^+ (\muM\\muM)']...
['TDN/PO_4^3^+ (\muM\\muM)']...
['NO_3^-/PO_4^3^+ (\muM\\muM)']...
['DON/PO_4^3^+ (\muM\\muM)']...
};
%% Graph variables

```

```
v_line_x = [1128 1128];
```

```

for i=1:length(k)
    c = k(i);

```

```
    n = figure;
```

```

    D1_x = D1(:,1);
    D1_y = D1(:,c);
    D1_x1 = D1_x(~isnan(D1_x));
    D1_y1 = D1_y(~isnan(D1_x));
    D1_y2 = D1_y1(~isnan(D1_y1));
    D1_x2 = D1_x1(~isnan(D1_y1));

```

```

    D2_x = D2(:,1);
    D2_y = D2(:,c);
    D2_x1 = D2_x(~isnan(D2_x));
    D2_y1 = D2_y(~isnan(D2_x));
    D2_y2 = D2_y1(~isnan(D2_y1));
    D2_x2 = D2_x1(~isnan(D2_y1));

```

```

    D3_x = D3(:,1);
    D3_y = D3(:,c);
    D3_x1 = D3_x(~isnan(D3_x));
    D3_y1 = D3_y(~isnan(D3_x));
    D3_y2 = D3_y1(~isnan(D3_y1));
    D3_x2 = D3_x1(~isnan(D3_y1));

```

```
    D4_x = D4(:,1);
```



```

D4_y = D4(:,c);
D4_x1 = D4_x(~isnan(D4_x));
D4_y1 = D4_y(~isnan(D4_x));
D4_y2 = D4_y1(~isnan(D4_y1));
D4_x2 = D4_x1(~isnan(D4_y1));

D5_x = D5(:,1);
D5_y = D5(:,c);
D5_x1 = D5_x(~isnan(D5_x));
D5_y1 = D5_y(~isnan(D5_x));
D5_y2 = D5_y1(~isnan(D5_y1));
D5_x2 = D5_x1(~isnan(D5_y1));

D6_x = D6(:,1);
D6_y = D6(:,c);
D6_x1 = D6_x(~isnan(D6_x));
D6_y1 = D6_y(~isnan(D6_x));
D6_y2 = D6_y1(~isnan(D6_y1));
D6_x2 = D6_x1(~isnan(D6_y1));

plot(D6_x2,D6_y2,'.-',...
     D3_x2,D3_y2,'.-',...
     D4_x2,D4_y2,'.-',...
     D5_x2,D5_y2,'.-',...
     D1_x2,D1_y2,'.-',...
     D2_x2,D2_y2,'.-')
colormap(jet)

xlim([0 1300])
ax = axis;
v_line_y = [ax(3) ax(4)];
vert_line = line(v_line_x,v_line_y, 'color','r','linestyle','--');

legend('Feb', 'Apr', 'Jun', 'Aug', 'Sep', 'Nov')
[LEGH,OBJH,OUTH,OUTM] = legend;
legend([OUTH;vert_line],OUTM{:}, 'tributary',...
       'location','southoutside',...
       'orientation','horizontal')

title(label(i))
xlabel('Distance downstream from source (m)')

%{
set(gcf, 'PaperUnits', 'inches');
set(gcf, 'PaperSize', [6.5 2.5]);
set(gcf, 'PaperPositionMode', 'manual');

```

```
set(gcf, 'PaperPosition', [0 0 6.5 2.5]);  
set(gcf, 'renderer', 'painters');  
print(gcf, '-dpng', ['Longitudnal' num2str(i) '.png']);  
%}
```

```
end
```

## CITATIONS

- Aber, J., W. McDowell, K. Nadelhoffer, A. Magill, G. Berntson, M. Kamakea, S. McNulty, W. Currie, L. Rustad, and I. Fernandez. 1998. Nitrogen saturation in temperate forest ecosystems. *BioScience* 48(11):921-934.
- Aber, J. D., C. L. Goodale, S. V. Ollinger, M.-L. Smith, A. H. Magill, M. E. Martin, R. A. Hallett, and J. L. Stoddard. 2003. Is nitrogen deposition altering the nitrogen status of northeastern forests? *BioScience* 53(4):375-389.
- Acuña, V., I. Muñoz, A. Giorgi, M. Omella, F. Sabater, and S. Sabater. 2005. Drought and postdrought recovery cycles in an intermittent Mediterranean stream: structural and functional aspects. *Journal of the North American Benthological Society* 24(4):919-933.
- Adams, M. B., W. T. Peterjohn, and F. S. Gilliam. 2006. Acidification and nutrient cycling. In *The Fernow Watershed Acidification Study*, 207-236. Springer.
- Alexander, R. B., E. W. Boyer, R. A. Smith, G. E. Schwarz, and R. B. Moore. 2007. The role of headwater streams in downstream water quality. *Journal of the American Water Resources Association* 43(1):41-59.
- Alexander, R. B., R. A. Smith, and G. E. Schwarz. 2000. Effect of stream channel size on the delivery of nitrogen to the Gulf of Mexico. *Nature* 403(6771):758-761.
- Altieri, K. E., B. J. Turpin, and S. P. Seitzinger. 2009. Composition of dissolved organic nitrogen in continental precipitation investigated by ultra-high resolution FT-ICR mass spectrometry. *Environmental science & technology* 43(18):6950-6955.
- Angier, J., G. McCarty, T. Gish, and C. Daughtry. 2001. Impact of a first-order riparian zone on nitrogen removal and export from an agricultural ecosystem. *The Scientific World Journal* 1(S2):642-651.
- Angier, J. T., and G. W. McCarty. 2008. Variations in base-flow nitrate flux in a first-order stream and riparian zone. *Journal of the American Water Resources Association* 44(2):367-380.
- Angier, J. T., G. W. McCarty, and K. L. Prestegard. 2005. Hydrology of a first-order riparian zone and stream, mid-Atlantic coastal plain, Maryland. *Journal of Hydrology* 309(1):149-166.
- Arango, C., J. Tank, L. Johnson, and S. Hamilton. 2008. Assimilatory uptake rather than nitrification and denitrification determines nitrogen removal patterns in streams of varying land use. *Limnology and Oceanography* 53(6):2558-2572.
- Arango, C., and J. L. Tank. 2008. Land use influences the spatiotemporal controls on nitrification and denitrification in headwater streams. *Journal of the North American Benthological Society* 27(1):90-107.
- Argerich, A., E. Martí, F. Sabater, R. Haggerty, and M. Ribot. 2011. Influence of transient storage

on stream nutrient uptake based on substrata manipulation. *Aquatic Sciences* 73(3):365-376.

Ashkenas, L. R., S. L. Johnson, S. V. Gregory, J. L. Tank, and W. M. Wollheim. 2004. A stable isotope tracer study of nitrogen uptake and transformation in an old-growth forest stream. *Ecology* 85(6):1725-1739.

Ator, S. W., and J. M. Denver. 2012. Estimating contributions of nitrate and herbicides from groundwater to headwater streams, Northern Atlantic Coastal Plain, United States. *Journal of the American Water Resources Association* 48(6):1075-1090.

Aubertin, G., and J. Patric. 1974. Water quality after clearcutting a small watershed in West Virginia. *Journal of Environmental Quality* 3(3):243-249.

Aumen, N. G., C. P. Hawkins, and S. V. Gregory. 1990. Influence of woody debris on nutrient retention in catastrophically disturbed streams. *Hydrobiologia* 190(3):183-192.

Bachman, L. J., B. Lindsey, J. Brakebill, and D. S. Powars. 1998. *Ground-water discharge and base-flow nitrate loads of nontidal streams, and their relation to a hydrogeomorphic classification of the Chesapeake Bay Watershed, middle Atlantic coast*. USGS Water-Resources Investigations Report 98-4059. US Department of the Interior, US Geological Survey.

Baker, D. W., B. P. Bledsoe, and J. M. Price. 2012. Stream nitrate uptake and transient storage over a gradient of geomorphic complexity, north-central Colorado, USA. *Hydrological Processes* 26(21):3241-3252.

Baker, M. A., C. N. Dahm, and H. M. Valett. 1999. Acetate retention and metabolism in the hyporheic zone of a mountain stream. *Limnology and Oceanography* 44(6):1530-1539.

Band, L., C. Tague, P. Groffman, and K. Belt. 2001. Forest ecosystem processes at the watershed scale: Hydrological and ecological controls of nitrogen export. *Hydrological Processes* 15(10):2013-2028.

Barnes, R. T., R. L. Smith, and G. R. Aiken. 2012. Linkages between denitrification and dissolved organic matter quality, Boulder Creek watershed, Colorado. *Journal of Geophysical Research: Biogeosciences* 117(G01014):1-14.

Bascom, F. 1902. *The geology of the crystalline rocks of Cecil County*. Maryland Geological Survey and the Johns Hopkins Press, Baltimore, MD.

Battin, T. J., L. A. Kaplan, J. D. Newbold, and S. P. Hendricks. 2003. A mixing model analysis of stream solute dynamics and the contribution of a hyporheic zone to ecosystem function. *Freshwater Biology* 48(6):995-1014.

Benson, B. B., and D. Krause Jr. 1984. The concentration and isotopic fractionation of oxygen dissolved in freshwater and seawater in equilibrium with the atmosphere. *Limnology and Oceanography* 29(3):620-632.

Berman, T., and D. A. Bronk. 2003. Dissolved organic nitrogen: A dynamic participant in aquatic

ecosystems. *Aquatic Microbial Ecology* 31(3):279-305.

Bernal, S., A. Butturini, and F. Sabater. 2005. Seasonal variations of dissolved nitrogen and DOC:DON ratios in an intermittent Mediterranean stream. *Biogeochemistry* 75(2):351-372.

Bernhardt, E., G. Likens, D. Buso, and C. Driscoll. 2003. In-stream uptake dampens effects of major forest disturbance on watershed nitrogen export. *Proceedings of the National Academy of Sciences* 100(18):10304-10308.

Bernhardt, E. S., and G. E. Likens. 2002. Dissolved organic carbon enrichment alters nitrogen dynamics in a forest stream. *Ecology* 83(6):1689-1700.

Bernhardt, E. S., G. E. Likens, R. O. Hall Jr., D. C. Buso, S. G. Fisher, T. M. Burton, J. L. Meyer, W. H. McDowell, M. S. Mayer, and W. B. Bowden. 2005. Can't see the forest for the stream? In-stream processing and terrestrial nitrogen exports. *BioScience* 55(3):219-230.

Bernot, M. J., and W. K. Dodds. 2005. Nitrogen retention, removal, and saturation in lotic ecosystems. *Ecosystems* 8(4):442-453.

Böhlke, J., and J. Denver. 1995. Combined use of groundwater dating, chemical, and isotopic analyses to resolve the history and fate of nitrate contamination in two agricultural watersheds, Atlantic coastal plain, Maryland. *Water Resources Research* 31(9):2319-2339.

Böhlke, J. K., and R. L. Michel. 2009. Contrasting residence times and fluxes of water and sulfate in two small forested watersheds in Virginia, USA. *Science of the Total Environment* 407(14):4363-4377.

Boring, L. R., W. T. Swank, J. B. Waide, and G. S. Henderson. 1988. Sources, fates, and impacts of nitrogen inputs to terrestrial ecosystems: Review and synthesis. *Biogeochemistry* 6(2):119-159.

Bott, T. L. 2006. Primary productivity and community respiration. In *Methods in stream ecology*, 663-690. R. Hauer, and G. A. Lamberti, eds: Academic Press.

Bott, T. L., J. T. Brock, C. S. Dunn, R. J. Naiman, R. W. Ovink, and R. C. Petersen. 1985. Benthic community metabolism in four temperate stream systems: An inter-biome comparison and evaluation of the river continuum concept. *Hydrobiologia* 123(1):3-45.

Bott, T. L., J. D. Newbold, and D. B. Arscott. 2006. Ecosystem metabolism in Piedmont streams: Reach geomorphology modulates the influence of riparian vegetation. *Ecosystems* 9(3):398-421.

Boulton, A. J., S. Findlay, P. Marmonier, E. H. Stanley, and H. M. Valett. 1998. The functional significance of the hyporheic zone in streams and rivers. *Annual Review of Ecology and Systematics* 29:59-81.

Brookshire, E., H. Valett, and S. Gerber. 2009. Maintenance of terrestrial nutrient loss signatures during in-stream transport. *Ecology* 90(2):293-299.

Brookshire, E. N. J., H. M. Valett, S. A. Thomas, and J. R. Webster. 2007. Atmospheric N

- deposition increases organic N loss from temperate forests. *Ecosystems* 10(2):252-262.
- Brunke, M., and T. Gonser. 1997. The ecological significance of exchange processes between rivers and groundwater. *Freshwater Biology* 37(1):1-33.
- Brush, G. S. 2009. Historical land use, nitrogen, and coastal eutrophication: A paleoecological perspective. *Estuaries and Coasts* 32(1):18-28.
- Buda, A. R., and D. R. DeWalle. 2009. Dynamics of stream nitrate sources and flow pathways during stormflows on urban, forest and agricultural watersheds in central Pennsylvania, USA. *Hydrological Processes* 23(23):3292-3305.
- Buffam, I., J. N. Galloway, L. K. Blum, and K. J. McGlathery. 2001. A stormflow/baseflow comparison of dissolved organic matter concentrations and bioavailability in an Appalachian stream. *Biogeochemistry* 53(3):269-306.
- Bukaveckas, P. A. 2007. Effects of channel restoration on water velocity, transient storage, and nutrient uptake in a channelized stream. *Environmental science & technology* 41(5):1570-1576.
- Burgin, A. J., and S. K. Hamilton. 2007. Have we overemphasized the role of denitrification in aquatic ecosystems? A review of nitrate removal pathways. *Frontiers in Ecology and the Environment* 5(2):89-96.
- Burns, D. A. 1998. Retention of NO<sub>3</sub><sup>-</sup> in an upland stream environment: A mass balance approach. *Biogeochemistry* 40(1):73-96.
- Burns, D. A., and C. Kendall. 2002. Analysis of δ<sup>15</sup>N and δ<sup>18</sup>O to differentiate NO<sub>3</sub><sup>-</sup> sources in runoff at two watersheds in the Catskill Mountains of New York. *Water Resources Research* 38(5):1-11.
- Burns, D. A., and P. S. Murdoch. 2005. Effects of a clearcut on the net rates of nitrification and N mineralization in a northern hardwood forest, Catskill Mountains, New York, USA. *Biogeochemistry* 72(1):123-146.
- Burns, D. A., P. S. Murdoch, G. B. Lawrence, and R. L. Michel. 1998. Effect of groundwater springs on NO<sub>3</sub><sup>-</sup> concentrations during summer in Catskill Mountain streams. *Water Resources Research* 34(8):1987-1996.
- Butler, T., and G. Likens. 1995. A direct comparison of throughfall plus stemflow to estimates of dry and total deposition for sulfur and nitrogen. *Atmospheric Environment* 29(11):1253-1265.
- Butturini, A., T. J. Battin, and F. Sabater. 2000. Nitrification in stream sediment biofilms: The role of ammonium concentration and DOC quality. *Water Research* 34(2):629-639.
- Campbell, J., J. Hornbeck, W. McDowell, D. Buso, J. Shanley, and G. Likens. 2000. Dissolved organic nitrogen budgets for upland, forested ecosystems in New England. *Biogeochemistry* 49(2):123-142.

Campbell, J. L., J. W. Hornbeck, M. J. Mitchell, M. B. Adams, M. S. Castro, C. T. Driscoll, J. S. Kahl, J. N. Kochenderfer, G. E. Likens, and J. A. Lynch. 2004. Input-output budgets of inorganic nitrogen for 24 forest watersheds in the northeastern United States: A review. *Water, Air, and Soil Pollution* 151(1-4):373-396.

Cardinale, B. J. 2011. Biodiversity improves water quality through niche partitioning. *Nature* 472(7341):86-89.

Castro, M. S., K. N. Eshleman, L. F. Pitelka, G. Frech, M. Ramsey, W. S. Currie, K. Kuers, J. A. Simmons, B. R. Pohlrad, and C. L. Thomas. 2007. Symptoms of nitrogen saturation in an aggrading forested watershed in western Maryland. *Biogeochemistry* 84(3):333-348.

Castro, M. S., and R. P. Morgan II. 2000. Input-output budgets of major ions for a forested watershed in western Maryland. *Water, Air, and Soil Pollution* 119(1-4):121-137.

Cirno, C. P., and C. T. Driscoll. 1993. Beaver pond biogeochemistry: Acid neutralizing capacity generation in a headwater wetland. *Wetlands* 13(4):277-292.

Cirno, C. P., and J. J. McDonnell. 1997. Linking the hydrologic and biogeochemical controls of nitrogen transport in near-stream zones of temperate-forested catchments: A review. *Journal of Hydrology* 199(1):88-120.

Claessens, L., C. L. Tague, P. M. Groffman, and J. M. Melack. 2010. Longitudinal and seasonal variation of stream N uptake in an urbanizing watershed: Effect of organic matter, stream size, transient storage and debris dams. *Biogeochemistry* 98(1-3):45-62.

Cornell, S., T. Jickells, J. Cape, A. Rowland, and R. Duce. 2003. Organic nitrogen deposition on land and coastal environments: A review of methods and data. *Atmospheric Environment* 37(16):2173-2191.

Cornell, S. E. 2011. Atmospheric nitrogen deposition: Revisiting the question of the importance of the organic component. *Environmental Pollution* 159(10):2214-2222.

Correll, D. L., T. E. Jordan, and D. E. Weller. 1997. Failure of agricultural riparian buffers to protect surface waters from groundwater nitrate contamination. In *Groundwater/surface water ecotones: biological and hydrological interactions and management options*, 162-165. J. Gibert, J. Mathieu, and F. Fournier, eds: Cambridge University Press Cambridge.

Correll, D. L., T. E. Jordan, and D. E. Weller. 1999. Effects of precipitation and air temperature on nitrogen discharges from Rhode River watersheds. *Water, Air, and Soil Pollution* 115(1-4):547-575.

Correll, D. L., T. E. Jordan, and D. E. Weller. 2000. Beaver pond biogeochemical effects in the Maryland Coastal Plain. *Biogeochemistry* 49(3):217-239.

Correll, D. L., and D. E. Weller. 1997. Nitrogen input-output budgets for forests in the Chesapeake Bay Watershed. In *Atmospheric deposition of contaminants to the Great Lakes and coastal waters: Proceedings from a session at the SETAC 15th annual meeting, Denver, Colorado*, 431-442.

Pensacola, Florida: Society of Environmental Toxicology and Chemistry.

Cory, R. M., and L. A. Kaplan. 2012. Biological lability of streamwater fluorescent dissolved organic matter. *Limnology and Oceanography* 57(5):1347-1360.

Cosby, B. J., P. F. Ryan, J. R. Webb, G. M. Hornberger, and J. N. Galloway. 1991. Acidic deposition and aquatic ecosystems: Regional case studies. 297-318. D. F. Charles, and S. Christie, eds. New York, NY: Springer-Verlag.

Craig, L. S., M. A. Palmer, D. C. Richardson, S. Filoso, E. S. Bernhardt, B. P. Bledsoe, M. W. Doyle, P. M. Groffman, B. A. Hassett, and S. S. Kaushal. 2008. Stream restoration strategies for reducing river nitrogen loads. *Frontiers in Ecology and the Environment* 6(10):529-538.

Crenshaw, C., H. Valett, and J. Webster. 2002. Effects of augmentation of coarse particulate organic matter on metabolism and nutrient retention in hyporheic sediments. *Freshwater Biology* 47(10):1820-1831.

Curtis, C. J., C. D. Evans, C. L. Goodale, and T. H. Heaton. 2011. What have stable isotope studies revealed about the nature and mechanisms of N saturation and nitrate leaching from semi-natural catchments? *Ecosystems* 14(6):1021-1037.

Dahm, C. N., M. A. Baker, D. I. Moore, and J. R. Thibault. 2003. Coupled biogeochemical and hydrological responses of streams and rivers to drought. *Freshwater Biology* 48(7):1219-1231.

Dahm, C. N., N. B. Grimm, P. Marmonier, H. M. Valett, and P. Vervier. 1998. Nutrient dynamics at the interface between surface waters and groundwaters. *Freshwater Biology* 40(3):427-451.

Daniluk, T. L., L. K. Lutz, R. P. Gordon, and T. A. Endreny. 2012. Surface water-groundwater interaction at restored streams and associated reference reaches. *Hydrological Processes* 27(25):3730-3746.

Dawson, T. E., and K. A. Simonin. 2011. The roles of stable isotopes in forest hydrology and biogeochemistry. In *Forest Hydrology and Biogeochemistry*, 137-161. D. F. Levia, D. Carlyle-Moses, and T. Tanaka, eds: Springer Netherlands.

Devito, K. J., and P. J. Dillon. 1993. Importance of runoff and winter anoxia to the P and N dynamics of a beaver pond. *Canadian Journal of Fisheries and Aquatic Sciences* 50(10):2222-2234.

DeWalle, D., A. Buda, J. Eismeier, W. Sharpe, B. Swistock, P. Craig, M. O'Driscoll, L. Heathwaite, B. Webb, and D. Rosenberry. 2005. Nitrogen cycling on five headwater forested catchments in Mid-Appalachians of Pennsylvania. In *Seventh Scientific Assembly of the International Association of Hydrological Sciences: Dynamics and Biogeochemistry of River Corridors and Wetlands*. Foz do Iguaço, Brazil: IAHS Press.

DeWalle, D. R., P. J. Edwards, B. R. Swistock, R. Aravena, and R. J. Drimmie. 1997. Seasonal isotope hydrology of three Appalachian forest catchments. *Hydrological Processes* 11(15):1895-1906.



- DeWalle, D. R., and H. B. Pionke. 1994. Nitrogen export from forest land in the Chesapeake Bay region. In *Toward a Sustainable Coastal Watershed: The Chesapeake Experiment*. Norfolk, VA: Chesapeake Research Consortium.
- Dhillon, G. S., and S. Inamdar. 2013. Extreme storms and changes in particulate and dissolved organic carbon in runoff: Entering uncharted waters? *Geophysical Research Letters* 40(7):1322-1327.
- Dodds, W. K. 2003. The role of periphyton in phosphorus retention in shallow freshwater aquatic systems. *Journal of Phycology* 39(5):840-849.
- Dodds, W. K., M. A. Evans-White, N. M. Gerlanc, L. Gray, D. A. Gudder, M. J. Kemp, A. L. Lopez, D. Stagliano, E. A. Strauss, and J. L. Tank. 2000. Quantification of the nitrogen cycle in a prairie stream. *Ecosystems* 3(6):574-589.
- Dodds, W. K., E. Martí, J. L. Tank, J. Pontius, S. K. Hamilton, N. B. Grimm, W. B. Bowden, W. H. McDowell, B. J. Peterson, and H. M. Valett. 2004. Carbon and nitrogen stoichiometry and nitrogen cycling rates in streams. *Oecologia* 140(3):458-467.
- Dow, C. L., and D. R. DeWalle. 1997. Sulfur and nitrogen budgets for five forested Appalachian plateau basins. *Hydrological Processes* 11(7):801-816.
- Elgood, Z., W. Robertson, S. Schiff, and R. Elgood. 2010. Nitrate removal and greenhouse gas production in a stream-bed denitrifying bioreactor. *Ecological Engineering* 36(11):1575-1580.
- Ensign, S. H., and M. W. Doyle. 2005. In-channel transient storage and associated nutrient retention: Evidence from experimental manipulations. *Limnology and Oceanography* 50(6):1740-1751.
- Eshleman, K. N., R. H. Gardner, S. W. Seagle, N. M. Castro, D. A. Fiscus, J. R. Webb, J. N. Galloway, F. A. Deviney, and A. T. Herlihy. 2000. Effects of disturbance on nitrogen export from forested lands of the Chesapeake Bay watershed. *Environmental Monitoring and Assessment* 63(1):187-197.
- Eshleman, K. N., K. M. Kline, R. P. Morgan II, N. M. Castro, and T. L. Negley. 2008. Contemporary trends in the acid-base status of two acid-sensitive streams in western Maryland. *Environmental science & technology* 42(1):56-61.
- Eshleman, K. N., R. P. Morgan II, J. R. Webb, F. A. Deviney, and J. N. Galloway. 1998. Temporal patterns of nitrogen leakage from mid-Appalachian forested watersheds: Role of insect defoliation. *Water Resources Research* 34(8):2005-2016.
- Fairchild, G. W., and D. J. Velinsky. 2006. Effects of small ponds on stream water chemistry. *Lake and Reservoir Management* 22(4):321-330.
- Fanelli, R. M., and L. K. Lautz. 2008. Patterns of water, heat, and solute flux through streambeds around small dams. *Ground Water* 46(5):671-687.

- Filoso, S., and M. A. Palmer. 2011. Assessing stream restoration effectiveness at reducing nitrogen export to downstream waters. *Ecological Applications* 21(6):1989-2006.
- Findlay, S. 1995. Importance of surface-subsurface exchange in stream ecosystems: The hyporheic zone. *Limnology and Oceanography* 40(1):159-164.
- Fisher, D. C., and M. Oppenheimer. 1991. Atmospheric nitrogen deposition and the Chesapeake Bay estuary. *Ambio* 20(3/4):102-108.
- Fisher, S. G., N. B. Grimm, E. Martí, and R. Gómez. 1998. Hierarchy, spatial configuration, and nutrient cycling in a desert stream. *Australian Journal of Ecology* 23(1):41-52.
- Fisher, S. G., and G. E. Likens. 1973. Energy flow in Bear Brook, New Hampshire: An integrative approach to stream ecosystem metabolism. *Ecological Monographs* 43(4):421-439.
- Franken, R. J., R. G. Storey, and D. D. Williams. 2001. Biological, chemical and physical characteristics of downwelling and upwelling zones in the hyporheic zone of a north-temperate stream. *Hydrobiologia* 444(1-3):183-195.
- Galloway, J. N., J. D. Aber, J. W. Erisman, S. P. Seitzinger, R. W. Howarth, E. B. Cowling, and B. J. Cosby. 2003. The nitrogen cascade. *BioScience* 53(4):341-356.
- Gibson, C. A., and C. M. O'Reilly. 2012. Organic matter stoichiometry influences nitrogen and phosphorus uptake in a headwater stream. *Freshwater Science* 31(2):395-407.
- Goodale, C. L., S. A. Thomas, G. Fredriksen, E. M. Elliott, K. M. Flinn, T. J. Butler, and M. T. Walter. 2009. Unusual seasonal patterns and inferred processes of nitrogen retention in forested headwaters of the Upper Susquehanna River. *Biogeochemistry* 93(3):197-218.
- Grigal, D. 2012. Atmospheric deposition and inorganic nitrogen flux. *Water, Air, & Soil Pollution* 223(6):3565-3575.
- Grimm, N. B. 1987. Nitrogen dynamics during succession in a desert stream. *Ecology* 68(5):1157-1170.
- Grimm, N. B., S. G. Fisher, and W. Minckley. 1981. Nitrogen and phosphorus dynamics in hot desert streams of Southwestern USA. *Hydrobiologia* 83(2):303-312.
- Groffman, P. M., K. Butterbach-Bahl, R. W. Fulweiler, A. J. Gold, J. L. Morse, E. K. Stander, C. Tague, C. Tonitto, and P. Vidon. 2009. Challenges to incorporating spatially and temporally explicit phenomena (hotspots and hot moments) in denitrification models. *Biogeochemistry* 93(1-2):49-77.
- Groffman, P. M., A. M. Dorsey, and P. M. Mayer. 2005. N processing within geomorphic structures in urban streams. *Journal of the North American Benthological Society* 24(3):613-625.
- Groffman, P. M., N. L. Law, K. T. Belt, L. E. Band, and G. T. Fisher. 2004. Nitrogen fluxes and retention in urban watershed ecosystems. *Ecosystems* 7(4):393-403.

- Gulis, V., and K. Suberkropp. 2003. Leaf litter decomposition and microbial activity in nutrient-enriched and unaltered reaches of a headwater stream. *Freshwater Biology* 48(1):123-134.
- Haack, T. K., and G. A. McFeters. 1982. Nutritional relationships among microorganisms in an epilithic biofilm community. *Microbial Ecology* 8(2):115-126.
- Hagy, J. D., W. R. Boynton, C. W. Keefe, and K. V. Wood. 2004. Hypoxia in Chesapeake Bay, 1950–2001: Long-term change in relation to nutrient loading and river flow. *Estuaries* 27(4):634-658.
- Hall Jr., R. O., E. S. Bernhardt, and G. E. Likens. 2002. Relating nutrient uptake with transient storage in forested mountain streams. *Limnology and Oceanography* 47(1):255-265.
- Hall Jr., R. O., and J. L. Tank. 2003. Ecosystem metabolism controls nitrogen uptake in streams in Grand Teton National Park, Wyoming. *Limnology and Oceanography* 48(3):1120-1128.
- Hayhoe, K., C. P. Wake, T. G. Huntington, L. Luo, M. D. Schwartz, J. Sheffield, E. Wood, B. Anderson, J. Bradbury, A. DeGaetano, T. J. Troy, and D. Wolfe. 2007. Past and future changes in climate and hydrological indicators in the US Northeast. *Climate Dynamics* 28(4):381-407.
- Heatherly, T., M. R. Whiles, T. V. Royer, and M. B. David. 2007. Relationships between water quality, habitat quality, and macroinvertebrate assemblages in Illinois streams. *Journal of Environmental Quality* 36(6):1653-1660.
- Hedin, L. O., J. C. von Fischer, N. E. Ostrom, B. P. Kennedy, M. G. Brown, and G. P. Robertson. 1998. Thermodynamic constraints on nitrogen transformations and other biogeochemical processes at soil-stream interfaces. *Ecology* 79(2):684-703.
- Heim Jr., R. R. 2002. A review of twentieth-century drought indices used in the United States. *Bulletin of the American Meteorological Society* 83(8):1149-1165.
- Herrmann, M., W. E. Sharpe, D. R. DeWalle, and B. R. Swistock. 2001. Nitrogen export from a watershed subjected to partial salvage logging. *The Scientific World Journal* 1:440-448.
- Hester, E. T., and M. N. Gooseff. 2010. Moving beyond the banks: Hyporheic restoration is fundamental to restoring ecological services and functions of streams. *Environmental science & technology* 44(5):1521-1525.
- Hill, A. R. 1996. Nitrate removal in stream riparian zones. *Journal of Environmental Quality* 25(4):743-755.
- Hill, A. R., C. F. Labadia, and K. Sanmugadas. 1998a. Hyporheic zone hydrology and nitrogen dynamics in relation to the streambed topography of a N-rich stream. *Biogeochemistry* 42(3):285-310.
- Hill, B. H., A. T. Herlihy, and P. R. Kaufmann. 2002. Benthic microbial respiration in Appalachian Mountain, Piedmont, and Coastal Plains streams of the eastern U.S.A. *Freshwater Biology* 47(2):185-194.

- Hill, B. H., A. T. Herlihy, P. R. Kaufmann, and R. L. Sinsabaugh. 1998b. Sediment microbial respiration in a synoptic survey of mid-Atlantic region streams. *Freshwater Biology* 39(3):493-501.
- Hill, W. R., P. J. Mulholland, and E. R. Marzolf. 2001. Stream ecosystem responses to forest leaf emergence in spring. *Ecology* 82(8):2306-2319.
- Hoellein, T., J. Tank, S. Entekin, E. Rosi-Marshall, M. Stephen, and G. Lamberti. 2012. Effects of benthic habitat restoration on nutrient uptake and ecosystem metabolism in three headwater streams. *River Research and Applications* 28(9):1451-1461.
- Hoellein, T. J., J. L. Tank, E. J. Rosi-Marshall, and S. A. Entekin. 2009. Temporal variation in substratum-specific rates of N uptake and metabolism and their contribution at the stream-reach scale. *Journal of the North American Benthological Society* 28(2):305-318.
- Hoellein, T. J., J. L. Tank, E. J. Rosi-Marshall, S. A. Entekin, and G. A. Lamberti. 2007. Controls on spatial and temporal variation of nutrient uptake in three Michigan headwater streams. *Limnology and Oceanography* 52(5):1964-1977.
- Holland, E. A., B. H. Braswell, J. Sulzman, and J.-F. Lamarque. 2005. Nitrogen deposition onto the United States and Western Europe: Synthesis of observations and models. *Ecological Applications* 15(1):38-57.
- Howarth, R. W., G. Billen, D. Swaney, A. Townsend, N. Jaworski, K. Lajtha, J. Downing, R. Elmgren, N. Caraco, and T. Jordan. 1996. Regional nitrogen budgets and riverine N & P fluxes for the drainages to the North Atlantic Ocean: Natural and human influences. *Biogeochemistry* 35(1):75-139.
- Inamdar, S., G. Dhillon, S. Singh, S. Dutta, D. Levia, D. Scott, M. Mitchell, J. Van Stan, and P. McHale. 2013. Temporal variation in end-member chemistry and its influence on runoff mixing patterns in a forested, piedmont catchment. *Water Resources Research* 49(4):1828-1844.
- Inamdar, S., N. Finger, S. Singh, M. Mitchell, D. Levia, H. Bais, D. Scott, and P. McHale. 2011a. Dissolved organic matter (DOM) concentration and quality in a forested mid-Atlantic watershed, USA. *Biogeochemistry* 108(1-3):55-76.
- Inamdar, S., S. Singh, S. Dutta, D. Levia, M. Mitchell, D. Scott, H. Bais, and P. McHale. 2011b. Fluorescence characteristics and sources of dissolved organic matter for stream water during storm events in a forested mid-Atlantic watershed. *Journal of Geophysical Research: Biogeosciences* 116(G03043):1-23.
- Inamdar, S. P., and M. J. Mitchell. 2007. Storm event exports of dissolved organic nitrogen (DON) across multiple catchments in a glaciated forested watershed. *Journal of Geophysical Research: Biogeosciences* 112(G2):1-18.
- Izagirre, O., A. Argerich, E. Martí, and A. Elosegi. 2012. Nutrient uptake in a stream affected by hydropower plants: Comparison between stream channels and diversion canals. *Hydrobiologia*:1-12.

- Jaworski, N. A., P. M. Groffman, A. A. Keller, and J. C. Prager. 1992. A watershed nitrogen and phosphorus balance: The upper Potomac River basin. *Estuaries* 15(1):83-95.
- Jin, L., D. M. Andrews, G. H. Holmes, H. Lin, and S. L. Brantley. 2011. Opening the “black box”: Water chemistry reveals hydrological controls on weathering in the Susquehanna Shale Hills Critical Zone Observatory *Vadose Zone Journal* 10(3):928-942.
- Johnson, L. T., and J. L. Tank. 2009. Diurnal variations in dissolved organic matter and ammonium uptake in six open-canopy streams. *Journal of the North American Benthological Society* 28(3):694-708.
- Johnson, L. T., J. L. Tank, and C. P. Arango. 2009. The effect of land use on dissolved organic carbon and nitrogen uptake in streams. *Freshwater Biology* 54(11):2335-2350.
- Jones Jr., J. B., R. A. Berner, P. S. Meadows, B. Durand, and G. Eglinton. 1985. Microbes and microbial processes in sediments. *Philosophical Transactions of the Royal Society of London. Series A, Mathematical and Physical Sciences* 315(1531):3-17.
- Jones Jr., J. B., S. G. Fisher, and N. B. Grimm. 1995. Nitrification in the hyporheic zone of a desert stream ecosystem. *Journal of the North American Benthological Society* 14(2):249-258.
- Jordan, T. E., D. L. Correll, and D. E. Weller. 1993. Nutrient interception by a riparian forest receiving inputs from adjacent cropland. *Journal of Environmental Quality* 22(3):467-473.
- Jordan, T. E., D. L. Correll, and D. E. Weller. 1997a. Nonpoint source discharges of nutrients from Piedmont watersheds of Chesapeake Bay. *Journal of the American Water Resources Association* 33(3):631-645.
- Jordan, T. E., D. L. Correll, and D. E. Weller. 1997b. Relating nutrient discharges from watersheds to land use and streamflow variability. *Water Resources Research* 33(11):2579-2590.
- Jordan, T. E., D. L. Correll, D. E. Weller, and N. M. Goff. 1995. Temporal variation in precipitation chemistry on the shore of the Chesapeake Bay. *Water, Air, and Soil Pollution* 83(3-4):263-284.
- Kaplan, L. A., R. A. Larson, and T. L. Bott. 1980. Patterns of dissolved organic carbon in transport. *Limnology and Oceanography* 25(6):1034-1043.
- Kaplan, L. A., T. N. Wiegner, J. Newbold, P. H. Ostrom, and H. Gandhi. 2008. Untangling the complex issue of dissolved organic carbon uptake: A stable isotope approach. *Freshwater Biology* 53(5):855-864.
- Kasahara, T., and A. R. Hill. 2006. Effects of riffle step restoration on hyporheic zone chemistry in N-rich lowland streams. *Canadian Journal of Fisheries and Aquatic Sciences* 63(1):120-133.
- Kaushal, S. S., and W. M. Lewis, Jr. 2005. Fate and transport of organic nitrogen in minimally disturbed montane streams of Colorado, USA. *Biogeochemistry* 74(3):303-321.
- Keene, W., J. Montag, J. Maben, M. Southwell, J. Leonard, T. Church, J. Moody, and J. Galloway.

2002. Organic nitrogen in precipitation over Eastern North America. *Atmospheric Environment* 36(28):4529-4540.
- Kemp, M. J., and W. K. Dodds. 2002. Comparisons of nitrification and denitrification in prairie and agriculturally influenced streams. *Ecological Applications* 12(4):998-1009.
- Kent, R., K. Belitz, and C. A. Burton. 2005. Algal productivity and nitrate assimilation in an effluent dominated concrete lined stream. *Journal of the American Water Resources Association* 41(5):1109-1128.
- Klingaman, N. P., D. F. Levia, and E. E. Frost. 2007. A comparison of three canopy interception models for a leafless mixed deciduous forest stand in the Eastern United States. *Journal of Hydrometeorology* 8(4):825-836.
- Klocker, C. A., S. S. Kaushal, P. M. Groffman, P. M. Mayer, and R. P. Morgan II. 2009. Nitrogen uptake and denitrification in restored and unrestored streams in urban Maryland, USA. *Aquatic Sciences* 71(4):411-424.
- Klotz, R. L. 2010. Reduction of high nitrate concentrations in a Central New York State stream impounded by beaver. *Northeastern Naturalist* 17(3):349-356.
- Knapp, C. W., W. K. Dodds, K. C. Wilson, J. M. O'Brien, and D. W. Graham. 2009. Spatial heterogeneity of denitrification genes in a highly homogenous urban stream. *Environmental science & technology* 43(12):4273-4279.
- Knowles, R. 1982. Denitrification. *Microbiological reviews* 46(1):43-70.
- Krause, S., D. Hannah, J. Fleckenstein, C. Heppell, D. Kaeser, R. Pickup, G. Pinay, A. Robertson, and P. Wood. 2011. Inter-disciplinary perspectives on processes in the hyporheic zone. *Ecohydrology* 4(4):481-499.
- Kuserk, F. T., L. A. Kaplan, and T. L. Bott. 1984. In situ measures of dissolved organic carbon flux in a rural stream. *Canadian Journal of Fisheries and Aquatic Sciences* 41(6):964-973.
- Lake, P. S. 2003. Ecological effects of perturbation by drought in flowing waters. *Freshwater Biology* 48(7):1161-1172.
- Lamberti, G. A., S. V. Gregory, L. R. Ashkenas, R. C. Wildman, and A. D. Steinman. 1989. Influence of channel geomorphology on retention of dissolved and particulate matter in a Cascade Mountain stream. US Department of Agriculture.
- Lautz, L., and R. Fanelli. 2008. Seasonal biogeochemical hotspots in the streambed around restoration structures. *Biogeochemistry* 91(1):85-104.
- Lawrence, G. B., G. M. Lovett, and Y. H. Baevsky. 2000. Atmospheric deposition and watershed nitrogen export along an elevational gradient in the Catskill Mountains, New York. *Biogeochemistry* 50(1):21-43.

Lefebvre, S., P. Marmonier, and J.-L. Peiry. 2006. Nitrogen dynamics in rural streams: Differences between geomorphologic units. *Annales de Limnologie* 42(1):43-52.

Levia, D., J. Van Stan II, S. Mage, and P. Kelley-Hauske. 2010. Temporal variability of stemflow volume in a beech-yellow poplar forest in relation to tree species and size. *Journal of Hydrology* 380(1):112-120.

Levia, D. F., J. T. Van Stan II, C. M. Siegert, S. P. Inamdar, M. J. Mitchell, S. M. Mage, and P. J. McHale. 2011. Atmospheric deposition and corresponding variability of stemflow chemistry across temporal scales in a mid-Atlantic broadleaved deciduous forest. *Atmospheric Environment* 45(18):3046-3054.

Lewis, G. P., and G. E. Likens. 2007. Changes in stream chemistry associated with insect defoliation in a Pennsylvania hemlock-hardwoods forest. *Forest ecology and management* 238(1):199-211.

Lindsey, B. D., S. W. Phillips, C. A. Donnelly, G. K. Speiran, L. N. Plummer, J.-K. Böhlke, M. J. Focazio, W. C. Burton, and E. Busenberg. 2003. *Residence times and nitrate transport in ground water discharging to streams in the Chesapeake Bay Watershed*. USGS Water-Resources Investigations Report 03-4035. US Department of the Interior, US Geological Survey, New Cumberland, Pennsylvania.

Liu, Z.-J., D. E. Weller, D. L. Correll, and T. E. Jordan. 2000. Effects of land cover and geology on stream chemistry in watersheds of Chesapeake Bay. *Journal of the American Water Resources Association* 36(6):1349-1365.

Lovett, G. M., K. C. Weathers, and W. V. Sobczak. 2000. Nitrogen saturation and retention in forested watersheds of the Catskill Mountains, New York. *Ecological Applications* 10(1):73-84.

Lowe, W. H., and G. E. Likens. 2005. Moving headwater streams to the head of the class. *BioScience* 55(3):196-197.

Lowrance, R., L. S. Altier, J. D. Newbold, R. R. Schnabel, P. M. Groffman, J. M. Denver, D. L. Correll, J. W. Gilliam, J. L. Robinson, and R. B. Brinsfield. 1997. Water quality functions of riparian forest buffers in Chesapeake Bay watersheds. *Environmental Management* 21(5):687-712.

Lutz, B. D., E. S. Bernhardt, B. J. Roberts, and P. J. Mulholland. 2011. Examining the coupling of carbon and nitrogen cycles in Appalachian streams: The role of dissolved organic nitrogen. *Ecology* 92(3):720-732.

Lynch, J. A., and E. S. Corbett. 1990. Evaluation of best management practices for controlling nonpoint pollution from silvicultural operations. *Journal of the American Water Resources Association* 26(1):41-52.

Lynch, J. A., and E. S. Corbett. 1991. Long-term implications of forest harvesting on nutrient cycling in central hardwood forests. In *8th Central Hardwood Forest Conference*. University Park, Pennsylvania: United States Department of Agriculture, Forest Service, Northeastern Forest Experimental Station.

- Lynch, J. A., and E. S. Corbett. 1994. Nitrate export from managed and unmanaged forested watersheds in the Chesapeake Bay Watershed. In *Toward a Sustainable Coastal Watershed: The Chesapeake Experiment*. Norfolk, VA: Chesapeake Research Consortium.
- Lynch, J. A., E. S. Corbett, and K. Mussallem. 1985. Best management practices for controlling nonpoint-source pollution on forested watersheds. *Journal of soil and water conservation* 40(1):164-167.
- Manzoni, S., and A. Porporato. 2011. Common hydrologic and biogeochemical controls along the soil–stream continuum. *Hydrological Processes* 25(8):1355-1360.
- Maret, T. J., M. Parker, and T. E. Fannin. 1987. The effect of beaver ponds on the nonpoint source water quality of a stream in southwestern Wyoming. *Water Research* 21(3):263-268.
- Margolis, B. E., M. S. Castro, and R. L. Raesly. 2001. The impact of beaver impoundments on the water chemistry of two Appalachian streams. *Canadian Journal of Fisheries and Aquatic Sciences* 58(11):2271-2283.
- Martin, R. A., and J. A. Harrison. 2011. Effect of high flow events on in-stream dissolved organic nitrogen concentration. *Ecosystems* 14(8):1328-1338.
- McClain, M. E., E. W. Boyer, C. L. Dent, S. E. Gergel, N. B. Grimm, P. M. Groffman, S. C. Hart, J. W. Harvey, C. A. Johnston, and E. Mayorga. 2003. Biogeochemical hot spots and hot moments at the interface of terrestrial and aquatic ecosystems. *Ecosystems* 6(4):301-312.
- McGuire, K. J., D. R. DeWalle, and W. J. Gburek. 2002. Evaluation of mean residence time in subsurface waters using oxygen-18 fluctuations during drought conditions in the mid-Appalachians. *Journal of Hydrology* 261(1–4):132-149.
- McHale, M. R., D. A. Burns, G. B. Lawrence, and P. S. Murdoch. 2007. Factors controlling soil water and stream water aluminum concentrations after a clearcut in a forested watershed with calcium-poor soils. *Biogeochemistry* 84(3):311-331.
- McMillan, S. K., M. F. Piehler, S. P. Thompson, and H. W. Paerl. 2010. Denitrification of nitrogen released from senescing algal biomass in coastal agricultural headwater streams. *Journal of Environmental Quality* 39(1):274-281.
- MDE. 2017. Previous conditions. Baltimore, MD: Maryland Department of the Environment, Water Supply Program.
- Meyer, J. 1994. The microbial loop in flowing waters. *Microbial Ecology* 28(2):195-199.
- Meyer, J., L. Kaplan, D. Newbold, D. Strayer, C. Woltemade, J. Zedler, R. Beilfuss, Q. Carpenter, R. Semlitsch, and M. Watzin. 2003. *Where rivers are born: The scientific imperative for defending small streams and wetlands*. American Rivers and the Sierra Club, Washington, DC.
- Meyer, J. L., J. B. Wallace, and S. L. Eggert. 1998. Leaf litter as a source of dissolved organic carbon in streams. *Ecosystems* 1(3):240-249.



- Miller, C. V., J. M. Denis, S. W. Ator, and J. W. Brakebill. 1997. Nutrients in streams during baseflow in selected environmental settings of the Potomac River Basin. *Journal of the American Water Resources Association* 33(6):1155-1171.
- Miltner, R. J., and E. T. Rankin. 1998. Primary nutrients and the biotic integrity of rivers and streams. *Freshwater Biology* 40(1):145-158.
- Minshall, G. 1978. Autotrophy in stream ecosystems. *BioScience* 28(12):767-771.
- Mitchell, M. J. 2001. Linkages of nitrate losses in watersheds to hydrological processes. *Hydrological Processes* 15(17):3305-3307.
- Morgan II, R. P., and K. M. Kline. 2011. Nutrient concentrations in Maryland non-tidal streams. *Environmental Monitoring and Assessment* 178(1-4):221-235.
- Morgan II, R. P., K. M. Kline, and J. B. Churchill. 2013. Estimating reference nutrient criteria for Maryland ecoregions. *Environmental Monitoring and Assessment* 185(3):2123-2137.
- Morrice, J. A., C. N. Dahm, H. M. Valett, P. V. Unnikrishna, and M. E. Campana. 2000. Terminal electron accepting processes in the alluvial sediments of a headwater stream. *Journal of the North American Benthological Society* 19(4):593-608.
- Mulholland, P. J. 1992. Regulation of nutrient concentrations in a temperate forest stream: Roles of upland, riparian, and instream processes. *Limnology and Oceanography* 37(7):1512-1526.
- Mulholland, P. J. 2004. The importance of in-stream uptake for regulating stream concentrations and outputs of N and P from a forested watershed: Evidence from long-term chemistry records for Walker Branch Watershed. *Biogeochemistry* 70(3):403-426.
- Mulholland, P. J., A. M. Helton, G. C. Poole, R. O. Hall, S. K. Hamilton, B. J. Peterson, J. L. Tank, L. R. Ashkenas, L. W. Cooper, and C. N. Dahm. 2008. Stream denitrification across biomes and its response to anthropogenic nitrate loading. *Nature* 452(7184):202-205.
- Mulholland, P. J., and W. R. Hill. 1997. Seasonal patterns in streamwater nutrient and dissolved organic carbon concentrations: Separating catchment flow path and in-stream effects. *Water Resources Research* 33(6):1297-1306.
- Mulholland, P. J., E. R. Marzolf, J. R. Webster, D. R. Hart, and S. P. Hendricks. 1997. Evidence that hyporheic zones increase heterotrophic metabolism and phosphorus uptake in forest streams. *Limnology and Oceanography* 42(3):443-451.
- Mulholland, P. J., and A. D. Rosemond. 1992. Periphyton response to longitudinal nutrient depletion in a woodland stream: Evidence of upstream-downstream linkage. *Journal of the North American Benthological Society* 11(4):405-419.
- Mulholland, P. J., J. L. Tank, D. M. Sanzone, W. M. Wollheim, B. J. Peterson, J. R. Webster, and J. L. Meyer. 2000. Nitrogen cycling in a forest stream determined by a <sup>15</sup>N tracer addition. *Ecological Monographs* 70(3):471-493.

- Munn, N. L., and J. L. Meyer. 1990. Habitat-specific solute retention in two small streams: An intersite comparison. *Ecology* 71(6):2069-2082.
- Nadelhoffer, K., M. Downs, B. Fry, A. Magill, and J. Aber. 1999. Controls on N retention and exports in a forested watershed. *Environmental Monitoring and Assessment* 55(1):187-210.
- Najjar, R. G., C. R. Pyke, M. B. Adams, D. Breitburg, C. Hershner, M. Kemp, R. Howarth, M. R. Mulholland, M. Paolisso, and D. Secor. 2010. Potential climate-change impacts on the Chesapeake Bay. *Estuarine, Coastal and Shelf Science* 86(1):1-20.
- Neff, J. C., E. A. Holland, F. J. Dentener, W. H. McDowell, and K. M. Russell. 2002. The origin, composition and rates of organic nitrogen deposition: A missing piece of the nitrogen cycle? *Biogeochemistry* 57(1):99-136.
- Nestler, A., M. Berglund, F. Accoe, S. Duta, D. Xue, P. Boeckx, and P. Taylor. 2011. Isotopes for improved management of nitrate pollution in aqueous resources: Review of surface water field studies. *Environmental Science and Pollution Research* 18(4):519-533.
- Newbold, J., T. Bott, L. Kaplan, B. Sweeney, and R. Vannote. 1997. Organic matter dynamics in White Clay Creek, Pennsylvania, USA. *Journal of the North American Benthological Society* 16(1):46-50.
- Newbold, J. D., T. L. Bott, L. A. Kaplan, C. L. Dow, J. K. Jackson, A. K. Aufdenkampe, L. A. Martin, D. J. V. Horn, and A. A. Long. 2006. Uptake of nutrients and organic C in streams in New York City drinking-water-supply watersheds. *Journal of the North American Benthological Society* 25(4):998-1017.
- Newbold, J. D., J. W. Elwood, M. S. Schulze, R. W. Stark, and J. C. Barmeier. 1983. Continuous ammonium enrichment of a woodland stream: Uptake kinetics, leaf decomposition, and nitrification. *Freshwater Biology* 13(2):193-204.
- Newbold, J. D., S. Herbert, B. W. Sweeney, P. Kiry, and S. J. Alberts. 2010. Water quality functions of a 15-year-old riparian forest buffer system. *Journal of the American Water Resources Association* 46(2):299-310.
- Newcomer, T. A., S. S. Kaushal, P. M. Mayer, A. R. Shields, E. A. Canuel, P. M. Groffman, and A. J. Gold. 2012. Influence of natural and novel organic carbon sources on denitrification in forest, degraded urban, and restored streams. *Ecological Monographs* 82(4):449-466.
- Nimick, D. A., C. H. Gammons, and S. R. Parker. 2011. Diel biogeochemical processes and their effect on the aqueous chemistry of streams: A review. *Chemical Geology* 283(1-2):3-17.
- NOAA. 2010. State of the Climate: Drought for September 2010. NOAA National Centers for Environmental Information.
- NOAA. 2012. NOAA solar calculator. Earth Systems Research Laboratory Global Monitoring Division.

NRCC. 2010. Northeast overview - September 2010. Ithaca, NY: Northeast Regional Climate Center.

O'Connor, B. L., M. Hondzo, and J. W. Harvey. 2009. Predictive modeling of transient storage and nutrient uptake: Implications for stream restoration. *Journal of Hydraulic Engineering* 136(12):1018-1032.

Olmsted, F. H., and A. G. Hely. 1962. *Relation between ground water and surface water in Brandywine Creek Basin, Pennsylvania*. USGS Professional Paper 417-A. US Government Printing Office.

Opdyke, M. R., M. B. David, and B. L. Rhoads. 2006. Influence of geomorphological variability in channel characteristics on sediment denitrification in agricultural streams. *Journal of Environmental Quality* 35(6):2103-2112.

Paerl, H. W. 1984. Alteration of microbial metabolic activities in association with detritus. *Bulletin of Marine Science* 35(3):393-408.

Pan, Y., J. Hom, R. Birdsey, and K. McCullough. 2004. Impacts of rising nitrogen deposition on N exports from forests to surface waters in the Chesapeake Bay Watershed. *Environmental Management* 33(1):S120-S131.

Passeport, E., P. Vidon, K. J. Forshay, L. Harris, S. S. Kaushal, D. Q. Kellogg, J. Lazar, P. Mayer, and E. K. Stander. 2013. Ecological engineering practices for the reduction of excess nitrogen in human-influenced landscapes: A guide for watershed managers. *Environmental Management* 51(2):392-413.

Pellerin, B. A., S. S. Kaushal, and W. H. McDowell. 2006. Does anthropogenic nitrogen enrichment increase organic nitrogen concentrations in runoff from forested and human-dominated watersheds? *Ecosystems* 9(5):852-864.

Peterjohn, W. T., M. B. Adams, and F. S. Gilliam. 1996. Symptoms of nitrogen saturation in two central Appalachian hardwood forest ecosystems. *Biogeochemistry* 35(3):507-522.

Peterjohn, W. T., and D. L. Correll. 1984. Nutrient dynamics in an agricultural watershed: Observations on the role of a riparian forest. *Ecology* 65(5):1466-1475.

Peterson, B. J., W. M. Wollheim, P. J. Mulholland, J. R. Webster, J. L. Meyer, J. L. Tank, E. Martí, W. B. Bowden, H. M. Valett, and A. E. Hershey. 2001. Control of nitrogen export from watersheds by headwater streams. *Science* 292(5514):86-90.

Peterson, E. W., and C. Benning. 2013. Factors influencing nitrate within a low-gradient agricultural stream. *Environmental Earth Sciences* 68(5):1233-1245.

Petrone, K. C., J. S. Richards, and P. F. Grierson. 2009. Bioavailability and composition of dissolved organic carbon and nitrogen in a near coastal catchment of south-western Australia. *Biogeochemistry* 92(1-2):27-40.

- Pionke, H., W. Gburek, R. Schnabel, A. Sharpley, and G. Elwinger. 1999. Seasonal flow, nutrient concentrations and loading patterns in stream flow draining an agricultural hill-land watershed. *Journal of Hydrology* 220(1):62-73.
- Plummer, L. N., E. Busenberg, J. K. Böhlke, D. L. Nelms, R. L. Michel, and P. Schlosser. 2001. Groundwater residence times in Shenandoah National Park, Blue Ridge Mountains, Virginia, USA: a multi-tracer approach. *Chemical Geology* 179(1-4):93-111.
- Powell, K. L., and V. Bouchard. 2010. Is denitrification enhanced by the development of natural fluvial morphology in agricultural headwater ditches? *Journal of the North American Benthological Society* 29(2):761-772.
- Powers, S. M., R. A. Johnson, and E. H. Stanley. 2012. Nutrient retention and the problem of hydrologic disconnection in streams and wetlands. *Ecosystems* 15(3):435-449.
- Prospero, J., K. Barrett, T. Church, F. Dentener, R. Duce, J. Galloway, H. Levy II, J. Moody, and P. Quinn. 1996. Atmospheric deposition of nutrients to the North Atlantic Basin. *Biogeochemistry* 35(1):27-73.
- Rathbun, T. 2010. DEP declares statewide drought watches, warnings: Below-normal rainfall leads to water deficits. Commonwealth of Pennsylvania, Department of Environmental Protection: Commonwealth News Bureau.
- Reddy, K. R., R. H. Kadlec, E. Flaig, and P. M. Gale. 1999. Phosphorus retention in streams and wetlands: A review. *Critical Reviews in Environmental Science and Technology* 29(1):83-146.
- Redfield, A. C. 1958. The biological control of chemical factors in the environment. *American scientist* 46(3):205-221.
- Rentch, J. S., and R. R. Hicks. 1999. *Nutrient fluxes for two small forested watersheds : Sixteen-year results from the West Virginia University forest*. Bulletin 724. West Virginia University, Agricultural and Forestry Experiment Station, Morgantown, WV.
- Riscassi, A. L., and T. M. Scanlon. 2009. Nitrate variability in hydrological flow paths for three mid-Appalachian forested watersheds following a large-scale defoliation. *Journal of Geophysical Research: Biogeosciences* 114(G2):1-11.
- Roberts, B., P. Mulholland, and W. Hill. 2007a. Multiple scales of temporal variability in ecosystem metabolism rates: Results from 2 years of continuous monitoring in a forested headwater stream. *Ecosystems* 10(4):588-606.
- Roberts, B. J., and P. J. Mulholland. 2007. In-stream biotic control on nutrient biogeochemistry in a forested stream, West Fork of Walker Branch. *Journal of Geophysical Research: Biogeosciences* 112(G04002):1-11.
- Roberts, B. J., P. J. Mulholland, and J. N. Houser. 2007b. Effects of upland disturbance and instream restoration on hydrodynamics and ammonium uptake in headwater streams. *Journal of the North American Benthological Society* 26(1):38-53.

- Robertson, W., and L. Merkley. 2009. In-stream bioreactor for agricultural nitrate treatment. *Journal of Environmental Quality* 38(1):230-237.
- Roley, S. S., J. L. Tank, M. L. Stephen, L. T. Johnson, J. J. Beaulieu, and J. D. Witter. 2012a. Floodplain restoration enhances denitrification and reach-scale nitrogen removal in an agricultural stream. *Ecological Applications* 22(1):281-297.
- Roley, S. S., J. L. Tank, and M. A. Williams. 2012b. Hydrologic connectivity increases denitrification in the hyporheic zone and restored floodplains of an agricultural stream. *Journal of Geophysical Research: Biogeosciences* 117(G00N04):1-16.
- Runkel, R. L. 2007. Toward a transport-based analysis of nutrient spiraling and uptake in streams. *Limnology and Oceanography: Methods* 5:50-62.
- Rupert, C., and K. O'Hara. 2010a. DRBC declares lower basin drought warning. West Trenton, NJ: Delaware River Basin Commission.
- Rupert, C., and K. O'Hara. 2010b. DRBC lifts lower basin drought warning. West Trenton, NJ: Delaware River Basin Commission.
- Rusanov, A. G., H.-P. Grossart, and M. T. Pusch. 2009. Periphytic bacterial and algal response to a hydraulic gradient under different light levels: Test of algal-bacterial coupling in the laboratory. *Fundamental and Applied Limnology/Archiv für Hydrobiologie* 175(4):339-353.
- Russell, K. M., J. N. Galloway, S. A. Macko, J. L. Moody, and J. R. Scudlark. 1998. Sources of nitrogen in wet deposition to the Chesapeake Bay region. *Atmospheric Environment* 32(14):2453-2465.
- Rutledge, A., and T. O. Mesko. 1996. *Regional Aquifer-System Analysis-Appalachian Valley and Piedmont: Estimated hydrologic characteristics of shallow aquifer systems in the Valley and Ridge, the Blue Ridge, and the Piedmont physiographic provinces based on analysis of streamflow recession and base flow*. USGS Professional Paper 1422-B.
- Sabater, S., H. Guasch, I. Muñoz, and A. Romani. 2006. Hydrology, light and the use of organic and inorganic materials as structuring factors of biological communities in Mediterranean streams. *Limnetica* 25(1-2):335-348.
- Scanlon, T. M., S. M. Ingram, and A. L. Riscassi. 2010. Terrestrial and in-stream influences on the spatial variability of nitrate in a forested headwater catchment. *Journal of Geophysical Research: Biogeosciences* 115(G02022):1-12.
- Scott, D., J. Harvey, R. Alexander, and G. Schwarz. 2007. Dominance of organic nitrogen from headwater streams to large rivers across the conterminous United States. *Global Biogeochemical Cycles* 21(GB1003):1-8.
- Scudlark, J., K. Russell, J. Galloway, T. Church, and W. Keene. 1998. Organic nitrogen in precipitation at the mid-Atlantic US coast—methods evaluation and preliminary measurements. *Atmospheric Environment* 32(10):1719-1728.

- Scudlark, J. R., J. A. Jennings, M. J. Roadman, K. B. Savidge, and W. J. Ullman. 2005. Atmospheric nitrogen inputs to the Delaware Inland Bays: The role of ammonia. *Environmental Pollution* 135(3):433-443.
- Seitzinger, S., J. A. Harrison, J. Böhlke, A. Bouwman, R. Lowrance, B. Peterson, C. Tobias, and G. V. Drecht. 2006. Denitrification across landscapes and waterscapes: A synthesis. *Ecological Applications* 16(6):2064-2090.
- Seitzinger, S., and R. Sanders. 1999. Atmospheric inputs of dissolved organic nitrogen stimulate estuarine bacteria and phytoplankton. *Limnology and Oceanography* 44(3):721-730.
- Servais, P., G. Billen, and M.-C. Hascoët. 1987. Determination of the biodegradable fraction of dissolved organic matter in waters. *Water Research* 21(4):445-450.
- Sheeder, S. A., J. A. Lynch, and J. Grimm. 2002. Modeling atmospheric nitrogen deposition and transport in the Chesapeake Bay watershed. *Journal of Environmental Quality* 31(4):1194-1206.
- Shields, C. A., L. E. Band, N. Law, P. M. Groffman, S. S. Kaushal, K. Savvas, G. T. Fisher, and K. T. Belt. 2008. Streamflow distribution of non-point source nitrogen export from urban-rural catchments in the Chesapeake Bay watershed. *Water Resources Research* 44(W09416):1-13.
- Simon, K. S., and E. F. Benfield. 2002. Ammonium retention and whole-stream metabolism in cave streams. *Hydrobiologia* 482(1-3):31-39.
- Sinnott, A., and E. M. Cushing. 1978. *Summary appraisals of the nation's ground-water resource - mid-Atlantic region*. USGS Professional Paper 813-I.
- Sinsabaugh, R. L. 1997. Large-scale trends for stream benthic respiration. *Journal of the North American Benthological Society* 16(1):119-122.
- Sivirichi, G. M., S. S. Kaushal, P. M. Mayer, C. Welty, K. T. Belt, T. A. Newcomer, K. D. Newcomb, and M. M. Grese. 2011. Longitudinal variability in streamwater chemistry and carbon and nitrogen fluxes in restored and degraded urban stream networks. *Journal of Environmental Monitoring* 13(2):288-303.
- Sloto, R. A. 2002. *Geohydrology and ground water quality, Big Elk Creek basin, Chester County, Pennsylvania, and Cecil County, Maryland*. USGS Water-Resources Investigations Report 02-4057. US Department of the Interior, US Geological Survey, Chester County Water Resources Authority, Chester County Health Department.
- Smith, M. 2010. DEP drought watches, warnings lifted for 46 Counties 21 western counties now under drought watch. Commonwealth of Pennsylvania, Department of Environmental Protection: Commonwealth News Bureau.
- Snyder, N., S. Mostaghimi, D. Berry, R. Reneau, S. Hong, P. W. McClellan, and E. Smith. 1998. Impact of riparian forest buffers on agricultural nonpoint source pollution. *Journal of the American Water Resources Association* 34(2):385-395.

- Sobczak, W. V., and S. Findlay. 2002. Variation in bioavailability of dissolved organic carbon among stream hyporheic flowpaths. *Ecology* 83(11):3194-3209.
- Sobczak, W. V., S. Findlay, and S. Dye. 2003. Relationships between DOC bioavailability and nitrate removal in an upland stream: An experimental approach. *Biogeochemistry* 62(3):309-327.
- Sophocleous, M. 2002. Interactions between groundwater and surface water: The state of the science. *Hydrogeology Journal* 10(1):52-67.
- Speiran, G. 2003. Polecat Creek Watershed, Virginia. In *Residence times and nitrate transport in ground water discharging to streams in the Chesapeake Bay Watershed*, 71-87. B. D. Lindsey, S. W. Phillips, C. A. Donnelly, G. K. Speiran, L. N. Plummer, J.-K. Böhlke, M. J. Focazio, W. C. Burton, and E. Busenberg, eds. New Cumberland, Pennsylvania: US Department of the Interior, US Geological Survey.
- Speiran, G. K. 2010. Effects of groundwater-flow paths on nitrate concentrations across two riparian forest corridors. *Journal of the American Water Resources Association* 46(2):246-260.
- Sprague, E., D. Burke, S. Claggett, and A. Todd. 2006. *The State of Chesapeake Forest*. Conservation Fund.
- Stanley, E. H., and M. W. Doyle. 2002. A geomorphic perspective on nutrient retention following dam removal. *BioScience* 52(8):693-701.
- Starry, O. S., H. M. Valett, and M. E. Schreiber. 2005. Nitrification rates in a headwater stream: Influences of seasonal variation in C and N supply. *Journal of the North American Benthological Society* 24(4):753-768.
- Stewart, R. J., W. M. Wollheim, M. N. Gooseff, M. A. Briggs, J. M. Jacobs, B. J. Peterson, and C. S. Hopkinson. 2011. Separation of river network-scale nitrogen removal among the main channel and two transient storage compartments. *Water Resources Research* 47(W00J10):1-19.
- Storey, R., R. Fulthorpe, and D. Williams. 1999. Perspectives and predictions on the microbial ecology of the hyporheic zone. *Freshwater Biology* 41(1):119-130.
- Strauss, E. A., and G. A. Lamberti. 2000. Regulation of nitrification in aquatic sediments by organic carbon. *Limnology and Oceanography* 45(8):1854-1859.
- Strauss, E. A., N. L. Mitchell, and G. A. Lamberti. 2002. Factors regulating nitrification in aquatic sediments: Effects of organic carbon, nitrogen availability, and pH. *Canadian Journal of Fisheries and Aquatic Sciences* 59(3):554-563.
- Sudduth, E. B., B. A. Hassett, P. Cada, and E. S. Bernhardt. 2011. Testing the field of dreams hypothesis: Functional responses to urbanization and restoration in stream ecosystems. *Ecological Applications* 21(6):1972-1988.
- Swank, W. T., and J. M. Vose. 1997. Long-term nitrogen dynamics of Coweeta Forested Watersheds in the southeastern United States of America. *Global Biogeochemical Cycles*

11(4):657-671.

Sweeney, B. W. 1992. Streamside forests and the physical, chemical, and trophic characteristics of piedmont streams in eastern North America. *Water Science and Technology* 26(12):2653-2673.

Tank, J. L., J. L. Meyer, D. M. Sanzone, P. J. Mulholland, J. R. Webster, B. J. Peterson, W. M. Wollheim, and N. E. Leonard. 2000. Analysis of nitrogen cycling in a forest stream during autumn using a <sup>15</sup>N-tracer addition. *Limnology and Oceanography* 45(5):1013-1029.

Tank, J. L., and J. Webster. 1998. Interaction of substrate and nutrient availability on wood biofilm processes in streams. *Ecology* 79(6):2168-2179.

Taylor, P. G., and A. R. Townsend. 2010. Stoichiometric control of organic carbon–nitrate relationships from soils to the sea. *Nature* 464(7292):1178-1181.

Thomas, S., H. Valett, P. Mulholland, C. Fellows, J. Webster, C. Dahm, and C. Peterson. 2001. Nitrogen retention in headwater streams: The influence of groundwater-surface water exchange. *The Scientific World Journal* 1:623-631.

Thomas, S. A., H. Maurice Valett, J. R. Webster, and P. J. Mulholland. 2003. A regression approach to estimating reactive solute uptake in advective and transient storage zones of stream ecosystems. *Advances in Water Resources* 26(9):965-976.

Thurman, E. M. 1985. *Organic geochemistry of natural waters*. Martinus Nijhoff/ Dr. W. Junk Publishers, Dordrecht, the Netherlands.

Tiedje, J. M., A. J. Sexstone, D. D. Myrold, and J. A. Robinson. 1983. Denitrification: Ecological niches, competition and survival. *Antonie van Leeuwenhoek* 48(6):569-583.

Trimmer, M., J. Grey, C. M. Heppell, A. G. Hildrew, K. Lansdown, H. Stahl, and G. Yvon-Durocher. 2012. River bed carbon and nitrogen cycling: State of play and some new directions. *Science of the Total Environment* 434:143–158.

Triska, F. J., J. H. Duff, and R. J. Avanzino. 1993. The role of water exchange between a stream channel and its hyporheic zone in nitrogen cycling at the terrestrial—aquatic interface. *Hydrobiologia* 251(1-3):167-184.

Valett, H., C. Dahm, M. Campana, J. Morrice, M. A. Baker, and C. Fellows. 1997. Hydrologic influences on groundwater-surface water ecotones: Heterogeneity in nutrient composition and retention. *Journal of the North American Benthological Society* 16(1):239-247.

Valett, H., J. Morrice, C. Dahm, and M. Campana. 1996. Parent lithology, surface-groundwater exchange, and nitrate retention in headwater streams. *Limnology and Oceanography* 41(2):333-345.

Valett, H., S. Thomas, P. Mulholland, J. Webster, C. Dahm, C. S. Fellows, C. Crenshaw, and C. Peterson. 2008. Endogenous and exogenous control of ecosystem function: N cycling in headwater streams. *Ecology* 89(12):3515-3527.



- Valett, H. M. 1993. Surface-hyporheic interactions in a Sonoran Desert stream: Hydrologic exchange and diel periodicity. *Hydrobiologia* 259(3):133-144.
- Valett, H. M., S. G. Fisher, N. B. Grimm, and P. Camill. 1994. Vertical hydrologic exchange and ecological stability of a desert stream ecosystem. *Ecology* 75(2):548-560.
- van Niel, E., P. Arts, B. Wesselink, L. Robertson, and J. Kuenen. 1993. Competition between heterotrophic and autotrophic nitrifiers for ammonia in chemostat cultures. *FEMS Microbiology Letters* 102(2):109-118.
- Van Stan II, J. T., C. M. Siegert, D. F. Levia, and C. E. Scheick. 2011. Effects of wind-driven rainfall on stemflow generation between codominant tree species with differing crown characteristics. *Agricultural and Forest Meteorology* 151(9):1277-1286.
- Vannote, R. L., G. W. Minshall, K. W. Cummins, J. R. Sedell, and C. E. Cushing. 1980. The river continuum concept. *Canadian Journal of Fisheries and Aquatic Sciences* 37(1):130-137.
- Vazquez, E., S. Amalfitano, S. Fazi, and A. Butturini. 2011. Dissolved organic matter composition in a fragmented Mediterranean fluvial system under severe drought conditions. *Biogeochemistry* 102(1-3):59-72.
- Verhagen, F. J., and H. J. Laanbroek. 1991. Competition for ammonium between nitrifying and heterotrophic bacteria in dual energy-limited chemostats. *Applied and Environmental Microbiology* 57(11):3255-3263.
- Vidon, P., C. Allan, D. Burns, T. P. Duval, N. Gurwick, S. Inamdar, R. Lowrance, J. Okay, D. Scott, and S. Sebestyen. 2010. Hot spots and hot moments in riparian zones: Potential for improved water quality management. *Journal of the American Water Resources Association* 46(2):278-298.
- Vidon, P. G., and A. R. Hill. 2004. Landscape controls on nitrate removal in stream riparian zones. *Water Resources Research* 40(3):1-14.
- Vitousek, P. M., J. D. Aber, R. W. Howarth, G. E. Likens, P. A. Matson, D. W. Schindler, W. H. Schlesinger, and D. G. Tilman. 1997. Human alteration of the global nitrogen cycle: Sources and consequences. *Ecological Applications* 7(3):737-750.
- Vitousek, P. M., J. R. Gosz, C. C. Grier, J. M. Melillo, W. A. Reiners, and R. L. Todd. 1979. Nitrate losses from disturbed ecosystems. *Science* 204(4392):469-474.
- Volk, C. J., C. B. Volk, and L. A. Kaplan. 1997. Chemical composition of biodegradable dissolved organic matter in streamwater. *Limnology and Oceanography* 42(1):39-44.
- Wall, G. R., P. J. Phillips, and K. Riva-Murray. 1998. Seasonal and spatial patterns of nitrate and silica concentrations in Canajoharie Creek, New York. *Journal of Environmental Quality* 27(2):381-389.
- Wallace, J. B., J. R. Webster, and J. L. Meyer. 1995. Influence of log additions on physical and biotic characteristics of a mountain stream. *Canadian Journal of Fisheries and Aquatic Sciences*

52(10):2120-2137.

Wang, X., D. A. Burns, R. D. Yanai, R. D. Briggs, and R. H. Germain. 2006. Changes in stream chemistry and nutrient export following a partial harvest in the Catskill Mountains, New York, USA. *Forest ecology and management* 223(1):103-112.

Webb, J., B. Cosby, F. Deviney Jr, K. Eshleman, and J. Galloway. 1995. Change in the acid-base status of an Appalachian mountain catchment following forest defoliation by the gypsy moth. *Water, Air, and Soil Pollution* 85(2):535-540.

Webster, J. R., P. J. Mulholland, J. L. Tank, H. M. Valett, W. K. Dodds, B. J. Peterson, W. B. Bowden, C. N. Dahm, S. Findlay, and S. V. Gregory. 2003. Factors affecting ammonium uptake in streams—an inter-biome perspective. *Freshwater Biology* 48(8):1329-1352.

Webster, J. R., and H. M. Valett. 2006. Solute dynamics. In *Methods in stream ecology*, 169-185. R. Hauer, and G. A. Lamberti, eds. New York, NY: Academic Press.

Wetzel, R. G., and B. A. Manny. 1972. Decomposition of dissolved organic carbon and nitrogen compounds from leaves in an experimental hard-water stream. *Limnology and Oceanography* 17(6):927-931.

Wiegner, T. N., S. P. Seitzinger, P. M. Glibert, and D. A. Bronk. 2006. Bioavailability of dissolved organic nitrogen and carbon from nine rivers in the eastern United States. *Aquatic Microbial Ecology* 43(3):277-287.

Willett, V. B., B. A. Reynolds, P. A. Stevens, S. J. Ormerod, and D. L. Jones. 2004. Dissolved organic nitrogen regulation in freshwaters. *Journal of Environmental Quality* 33(1):201-209.

Williams, D. D. 1993. Nutrient and flow vector dynamics at the hyporheic/groundwater interface and their effects on the interstitial fauna. *Hydrobiologia* 251(1-3):185-198.

Williard, K. W., D. R. DeWalle, P. J. Edwards, and R. R. Schnabel. 1997. Indicators of nitrate export from forested watersheds of the mid-Appalachians, United States of America. *Global Biogeochemical Cycles* 11(4):649-656.

Williard, K. W., D. R. DeWalle, P. J. Edwards, and W. E. Sharpe. 2001. <sup>18</sup>O isotopic separation of stream nitrate sources in mid-Appalachian forested watersheds. *Journal of Hydrology* 252(1):174-188.

Withers, P. J. A., and H. P. Jarvie. 2008. Delivery and cycling of phosphorus in rivers: A review. *Science of the Total Environment* 400(1-3):379-395.

Workshop, S. S. 1990. Concepts and methods for assessing solute dynamics in stream ecosystems. *Journal of the North American Benthological Society* 9(2):95-119.

Wynn, T., S. Mostaghimi, J. Frazee, P. McClellan, R. Shaffer, and W. Aust. 2000. Effects of forest harvesting best management practices on surface water quality in the Virginia coastal plain. *Transactions of the ASAE* 43(4):927-936.

Zarnetske, J. P., R. Haggerty, S. M. Wondzell, and M. A. Baker. 2011. Dynamics of nitrate production and removal as a function of residence time in the hyporheic zone. *Journal of Geophysical Research: Biogeosciences* 116(G01025):1-12.

Zheng, L., J. Gerritsen, J. Beckman, J. Ludwig, and S. Wilkes. 2008. Land use, geology, enrichment, and stream biota in the eastern ridge and valley ecoregion: Implications for nutrient criteria development. *Journal of the American Water Resources Association* 44(6):1521-1536.

Zhu, Q., J. P. Schmidt, A. R. Buda, R. B. Bryant, and G. J. Folmar. 2011. Nitrogen loss from a mixed land use watershed as influenced by hydrology and seasons. *Journal of Hydrology* 405(3):307-315.

Zika, U. 2008. Validating drainage and restoration approaches for restoring nutrient reduction in agricultural headwater streams. In *16th National Nonpoint Source Monitoring Workshop*. Columbus, OH.